

NASA-CP-2427 19880014488

NASA Conference Publication 2427

# Structural Ceramics

FOR REFERENCE

NOT TO BE TAKEN FROM THIS ROOM

~~FOR EARLY DOMESTIC DISSEMINATION~~

~~Because of its significant early commercial potential, this information, which has been developed under a U.S. Government program, is being disseminated within the United States in advance of general publication. This information may be duplicated and used by the recipient with the express limitation that it not be published. Release of this information to other domestic parties by the recipient shall be made subject to these limitations.~~

~~Foreign release may be made only with prior NASA approval and appropriate export licenses. This legend shall be marked on any reproduction of this information in whole or in part.~~

Date for general release May 1988

LIBRARY COPY

MAY 26 1986

LANGLEY RESEARCH CENTER  
LIBRARY, NASA  
HAMPTON, VIRGINIA

*Proceedings of a workshop sponsored by  
NASA Lewis Research Center  
Cleveland, Ohio  
May 20-21, 1986*

**NASA**





*NASA Conference Publication 2427*

# Structural Ceramics

*Proceedings of a workshop sponsored by  
NASA Lewis Research Center  
May 20-21, 1986*



National Aeronautics  
and Space Administration

**Scientific and Technical  
Information Branch**

1986



## PREFACE

Welcome to Lewis Research Center and the Materials Division. We are very pleased that you could visit us and hear about all the progress we, our contractors, and grantees have been making in ceramics. We feel ceramics and ceramic matrix composites are an exciting area of tailored structural materials research. NASA has made a strong commitment to advance this technology and we will work with U.S. industry to foster our national position in world markets. In fact, that is the job of the Materials Division in all areas of NASA technology needs.

If any of your organizations are interested in more detailed information on our programs, in joint research efforts, or in sending a research here for some extended on-site studies, feel free to call me and we will discuss it.

Sal Grisaffe

Chief, Materials Division

(216) 433-3193



# CONTENTS

	Page
Preface . . . . .	111
Ceramics for Turbine Engines	
Stanley R. Levine, NASA Lewis Research Center . . . . .	1
Friction and Wear of Ceramics	
Donald H. Buckley, NASA Lewis Research Center . . . . .	15
Some Design Considerations for Ceramic Components in Heat Engine Applications	
John P. Gyekenyesi, NASA Lewis Research Center . . . . .	23
Nondestructive Evaluation of Structural Ceramics	
Alex Vary, NASA Lewis Research Center . . . . .	35
Fracture Mechanics	
John L. Shannon, Jr., NASA Lewis Research Center . . . . .	47
Structural Ceramics Research	
J.I. Mueller, R.J.H. Bollard, and R.C. Bradt, University of Washington, . . . . .	59
Improved Silicon Carbide for Advanced Heat Engines	
Thomas J. Whalen and J.A. Mangels, Ford Motor Company . . . . .	63
Strength Optimization of $\alpha$ -SiC By Improved Processing	
Sunil Dutta, NASA Lewis Research Center . . . . .	89
Improved Silicon Nitride for Advanced Heat Engines	
H.C. Yeh, AiResearch Casting Company and J.M. Wimmer, Garrett Turbine Engine Company . . . . .	99
Improved Processing of $\text{Si}_3\text{N}_4$	
William A. Sanders, NASA Lewis Research Center and George Y. Baaklini, Cleveland State University . . . . .	119
Colloidal Characterization of Silicon Nitride and Silicon Carbide	
Donald L. Feke, Case Western Reserve University . . . . .	129
NDE of Structural Ceramics by Photoacoustic Microscopy	
P.K. Khandelwal, General Motors Corporation . . . . .	139
Molten Salt Corrosion of SiC and $\text{Si}_3\text{N}_4$	
N.S. Jacobson, J.L. Smialek, and D.S. Fox, NASA Lewis Research Center . . . . .	147
Thermal Cyclic Durability Testing of Ceramic Materials for Turbine Engines	
L.J. Lindberg, Garrett Turbine Engine Company . . . . .	163

	Page
Fractographic and Microstructural Evaluation of 3500-Hour Durability Specimens	
A.D. Miller, University of Washington . . . . .	173
Ceramic Matrix Composites	
James A. DiCarlo, NASA Lewis Research Center . . . . .	181
Polymer Precursors for SiC Ceramic Materials	
Morton H. Litt, Case Western Reserve University . . . . .	189
Polymer Precursors for Ceramic Composites	
Frances I. Hurwitz, NASA Lewis Research Center . . . . .	199
SiC Fiber Analysis	
Martha H. Jaskowiak, NASA Lewis Research Center . . . . .	203
SiC Fiber Reinforced Reaction-Bonded Si <sub>3</sub> N <sub>4</sub> Composites	
Ramakrishna T. Bhatt, NASA Lewis Research Center . . . . .	213

## CERAMICS FOR TURBINE ENGINES

Stanley R. Levine

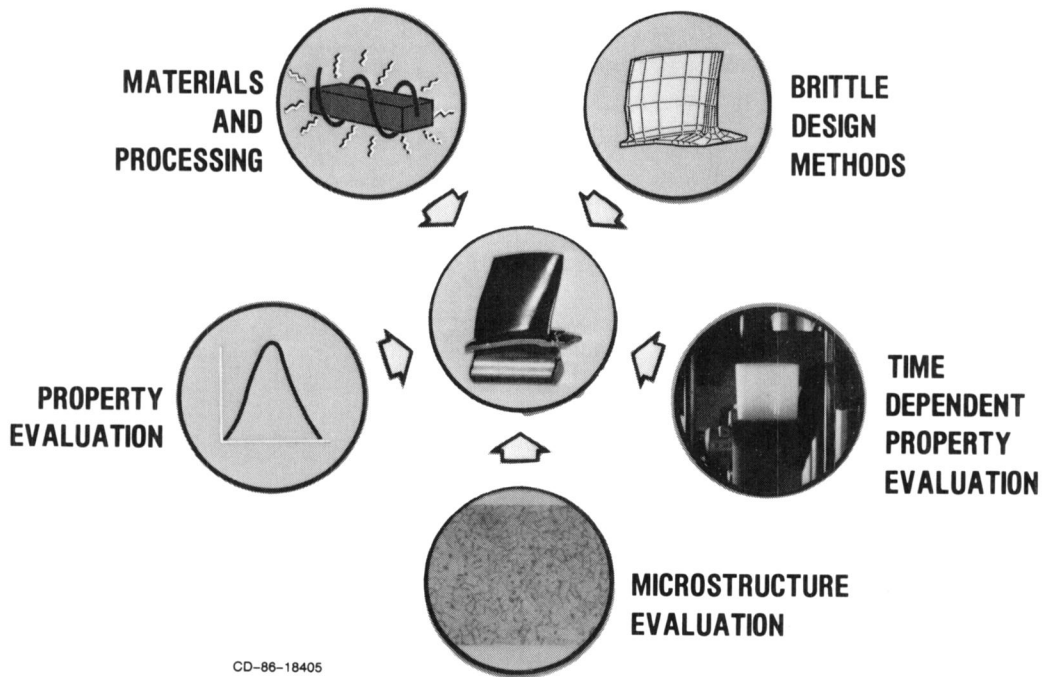
NASA Lewis Research Center  
Cleveland, Ohio 44135

The Ceramics for Turbine Engines Project is comprised of three main research thrusts with major elements as indicated:

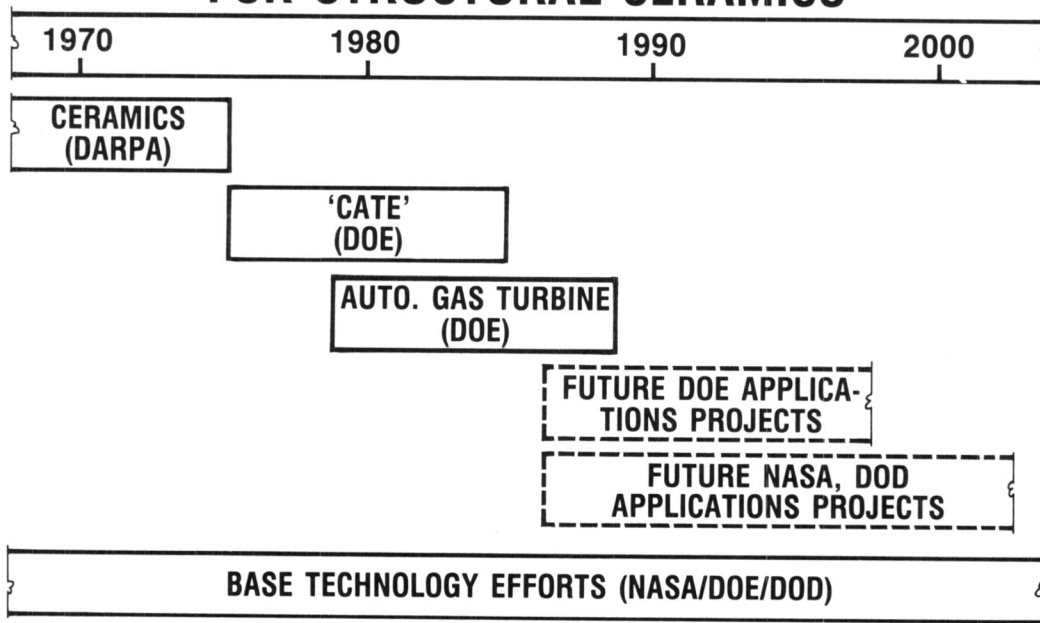
- Materials and Processing
  - Monolithics
  - Fiber reinforced
- Design Methodology
  - Design code
  - Tribology
- Life Prediction
  - Environmental effects
  - Non-destructive evaluation
  - Fracture and fatigue
  - Time dependent behavior

The overall objective of this program is to provide the ceramics technology base in materials and structures for aerospace propulsion and power applications programs. The effort is complementary to and coordinated with the Department of Energy funded Ceramic Technology for Advanced Heat Engines Project at Oak Ridge National Laboratory. From the NASA perspective an enhanced ceramics technology base directly supports aeronautics initiatives in small engine technology, high-performance turbine engine technology, and hypersonics. The Ceramics for Turbine Engines Project is funded at about \$2M per year and involves about 20 researchers in the Materials Division and the Structures Division at Lewis as well as contract and grant research. An overview of the program, which includes the technical objectives and content of each thrust, is provided in the following figures. This workshop reports on research efforts funded mainly by Ceramics for Turbine Engines. A major strength of the program is the increasingly interdisciplinary nature of the research being carried out in-house. Several of the papers presented will illustrate and demonstrate the benefits of such an approach.

# CERAMICS FOR TURBINE ENGINES



## GOVERNMENT-SPONSORED TECHNOLOGY PROGRAMS FOR STRUCTURAL CERAMICS





# DOE/NASA ADVANCED GAS TURBINE TECHNOLOGY DEVELOPMENT PROJECT

## OBJECTIVE

- DEVELOP A TECHNOLOGY BASE APPLICABLE TO A COMPETITIVE AUTOMOTIVE GAS TURBINE ENGINE

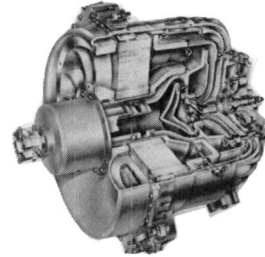
## TECHNOLOGY DEVELOPMENT GOALS

- 36% IMPROVEMENT IN FUEL ECONOMY OVER A CONVENTIONAL (SI) ENGINE IN A 3000 LB VEHICLE
- ADAPTABILITY TO ALTERNATIVE FUELS
- MEET OR EXCEED PRESENT EMISSION STANDARDS
- COMPETITIVE RELIABILITY, LIFE, AND COSTS

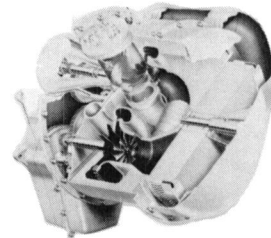
## APPROACH

- TWO ENGINE/AUTOMOBILE CONTRACTOR TEAMS (GARRETT/FORD AND ALLISON/PONTIAC)
  - DESIGN, FABRICATE, AND TEST ALL-CERAMIC HOT SECTION COMPONENTS
- SUPPORTING RESEARCH AND TECHNOLOGY EFFORT IN CRITICAL AREAS
- INITIATED 1980--PLANNED COMPLETION 1986

CD-85-17625

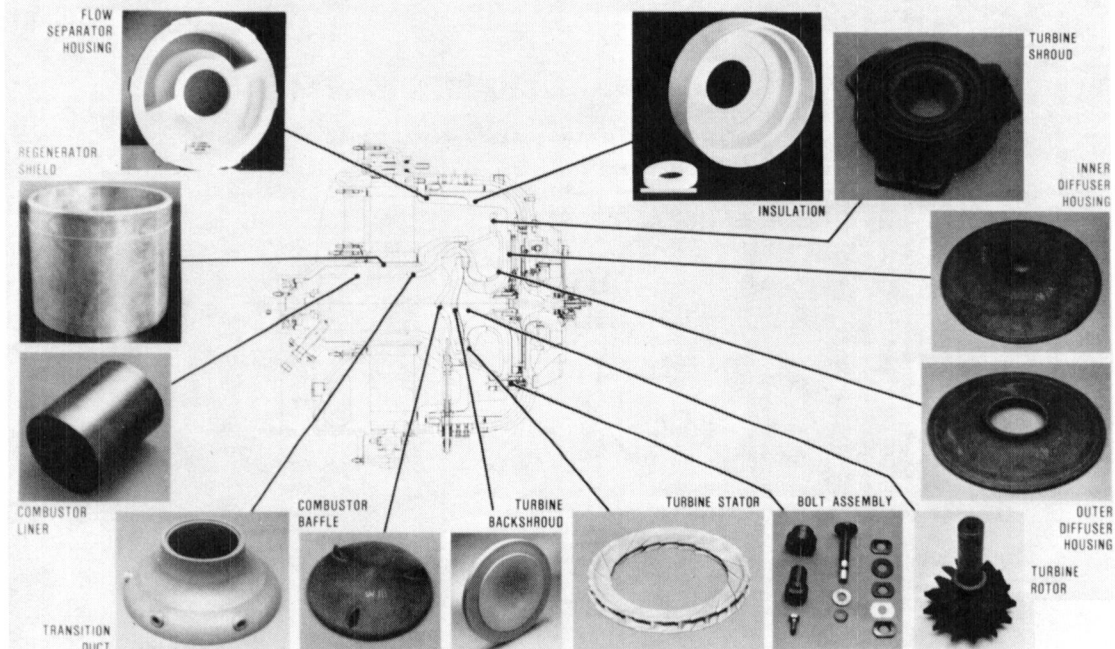


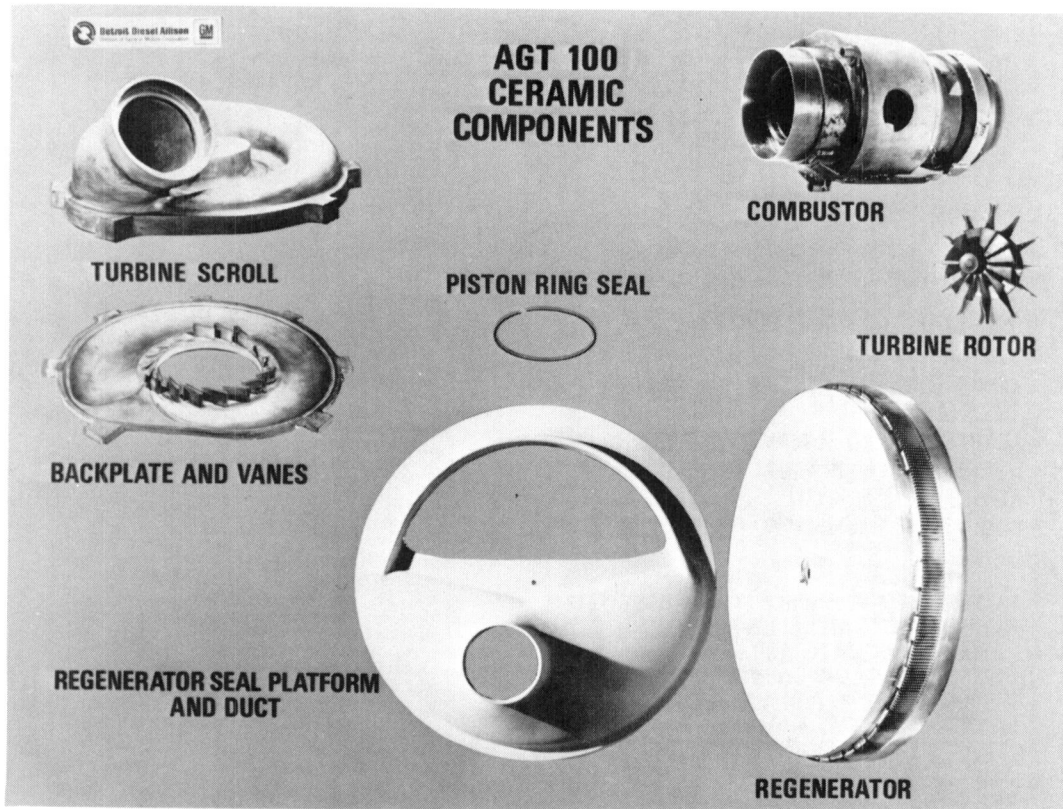
**AGT-101**



**AGT-100**

## AGT101 CERAMIC COMPONENTS





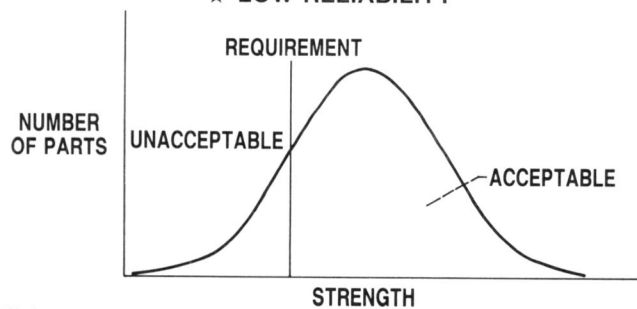
## STATUS OF MONOLITHIC CERAMIC MATERIALS

CERAMIC MATERIALS HAVE DEMONSTRATED:

- ★ GOOD HIGH TEMPERATURE STRENGTH
- ★ GOOD OXIDATION RESISTANCE
- ★ GOOD EROSION RESISTANCE
- ★ NET SHAPE FABRICATION CAPABILITY

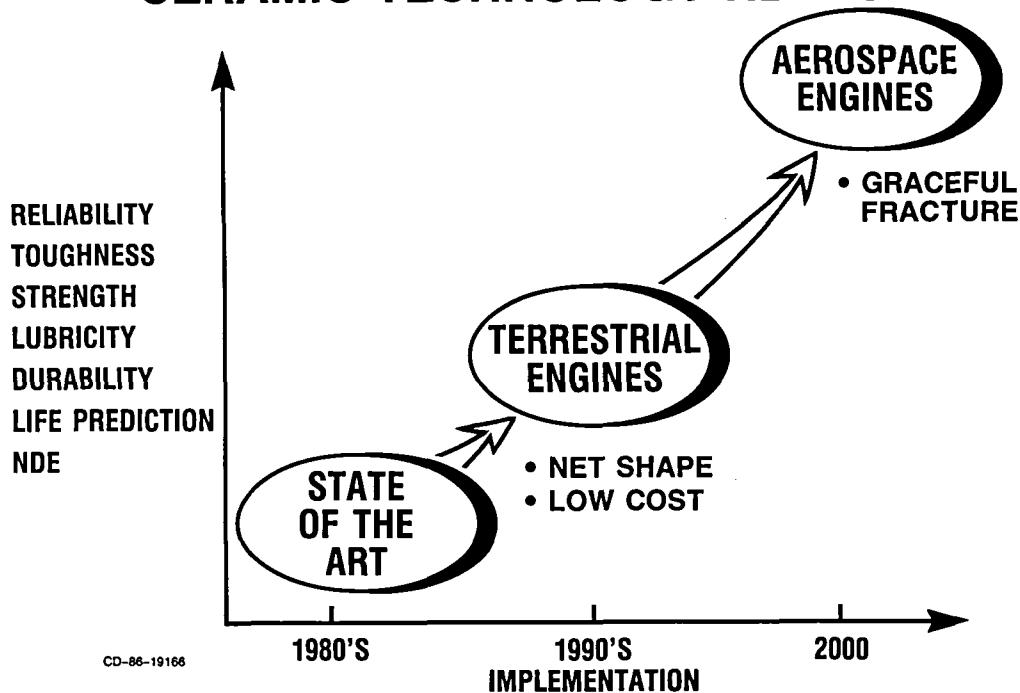
**BUT**

- ★ LOW RELIABILITY



CD-86-19177

## CERAMIC TECHNOLOGY NEEDS



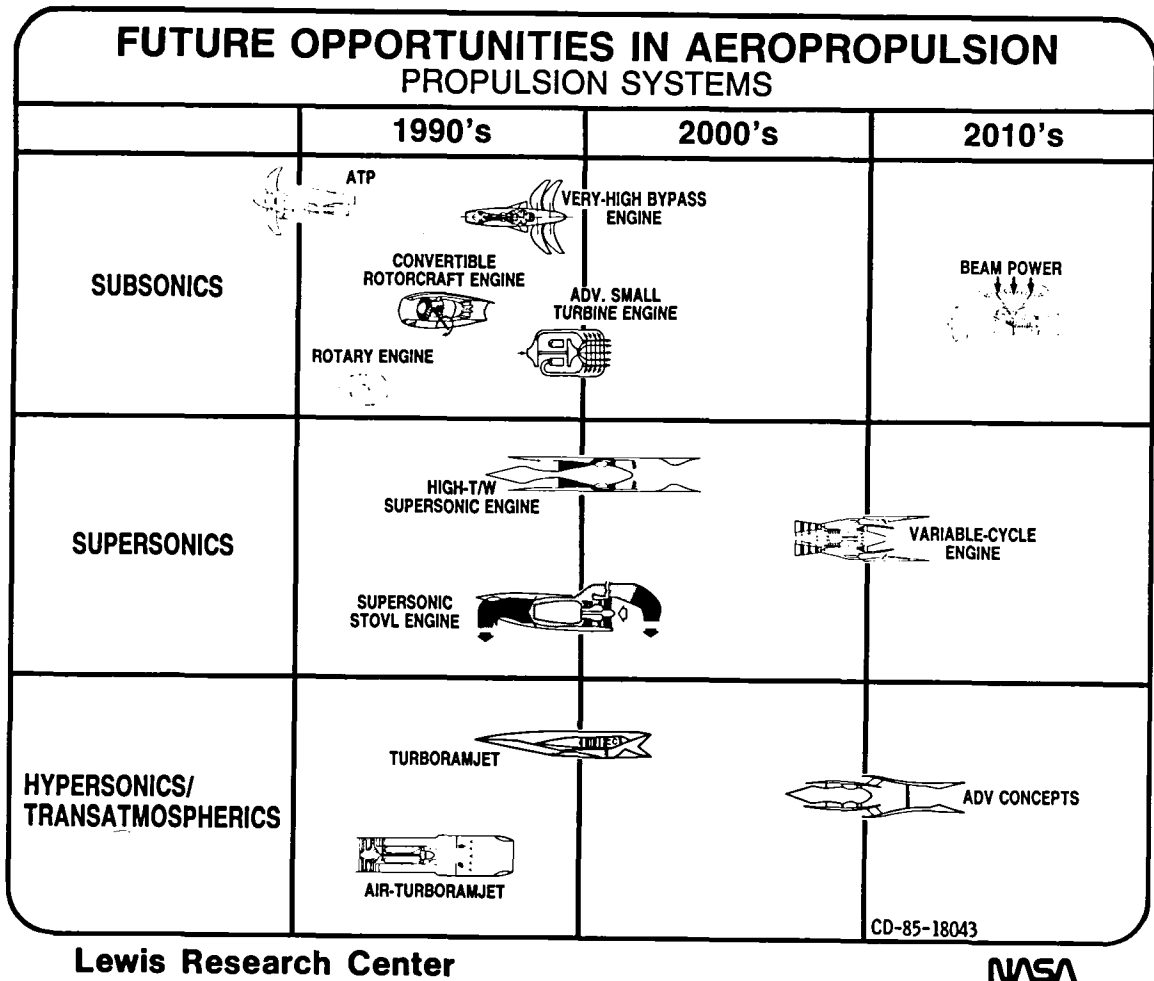
## STRATEGIC THRUSTS IN AERONAUTICS TO ESTABLISH TECHNOLOGY FOR 21st CENTURY ADVANCED AIRCRAFT

NASA OAST/AERONAUTICS - NOVEMBER 1984

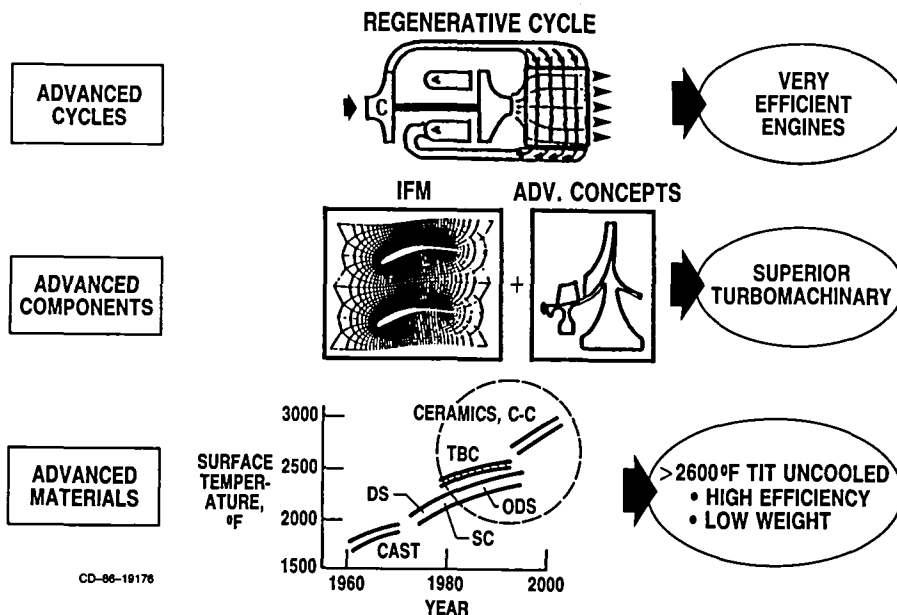
PRESIDENTIAL SCIENCE ADVISOR KEYWORTH - APRIL 1985

- DEVELOP ESSENTIAL TECHNOLOGIES FOR HIGH-EFFICIENCY SUBSONIC TRANSPORTS.
- ESTABLISH TECHNOLOGY READINESS FOR EFFICIENT SUPERSONIC CRUISE TRANSPORT AND FIGHTER/ATTACK AIRCRAFT.
- DEVELOP ESSENTIAL TECHNOLOGIES FOR REALIZATION OF PRACTICAL HYPERSONIC AND TRANSATMOSPHERIC FLIGHT AIRCRAFT.

CD-85-17934

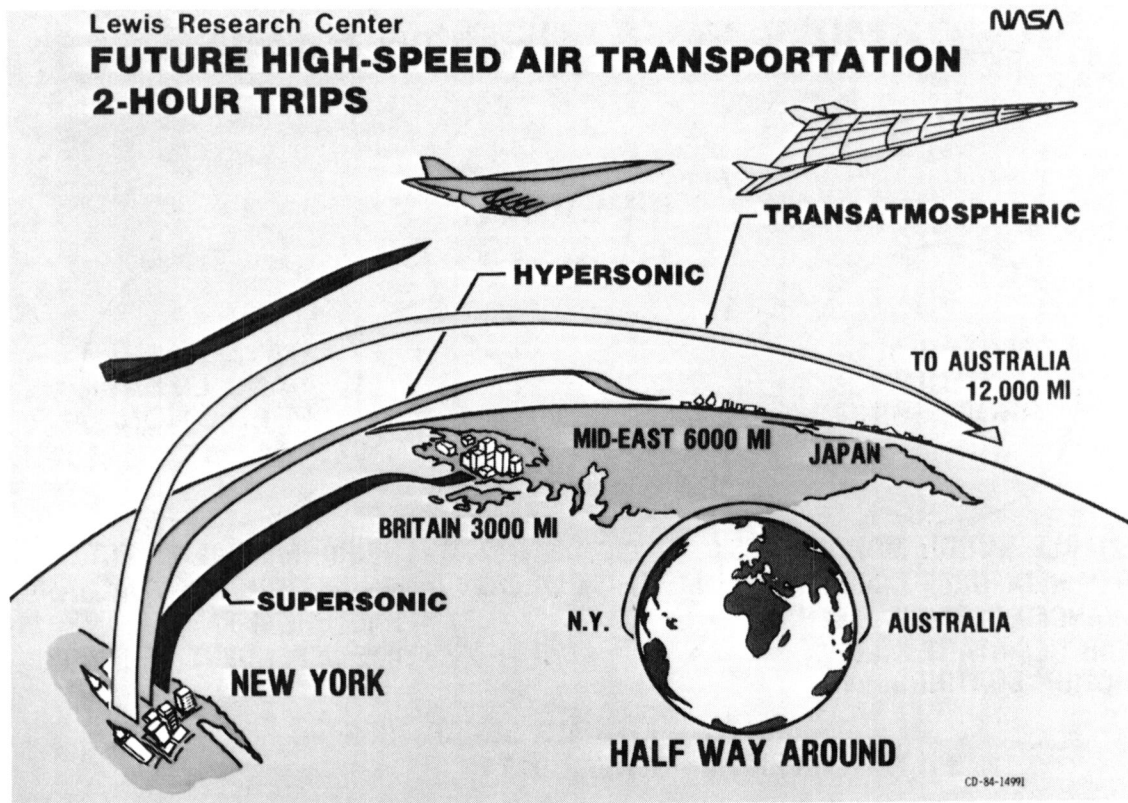
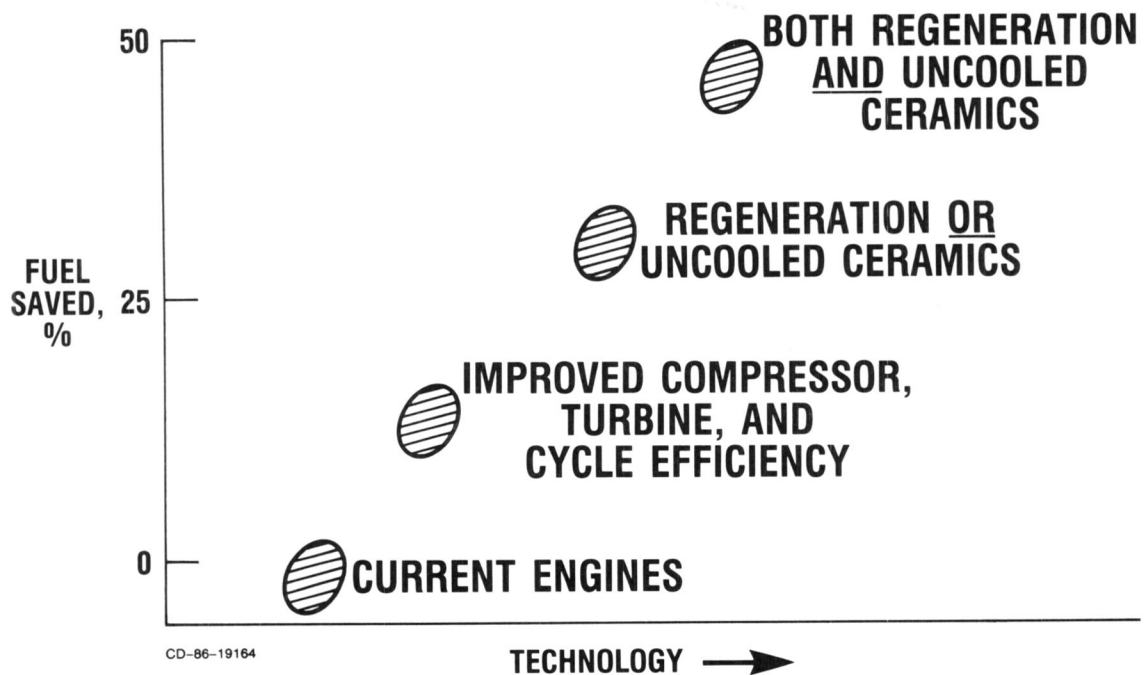


## SMALL ENGINE TECHNOLOGY OPPORTUNITIES



# TECHNOLOGY BENEFITS FROM CERAMICS

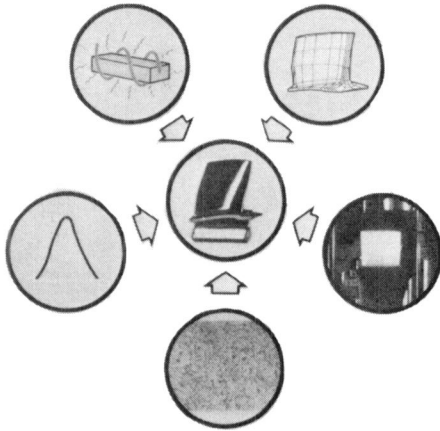
## TYPICAL-COMMUTER MISSION



# CERAMICS FOR TURBINE ENGINES

## OBJECTIVE

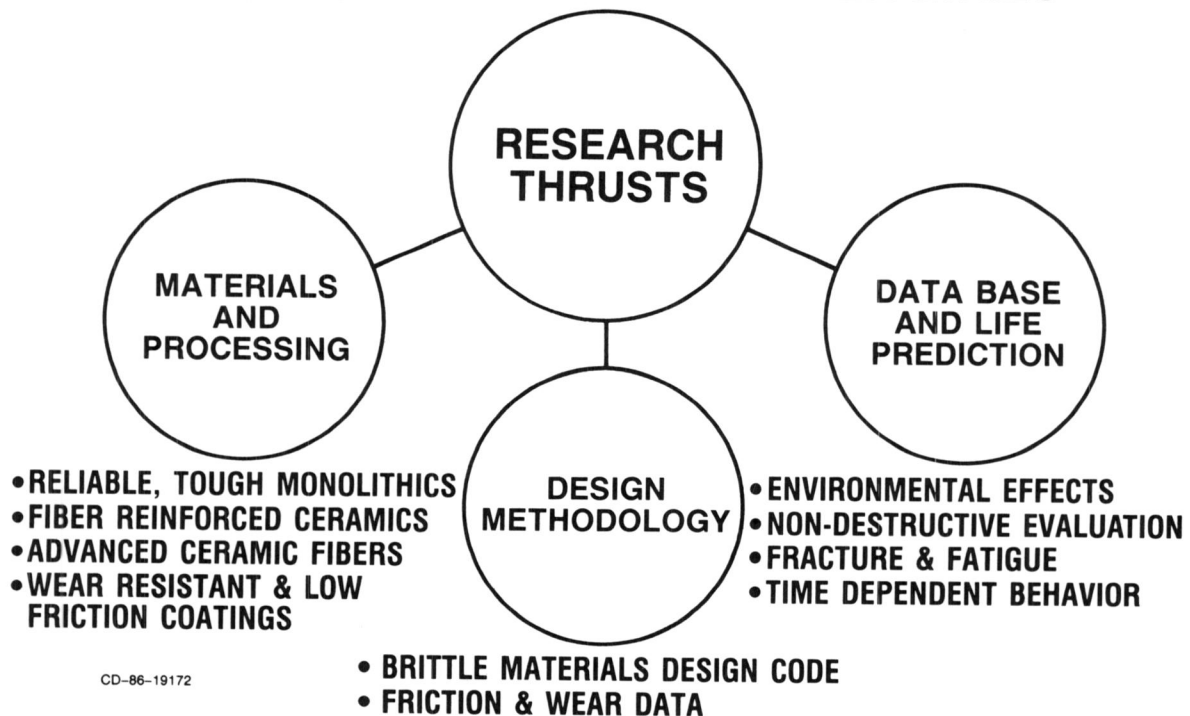
DEVELOP THE TECHNOLOGY  
REQUIRED TO IMPROVE STRUCTURAL  
CERAMIC RELIABILITY AND PERMIT  
USE OF CERAMICS IN ADVANCED  
HEAT ENGINES



## APPROACHES

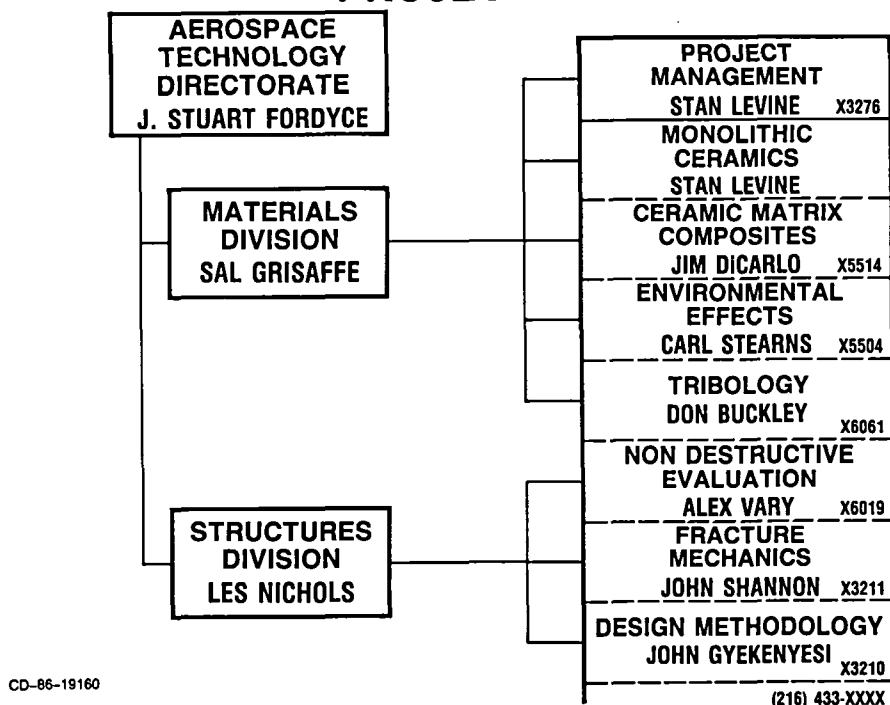
- MATERIALS AND PROCESSING
- DESIGN METHODOLOGY
- LIFE PREDICTION

# CERAMICS FOR TURBINE ENGINES

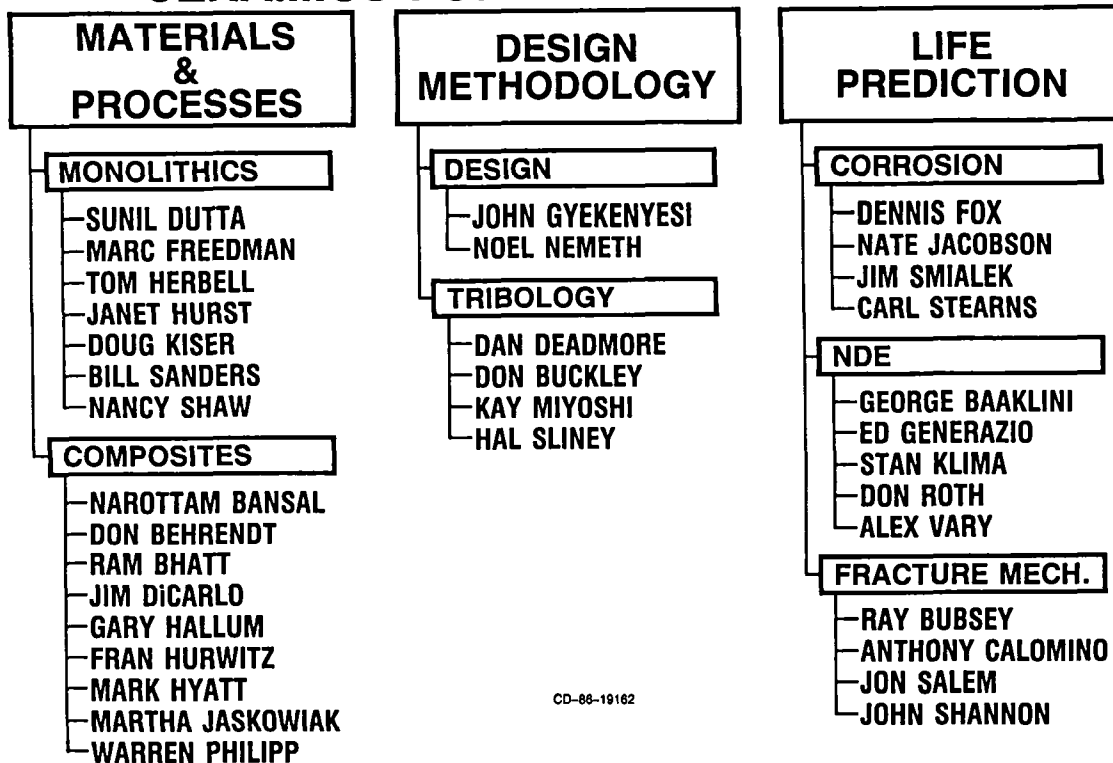


CD-86-19172

# CERAMICS FOR TURBINE ENGINES PROJECT TEAM



## CERAMICS FOR TURBINE ENGINES



# LEWIS CERAMICS CAPABILITIES

## FIBERS

FIBER COATING  
HIGH TEMPERATURE FIBER TESTING  
FIBER PHYSICAL/MECHANICAL PROPERTIES

## CERAMIC/CERAMIC COMPOSITE FABRICATION

FIBER/MATRIX TAPE FAB  
HOT PRESS  
REACTION BONDING  
HOT ISOSTATIC PRESS (2200 °C, 20 ksi)  
HIGH PRESSURE N<sub>2</sub> SINTERING (2150 °C, 1000 psi)  
CVD & CVI FABRICATION  
SOL GEL PROCESSING/CHARACTERIZATION  
POLYMER PROCESSING/CHARACTERIZATION  
POWDER PROCESSING/CHARACTERIZATION

## INTERDISCIPLINARY COLLABORATION

ENVIRONMENTAL EFFECTS - BURNER RIGS, H<sub>2</sub>/O<sub>2</sub> RIG, COATINGS  
NDE - RADIOGRAPHY ACOUSTIC MICROSCOPY, ULTRASONICS  
FRACTURE MECHANICS & FATIGUE  
STRUCTURAL ANALYSIS & DESIGN METHODOLOGY  
SURFACE SCIENCE - FRICTION, WEAR, COATINGS

CD-86-19167

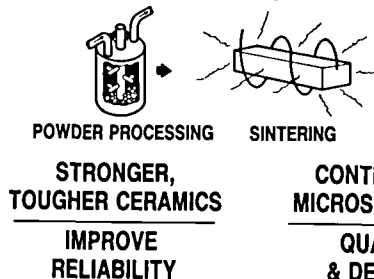
# CERAMICS FOR TURBINE ENGINES

## —MATERIALS AND PROCESSING—

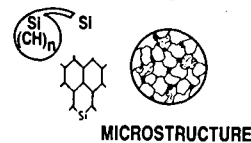
### OBJECTIVE:

IMPROVE RELIABILITY, STRENGTH AND TOUGHNESS OF CERAMICS/CERAMIC MATRIX COMPOSITES

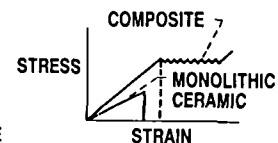
### APPROACH: POWDER DERIVED MATERIALS



### CHEMICALLY DERIVED MATERIALS



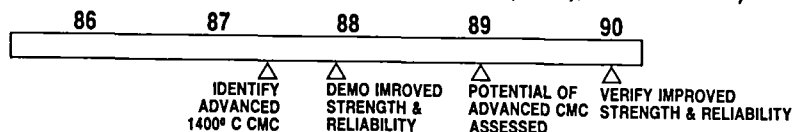
### COMPOSITES



### BENEFITS:

ADVANCED CERAMIC MATERIALS TECHNOLOGY FOR AEROSPACE PROPULSION AND POWER APPLICATIONS (E.G. ADVANCED SMALL ENGINE TECHNOLOGY (ASET), HYPERSONICS)

### SCHEDULE:

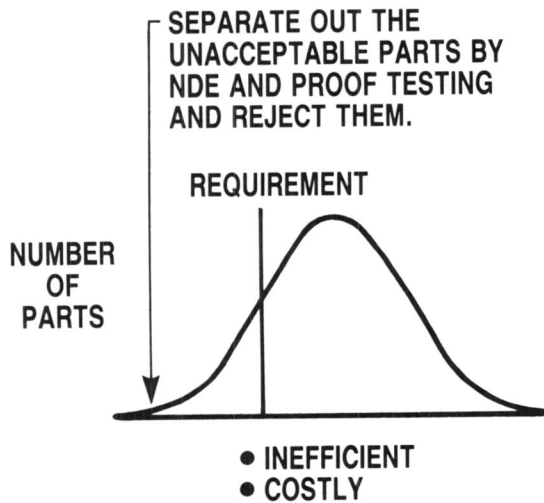


CD-85-18488



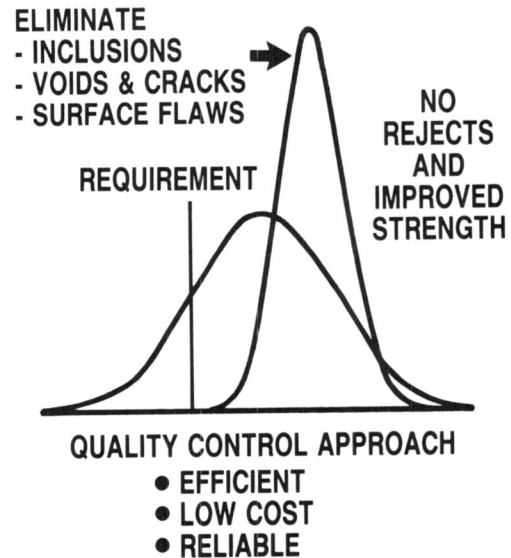
# APPROACHES TO CERAMIC RELIABILITY

## "INSPECT-IN" THE QUALITY



CD-86-19174

## IMPROVE THE PROCESS



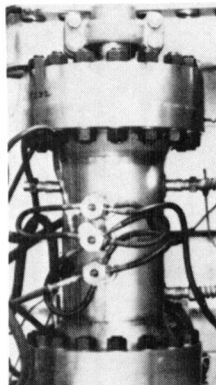
## MONOLITHIC CERAMICS

### OBJECTIVES:

- UNDERSTAND MICROSTRUCTURE/PROCESSING/ PROPERTIES/RELATIONSHIPS
- IMPROVE RELIABILITY

### APPROACHES

#### SINTERING/HIGH $P_{N_2}$



← SINTERED  $Si_3N_4$  (SSN)

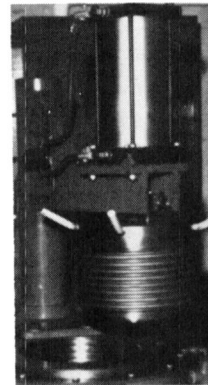
REACTION BONDED  
 $Si_3N_4$  (RBSN) →

← SINTERED REACTION  
BONDED  $Si_3N_4$  (SRBSN) →

← SINTERED  $SiC$  (SSC) →

CD-86-19178

#### HIP



# FIBER REINFORCED CERAMICS APPROACH TO RELIABILITY

INCORPORATE CONTINUOUS CERAMIC FILAMENTS HAVING  
GREATER STIFFNESS THAN MATRIX

## • ADVANTAGES

- IMPROVED TOUGHNESS IMPARTED BY CRACK DEFLECTION AND CRACK BRIDGING
- INCREASED MODULUS AND STRESS TO FAILURE
- "METAL-LIKE" STRESS-STRAIN BEHAVIOR
- GRACEFUL FAILURE

## • DISADVANTAGES

- PROCESSING MORE DIFFICULT
- AVAILABLE FIBERS LIMITED
- CONTROL OF FIBER-MATRIX BOND REQUIRED

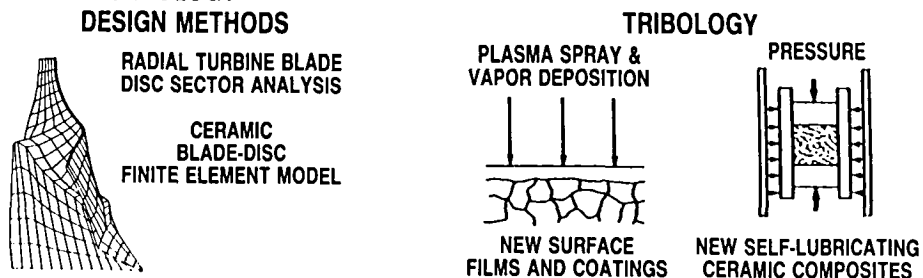
CD-86-19175

# CERAMICS FOR TURBINE ENGINES —DESIGN METHODOLOGY—

## OBJECTIVES:

- DEVELOP AND VERIFY MECHANICAL DESIGN METHODS FOR CERAMIC AND CERAMIC COMPOSITE COMPONENTS
- UNDERSTAND FRICTION/WEAR INTERACTIONS AND DEVELOP HIGH TEMPERATURE SOLID FILM AND COMPOSITE LUBRICANT TECHNOLOGY

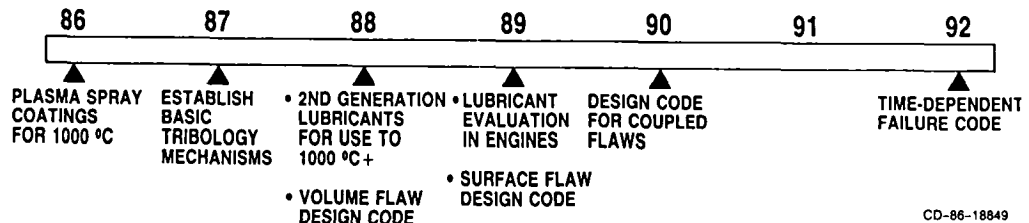
## APPROACH:



## BENEFITS:

ENABLING TECHNOLOGY TO PERMIT USE OF CERAMIC MATERIALS IN ADVANCED AEROSPACE PROPULSION AND POWER SYSTEMS

## SCHEDULE: AT GL



CD-86-18849

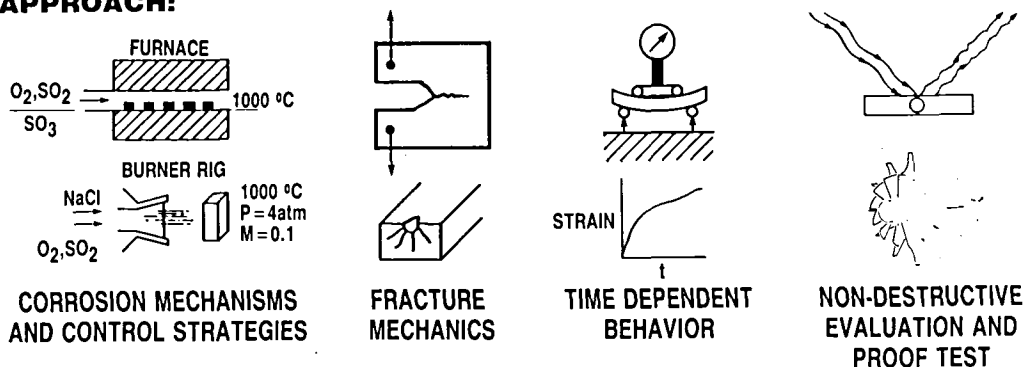
# CERAMICS FOR TURBINE ENGINES

## —LIFE PREDICTION—

### OBJECTIVE:

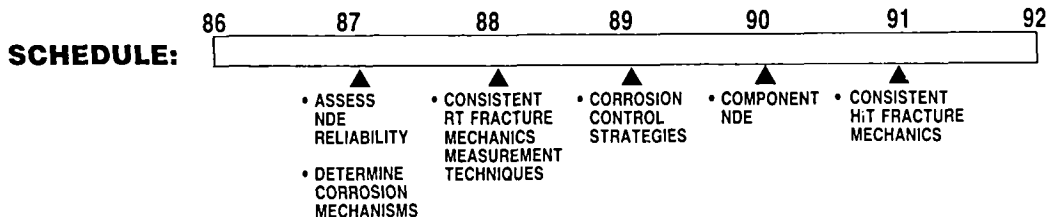
DEVELOP LIFE PREDICTION AND RELIABILITY ASSESSMENT TOOLS FOR STRUCTURAL CERAMICS

### APPROACH:



### BENEFITS:

- ENABLING TECHNOLOGY TO PERMIT RELIABLE DESIGN AND USE OF ADVANCED CERAMIC MATERIALS
- GUIDE DEVELOPMENT OF DURABLE CERAMICS FOR AEROSPACE PROPULSION AND POWER SYSTEMS



CD-86-18848

## FUTURE OPPORTUNITIES FOR CERAMICS

### SYSTEMS

- VEHICULAR AND STATIONARY POWER
- ADVANCED SMALL ENGINE TECHNOLOGY (ASET)
- HIGH-THRUST-TO-WEIGHT ENGINES (HPTE)
- AEROSPACEPLANE

### MATERIAL NEEDS

- HIGH-TEMPERATURE, NON-STRATEGIC MATERIALS AT LOW COST (2500 °F)
- VERY HIGH RELIABILITY, TOUGHNESS AND STRENGTH-TO-WEIGHT (2700 °F)
- ADVANCED RECUPERATORS/REGENERATORS (2200 °F)
- ASSEMBLY OF CERAMICS INTO A WORKABLE ENGINE SYSTEM
- VERY HIGH RELIABILITY, TOUGHNESS AND STRENGTH-TO-WEIGHT (3000 °F)
- SAME AS HPTE (3000 °F + +)
- DURABLE CERAMICS FOR USE IN  $O_2$  AT HIGH HEAT FLUX (EDGE INSERTS) AND IN  $H_2/O_2$  (ENGINE SEALS)

### OPPORTUNITY

- CONTINUE EMPHASIS ON RELIABILITY
- DEVELOP THERMALLY STABLE 10 TO 25  $\mu$  DIAMETER CERAMIC FIBER AND APPLY IN CERAMIC MATRIX COMPOSITES
- DEVELOP AND VERIFY POTENTIAL OF ADVANCED MATERIALS
- ADVANCED JOINING, NONJOINING AND CONTACT STRESS CONTROL TECHNOLOGY
- DESIGN AND LIFE PREDICTION
- FIBERS AND COMPOSITES
- FIBERS AND COMPOSITES
- IDENTIFY SUITABLE MATERIALS

CD-86-19169



## FRICITION AND WEAR OF CERAMICS

Donald H. Buckley  
NASA Lewis Research Center

The adhesion, friction, wear, and lubricated behaviors of both oxide and non-oxide ceramics are reviewed. Ceramics are examined in contact with themselves, other harder materials, and metals. Elastic, plastic, and fracture behavior of ceramics in solid state contact is discussed. The contact load necessary to initiate fracture in ceramics is shown to be appreciably reduced with tangential motion. Both friction and wear of ceramics are anisotropic and relate to crystal structure as with metals. Grit size effects in two- and three-body abrasive wear are observed for ceramics. Both the free energy of oxide formation and the d valence bond character of metals are related to the friction and wear characteristics for metals in contact with ceramics. Surface contaminants affect friction and adhesive wear. For example, carbon on silicon carbide and chlorine on aluminum oxide reduce friction while oxygen on metal surfaces in contact with ceramics increases friction. Lubrication increases the critical load necessary to initiate fracture of ceramics both in indentation and with sliding or rubbing.

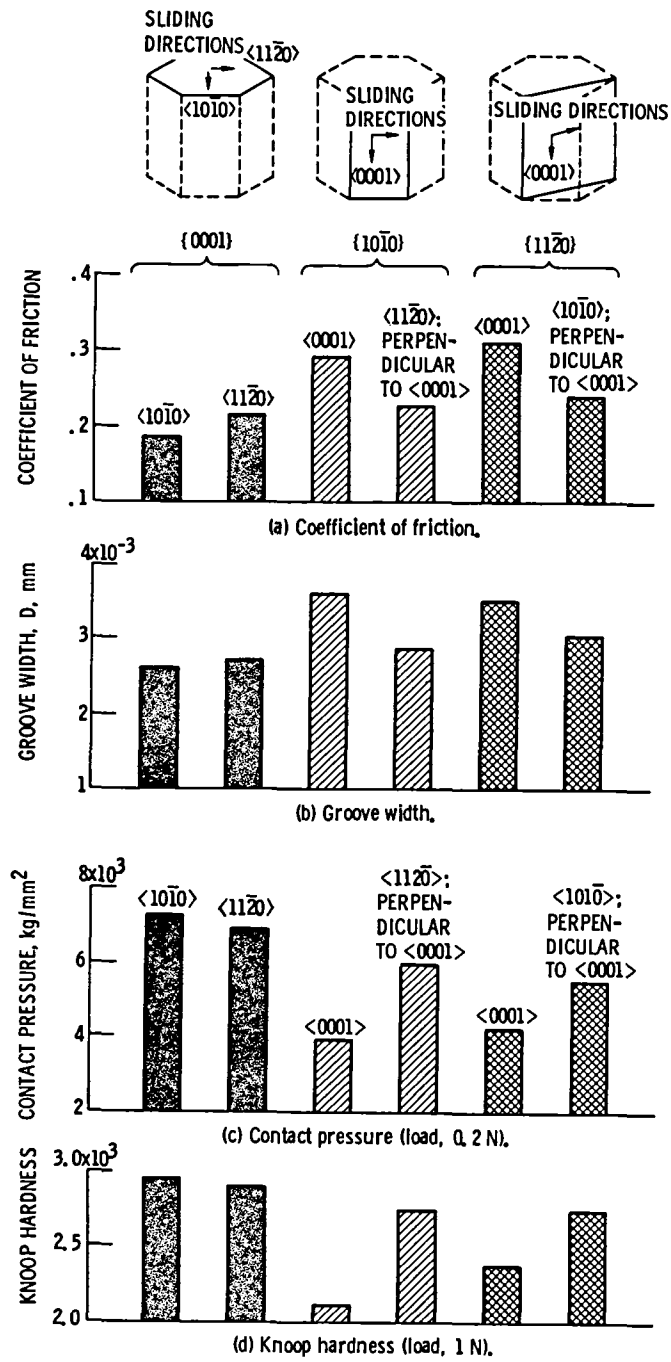


Figure 1. - Anisotropies on {0001}, {10 $\bar{1}$ 0}, and {11 $\bar{2}$ 0} surfaces of SiC.

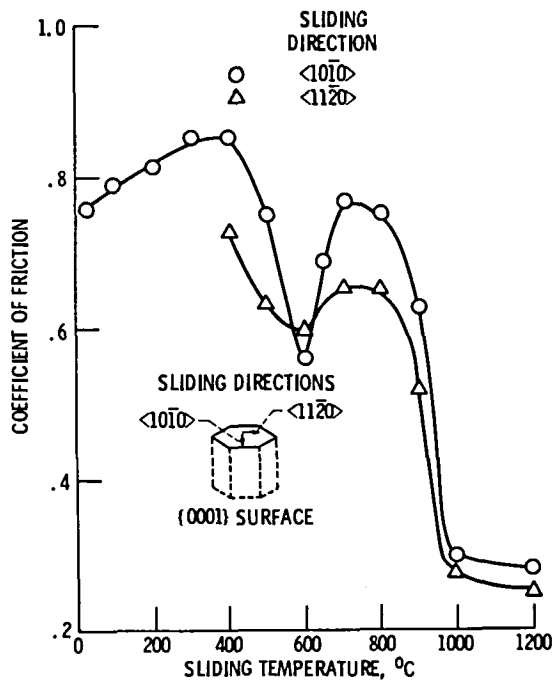


Figure 2. - Effect of temperature on coefficient of friction for silicon carbide {0001} surface sliding against an iron rider. The iron rider was argon ion sputter cleaned before experiments. Normal load, 0.2 N, vacuum, 10 nPa.

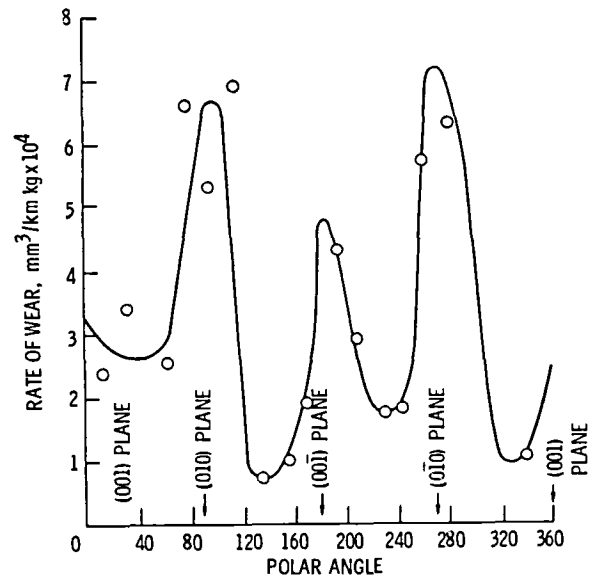


Figure 3. - Rate of wear of a rutile single-crystal sphere on a great circle in the plane of the a- and c-axes is normal to plane of sliding at 0 and 180°. Slide direction in plane of the great circle (ref. 8).

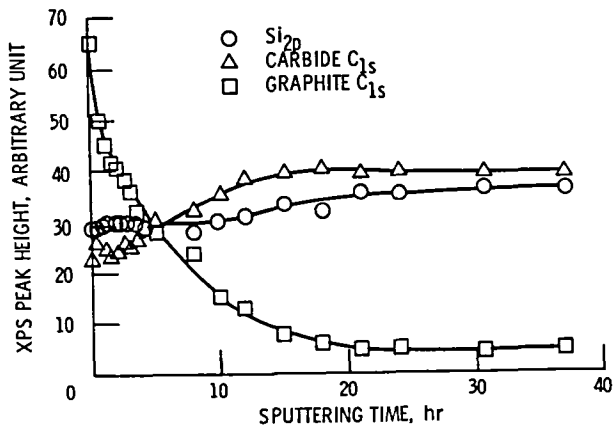


Figure 4. - Elemental depth profile of silicon carbide {0001} surface preheated a temperature of 1500° C for 1 hour.

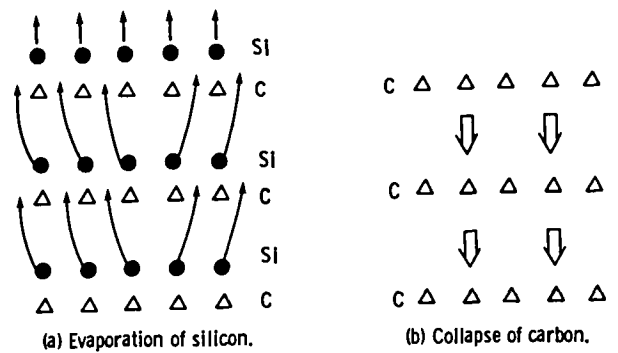


Figure 5. - Graphitization of silicon carbide surface.

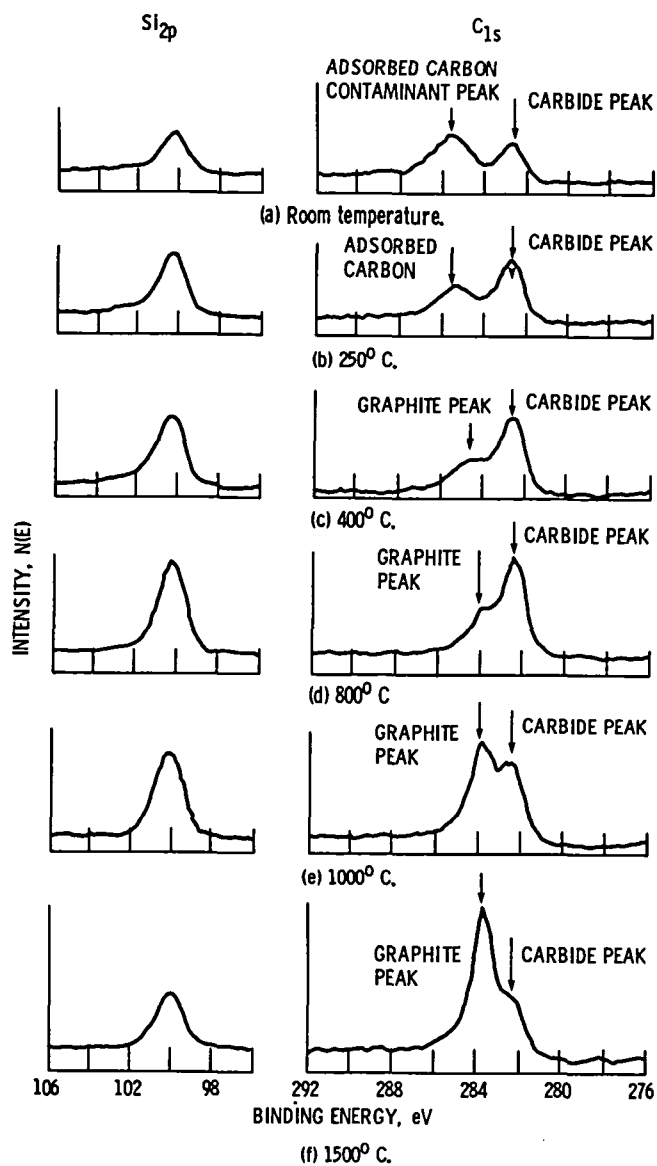


Figure 6. - Representative  $\text{Si } 2p$  and  $\text{C } 1s$  XPS peaks on silicon carbide  $\{0001\}$  surface preheated at various temperatures to  $1500^\circ\text{C}$ .



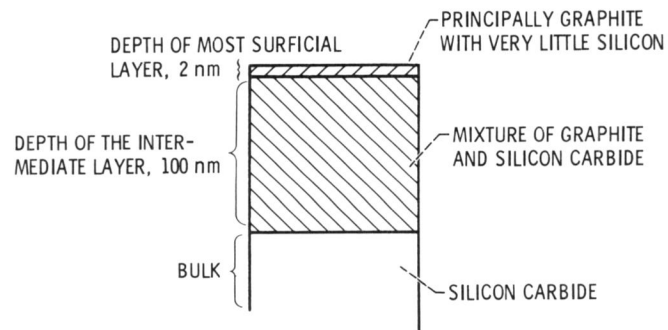


Figure 7. - Surface condition of silicon carbide after heating at temperatures above 1200° C.

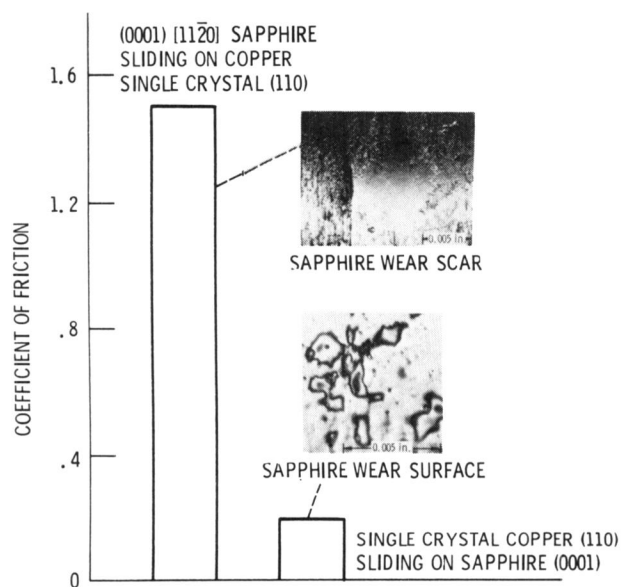


Figure 8. - Friction for copper in sliding contact with sapphire in vacuum 30 nPa; load, 100 g; sliding velocity, 0.013 cm/s.

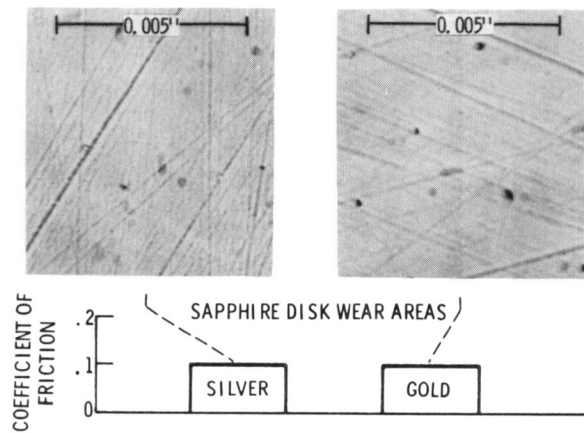


Figure 9. - Coefficient of friction for gold and silver riders sliding on sapphire in vacuum (30 nPa). Sliding velocity, 0.013 cm/s; ambient temperature, 25<sup>0</sup> C; duration, 1hr.

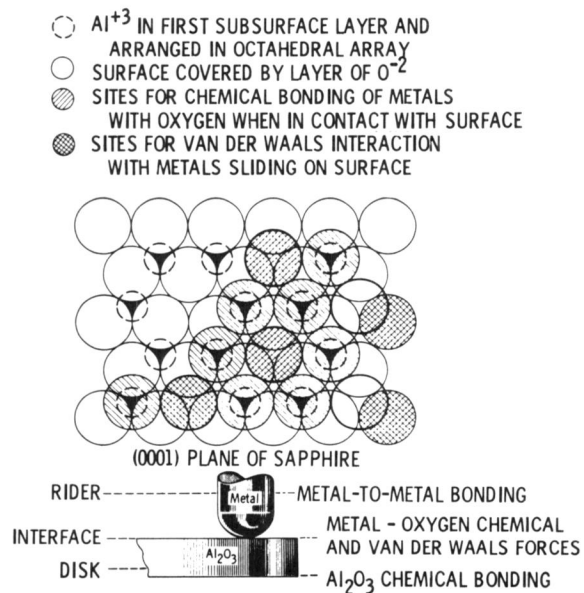


Figure 10. - Nature of surface interaction and bonding of metal to  $\text{Al}_2\text{O}_3$ .

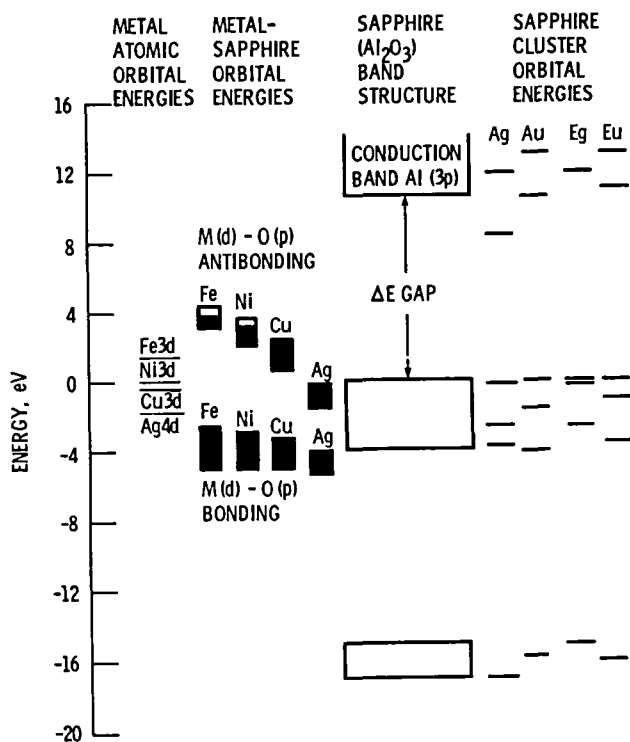
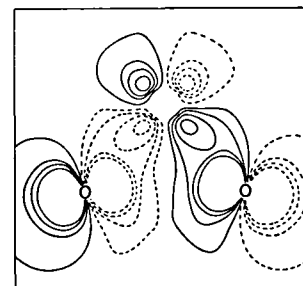
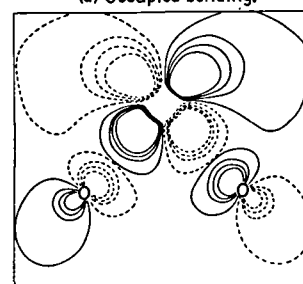


Figure 11. - Molecular-orbital energies, as determined by the self-consistent-field X-alpha scattered wave method, for clusters representing bulk sapphire and metal-sapphire interfaces

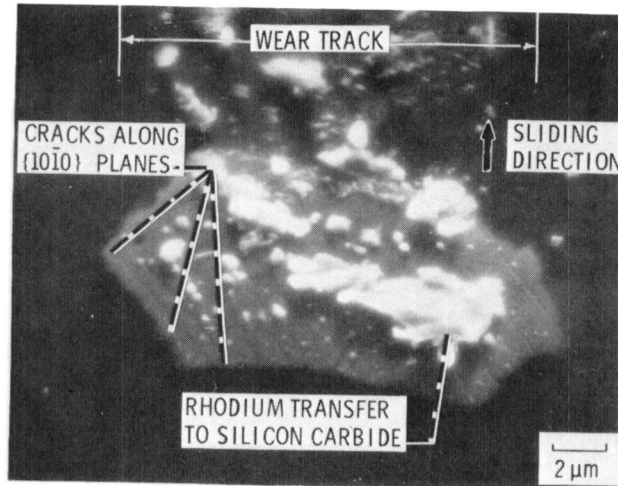


(a) Occupied bonding.

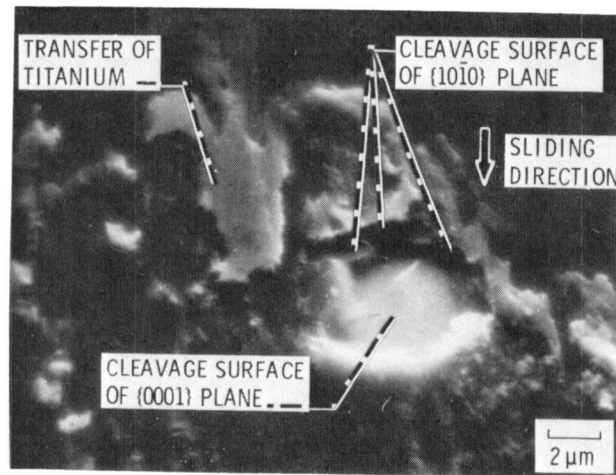


(b) Unoccupied antibonding.

Figure 12. - Fe(d) - O(p) molecular-orbital wave-function contour maps for an iron atom supported on sapphire, plotted in the plane of the iron atom and two surface oxygen atoms. The solid and dashed contours represent the positive and negative phases of the wave function



(a) Hexagonal cracking.



(b) Hexagonal pit.

Figure 13. - Scanning electron photomicrographs of wear tracks on the {0001} surface of single-crystal SiC in contact with rhodium and titanium as a result of ten passes of a rider in vacuum. Sliding direction,  $\langle 10\bar{1}0 \rangle$ ; sliding velocity,  $3 \text{ mm/min}^{-1}$ ; load, 0.3 N; room temperature; pressure, 30 nPa; metal pin rider, 0.79 mm radius.

## SOME DESIGN CONSIDERATIONS FOR CERAMIC COMPONENTS IN HEAT ENGINE APPLICATIONS

John P. Gyekenyesi  
NASA Lewis Research Center  
Cleveland, Ohio 44135

This presentation reviews the design methodology for brittle material structures which is being developed and used at the Lewis Research Center for sizing ceramic components in heat engine applications. Theoretical aspects of designing with structural ceramics are discussed, and a general purpose reliability program for predicting fast fracture response due to volume distributed flaws is described. Statistical treatment of brittle behavior, based on the Weibull model, is reviewed and its advantages, as well as drawbacks, are listed. A mechanistic statistical fracture theory, proposed by Batdorf to overcome the Weibull model limitations and based on Griffith fracture mechanics, is summarized. Failure probability predictions are made for rotating annular  $\text{Si}_3\text{N}_4$  disks using various fracture models, and the results are compared to actual failure data. The application of these design methods to Government funded ceramics engine demonstration programs is surveyed. The uncertainty in observed component performance emphasizes the need for proof testing and improved NDE technology to guarantee adequate structural integrity.

## POSSIBLE APPROACHES TO CERAMIC DESIGN

### A. PROTOTYPE TESTING

- NO STRESS ANALYSIS REQUIRED
- POLYAXIAL FRACTURE STRESS THEORY NOT NEEDED
- EVERY DESIGN IS UNIQUE
- EXPENSIVE

### B. SCALE MODEL EVALUATION

- VOLUME EFFECT MUST BE INCLUDED
- NO MECHANICAL STRESS ANALYSIS NEEDED
- POLYAXIAL FRACTURE STRESS THEORY NOT NEEDED
- THERMAL STRESS PROBLEM CANNOT BE SCALED
- EVERY DESIGN IS UNIQUE
- LESS EXPENSIVE

### C. USE OF TEST SPECIMEN TESTING

- VOLUME EFFECT MUST BE INCLUDED
- FULL THERMOMECHANICAL ANALYSIS REQUIRED
- COMBINED FRACTURE STRESS THEORY NEEDED
- CAN BE APPLIED TO ALL DESIGNS
- INEXPENSIVE

CD-86-19363

## POTENTIAL FAILURE MODES IN HEAT ENGINES

### A. TIME INDEPENDENT FAILURE MODES

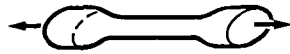
- FAST FRACTURE (TENSION-COMPRESSION)
- BUCKLING

### B. TIME DEPENDENT FAILURE MODES

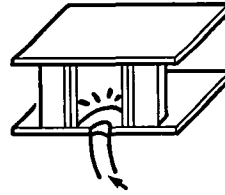
- STATIC FATIGUE
- DYNAMIC FATIGUE
- CREEP CRACK GROWTH
- STRESS CORROSION AND OXIDATION
- IMPACT AND DYNAMIC LOADING

CD-86-19359

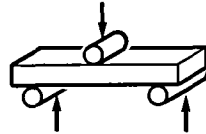
## SCHEMATICS OF STRENGTH TESTS



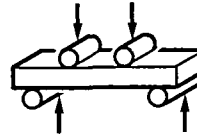
UNIAXIAL TENSILE STRENGTH



HYDROSTATIC TENSILE



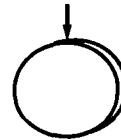
3-POINT BENDING



4-POINT BENDING



UNIAXIAL COMPRESSIVE



DIAMETRAL COMPRESSION

CD-86-19368

## BRITTLE MATERIAL DESIGN METHOD

### MATERIAL BRITTLENESS AND PRESENCE OF MICROCRACKS REQUIRES

- ALLOWANCE FOR STRENGTH DISPERSION - PROBABILISTIC APPROACH
- CONSIDERATION OF MATERIAL VOLUME UNDER STRESS (COMBINATION OF STRESS AND VOLUME DETERMINE INTEGRITY)
- REFINED THERMAL AND STRESS ANALYSIS - FIELD SOLUTIONS (EXAMINATION OF CRITICAL POINT IS NOT ADEQUATE)

### DESIGN PRACTICE

- FAILURE MODE IS FRACTURE DUE TO CRACK PROPAGATION
- PROOF TESTING AND/OR NDE REQUIRED TO TRUNCATE STRENGTH DISTRIBUTION - ESTABLISH ALLOWABLE STRESS
- NO DESIGN CODES AND ONLY LIMITED EXPERIENCE AVAILABLE

CD-86-19362

## FRACTURE THEORIES

### I. GRIFFITH (1920 AND 1924)

- CRACK SHAPE, SIZE, ORIENTATION SPECIFIED
- IGNORES VOLUME EFFECT
- USES MECHANISTIC FRACTURE CRITERION
- APPROACH IS DETERMINISTIC (BASIS FOR LEFM)

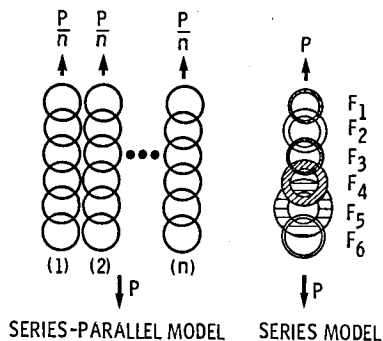
### II. WEIBULL (1939)

- CRACK SHAPE, SIZE, ORIENTATION NOT SPECIFIED
- INCLUDES ALLOWANCE FOR STRENGTH DISPERSION
- EXPLAINS VOLUME EFFECT
- USES EMPIRICAL FRACTURE CRITERION
- APPROACH IS PROBABILISTIC

## STATISTICAL TREATMENTS

### WEAKEST LINK THEORY FOR TENSILE LOADING

- MATERIAL CONTAINS  $N$  FLAWS OR LINKS
- EACH FLAW OR LINK HAS A  $\sigma_{cr}$
- UPON SINGLE LINK FAILURE, TWO REDISTRIBUTION MECHANISMS ARE POSSIBLE

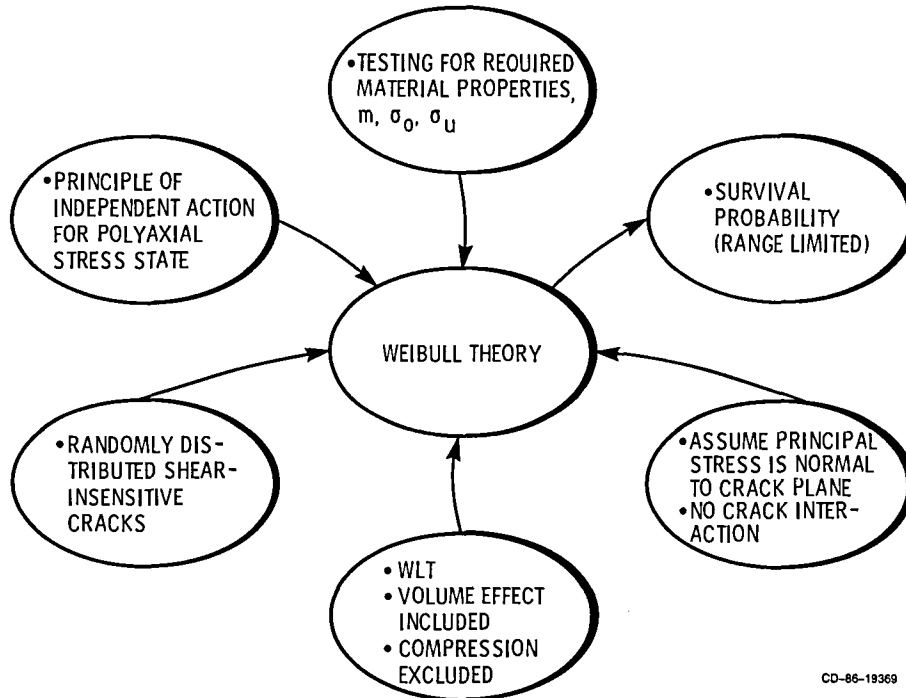


- STRUCTURAL CERAMICS ARE ASSUMED TO FOLLOW THE SERIES MODEL
- FAILURE OF SINGLE LINK IMPLIES COMPONENT FAILURE, NO CRACK ARREST MECHANISM EXISTS

CD-86-19372



## ELEMENTS OF WEIBULL'S THEORY (1)



CD-86-19369

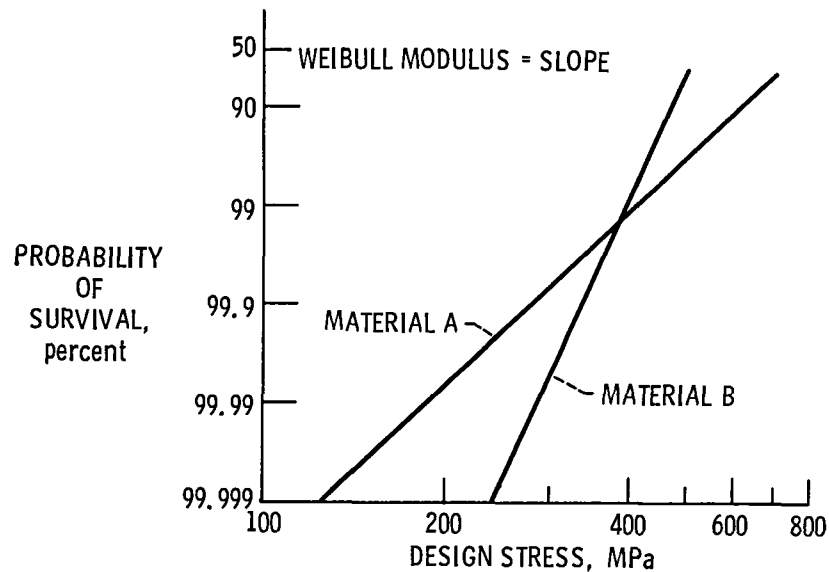
## WEIBULL THEORY (2) (CONTINUED)

SURVIVAL PROBABILITY	EQUATION
IN UNIAXIAL TENSION	$P_S(\sigma) = P_S^V(\sigma) \cdot P_S^A(\sigma)$
DUE TO VOLUME CRACKS	$P_S^V(\sigma) = \exp \left[ - \int_V \left( \frac{\sigma - \sigma_u^V}{\sigma_0^V} \right)^{m_V} dv \right]$
DUE TO SURFACE CRACKS	$P_S^A(\sigma) = \exp \left[ - \int_A \left( \frac{\sigma - \sigma_u^A}{\sigma_0^A} \right)^{m_A} dA \right]$
IN POLYAXIAL TENSION	$P_S(\sigma_1, \sigma_2, \sigma_3) = P_S(\sigma_1) \cdot P_S(\sigma_2) \cdot P_S(\sigma_3)$

WHERE  $\sigma$  = APPLIED STRESS AND  $\sigma_1, \sigma_2, \sigma_3$  = PRINCIPAL STRESSES.

CD-86-19371

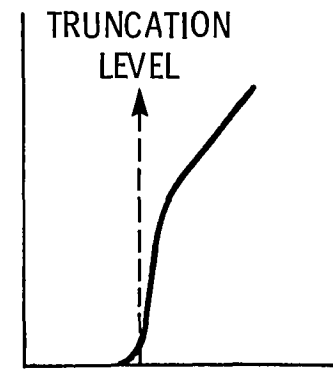
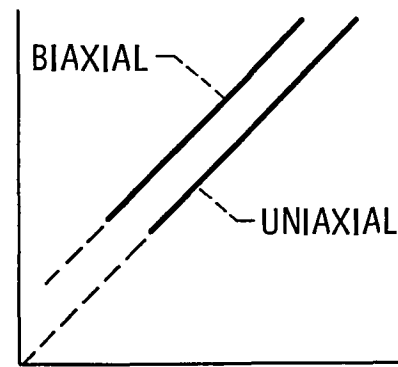
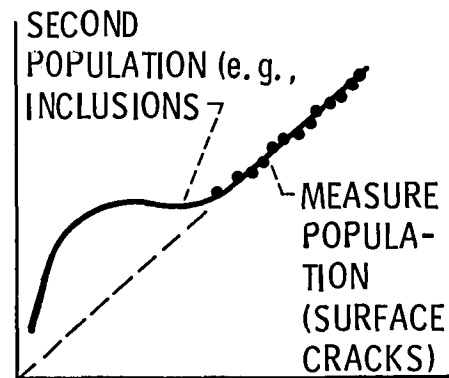
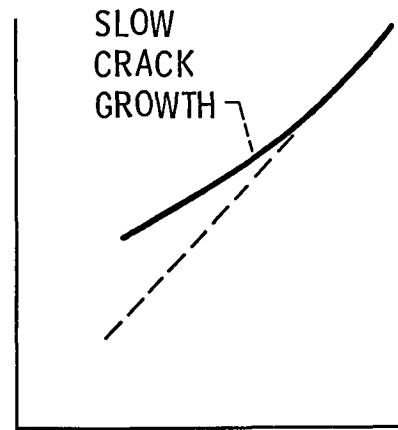
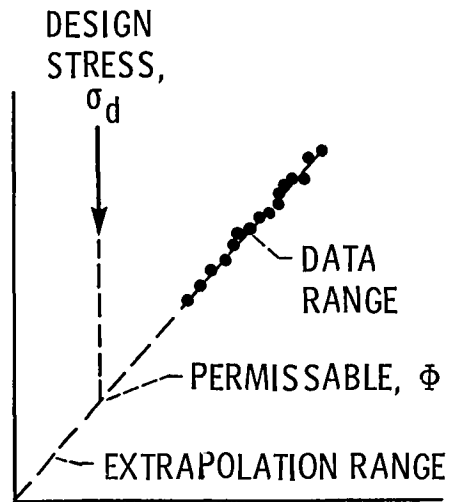
## HYPOTHETICAL EXAMPLE OF IMPORTANCE OF HIGH WEIBULL MODULUS FOR STRUCTURAL CERAMICS



## ADVANTAGES OF PROBABILISTIC DESIGN

- PERMITS EFFICIENT MATERIAL UTILIZATION
- INCLUDES TRADE-OFF BETWEEN HIGH STRENGTH AND LOW SCATTER
- ACCOUNTS FOR MATERIAL STRENGTH DISPERSION
- INCLUDES COMPONENT SIZE EFFECT

# LIMITATIONS OF THE DIRECT STATISTICAL APPROACH

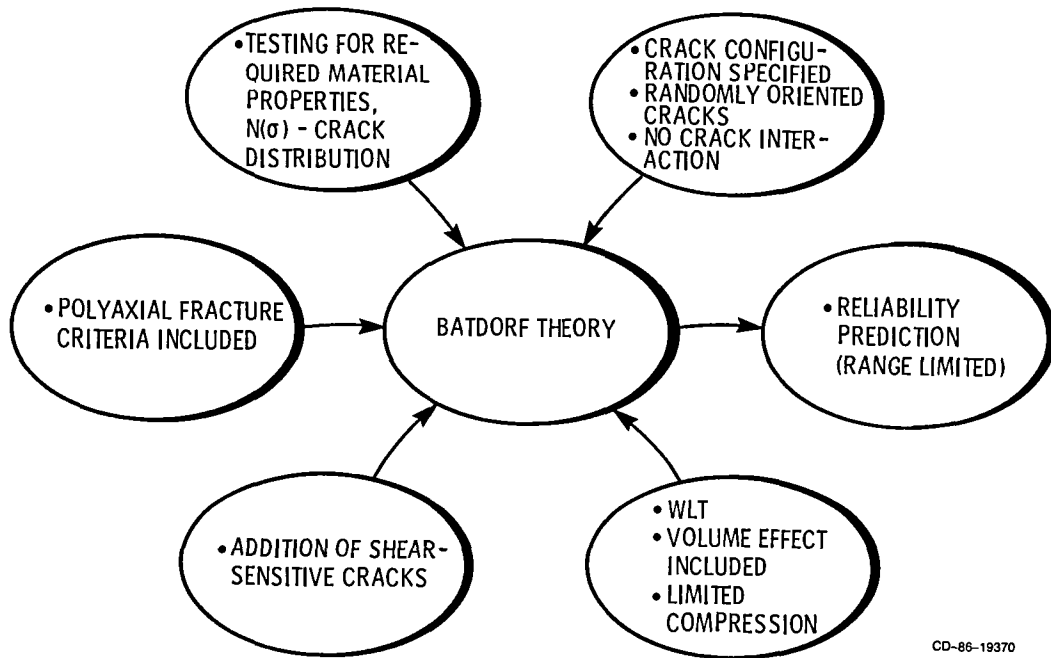


$$V(S/S_0)^m$$

STRESS STATE EFFECTS

TRUNCATION PROCEDURES

## ELEMENTS OF BATDORF'S THEORY (1)



CD-86-19370

## BATDORF THEORY (2) (CONTINUED)

$$P_s(\Sigma) = P_s^V \cdot P_s^A$$

$$P_s^V = \exp \left( - \int_V \int_0^{\sigma_1} \frac{\Omega}{4\pi} \frac{dN_1}{d\sigma_{cr}} d\sigma_{cr} dv \right)$$

$$P_s^A = \exp \left( - \int_A \int_0^{\sigma_1} \frac{\omega}{\pi} \frac{dN_2}{d\sigma_{cr}} d\sigma_{cr} dA \right)$$

$$N_1 = K_1 \sigma_{cr}^{m_1}$$

$$N_2 = K_2 \sigma_{cr}^{m_2}$$

$$\omega = f_1(\sigma_{cr}, \sigma_1, \sigma_2)$$

$$\Omega = f_2(\sigma_{cr}, \sigma_1, \sigma_2, \sigma_3, \alpha)$$

$$\sigma_e = f_3(\sigma_n, \tau), \text{ } f_3 \text{ DEPENDS UPON THE FRACTURE CRITERION SELECTED}$$

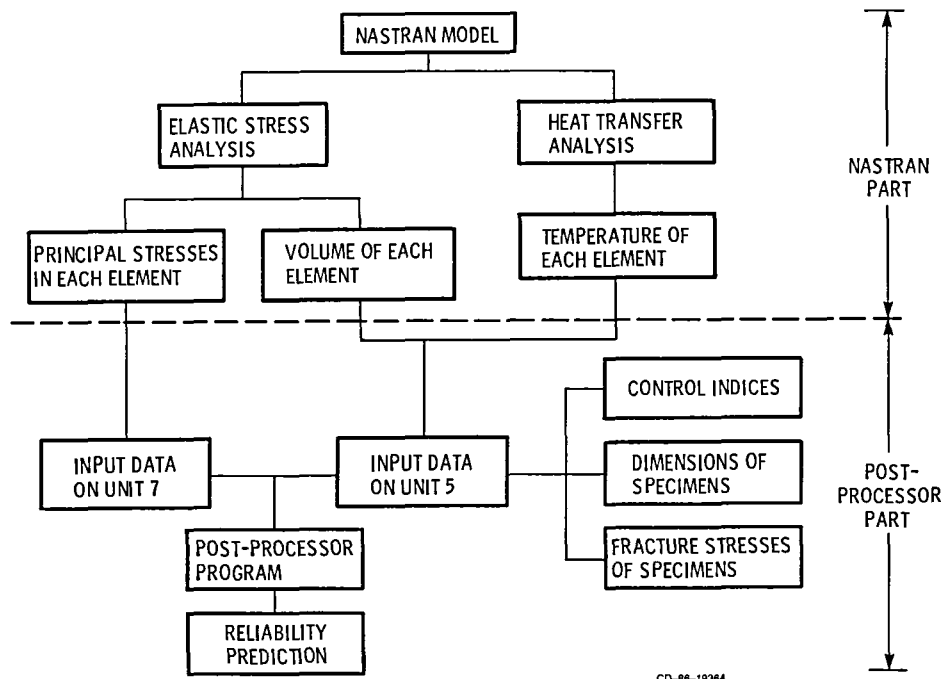
$$\sigma_n = f_4(\sigma_1, \sigma_2, \sigma_3, \alpha, \beta)$$

$$\tau = f_5(\sigma_1, \sigma_2, \sigma_3, \alpha, \beta)$$

CD-86-19373

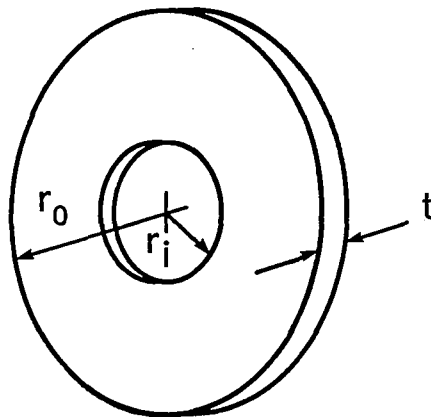
# FLOW CHART FOR RELIABILITY PREDICTION

(VOLUME FLAWS ONLY)



CD-86-19364

## EXAMPLE 1 - ROTATING ANNULAR DISK



### DATA:

NC - 132 HOT PRESSED  $\text{Si}_3\text{N}_4$

$m = 7.65$

$\sigma_0 = 74.82 \text{ MPa } m^{.3922}$

$\bar{k}_B = 16.30$

$r_i = 6.35 \text{ mm } (.25 \text{ in})$

$r_o = 41.275 \text{ mm } (1.625 \text{ in})$

$t = 3.80 \text{ mm } (.15 \text{ in})$

RPM RANGE - 70K TO 114K

CD-86-19366

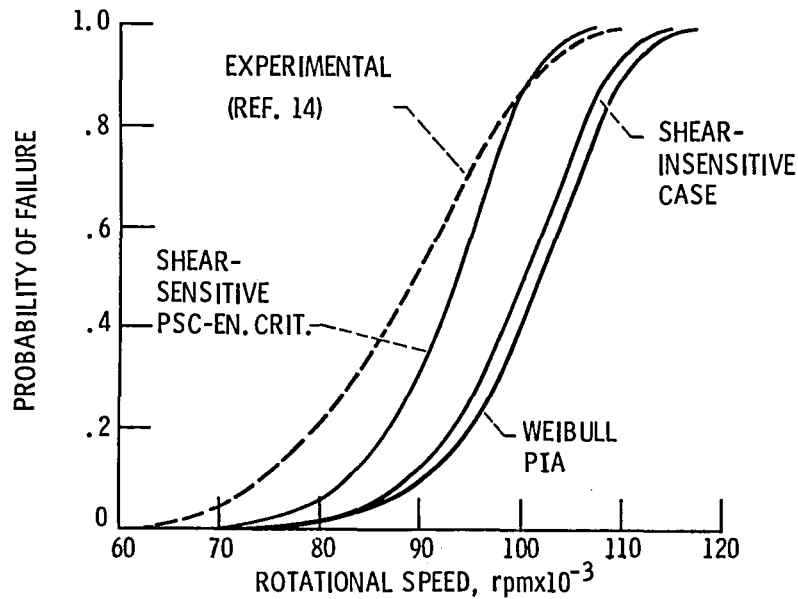
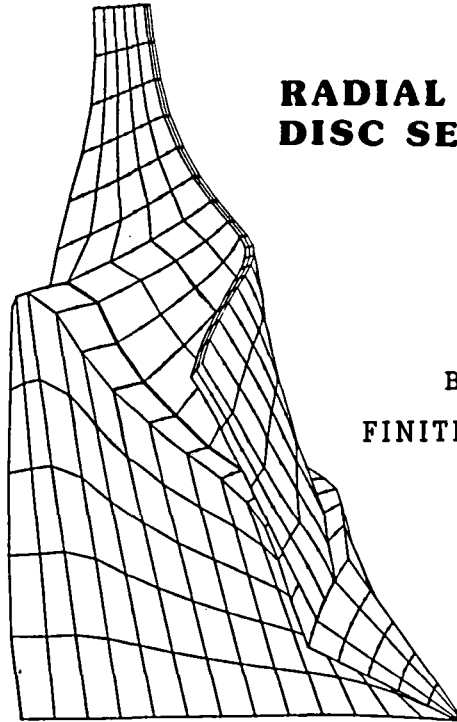


Fig. 7 Example 1 probability of failure vs disk rotational speed for various fracture models (SCARE2 data).

#### APPLICATION TO CERAMICS

- INITIALLY ONLY WEIBULL THEORY WAS USED (INCLUDES CATE, AGT, AND DARPA PROGRAMS)
- LIMITED SUCCESS AND ACCURACY OBTAINED
- BATDORF BRIDGES GAP BETWEEN FRACTURE THEORIES IN 1974 (GRAPHITE NOSE CONES)
- UNIVERSITY OF WASHINGTON (UW) APPLIES BATDORF'S THEORY TO CERAMICS (NASA GRANT)
- LeRC CORRECTS UW PUBLICATIONS AND DEVELOPS GENERAL PURPOSE DESIGN PROGRAM - SCARE
- SCARE INCLUDES WEIBULL AND BATDORF THEORIES
- SCARE RELEASED TO GM, FORD, TRW, BOEING, GE, AND NASA AND ARMY FOR INITIAL EVALUATION

CD-86-19360



## **RADIAL TURBINE BLADE DISC SECTOR ANALYSIS**

**CERAMIC  
BLADE - DISC  
FINITE ELEMENT MODEL**

### **CONCLUSIONS**

1. PROBABILISTIC DESIGN APPROACH AND WLT MUST BE USED FOR CERAMICS
2. FRACTURE MECHANICS MUST BE APPLIED TO IMPROVE MODELING OF:
  - MULTI-AXIALITY EFFECT
  - DELAYED FAILURE
3. PROOF-TESTING AND/OR NDE SHOULD BE USED TO AVOID DATA EXTRAPOLATION
4. MULTIPLE FLAW DISTRIBUTIONS SHOULD BE INCLUDED IN THE ANALYSIS
5. IMPROVED FRACTURE TOUGHNESS AND MATERIAL PROCESSING ARE NEEDED TO INCREASE CERAMIC STRENGTH

CD-86-19361



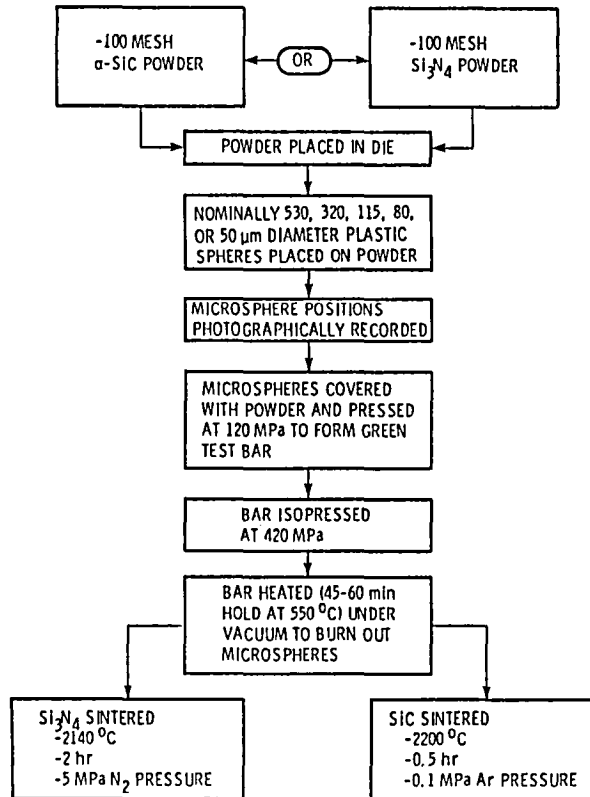


## NONDESTRUCTIVE EVALUATION OF STRUCTURAL CERAMICS\*

Alex Vary  
Lewis Research Center  
Cleveland, Ohio 44135

A review is presented on research for nondestructive evaluation (NDE) of structural ceramics for heat engine applications. Microfocus radiography and scanning laser acoustic microscopy are the NDE techniques highlighted in this review. The techniques were applied to research samples of sintered silicon nitride and silicon carbide in the form of modulus-of-rupture (MOR) bars. The strengths and limitations of the aforementioned techniques are given in terms of probability of detection for voids in green and sintered MOR bars. Voids for this purpose were introduced by seeding green ceramic bars and characterizing each void in terms of its size, shape, location, and nature before and after sintering. The effects of material density, microstructure, surface finish, thickness, void depth, and size characteristics on detectability are summarized. The review presented here is based on the work of Stanley Klima, Don Roth, George Baaklini, William Sanders, and James Kiser of Lewis Research Center, Cleveland, Ohio.

## FABRICATION OF MODULUS-OF-RUPTURE (MOR) BARS CONTAINING SEEDED INTERNAL VOIDS



### EXPERIMENTAL/ANALYTICAL

- SPECIALLY PREPARED MODULUS-OF-RUPTURE TYPE BARS WERE SYSTEMATICALLY SEEDED WITH CRITICAL SIZE VOIDS
- VOIDS RESULTED AFTER THE STYRENE DIVINYLBENZENE MICROSPHERES WERE DECOMPOSED IN THE GREEN CERAMICS AT 550° C
- POD STATISTICS WERE DETERMINED USING THE CUMULATIVE PROBABILITY FORMULA

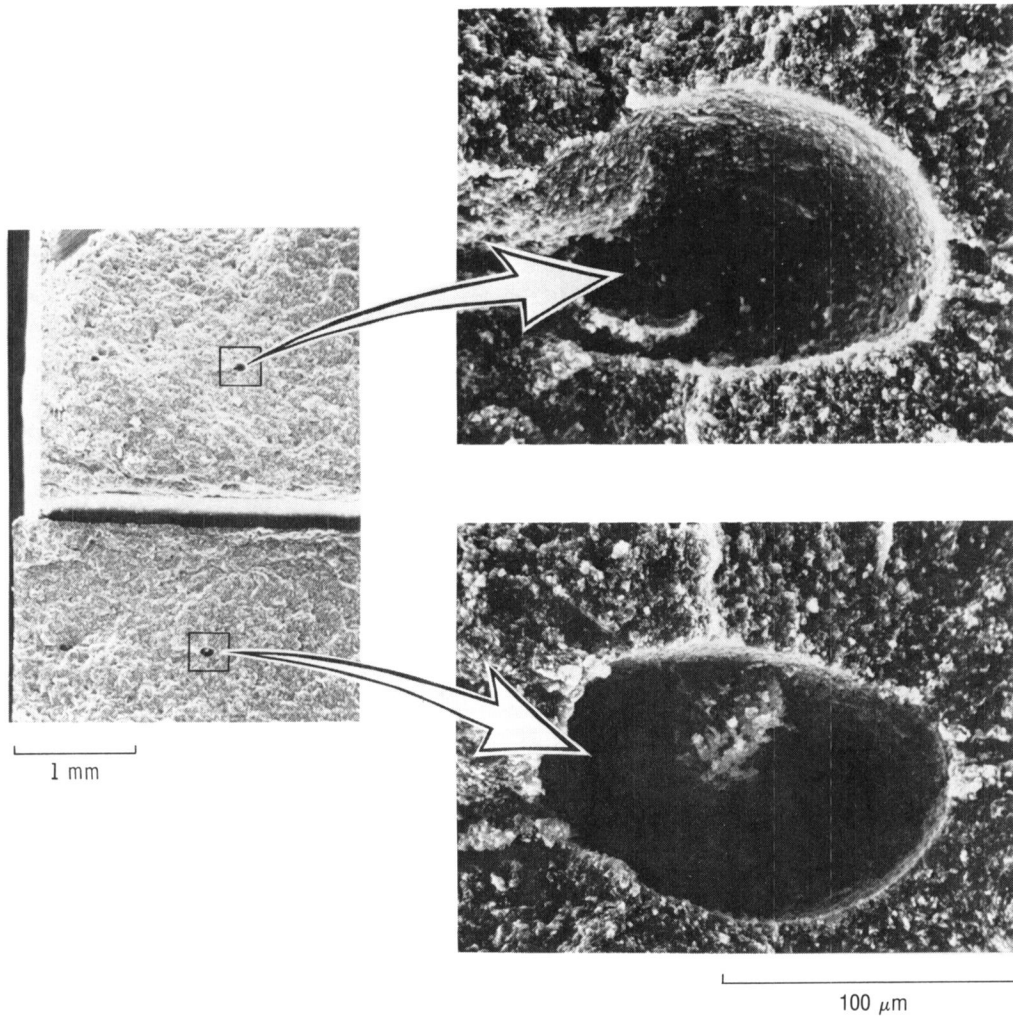
$$1 - G = \sum_{X=S}^N \frac{N!}{X! (N-X)!} P_L^X (1 - P_L)^{N-X}$$

WHERE  $P_L$  IS THE LOWER-BOUND PROBABILITY OF DETECTION,  $G$  IS THE CONFIDENCE LEVEL,  $N$  IS THE NUMBER OF VOIDS SEEDED, AND  $S$  IS THE NUMBER OF VOID DETECTED

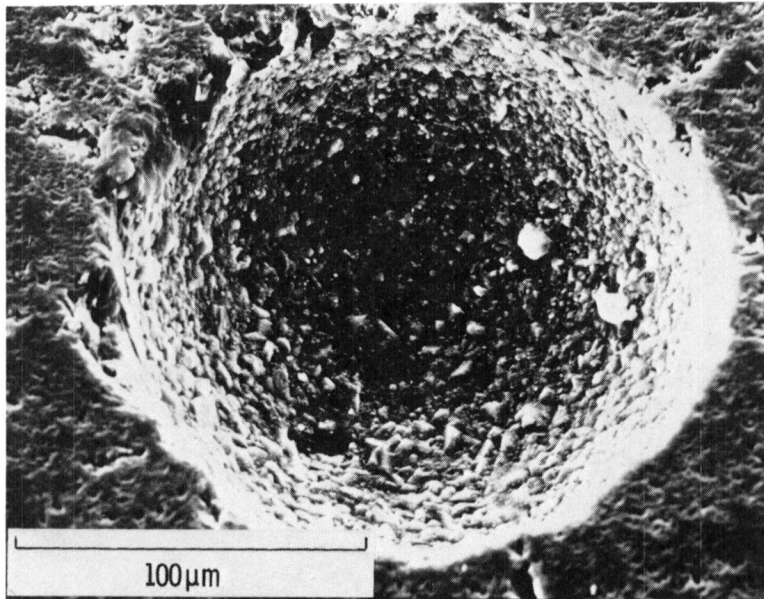
## DIMENSIONAL CHARACTERISTICS OF RESULTING INTERNAL VOIDS IN SINTERED MATERIALS

MATERIALS	SPECIMEN THICKNESS RANGE,	SPHERE diam, $\mu\text{m}$	NUMBER OF SPHERES SEEDED	RESULTING VOID DIMENSION			
				VOID DEPTH, $\mu\text{m}$		VOID DIAMETER, $\mu\text{m}$	
				MEAN	STANDARD DEVIATION	MEAN	STANDARD DEVIATION
$\text{Si}_3\text{N}_4$	2-7	80	69	20	4	25	6
		115	39	37	5	68	5
		200	31	133	17	139	8
		321	28	233	16	267	18
		528	21	307	14	386	15
SiC	2-7	50	50	32	3	58	3
		80	47	59	6	100	8
		115	68	77	10	131	8
		200	19	165	29	194	11
		321	39	297	19	307	15
		528	43	477	47	505	28

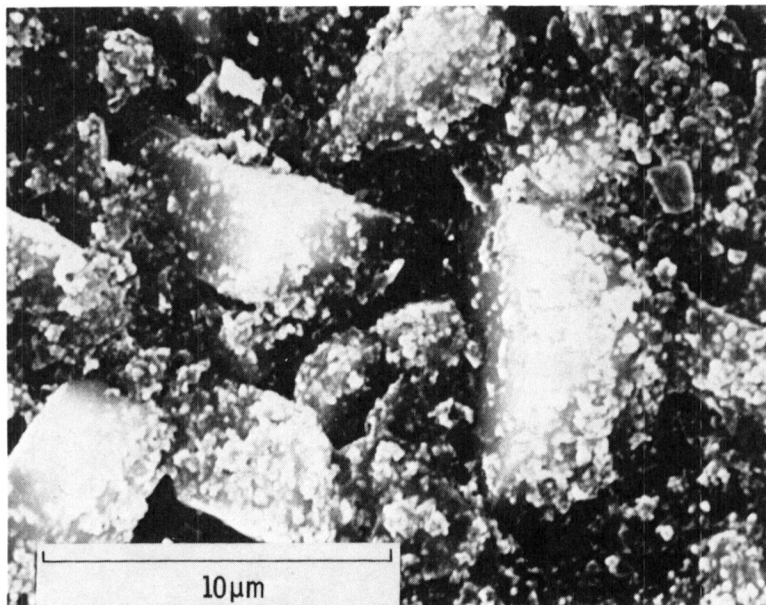
## SCANNING ELECTRON FRACTOGRAPHS SHOWING TYPICAL INTERNAL VOIDS IN GREEN SiC BARS



# SCANNING ELECTRON MICROGRAPHS OF A TYPICAL VOID IN SINTERED SiC BARS

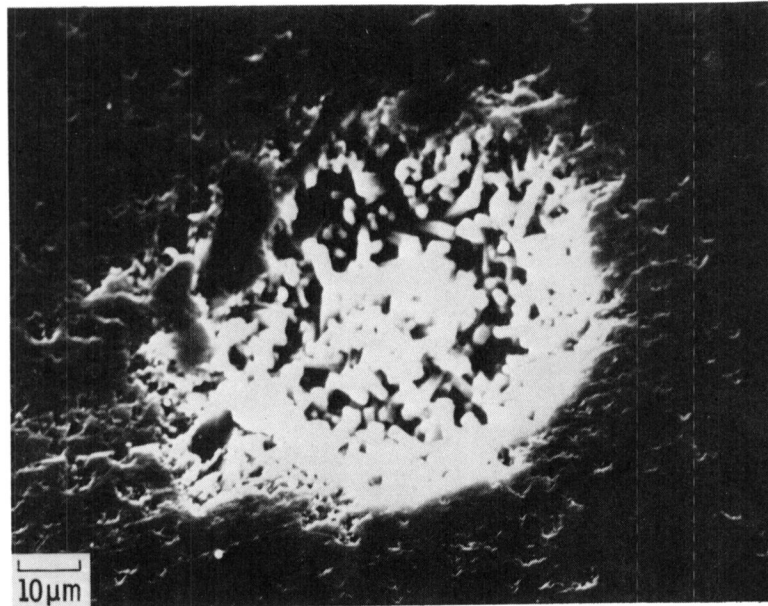


AS EXPOSED TO SURFACE

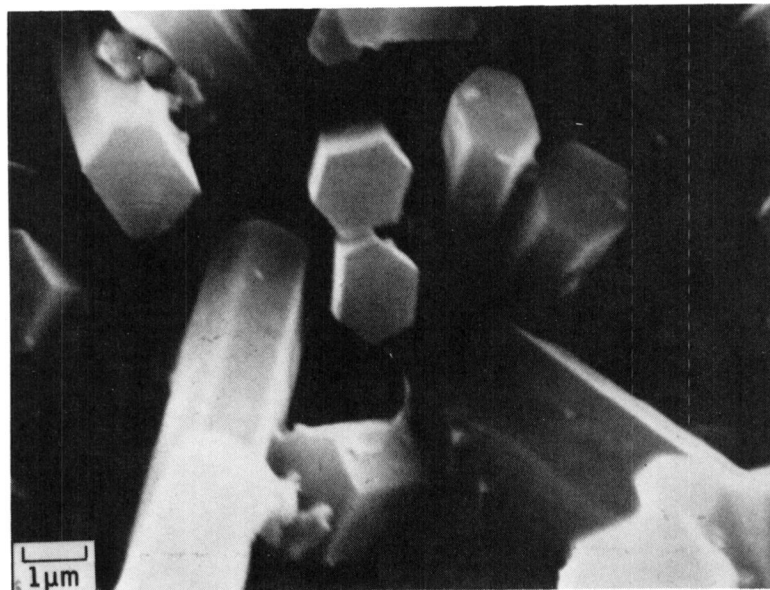


TEXTURE OF THE CAVITY-WALL-SURFACE

## SCANNING ELECTRON MICROGRAPHS OF TYPE A INTERNAL VOIDS IN SINTERED $\text{Si}_3\text{N}_4$

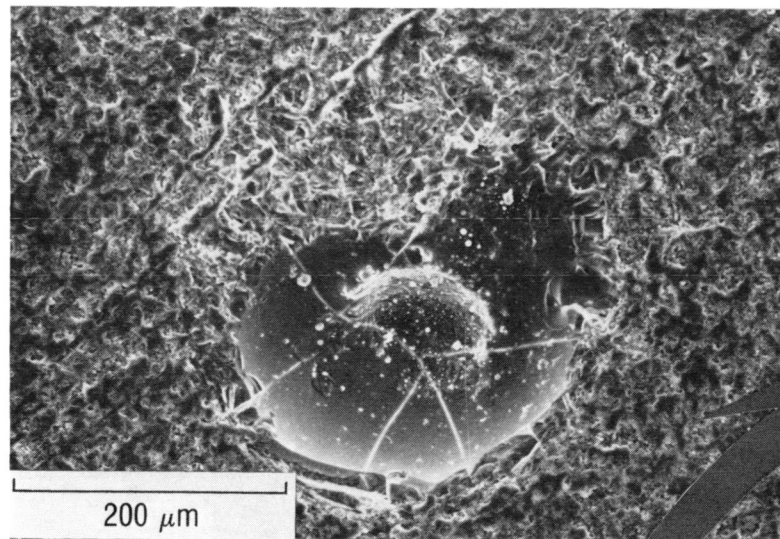


AS EXPOSED TO SURFACE

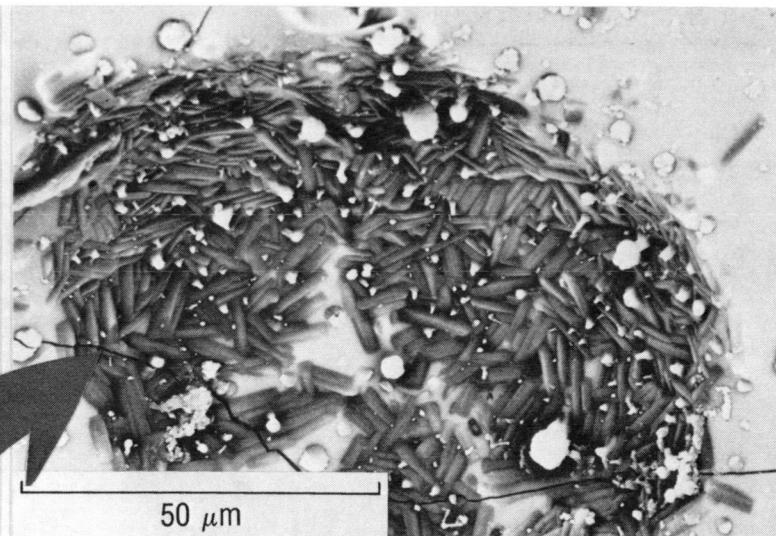


CLUSTERS OF GRAINS PROJECTING FROM THE CAVITY WALLS

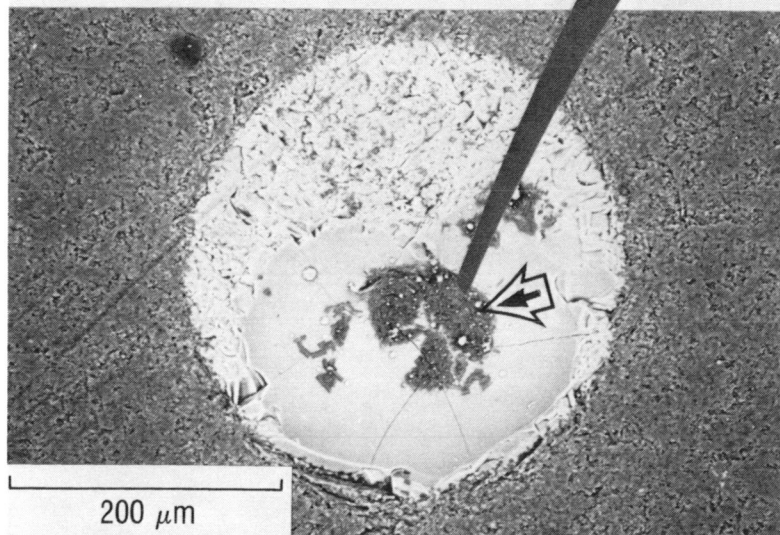
# SCANNING ELECTRON MICROGRAPHS OF TYPE B INTERNAL VOIDS IN SINTERED $\text{Si}_3\text{N}_4$



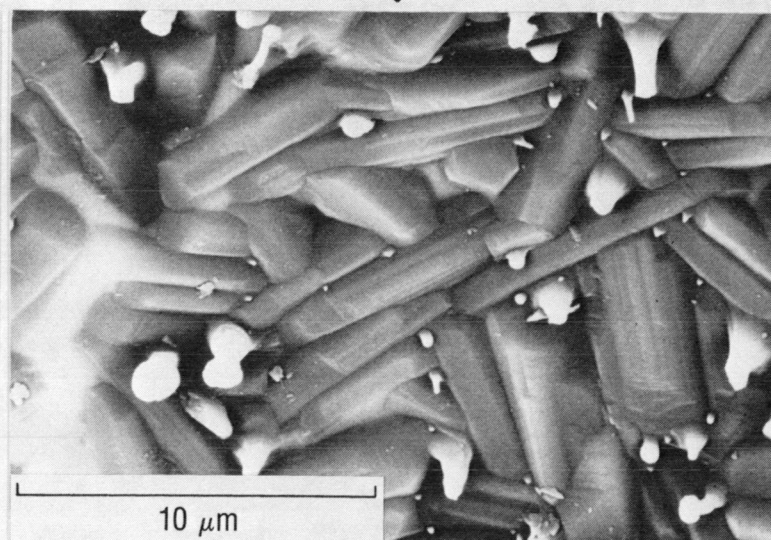
AS EXPOSED TO SURFACE



BACKSCATTERED ELECTRON IMAGE AT MODERATE  
MAGNIFICATION

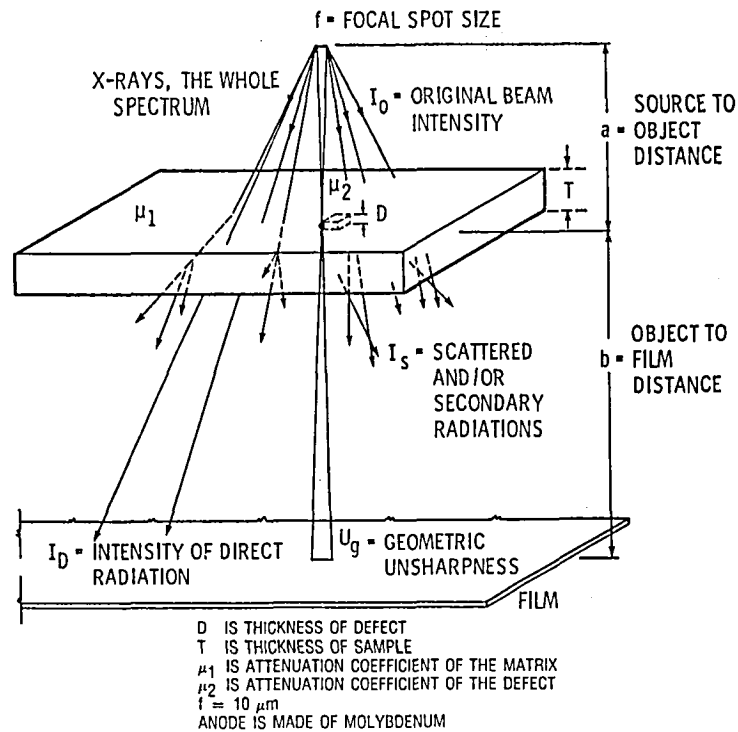


BACKSCATTERED ELECTRON IMAGE



BACKSCATTERED ELECTRON IMAGE AT HIGH MAGNIFICATION

## A SCHEMATIC CONFIGURATION OF MICROFOCUS PROJECTION RADIOGRAPHY



## MICROFOCUS RADIOGRAPHY

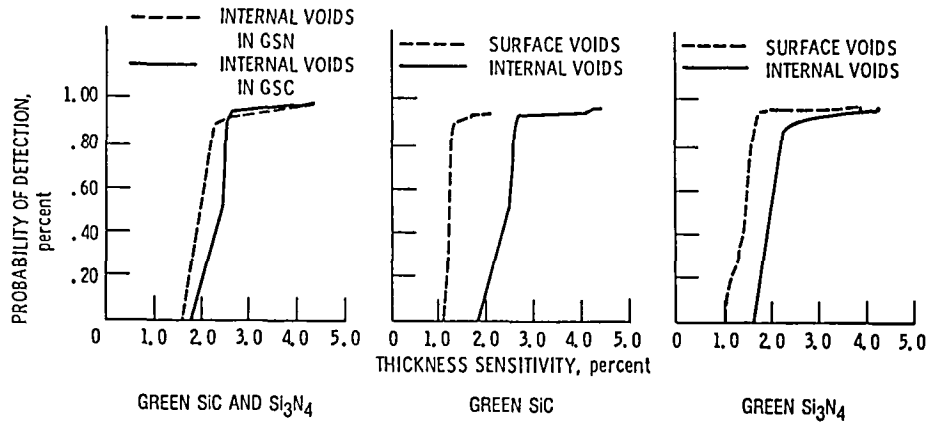
### SUMMARY OF POD STATISTICS FOR INTERNAL AND SURFACE VOIDS IN GREEN AND SINTERED SiC AND Si<sub>3</sub>N<sub>4</sub>

MATERIALS		OPTIMUM SENSITIVITY AT 90/95 POD/CL • (GIVEN AS PERCENT OF SAMPLE THICKNESS)	
		INTERNAL VOIDS	SURFACE VOIDS
SiC	GREEN	2.6	1.4
	SINTERED	1.5	1.7
Si <sub>3</sub> N <sub>4</sub>	GREEN	2.4	1.5
	SINTERED	0.6	1.5

- 90/95 POD/CL (PROBABILITY OF DETECTION/CONFIDENCE LEVEL) MEANS THAT THERE IS A 5% PROBABILITY THAT THE 90% IS AN OVERESTIMATE OF THE PROBABILITY OF DETECTION

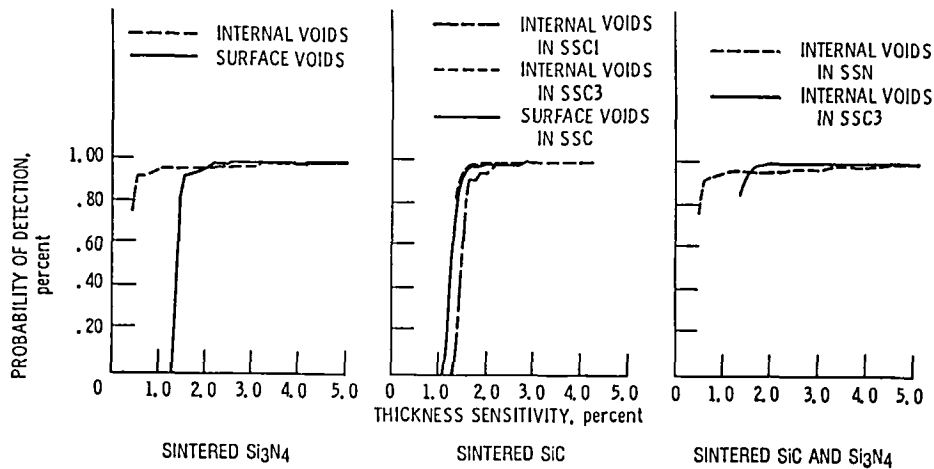


# **LOWER BOUND PROBABILITY OF DETECTION OF SURFACE AND INTERNAL VOIDS IN GREEN ISOPRESSED SiC (GSC) AND Si<sub>3</sub>N<sub>4</sub> (GSN) BARS**



- POD CURVES WERE CALCULATED AT 95 PERCENT CONFIDENCE LEVEL
- THICKNESS SENSITIVITY % = 100 (VOID DIMENSION IN X-RAY BEAM DIRECTION)/  
(THICKNESS OF SPECIMEN IN SAME DIRECTION)

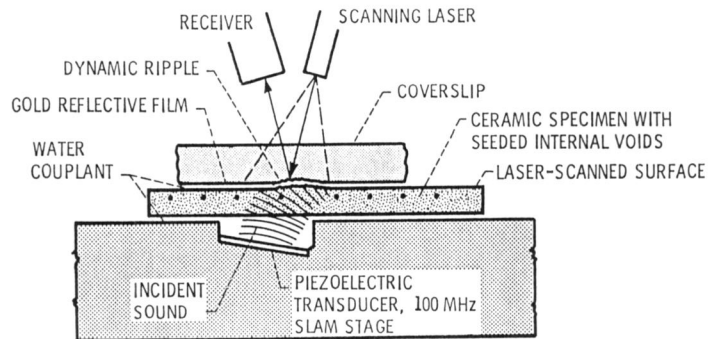
# **LOWER BOUND PROBABILITY OF DETECTION OF SURFACE AND INTERNAL VOIDS IN SINTERED SiC (SSC) AND Si<sub>3</sub>N<sub>4</sub> (SSN) BARS**



- POD CURVES WERE CALCULATED AT 95 PERCENT CONFIDENCE LEVEL
- THICKNESS SENSITIVITY % = 100 (VOID DIMENSION IN X-RAY BEAM DIRECTION)/(THICKNESS OF SPECIMEN IN SAME DIRECTION)

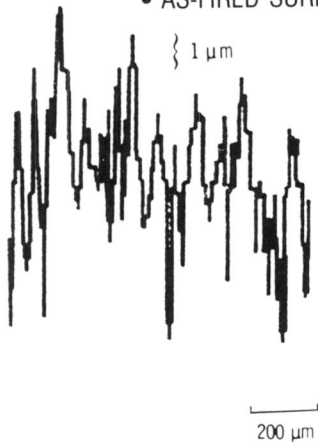


# SCHEMATIC ILLUSTRATION OF THE SCANNING LASER ACOUSTIC MICROSCOPE

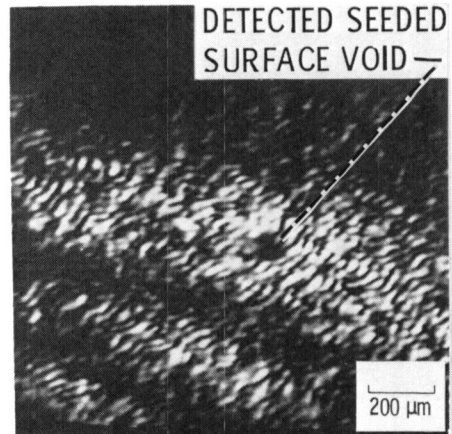


## EFFECT OF SPECIMEN SURFACE CONDITION ON SLAM IMAGE CLARITY

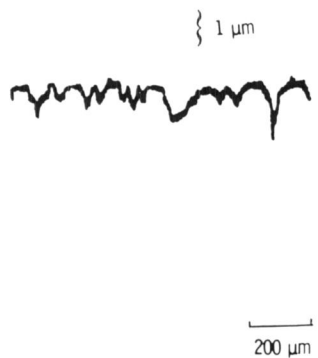
- AS-FIRED SURFACE PRODUCES A HIGHER BACKGROUND NOISE LEVEL



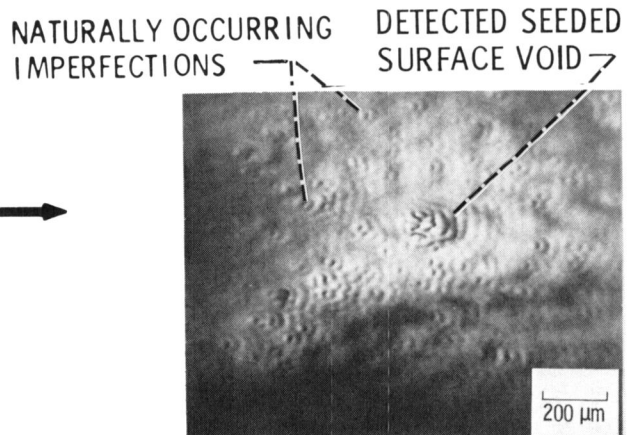
AS-FIRED SURFACE PROFILE.



ACOUSTIC MICROGRAPH OF AS-FIRED SPECIMEN.

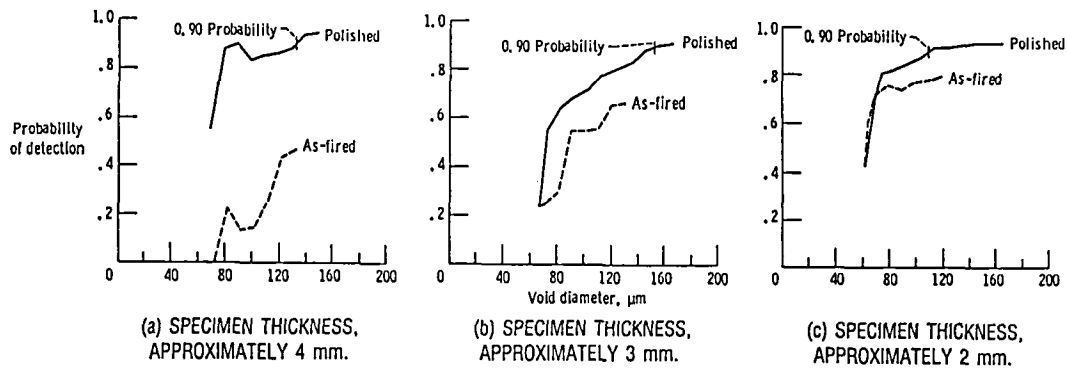


HAND-POLISHED SURFACE PROFILE.



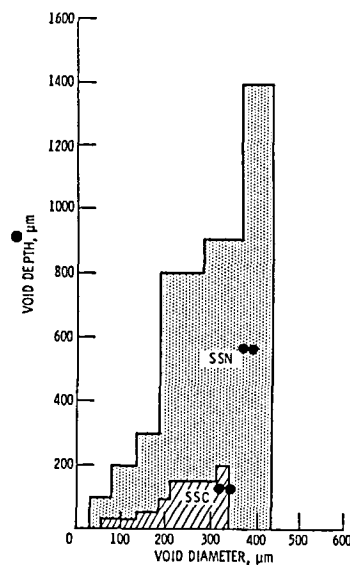
ACOUSTIC MICROGRAPH OF HAND-POLISHED SPECIMEN.

## EFFECT OF SURFACE FINISH AND SPECIMEN THICKNESS ON DETECTION OF VOIDS IN SSN



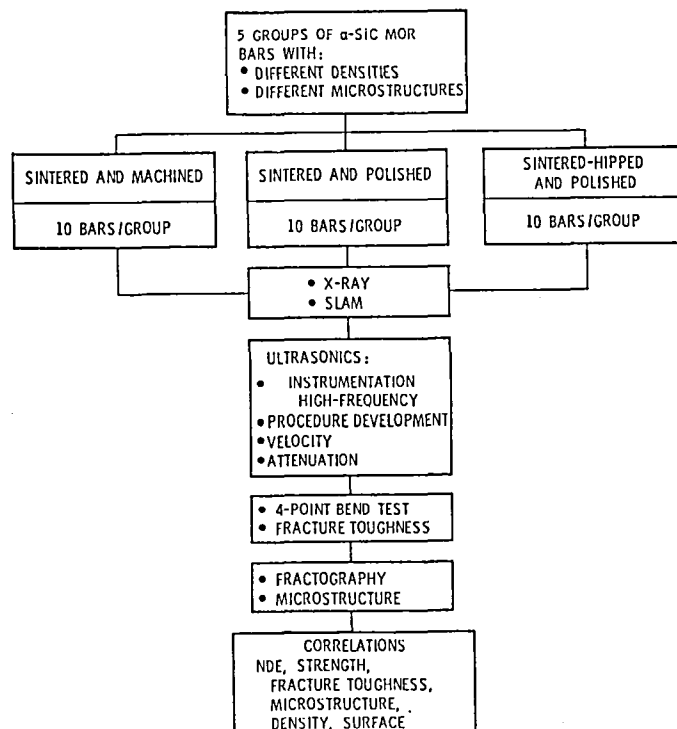
## EFFECT OF VOID DIAMETER, VOID DEPTH, AND MATRIX MATERIAL ON PROBABILITY OF DETECTION BY SLAM

90% PROBABILITY OF DETECTION AT 95% CONFIDENCE LIMIT



- DEPTH BELOW WHICH A VOID WITH A SPECIFIED DIAMETER CANNOT BE DETECTED AT  $\text{POD/CL} = 90/95$
- DETECTABILITY OF SMALLER, DEEPER VOIDS IN SSN MAY BE ATTRIBUTABLE TO FINER GRAINS AND GREATER DENSITY (SSN AT  $> 99\%$  VS SSC AT  $\sim 97\%$  THEORETICAL DENSITY)

## NDE FOR CHARACTERIZING CERAMIC MICROSTRUCTURES



ASSESSMENT OF FRACTURE ORIGINS FOR NASA 6Y SINTERED  $\text{Si}_3\text{N}_4$

			SUB-SURFACE PORE	SURFACE PORE	SEAM	SUB-SURFACE AGGLOMERATE	COLUMNAR GRAIN	SURFACE DEFECT	METALLIC INCLUSION
R. T. FLEXURE TEST	TOTAL FRACTURE ORIGINS IDENTIFIED	192 <sup>a</sup>	56	44	28	25	17	13	9
	PERCENT OF TOTAL	100	29	23	14	13	9	7	5
1200 °C FLEXURE TEST	TOTAL FRACTURE ORIGINS IDENTIFIED	90 <sup>a</sup>	23	19	9	7	14	0	18
	PERCENT OF TOTAL	100	26	21	10	8	15	0	20
1370 °C FLEXURE TEST	TOTAL FRACTURE ORIGINS IDENTIFIED	127 <sup>a</sup>	30	15	25	3	32	0	22
	PERCENT OF TOTAL	100	24	12	20	2	25	0	17

<sup>a</sup>NUMBER EXCLUDES 111, 47, AND 41 BARS FOR R.T., 1200 °C, AND 1370 °C, RESPECTIVELY, WHERE FLAW REGION OR FLAW TYPE COULD NOT BE DETERMINED.

## **SUMMARY**

### **SCANNING LASER ACOUSTIC MICROSCOPY**

**VOID DETECTABILITY WAS AFFECTED BY MATERIAL, MICROSTRUCTURE, SURFACE FINISH, SPECIMEN THICKNESS, VOID DEPTH, AND VOID SIZE.**

- **VOIDS WERE MORE EASILY DETECTED IN SINTERED SILICON NITRIDE (SSN) THAN IN SINTERED SILICON CARBIDE (SSC). SSN GRAIN SIZE WAS AN ORDER OF MAGNITUDE SMALLER THAN IN SSC.**
- **VOID DETECTABILITY WAS SIGNIFICANTLY IMPROVED BY SURFACE GRINDING. IN SPECIMENS WITH AS-FIRED SURFACES, 0.90/0.95 POD/CL WAS NOT ACHIEVED FOR ANY VOID SIZE UP TO 160  $\mu\text{m}$ .**
- **LITTLE OR NO THICKNESS EFFECT ON DETECTABILITY WAS OBSERVED IN SPECIMENS WITH GROUND SURFACES. IN SPECIMENS WITH AS-FIRED SURFACES, DETECTABILITY IMPROVED WITH DECREASING THICKNESS.**

### **MICROFOCUS X-RAY RADIOGRAPHY**

**DETECTABILITY OF VOIDS WAS AFFECTED BY PHOTON ENERGY LEVEL, MATERIAL COMPOSITION IN THE VICINITY OF THE VOID, DENSITY VARIATIONS, SAMPLE THICKNESS AND VOID SIZE.**

- **LOW PHOTON ENERGY LEVELS ( $\leq 20$  KeV) PRODUCED BETTER RADIOGRAPHIC FILM CONTRAST AND HENCE BETTER VOID DETECTABILITY THAN HIGHER ENERGY LEVELS.**
- **YITTRIUM MIGRATING TO THE WALLS OF SEEDED VOIDS AIDED DETECTION OF SOME BUT NOT ALL VOIDS IN SSN. YITTRIA SINTERING AID WAS THE SOURCE.**
- **DETECTABILITY OF VOIDS DID NOT APPEAR TO BE ADVERSELY AFFECTED BY AS-FIRED SURFACES RELATIVE TO DIAMOND GROUND SURFACES.**
- **THE THRESHOLD LEVEL OF DETECTION OF VOIDS WAS 1.5 PERCENT OF SPECIMEN THICKNESS OR 50  $\mu\text{m}$ , WHICHEVER IS GREATER, WHEN THE 0.90/0.95 POD/CL CRITERIA WAS APPLIED.**

## FRACTURE MECHANICS

John L. Shannon, Jr.  
NASA Lewis Research Center  
Cleveland, Ohio 44135

The application of fracture mechanics to the design of ceramic structures will require the precise measurement of crack growth and fracture resistance of these materials over their entire range of anticipated service temperatures and standardized test methods for making such measurements. The development of a standard test for measuring the plane strain fracture toughness is the initial objective of our ceramics fracture mechanics program.

Current fracture tests make use of a variety of specimen types (single-edge-notched bend, double torsion, double cantilever bend, and surface flawed specimens) having either blunt notches produced by saw cutting, or cracks produced by wedge loading, indenting, or local thermal shock. Specimens with blunt notches can overestimate the fracture toughness. Precracked specimens are difficult to prepare in a reproducible manner, and the initial crack front often cannot be seen on the fracture surface after testing, which makes it impossible to measure the initial crack length. These difficulties can be circumvented by using a specimen containing a chevron notch in which a crack originates at the tip of the triangular ligament during the early stage of specimen loading. Specimens with a chevron notch were first used by Nakayama in fracture studies (ref. 1). Later they were used by Tattersall and Tappin for fracture surface energy measurements (ref. 2) and more recently, by Barker for plane strain fracture toughness measurements (ref. 3). The essential features of the chevron-notch specimen are that (1) a sharp natural crack is produced during the early stage of loading (no precracking is required) and (2) the load passes through a maximum at a constant material-independent crack length-to-width ratio for a specific specimen geometry (no post-test crack length measurement is required). For materials with flat crack growth resistance curves, the plane strain fracture toughness is proportional to the maximum test load and a function of the specimen geometry and elastic compliance.

Stress intensity factor coefficients have been determined for three varieties of chevron-notch specimens, and fracture toughness measurements have been made on silicon nitride, silicon carbide, and aluminum oxide to assess the performance of each specimen variety. It has been determined that silicon nitride and silicon carbide have flat crack growth resistance curves, but aluminum oxide does not. Additionally, batch-to-batch differences have been noticed for the aluminum oxide. Experiments are continuing to explain the rising crack growth resistance and batch-to-batch variations for the aluminum oxide.

## REFERENCES

1. Nakayama, J.: Direct Measurement of Fracture Energies of Brittle Heterogeneous Materials. J. Am. Ceram. Soc., vol. 48, no. 11, 1965, pp. 583-587.
2. Tattersall, H.G.; and Tappin, G.: The Work of Fracture and Its Measurement in Metals, Ceramics and other Materials. J. Mater. Sci., vol. 1, no. 3, 1966, pp. 296-301.
3. Barker, L.M.: A Simplified Method for Measuring Plane Strain Fracture Toughness. Eng. Fracture Mech., vol. 9, no. 2, 1977, pp. 361-369.

# PLANE STRAIN ELASTIC STRESS FIELD IN VICINITY OF CRACK TIP

$$\sigma_x = \frac{K_I}{(2\pi r)^{1/2}} \cos \frac{\theta}{2} \left( 1 - \sin \frac{\theta}{2} \sin \frac{3\theta}{2} \right) + \dots$$

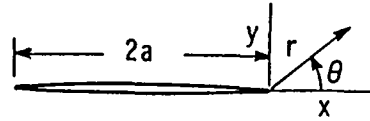
$$\sigma_y = \frac{K_I}{(2\pi r)^{1/2}} \cos \frac{\theta}{2} \left( 1 + \sin \frac{\theta}{2} \sin \frac{3\theta}{2} \right) + \dots$$

$$\tau_{xy} = \frac{K_I}{(2\pi r)^{1/2}} \sin \frac{\theta}{2} \cos \frac{\theta}{2} \cos \frac{3\theta}{2} + \dots$$

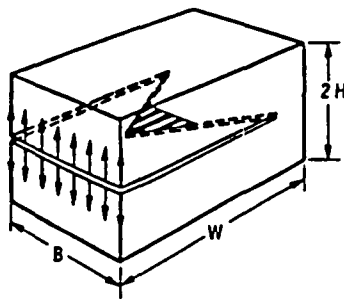
$$\sigma_z = \nu(\sigma_x + \sigma_y); \tau_{xz} = \tau_{yz} = 0$$

$K_I$  IS THE "STRESS INTENSITY FACTOR"

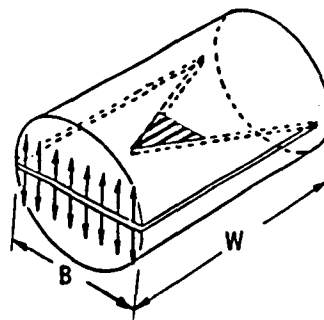
$K_{Ic}$  IS THE "FRACTURE TOUGHNESS"



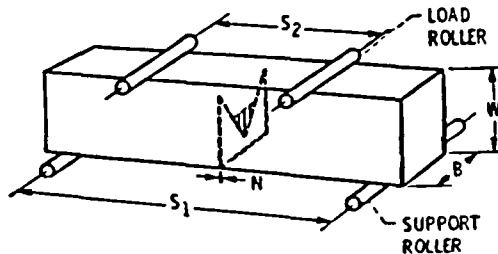
## CHEVRON-NOTCH SPECIMENS



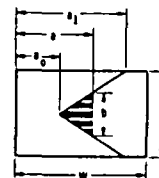
SHORT BAR



SHORT ROD



FOUR-POINT BEND



CRACK PLANE  
SECTION

# THEORETICAL BASIS FOR CHEVRON-NOTCH SPECIMEN $K_{Ic}$ MEASUREMENT

AVAILABLE ENERGY FOR EXTENSION OF CRACK BY  $\Delta a$ :

$$\Delta U = \frac{p^2}{2W} \cdot \frac{dC_{tr}}{da} \cdot \Delta a$$

NECESSARY ENERGY FOR EXTENSION OF CRACK BY  $\Delta a$ :

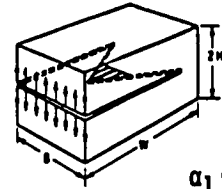
$$\Delta \bar{W} = G_{Ic} \cdot b \cdot \Delta a = \frac{K_{Ic}^2}{E} \cdot b \cdot \Delta a$$

DURING CRACK EXTENSION  $\Delta U = \Delta \bar{W}$ , AND:

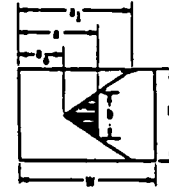
$$K_{Ic} = P \left[ \frac{E}{2bW} \frac{dC_{tr}}{da} \right]^{1/2}$$

$$\text{AND SINCE } b = B \left[ \frac{a - a_0}{a_1 - a_0} \right] = B \left[ \frac{\alpha - \alpha_0}{\alpha_1 - \alpha_0} \right]$$

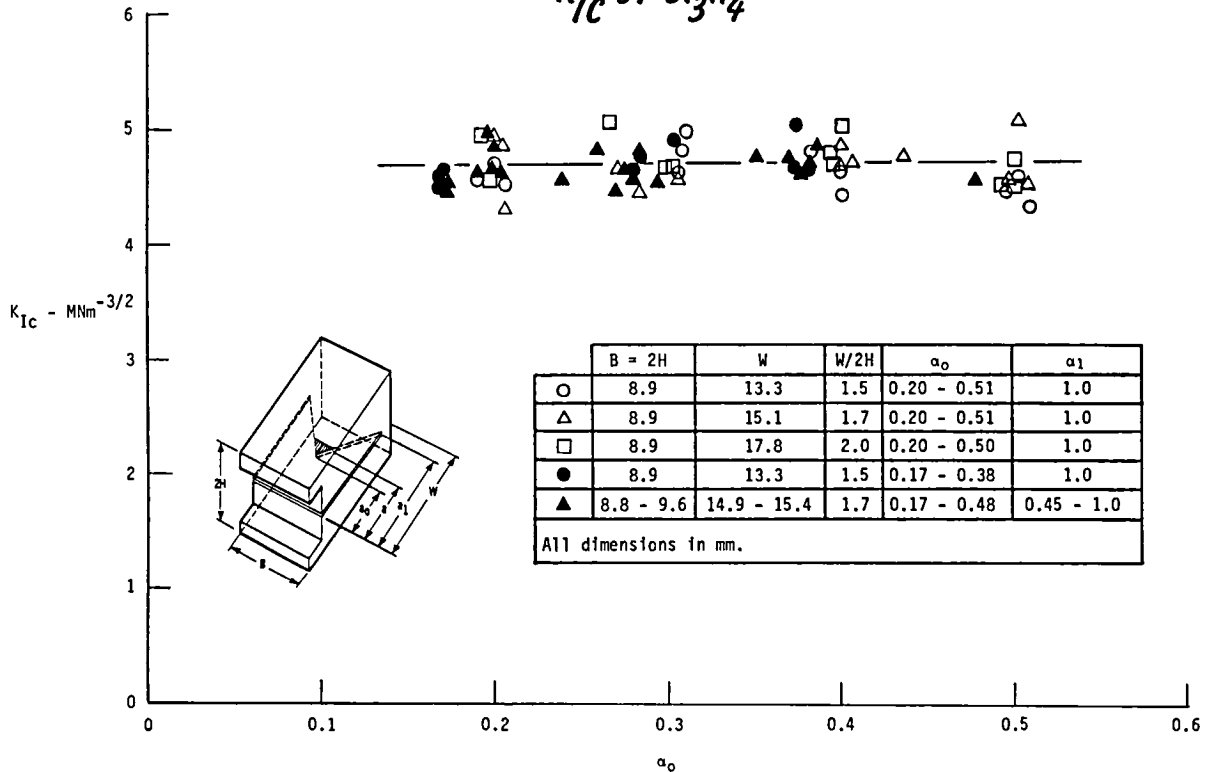
$$K_{Ic} = P \left[ \frac{E}{2WB \left( \frac{\alpha - \alpha_0}{\alpha_1 - \alpha_0} \right)} \frac{dC_{tr}}{da} \right]^{1/2} = \frac{P}{B\sqrt{W}} \left[ \frac{EB}{2} \frac{dC_{tr}}{da} \left( \frac{\alpha_1 - \alpha_0}{\alpha - \alpha_0} \right) \right]^{1/2} = \frac{P}{B\sqrt{W}} Y^*$$



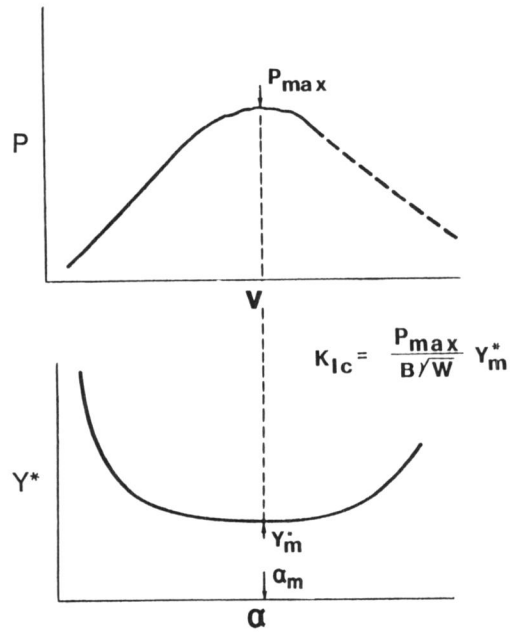
$$\begin{aligned} \alpha_1 &= a_1/W \\ \alpha &= a/W \\ \alpha_0 &= a_0/W \end{aligned}$$



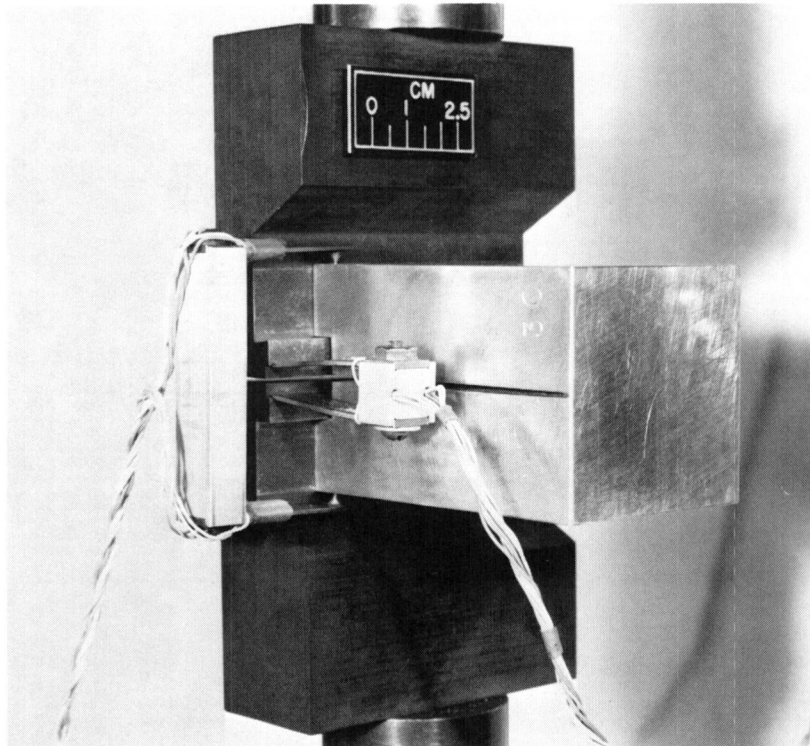
## $K_{Ic}$ OF $Si_3N_4$



*CHEVRON-NOTCH SPECIMEN  $K_{Ic}$  FROM  $P_{max}$  AND  $Y_m^*$*

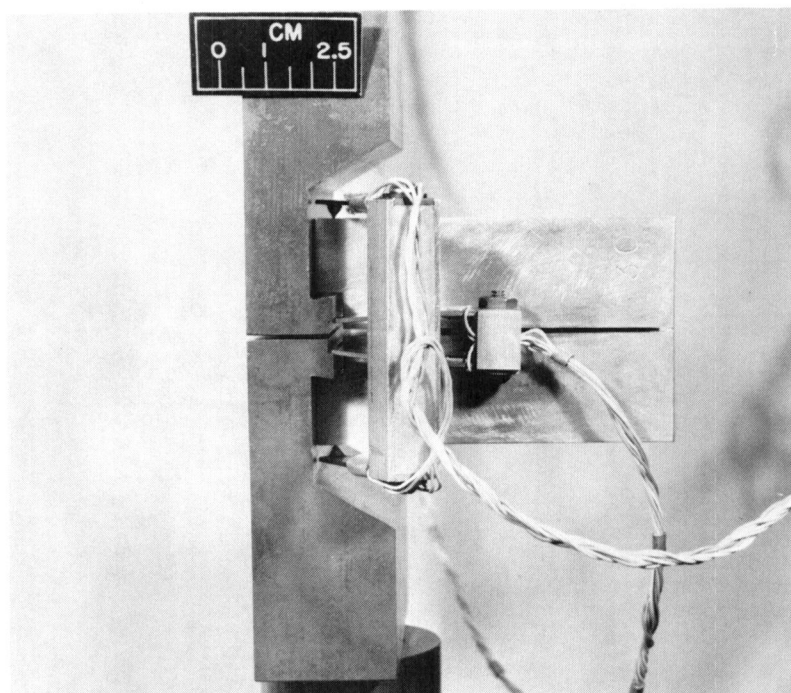


***CHEVRON-NOTCH SPECIMEN K CALIBRATION SETUP***

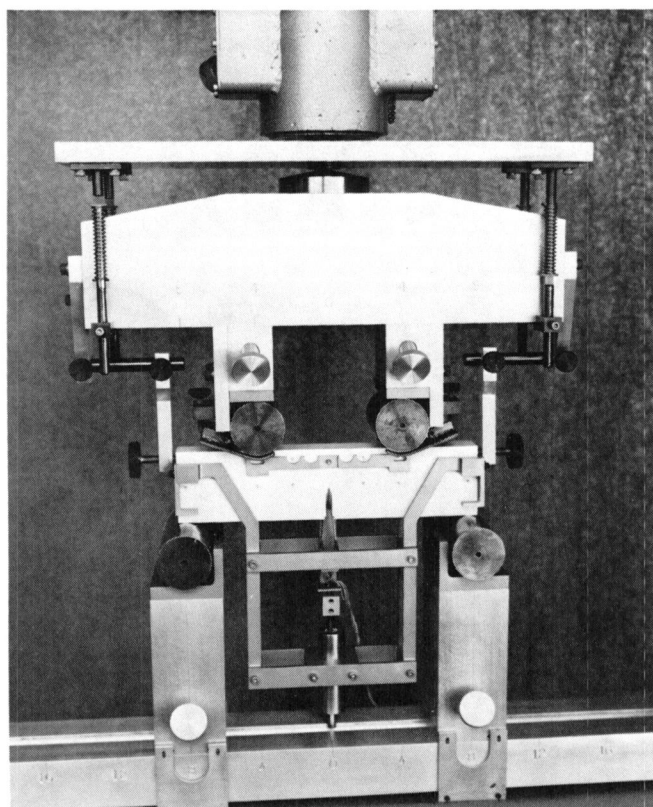




***CHEVRON-NOTCH SPECIMEN K CALIBRATION SETUP***



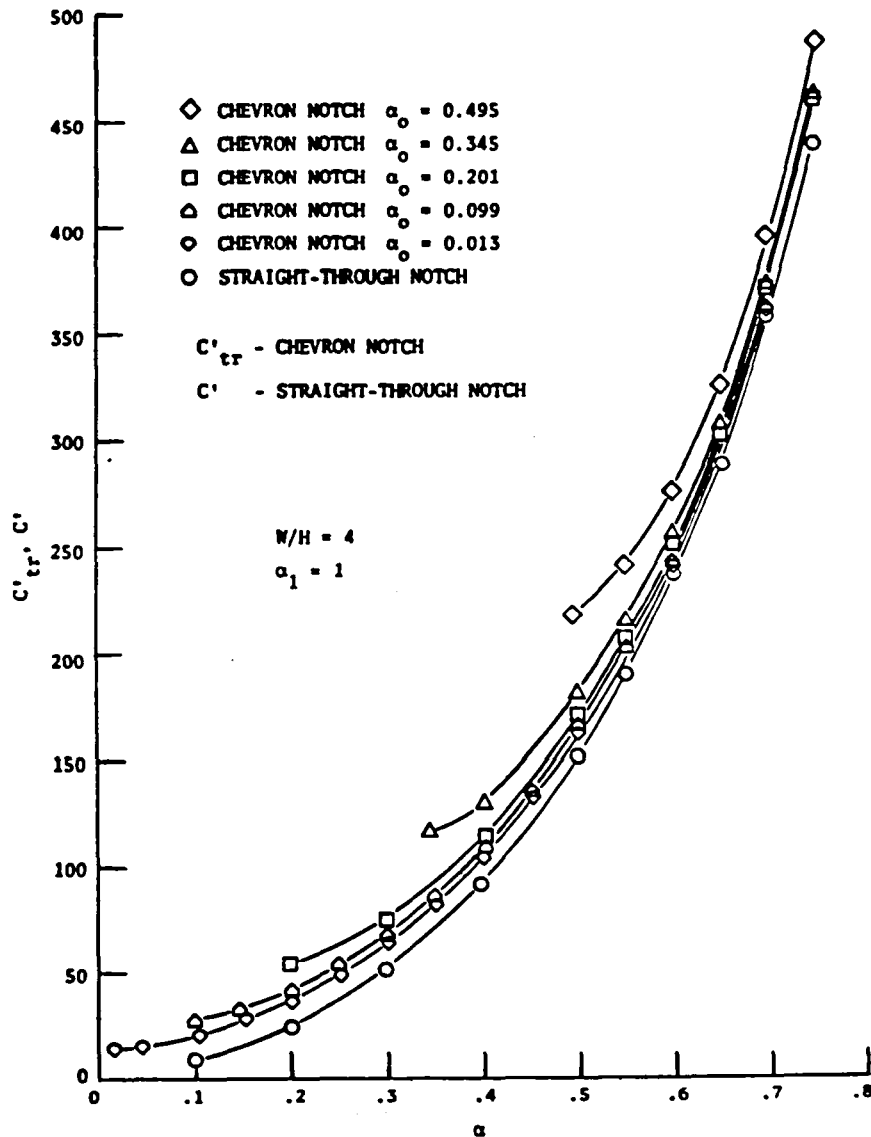
***CHEVRON-NOTCH SPECIMEN K CALIBRATION SETUP***



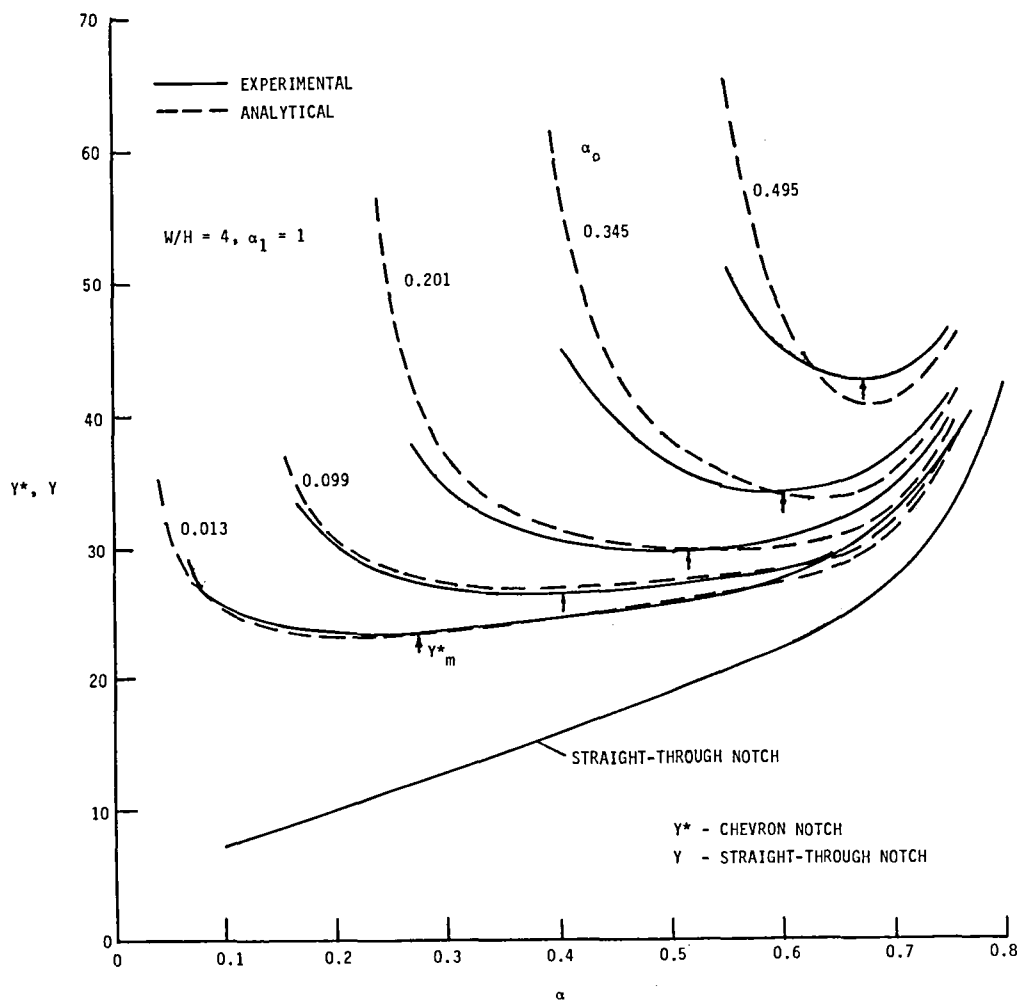
*CHEVRON-NOTCH SPECIMEN K CALIBRATION SETUP*

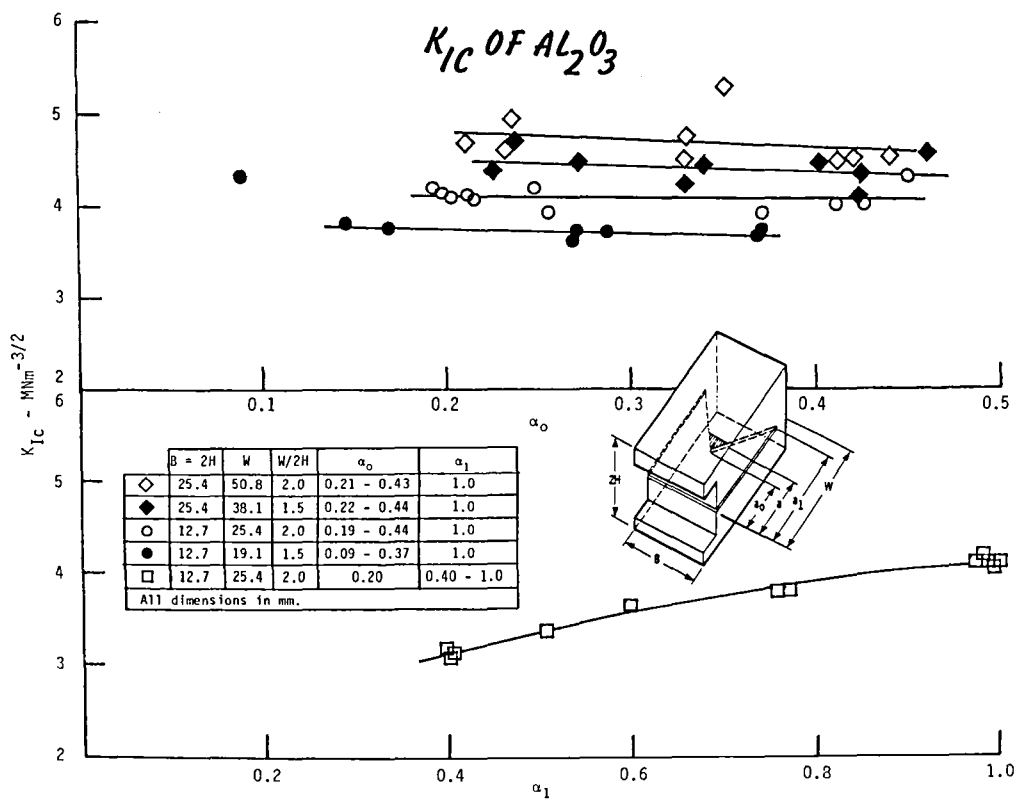
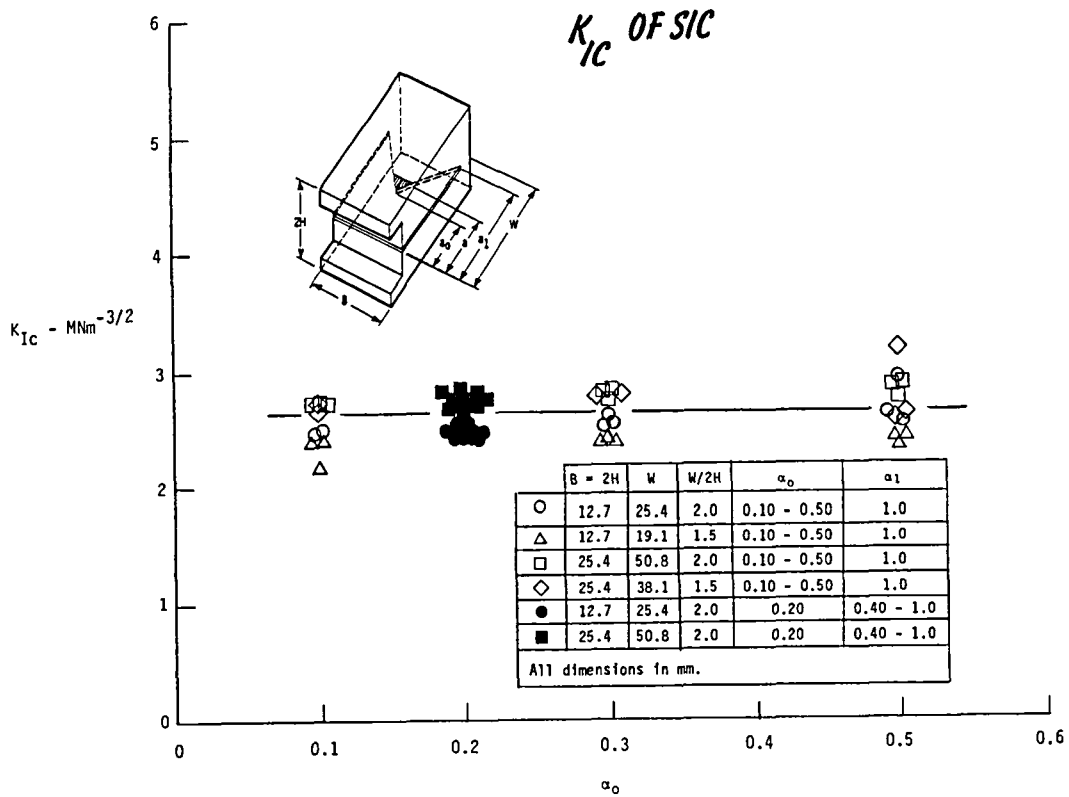


# CHEVRON-NOTCH SHORT BAR SPECIMEN DIMENSIONLESS COMPLIANCE



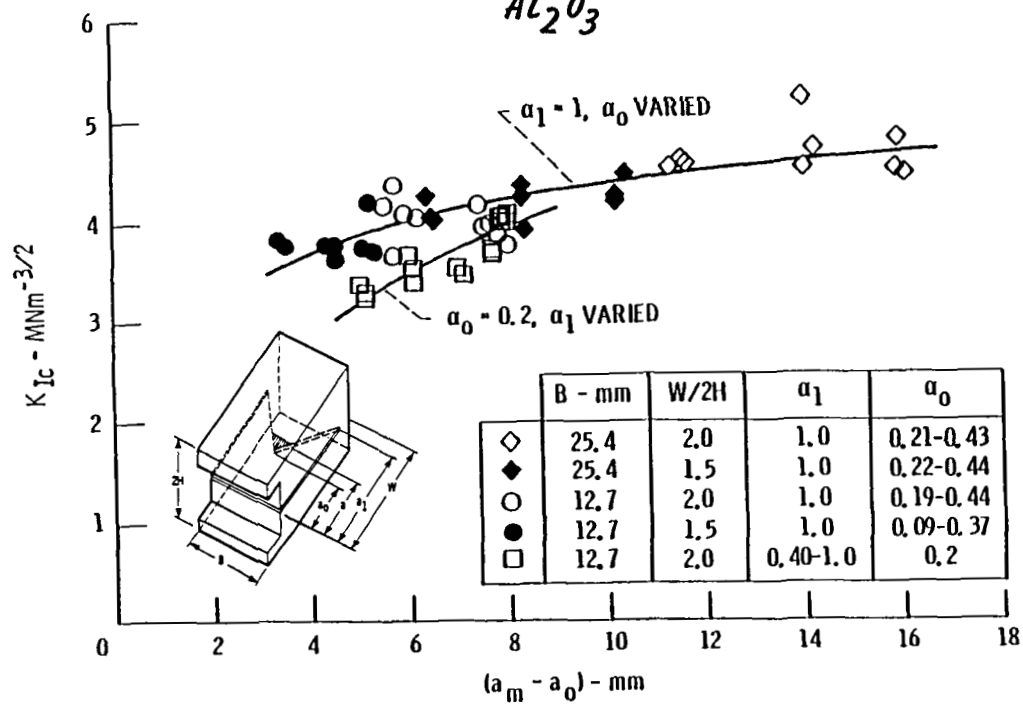
# CHEVRON-NOTCH SHORT BAR SPECIMEN STRESS INTENSITY FACTOR COEFFICIENTS



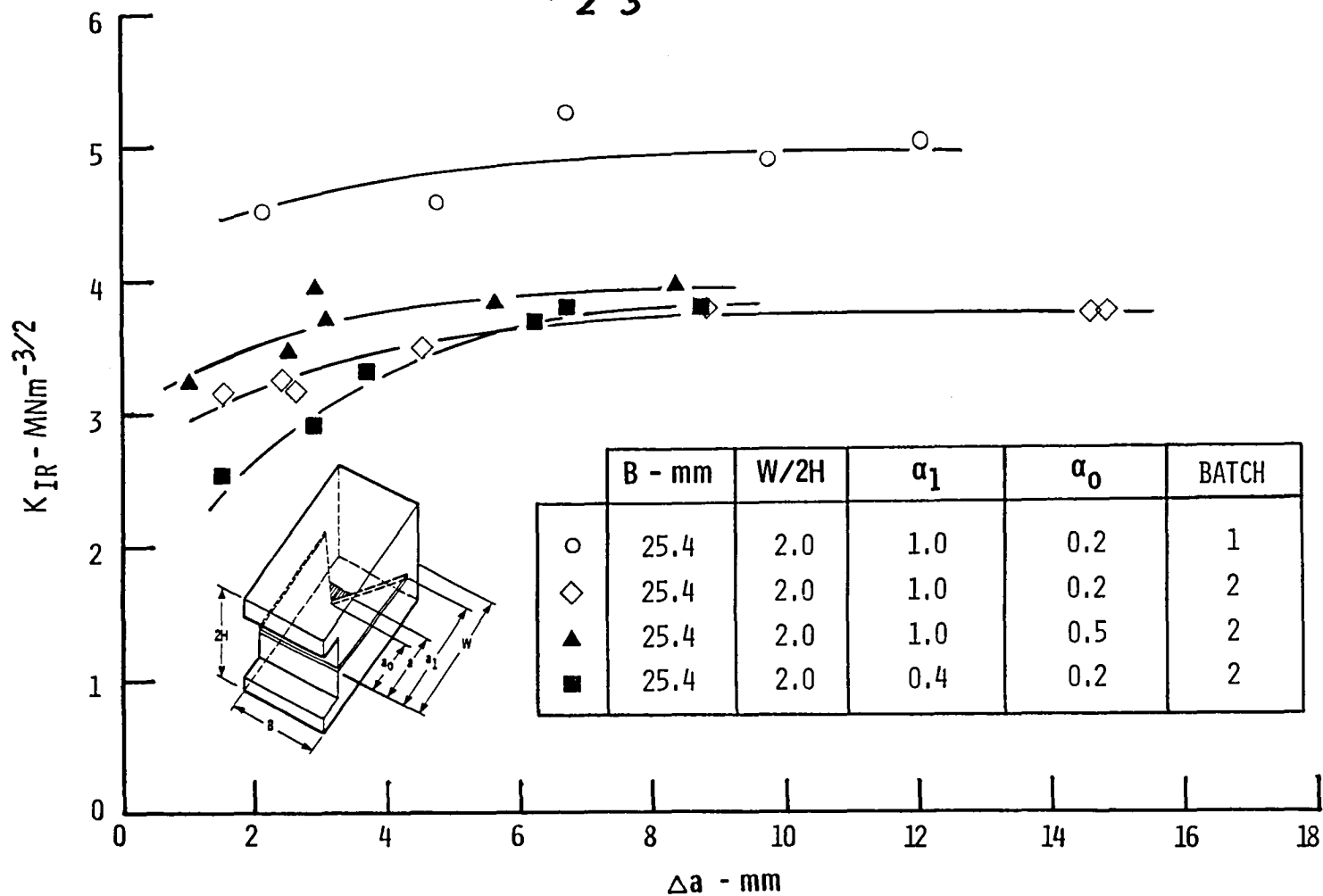


# VARIATION IN $K_{IC}$ WITH CRACK EXTENSION TO $P_{MAX}$

$Al_2O_3$



# $Al_2O_3$ R-CURVES







## STRUCTURAL CERAMICS RESEARCH

J.I. Mueller, R.J.H. Bollard, and R.C. Bradt  
University of Washington  
Seattle, Washington

### OUTLINE

CERAMIC RESEARCH AT U. OF W.

BRITTLE MATERIALS DESIGN PROGRAM

NASA PROGRAM RESEARCH AT U. OF W.

## **STRUCTURAL CERAMIC RESEARCH at U. of W.**

AKSAY, I.	MSE	powder processing, sintering
BERG, J.	ChE	colloidal studies
BJORKSTAM, J.	EE	NDE/NDT
BOLLARD, R.J.H.	AA	evaluation, design
BRADT, R.	MSE	mechanical properties
DASH, G.	PHY	thermal conditions
EMERY, A.	ME	thermal stresses
FISCHBACH, D.	MSE	fiber composite, carbon
HARTZ, B.	CE	design
KIKUCHI, R.	MSE	theoretical modeling
KOBAYASHI, A.	ME	mechanical prop., dynamic fracture
LIN, K.	AA	elast. mechanical comp.
MILLER, A.	MSE	processing, environ. effects
RAMULU, M.	ME	dynamic fracture, machining
RAO, Y.	MSE	nitridation Si
REED, D.	CE	design
SARIKAYA, M.	MSE	characterization
SCOTT, W.	MSE	oxidation
STOEBE, T.	MSE	nitridation, defects
TAGGART, R.	ME	design
TAYA, M.	ME	comp. mechanics
WHITTEMORE, O.	MSE	processing

## **BRITTLE MATERIALS DESIGN PROGRAM (COURSE)**

BRITTLE MATERIALS

PROCESSING of CERAMICS

ELASTICITY

MECHANICAL CHARACTERIZATION

MICROSTRUCTURE/MECHANICAL PROPERTIES

ENGINEERING PROPERTIES of CERAMICS

STRENGTH and FAILURE THEORIES

NDE/NDT

DESIGN of COMPONENTS

LABORATORY (PP) COMPONENT MANUFACTURE

## **CURRENT NASA RESEARCH PROGRAM AT UW**

### **I. PROCESSING AND CHARACTERIZATION**

STOEBE - Lattice Defects in  $\text{Si}_3\text{N}_4$

RAO - Nitridation of Si

AKSAY - Powder Consolidation by Injection Molding

SCOTT - Oxidation Resistance of  $\text{Si}_3\text{N}_4$

### **II. MECHANICAL PROPERTIES**

MILLER - Environmental Effects on  $\text{Si}_3\text{N}_4$ , SiC

EMERY - Thermal Fracture

KOBAYASHI - Impact, Erosion, Dynamic Fracture

BOLLARD - Evaluation of Mechanical Tests

BRADT/REED - Micromechanical Stresses

### **PROPOSED 86/87 CERAMIC/COMPOSITES RESEARCH TOPICS**

AKSAY - POWDER PROCESSING

RAO - NITRIDATION

MILLER - COMPOSITE NITRIDATION

BERG - COLLOIDAL PROCESSING OF  
COMPOSITES

EMERY - THERMAL PROPERTIES

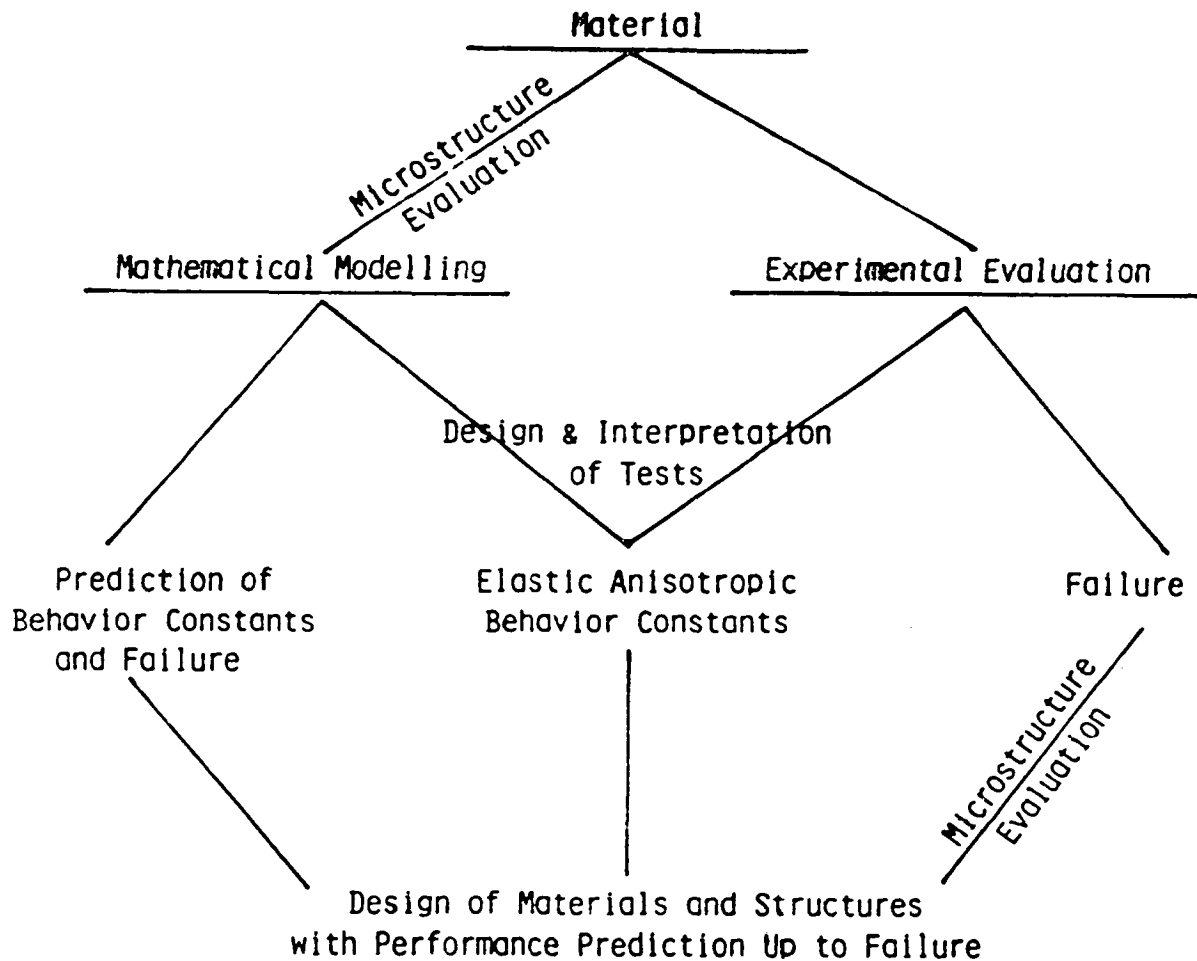
KOBAYASHI - DYNAMIC MECHANICAL  
PROPERTIES

TAYA - THERMAL CYCLING FATIGUE

BRADT/REED - ANISOTROPIC RESIDUAL  
STRESSES

BOLLARD - MECHANICAL CHARACTERIZATION

## COMPOSITE CHARACTERIZATION



## IMPROVED SILICON CARBIDE FOR ADVANCED HEAT ENGINES\*

Thomas J. Whalen and J.A. Mangels  
Ford Motor Company

This report describes work performed in the first year of the program conducted for NASA to develop silicon carbide materials of high strength and to form components of complex shape and high reliability. The approach has been to adapt a beta-SiC powder and binder system to the injection molding process and to develop procedures and process parameters capable of providing a sintered silicon carbide material with improved properties.

The initial effort has been to characterize the baseline precursor materials (beta silicon carbide powder and boron and carbon sintering aids), develop mixing and injection molding procedures for fabricating test bars, and characterize the properties of the sintered materials. Parallel studies of various mixing, dewaxing, and sintering procedures have been performed in order to distinguish process routes for improving material properties.

A total of 276 MOR bars of the baseline material have been molded, and 122 bars have been fully processed to a sinter density of approximately 95 percent. The material has a mean MOR room temperature strength of 43.3 ksi (299 mPa), a Weibull characteristic strength of 45.8 ksi (315 mPa) and a Weibull modulus of 8.0. Mean values of the MOR strengths at 1000 °C, 1200 °C and 1400 °C are 41.4 ksi, 43.2 ksi and 47.2 ksi, respectively. Strength controlling flaws in this material were found to consist of regions of high porosity and were attributed to agglomerates originating in the initial mixing procedures.

New fluid mixing techniques have been developed which significantly reduce flaw size and improve the strength of the material. Initial MOR tests indicate the strength of the fluid-mixed material exceeds the baseline property by more than 33 percent.

Plans for the development of the fluid-mixing process to reduce flaw size and increase density and the optimization of sinter-body microstructure to increase toughness of the silicon carbide materials will be reviewed.

Contributions to this program were made by the following.

Ford Motor Company: R. Govila, B.N. Juterbock, J.A. Mangels, V. Mindroiu, L.R. Reatherford, S.S. Shinozaki, W. Trela, T.J. Whalen, R.M. Williams, and W.L. Winterbottom

NASA: S. Levine and N. Shaw

---

\*Work performed under NASA Contract No. NAS3-24384

## **FIRST YEAR REVIEW**

**T. J. Whalen**

**J. A. Mangels**

**May 21, 1986**

### **OBJECTIVE :**

**Develop High Strength, High Reliability Silicon Carbide Parts Having Complex Shapes by a Method Adaptable to Mass Production on an Economically Sound Basis.**

### **APPROACH :**

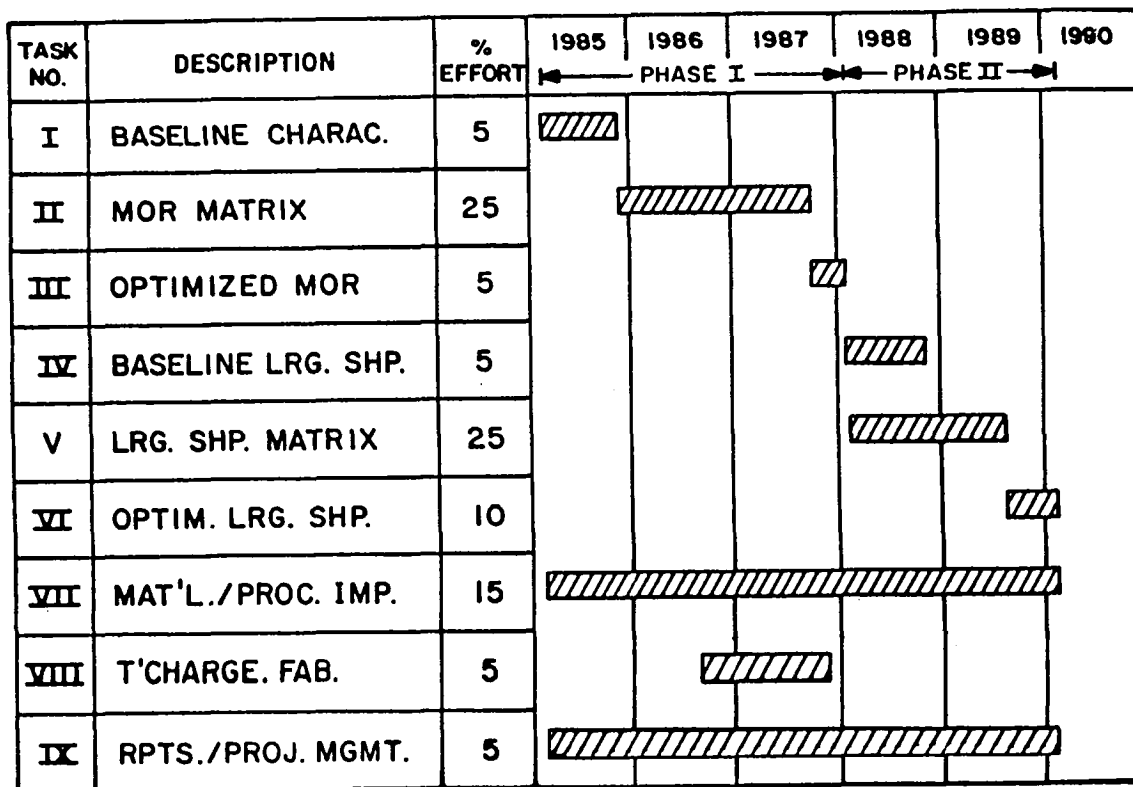
**Adapt Powder and Binder System to Injection Molding Process and Develop Procedures and Optimize Process Parameters Leading to a Sintered Silicon Carbide Material with Improved Properties.**

### **BENEFITS :**

**Silicon Carbide Parts for Advanced Gas Turbines and Other Heat Engines Would Permit Higher Temperature Operation with Resulting Fuel Efficiencies.**

### **START / FINISH :**

**February, 1985 to February, 1988**



Timing Chart

# OUTLINE

## TASK I

T. J. WHALEN

- \* BASELINE POWDERS CHARACTERIZATION
- \* BASELINE COMPOSITION SELECTION
- \* BASELINE RESULTS

## TASK VII AND PLANS

J. A. MANGELS

- \* PROCESSING AND COMPOSITION IMPROVEMENTS
- \* PLANNING

# TASK I

## BASELINE CHARACTERIZATION

### POWDERS

#### CHEMICAL ANALYSIS - BASELINE MATERIAL

ELEMENT	UF-SiC	BORON	CARBON
C	30.4 <sup>*</sup>	0.36	98.6
O	0.85	1.71	1.12
Al	0.046	0.040	
Fe	0.043	0.17	<0.005
Ca	0.019	0.046	
Mg	0.015	0.55	
Ti	0.005	0.047	
Zr	0.005		
S			0.25

<sup>\*</sup> Weight Percent

#### B.E.T. SURFACE AREA

##### As Received Powders for Baseline Bars

Ibiden UF	Lot 0166	SiC	21.5 M <sup>2</sup> /g
Starck	Lot S-3506	B	12.1 M <sup>2</sup> /g
Monsanto	Lot TL-246	C	53.1 M <sup>2</sup> /g



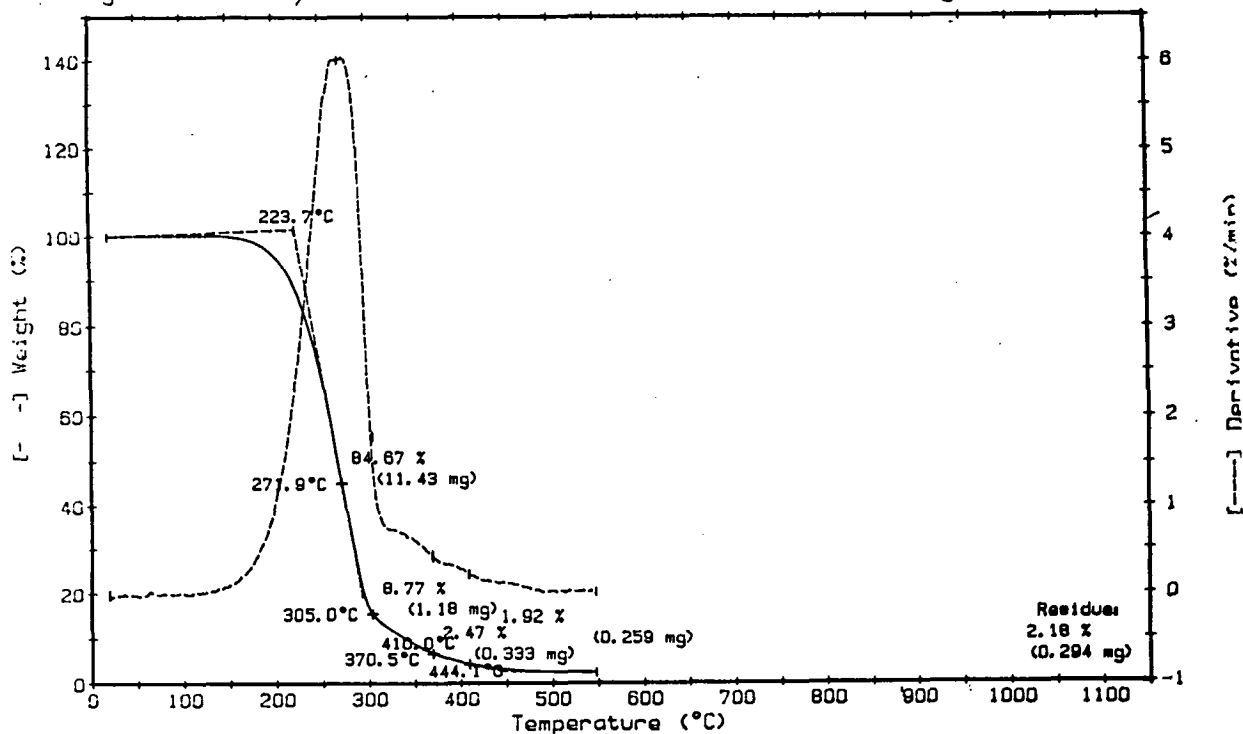
PARTICLE DIAMETER, SPECIFIC GRAVITY, PACK DENSITY,  
AND POLYPHASE ANALYSIS OF SIC POWDER FOR BASELINE BARS

Particle Diameter	Volume Dist.	Frequency Dist
<u>UF Lot 0166</u>		
Median	1.05	0.61
Mode	1.16	0.64
Geometric Mean	1.04	0.59
Arithmetic Mean	1.18	0.65
Specific Gravity		
		3.161 gm/cm <sup>3</sup>
Pack Density		
		0.787 gm/cm <sup>3</sup>
<u>X-ray Polyphase Analysis</u>		
3C Phase		84.0 %
Disordered Phase		16.0 %

Sample: RMW-PARAFFIN CARNUBA L.O.  
 Size: 13.50 mg  
 Rate: 5C/MIN 100ML/MIN ARG  
 Program: TGA Analysis V2.0

TGA

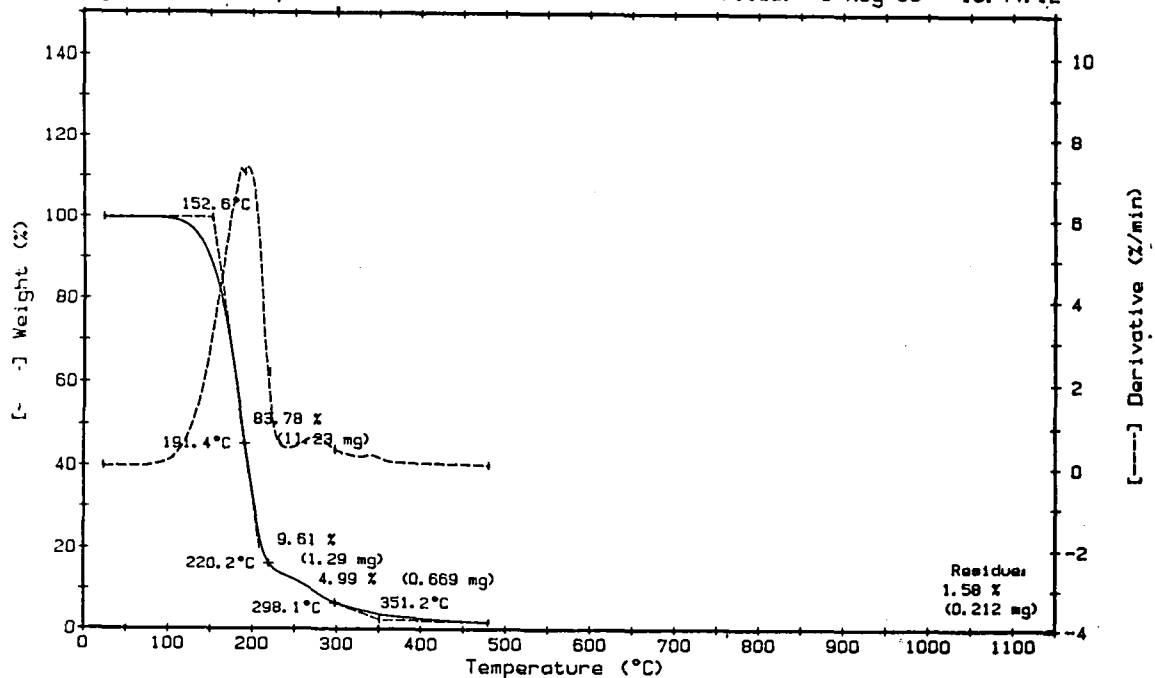
Date: 26-Aug-85 Time: 8:11:08  
 File: TGA.01 TGA.8AUG.1985  
 Operator: L.SKEWES  
 Plotted: 26-Aug-85 10:56:43



Sample: RMW-PARAFFIN LOW CARNUBA  
 Size: 13.41 mg  
 Rate: 5C/MIN 8mm Hg  
 Program: TGA Analysis V2.0

TGA

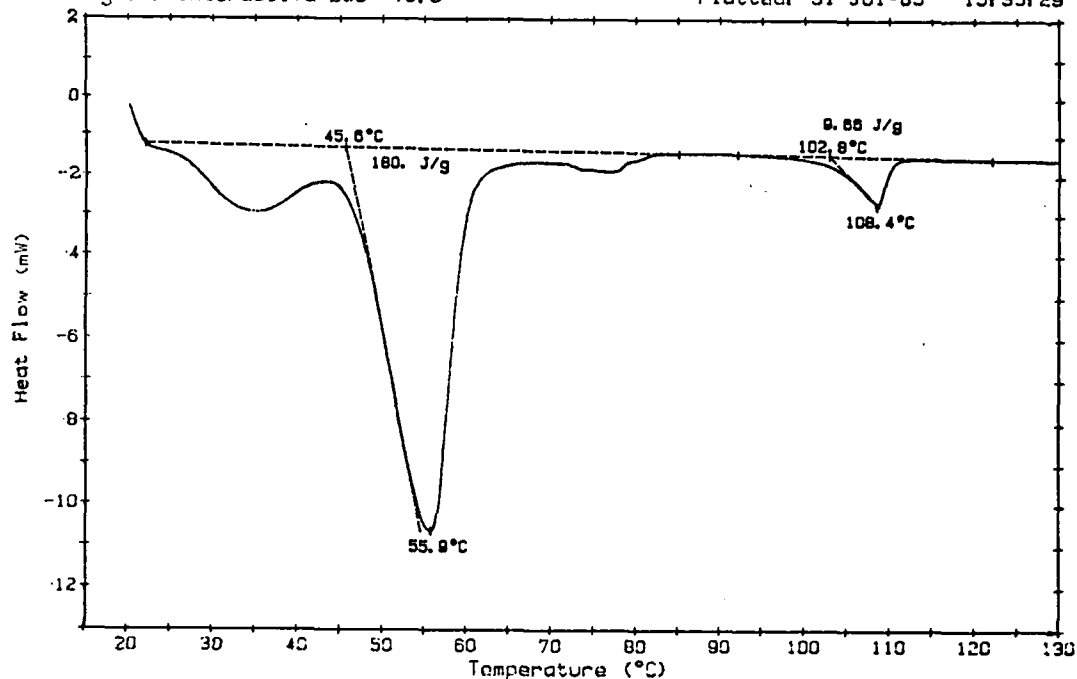
Date: 5-Aug-85 Time: 13:56:50  
 File: TGA.13 TGA.7JULY.1985  
 Operator: L. SKEWES  
 Plotted: 5-Aug-85 15:44:12



Sample: RMV-PARAFFIN LOW CARNUBA  
 Size: 7.673MG  
 Rate: 5C/MIN ARG  
 Program: Interactive DSC V3.0

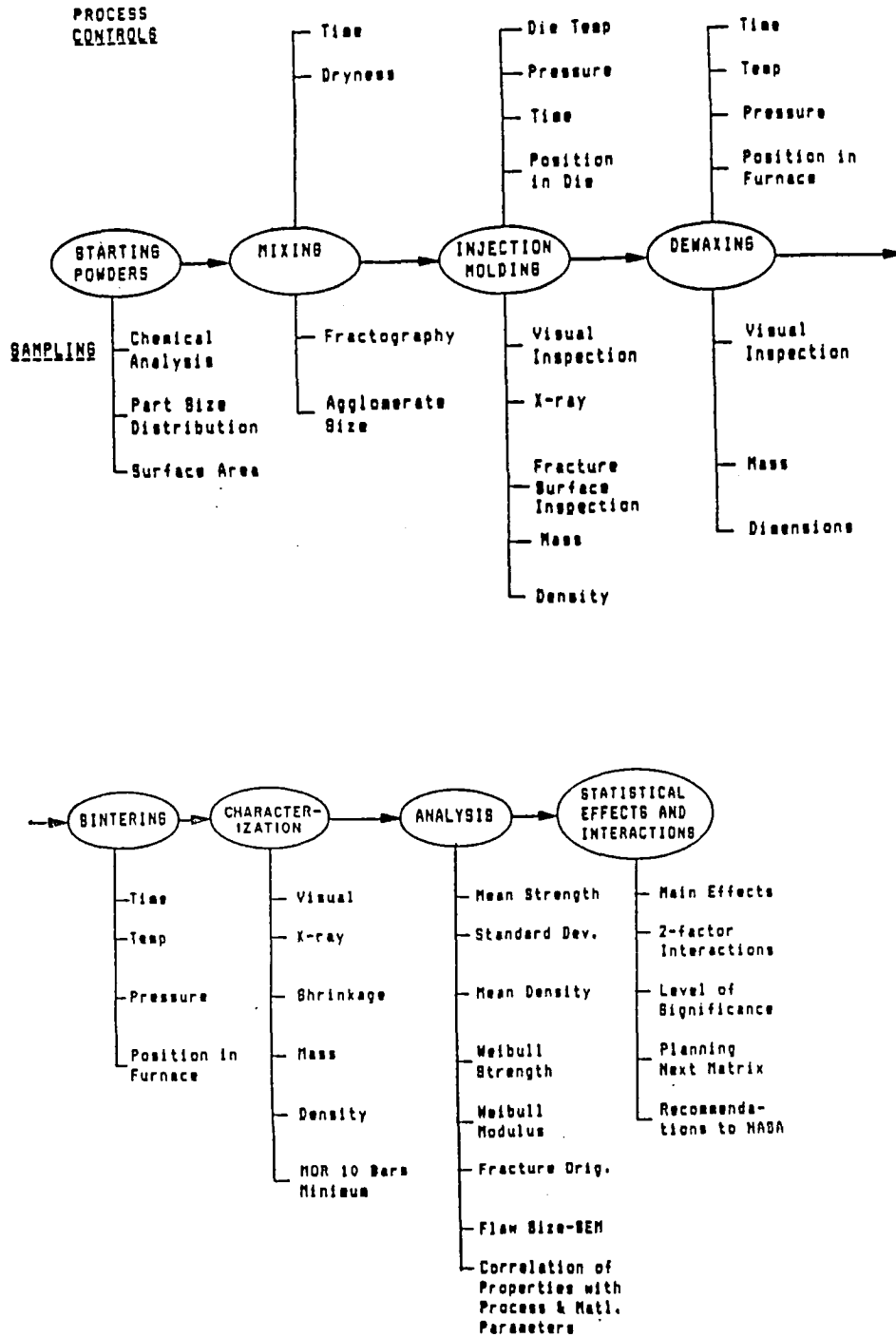
DSC

Date: 30-JUL-85 Time: 13:23:47  
 File: DSC.03 DSC.3JULY85  
 Operator: L. SKEWES  
 Plotted: 31-JUL-85 15:35:29



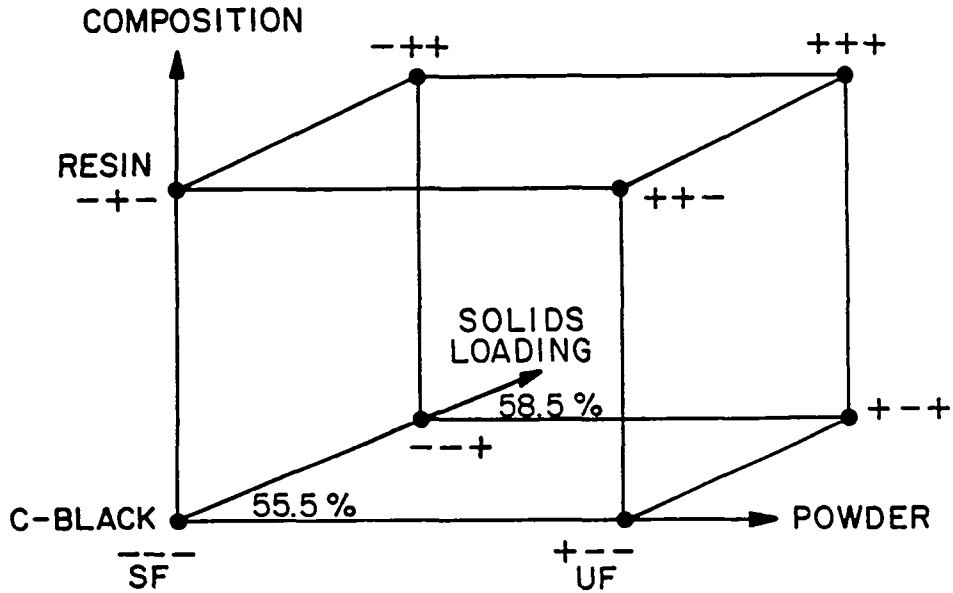
# TASK I

## BASELINE CHARACTERIZATION PROCESS



## 2<sup>3</sup> EXPERIMENT TO

### DETERMINE BASELINE COMPOSITION



### 2<sup>3</sup> BASELINE EXPERIMENT

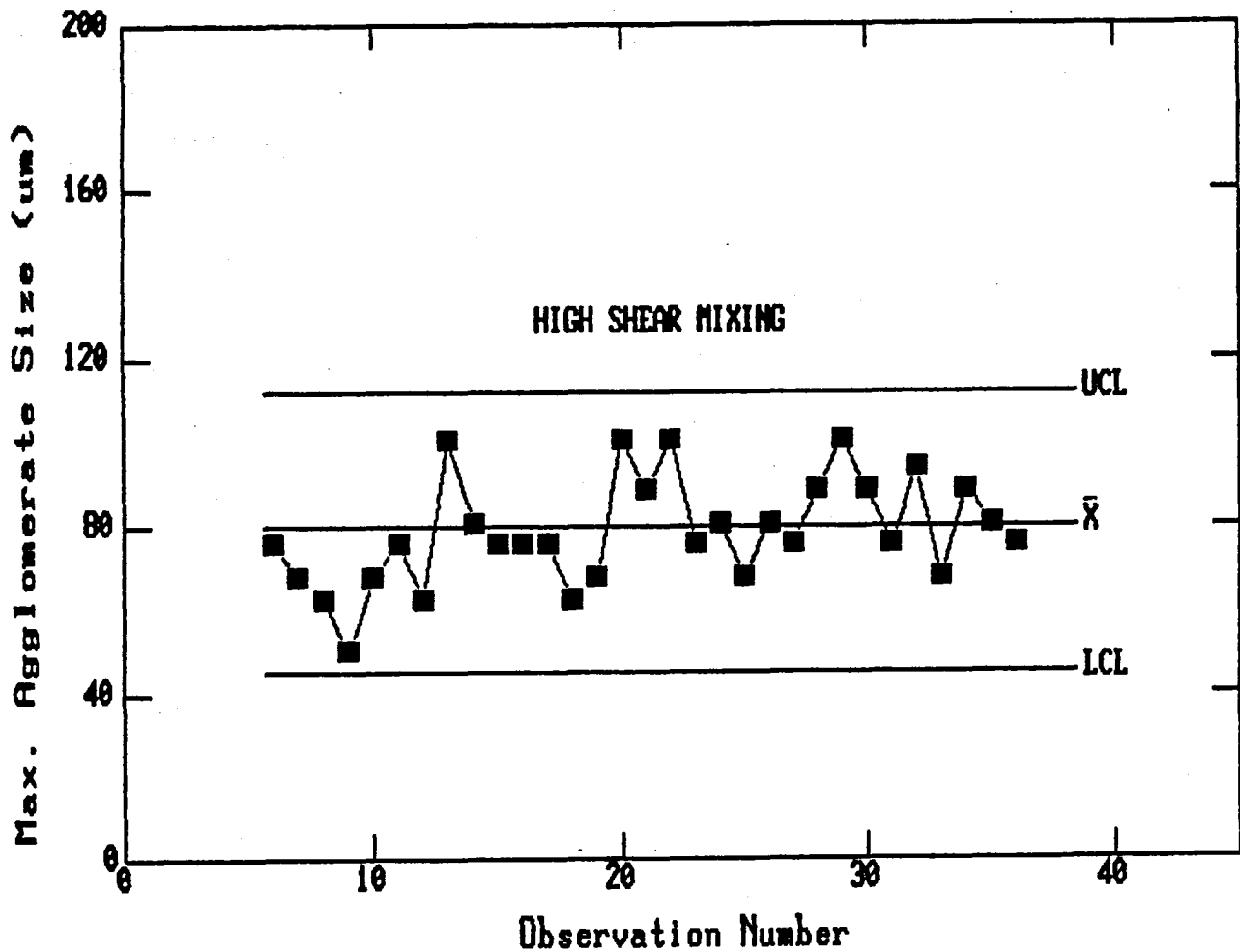
<u>NASA #</u>	<u>SOLIDS LOADING LEVEL</u>	<u>CARBON SOURCE</u>	<u>SIC SOURCE</u>	<u>%T.D.</u>
4	55.5	C-BLACK	UF	93
	58.5			94
5	55.5	C-BLACK	SF	91
	58.5			90
7	55.5	RESIN	UF	88
	58.5			--
8	55.5	RESIN	SF	88
	58.5			88

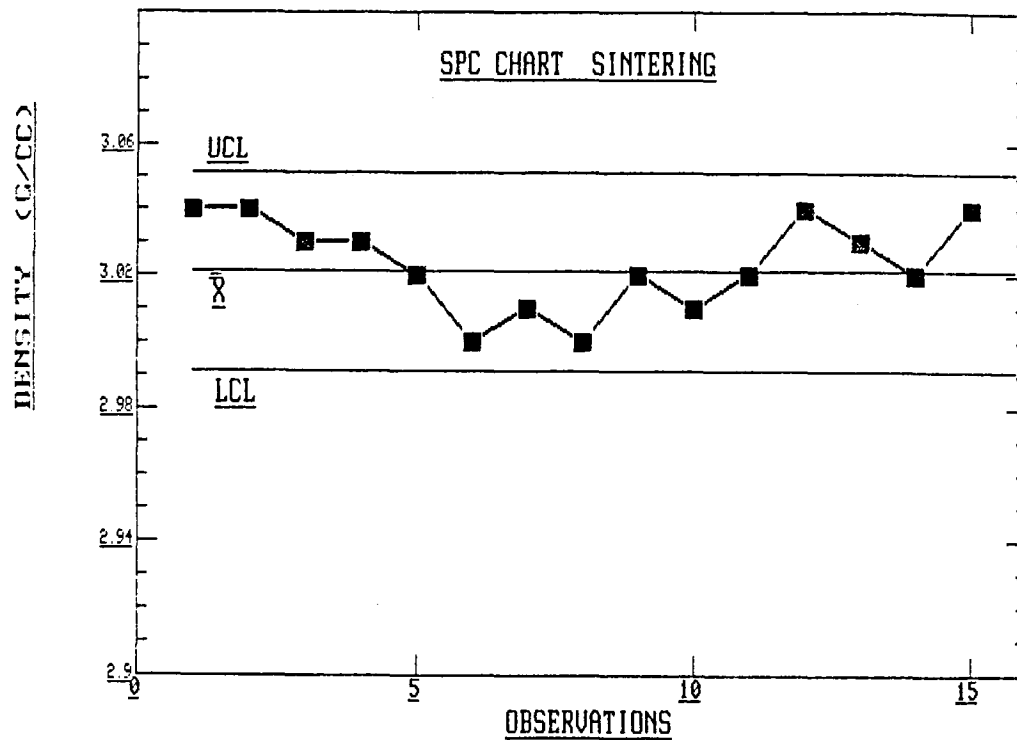
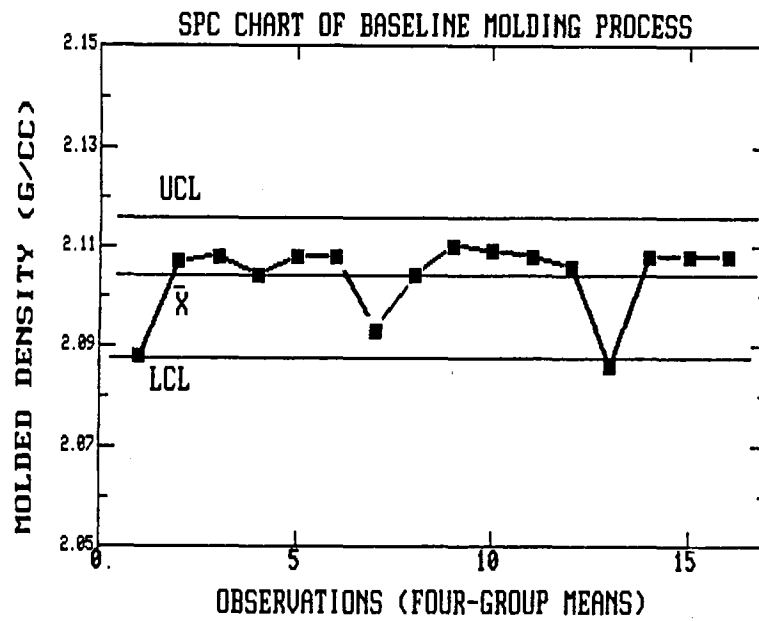
**BASELINE COMPOSITION**

(From 2<sup>nd</sup> Experiment)

**2% C - 1%B - 97% SiC**

**55.5% Solids Loading**





NASA 4G BASELINE  
FRACTOGRAPHY AND X-RAY

<u>M.O.R. BARS</u>			<u>FRACTURE ORIGIN</u>	<u>X-RAY</u>
<u>n</u>	<u>Ksi</u>	<u>S.D.</u>		
5	39.9	6.2	3 - Sub Surface Porosity 2 - Surface Porosity	Large inclusions, Comp. Surface
5	41.1	5.3	4 - Sub Surface Porosity 1 - Surface Porosity	Large inclusions, Center Line
5	37.3	6.7	3 - Sub Surface Porosity 2 - Surface Porosity	Clean
5	42.3	3.9	3 - Sub Surface Porosity 2 - Surface Porosity	Small inclusions

M.O.R. BASELINE SUMMARY

Molded		276*
X-ray acceptable		210
Dewaxed (1 run)		127
Sintered (3 runs)		122
Room Temp. M.O.R.		30
1000°C	FF SR	6 6 (est)
1200°C	FF SR	6 6 (est)
1400°C	FF SR	6 6 (est)

\* Number of M.O.R. Bars  
FF Fast Fracture Test  
SR Stress Rupture Test

# TASK I

## BASELINE CHARACTERIZATION

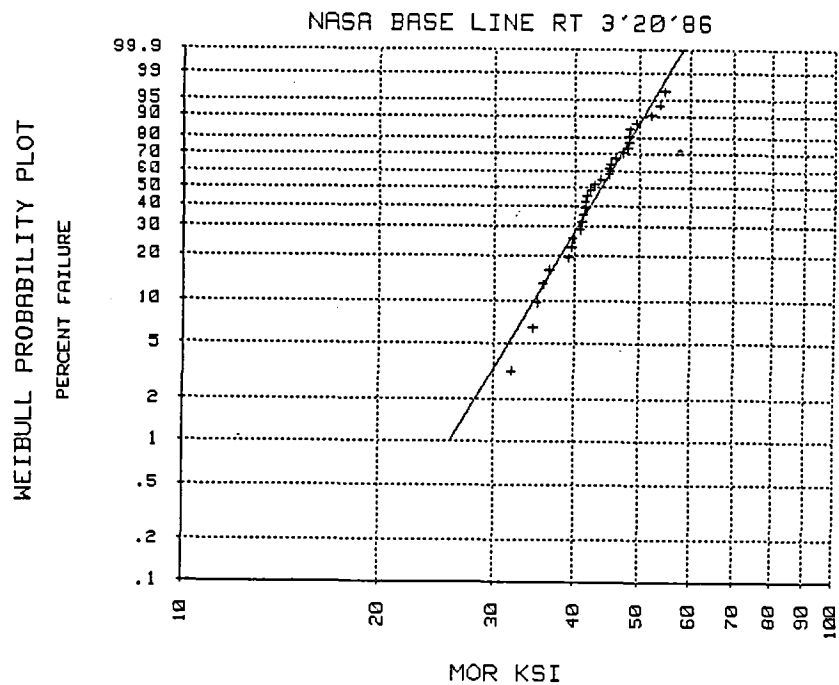
### M.O.R. Results

#### M.O.R. BASELINE RESULTS

		RT	1000°C	1200°C	1400°C
K <sub>1</sub>	K <sub>1</sub>	43.3	41.4	43.2	47.2
	mPa	(299)	(285)	(298)	(325)
n		30	6	6	6
K <sub>2</sub>	K <sub>2</sub>	45.8	WEIBULL SAMPLES TOO SMALL FOR ACCEPTABLE ACCURACY		
	mPa	(315)			
m		8			

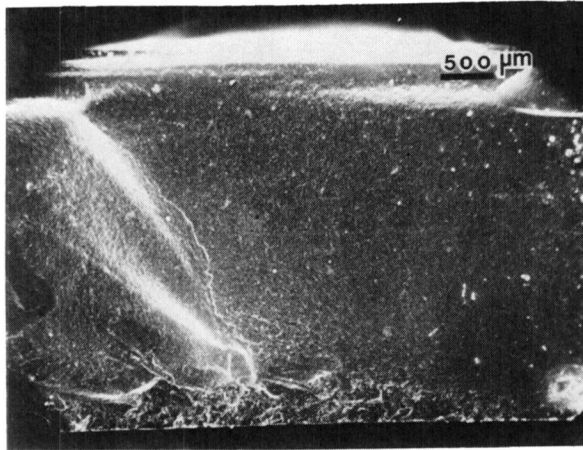
MOR KSI	PROB. OF FAILURE	EXPECTED VALUE
	1.00	25.72
	10.00	34.55
	50.00	43.76
	63.00	45.79
	90.00	50.88
	95.00	52.59
	99.00	55.51
	99.90	58.41

NUMBER OF SAMPLES = 30.00  
 WEIBULL CHARACTERISTIC VALUE = 45.82  
 WEIBULL SLOPE = 7.97  
 DISTRIBUTION MEAN = 43.14  
 STANDARD DEVIATION = 6.43



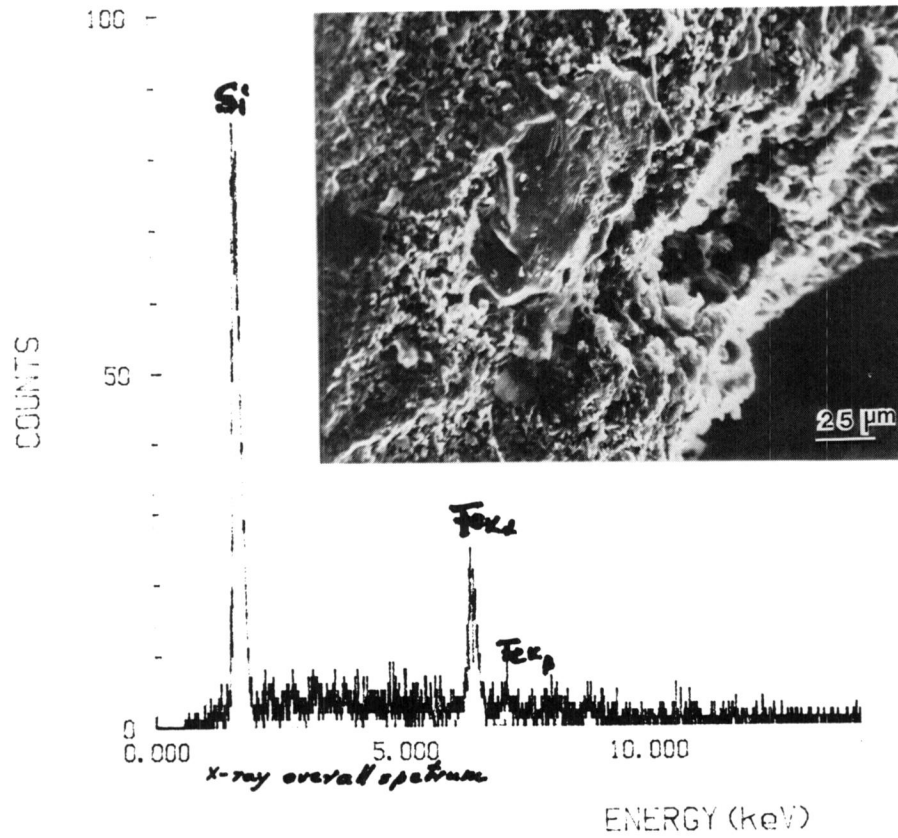


# **FRACTURE SURFACE FLAW ORIGIN — IRON RICH**

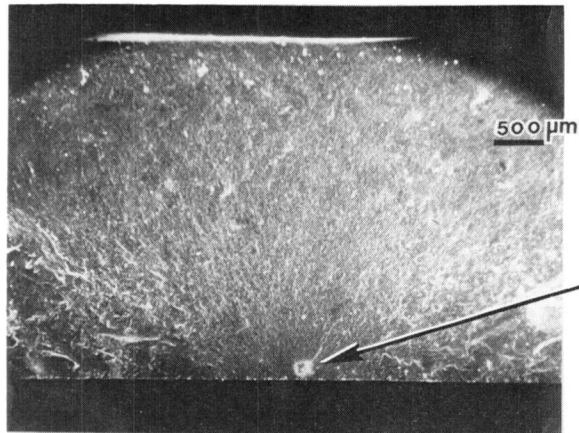


← FRACTURE ORIGIN

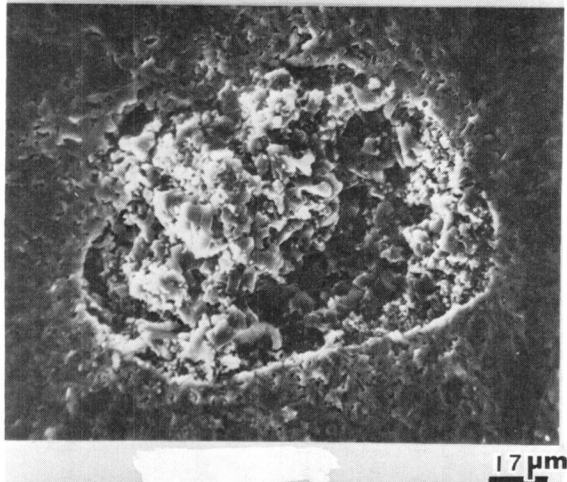
LT= 300 SECS



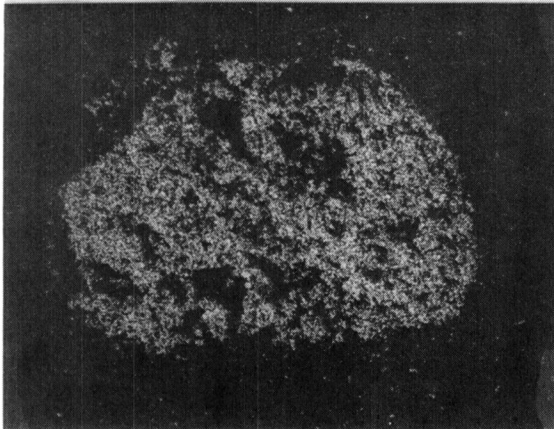
**FRACTURE SURFACE  
FLAW ORIGIN — BORON RICH**



**FRACTURE ORIGIN**

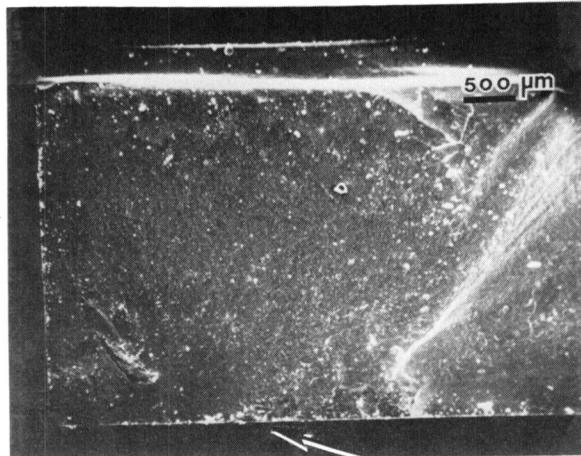


**FLAW**



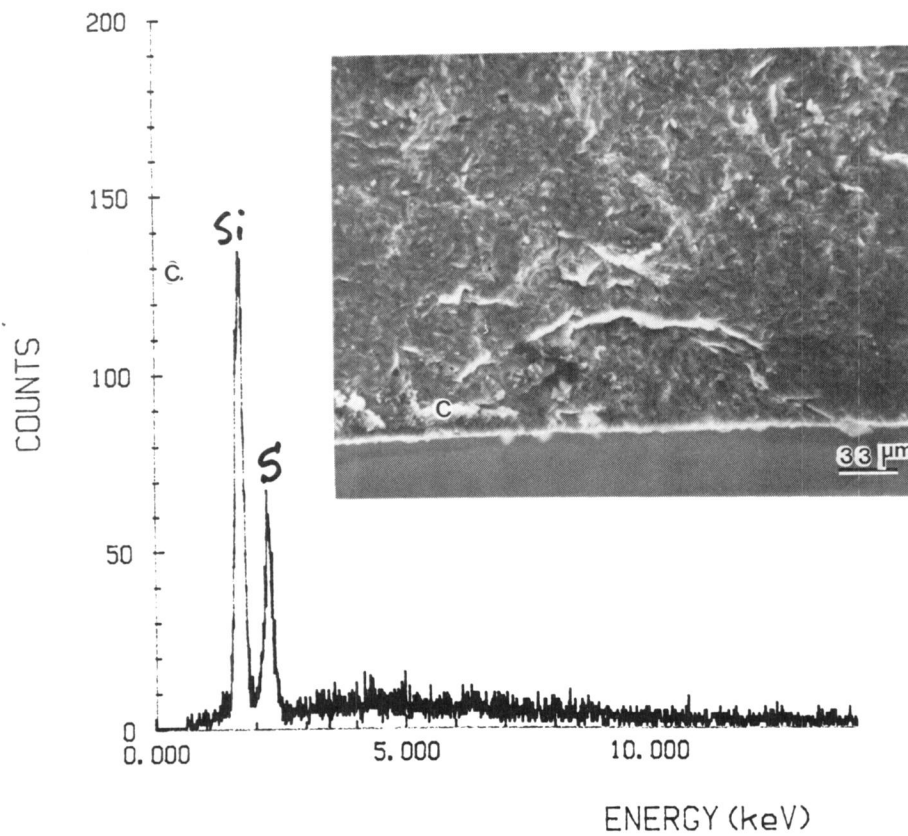
**BORON MAP**

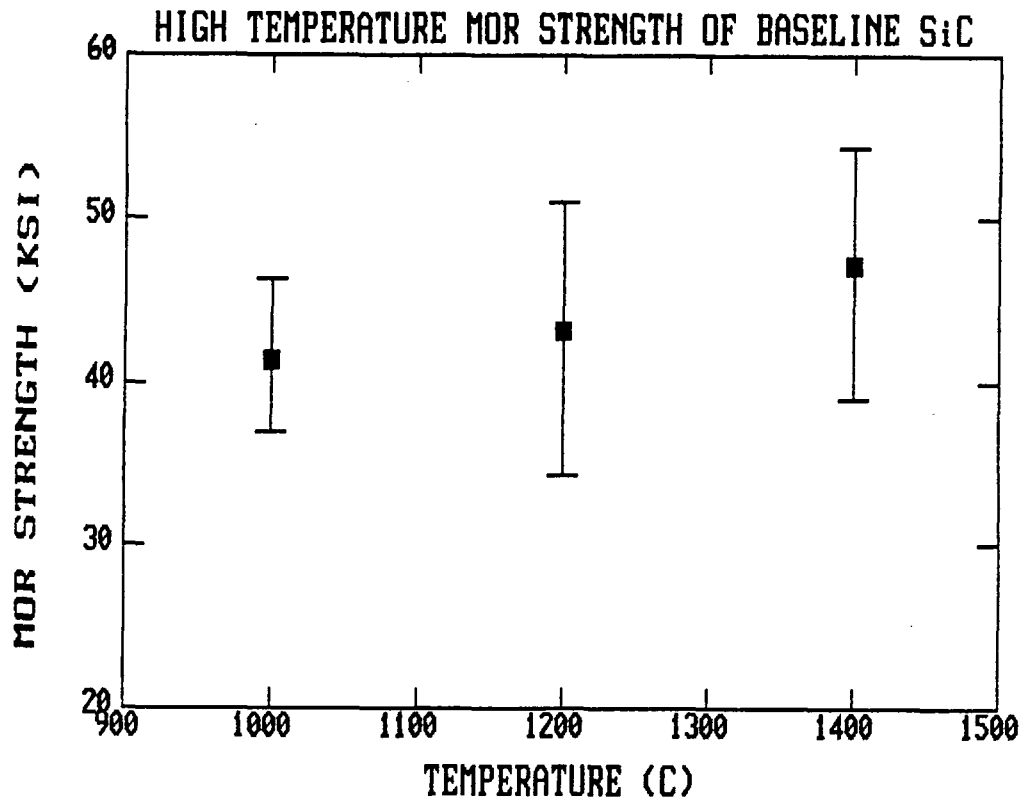
**FRACTURE SURFACE  
FLAW ORIGIN — SULFUR RICH**



LT= 300 SECS

**FRACTURE ORIGIN**





#### **TASK VII**

**OBJECTIVE:**

**CONTINUOUS THROUGHOUT THE PROGRAM**

**"ADVANCE THE STATE OF THE ART OF  
SiC TECHNOLOGY"**

**PROVIDE INPUT TO TASKS I AND II**

**WAYS TO IMPROVE THE STRENGTH OF A  
CERAMIC...**

$$\sigma \propto K_I E / c^{1/2}$$

**INCREASE THE FRACTURE TOUGHNESS  
(MICROSTRUCTURE)**

**INCREASE THE ELASTIC MODULUS  
(DENSITY) \*\***

**REDUCE THE FLAW SIZE \*\***

**\*\* ADDRESSED IN TASK VII**

**INJECTION MOLDED SiC  
PROCESS FLOW SHEET**

**POWDER PREPARATION**

**BLEND SINTERING ADDITIVES  
WITH SiC \*\***

**MIX SOLIDS WITH INJECTION MOLDING  
BINDERS \*\***

**INJECTION MOLD \*\***

**BINDER REMOVAL \*\***

**SINTER \*\***

**MACHINE**

**STRENGTH EVALUATION**

**\*\* ADDRESSED IN TASK VII**

**DEVELOPMENT OF IMPROVED MIXING  
TECHNIQUES**

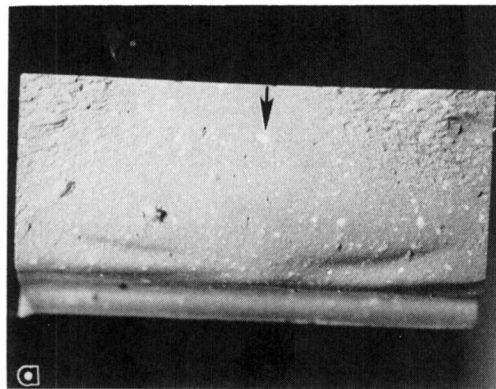
**FRACTURE ORIGINS IDENTIFIED AS  
PROCESSING FLAWS**

**FLAWS IDENTIFIED AS AGGLOMERATES IN  
THE INJECTION MOLDING BATCH**

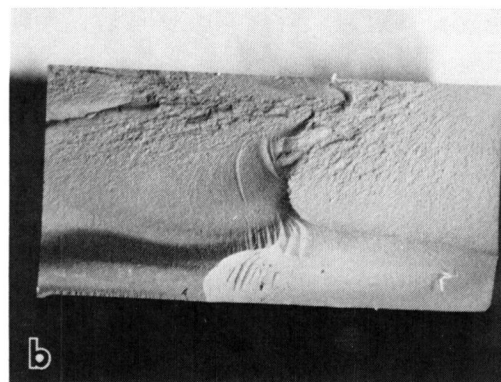
**AGGLOMERATES WERE DETECTED IN THE  
"MIXING" STAGE OF THE PROCESS**

**"GREEN" INJECTION MOLDED TEST BARS**

**STRENGTH CONTROLLING AGGLOMERATES  
(UF POWDER)**



**NO AGGLOMERATES OBSERVED  
(SF POWDER)**



1 mm

**DRY MIXING PROCESS  
(METHOD 1)**

**POWDER PREPARATION**

DRY BLEND SINTERING ADDITIVES  
WITH SiC

MIX SOLIDS WITH INJECTION MOLDING  
BINDER USING DOUBLE PLANETARY  
MIXER \*\*

INJECTION MOLD \*\*

**\*\* AGGLOMERATES OBSERVED**

**DRY MIXING PROCESS  
(METHOD 2)**

**POWDER PREPARATION**

DRY BLEND SINTERING ADDITIVES  
WITH SiC

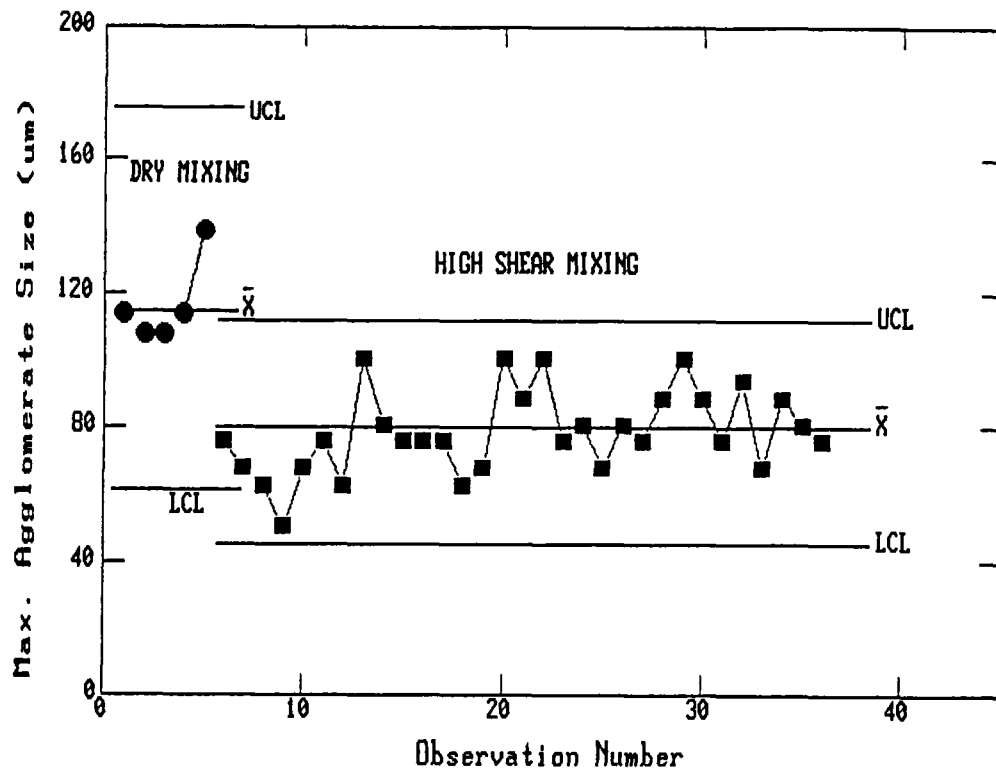
MIX SOLIDS WITH INJECTION MOLDING  
BINDER USING DOUBLE PLANETARY  
MIXER \*\*

RE-MIX MOLDING BATCH IN HIGH SHEAR  
HAAKE MIXER \*\*

INJECTION MOLD \*\*

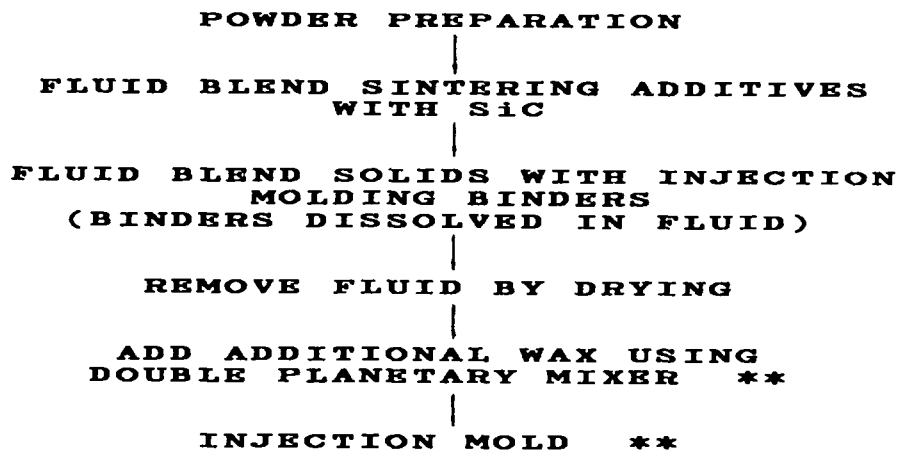
**\*\* AGGLOMERATES OBSERVED**

**HIGH SHEAR MIXING WAS FOUND TO REDUCE  
THE AGGLOMERATE SIZE**



**FLUID MIXING WAS INVESTIGATED  
TO REDUCE AGGLOMERATE SIZE**

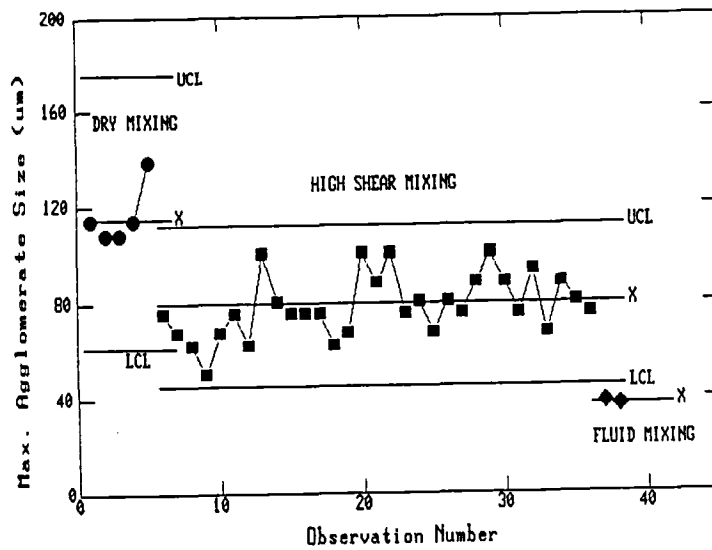
**FLUID MIXING PROCESS  
(METHOD 1)**



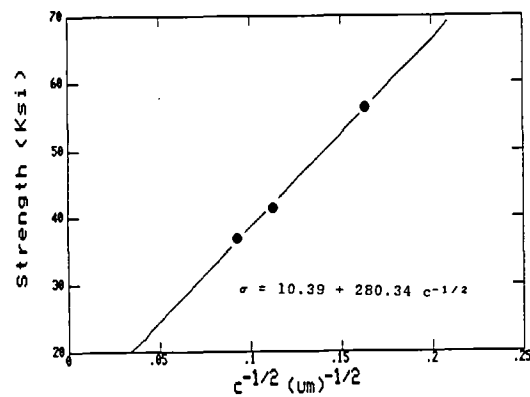
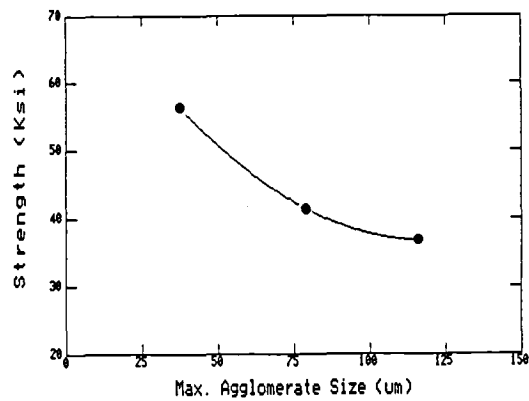
**\*\* AGGLOMERATES OBSERVED**



FLUID MIXING WAS FOUND TO FURTHER  
REDUCE THE AGGLOMERATE SIZE



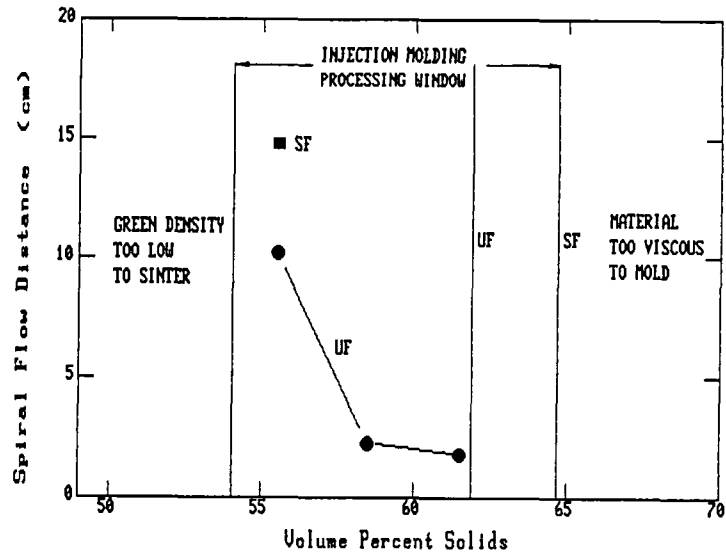
REGRESSION MODEL ILLUSTRATES THE  
RELATION BETWEEN STRENGTH AND  
AGGLOMERATE SIZE



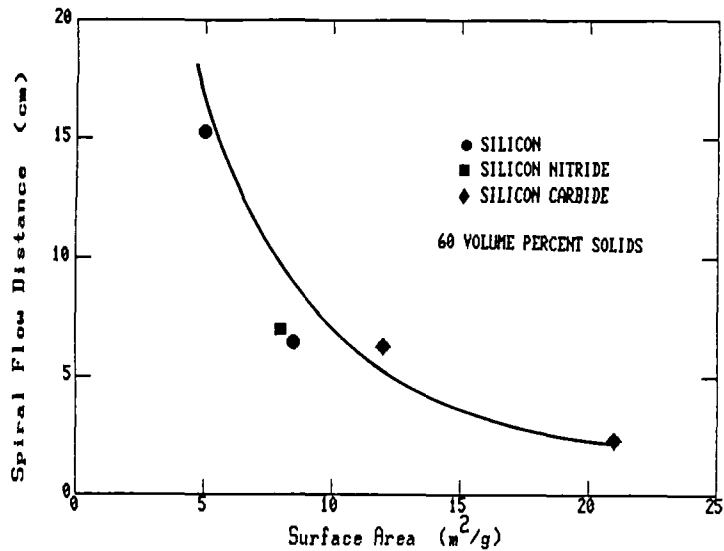
FLUID MIXING PROCESS WILL  
BE USED IN THE REMAINDER  
OF THE PROGRAM (TASK II)

# INJECTION MOLDING

INJECTION MOLDING PROCESSING WINDOW  
WAS IDENTIFIED



INJECTION MOLDING BEHAVIOR OF ALL  
SILICON BASED CERAMIC POWDERS  
IS A FUNCTION OF SURFACE AREA



**INJECTION MOLDING PROCESS YIELDS  
WERE IMPROVED THROUGH EQUIPMENT  
MODIFICATION**

**COMPOSITION: 12A - 60.0 VOL % SOLIDS**

**ORIGINAL SYSTEM:**

**332 BARS MOLDED  
221 BARS VOID FREE**

**66.6 % YIELD**

**IMPROVED VACUUM SYSTEM:**

**24 BARS MOLDED  
23 BARS VOID FREE**

**95.8 % YIELD**

**BINDER REMOVAL - SINTERING**

**CURRENT PROCESS USES  
VACUUM FOR BINDER REMOVAL  
VACUUM FOR SINTERING**

**VACUUM PROCESSING RESULTS IN CRACK  
FREE TEST BARS HAVING GOOD DENSITY**

**PROBLEMS ARE ANTICIPATED WITH  
VACUUM PROCESSING:**

**CRACKING IN THICK CROSS SECTION  
COMPONENTS**

**LOW DENSITY AREAS ON AS SINTERED  
SURFACES**

EXPERIMENTS WERE INITIATED TO  
INVESTIGATE ALTERNATIVES TO VACUUM  
PROCESSING DURING BINDER REMOVAL  
AND SINTERING.

## BINDER REMOVAL

### 22 EXPERIMENTAL DESIGN

VARIABLES:  
HEATING RATE  
PRESSURE

EXP.			PERCENT BINDER REMOVAL	VACUUM SINTERED DENSITY
1)	-	-	91.7	93.5
2)	+	-	91.4	93.6
3)	-	+	95.8	93.5
4)	+	+	96.4	93.8

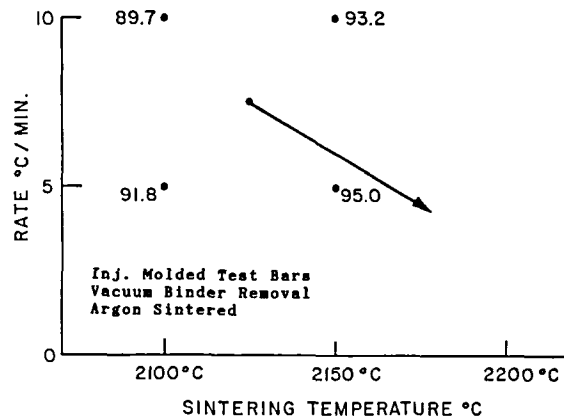
EXP. 1 USED FOR BASELINE PROCESSING

EXP. 3 OFFERS POTENTIAL FOR  
PROCESSING LARGE COMPONENTS

## SINTERING

ARGON SINTERING POTENTIAL  
DEMONSTRATED

### SINTERED DENSITY VS SINTERING VARIABLES



## **FUTURE PLANS**

### **TASK II**

$$\sigma \propto K_I E / c^{1/2}$$

#### **FIRST ITERATION:**

**REDUCE PROCESSING FLAW SIZE  
(AGGLOMERATES)**

#### **SECOND ITERATION:**

**INCREASE DENSITY (ELASTIC MODULUS)  
OPTIMIZE MICROSTRUCTURE (INCREASE  
FRACTURE TOUGHNESS)**

## **FUTURE PLANS**

### **TASK VII**

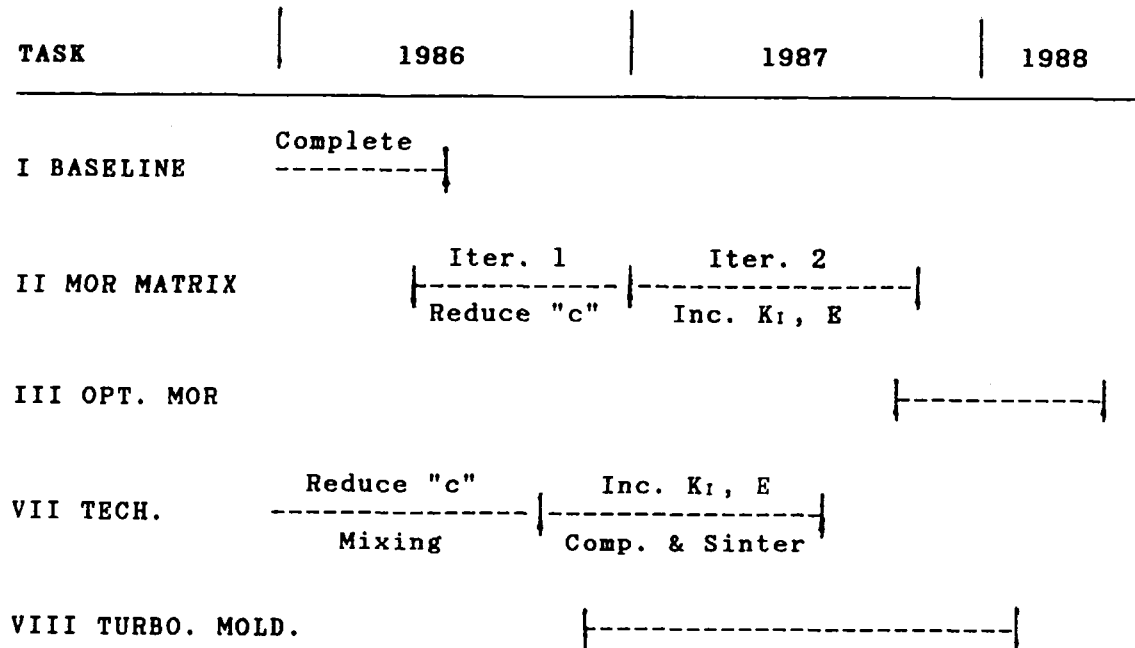
**CONTINUE TO STUDY WAYS TO REDUCE  
AGGLOMERATE SIZE**

**CONTINUE TO INVESTIGATE BINDER  
REMOVAL TECHNIQUES**

**CONTINUE TO STUDY THE INTERRELATION  
BETWEEN BINDER REMOVAL AND SINTERING**

**INITIATE WORK TO INCREASE SINTERED  
DENSITY AND IMPROVE SINTERED  
MICROSTRUCTURE**

# **PROGRAM TIMING CHART** **PHASE I**



## STRENGTH OPTIMIZATION OF $\alpha$ -SiC BY IMPROVED PROCESSING

Sunil Dutta  
NASA Lewis Research Center  
Cleveland, Ohio 44135

Silicon carbide is of great interest for structural use in aircraft and automobile engines. This ceramic combines high thermal conductivity and low coefficient of thermal expansion, and consequently has good thermal shock resistance. However, like other ceramics, silicon carbide shows strength variability due to processing flaws such as large voids, shrinkage cracks, inclusions, etc. Agglomerates in the starting powder seem to be the predominant cause for such defects. Improved processing techniques such as slurry pressing and hot isostatic pressing were employed to minimize these defects and to improve strength and reliability in the fabricated material. For this purpose 2-inch diameter discs were fabricated by various consolidation techniques. These include: (1) dry pressing and sintering, (2) slurry pressing and sintering, and (3) slurry pressing and HIPing. High density (>96 percent of theoretical) was produced by sintering at 2150 - 2200 °C. By contrast, a much lower temperature (1850-1900 °C) was required by HIPing to achieve high final density specimens. Dry pressing and sintering yielded an average flexure strength (4-point bend) of 350 MPa (50 ksi), while slurry pressing and sintering produced an average strength of 430 MPa (62 ksi), a 30 percent improvement in strength. Further, slurry pressing and HIPing yielded an average strength of 580 MPa (84 ksi). This strength value is 60 percent higher than the dry-pressed/sintered strength, and 30 percent higher than the slurry-pressed/sintered strength. The HIP silicon carbide exhibited an ultrafine grained microstructure (0.3-3  $\mu$ m) as compared to 1-30  $\mu$ m produced by sintering. Process related defects such as large isolated voids, shrinkage cracks, etc. were not observed in HIPed silicon carbide.

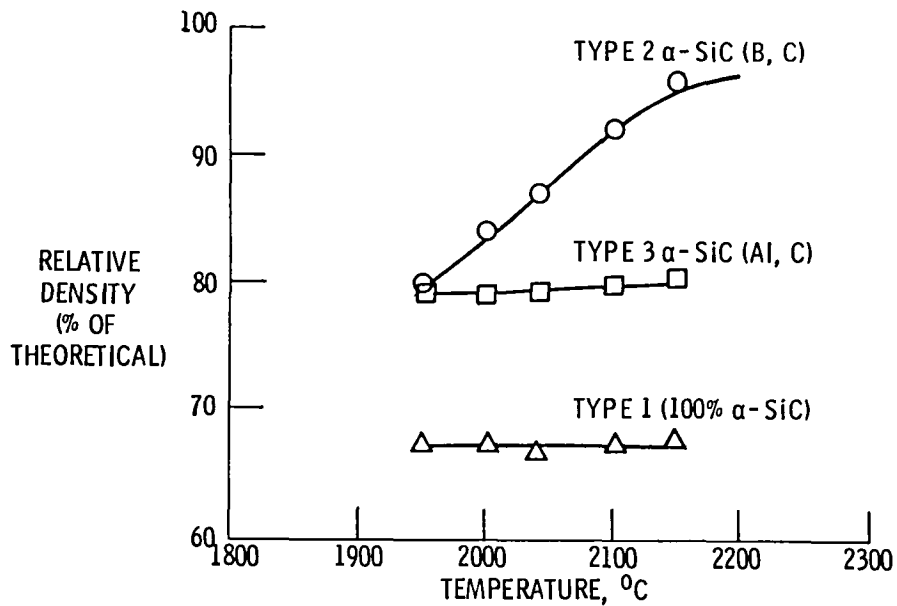
TABLE 1 ANALYSIS OF AS-RECEIVED  $\alpha$  - SiC POWDERS

	IMPURITY ANALYSIS (PPM)		
	TYPE 1	TYPE 2	TYPE 3
ELEMENT	$\alpha$ - SiC (100%)	$\alpha$ - SiC (B, C)	$\alpha$ - SiC (Al, C)
Al	50	140	1.2*
Ca	70	40	20
Fe	10	10	40
Ti	20	30	50
V	20	20	40
B	—	0.60*	—
FREE C	1.66*	7.31*	6.10*
SURFACE AREA (BET) m <sup>2</sup> /gm	31.47	4.19	11.38

\*WT PERCENT

CD-86-19198

RELATIVE DENSITY OF THREE TYPES OF STARCK  $\alpha$ -SiC POWDER  
SINTERED FOR 30 min AT DIFFERENT TEMPERATURES



V-1270

CS-83-1723

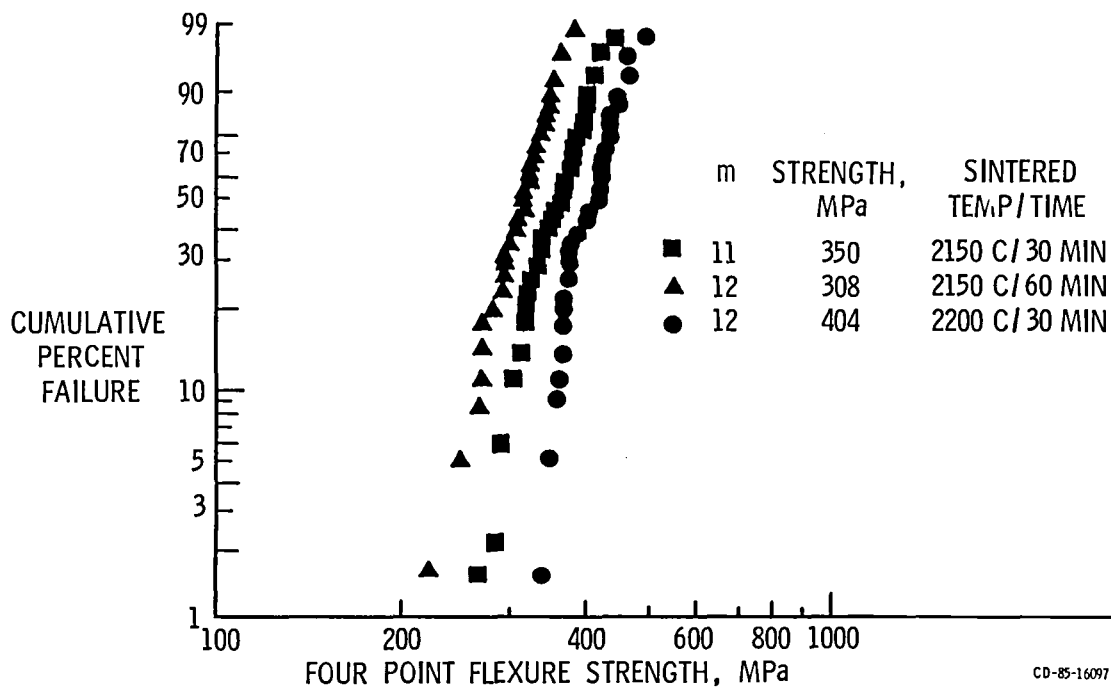


# PROCESSING AND PROPERTIES OF TYPE 2 (AS-RECEIVED) $\alpha$ - SiC (B, C) MATERIAL

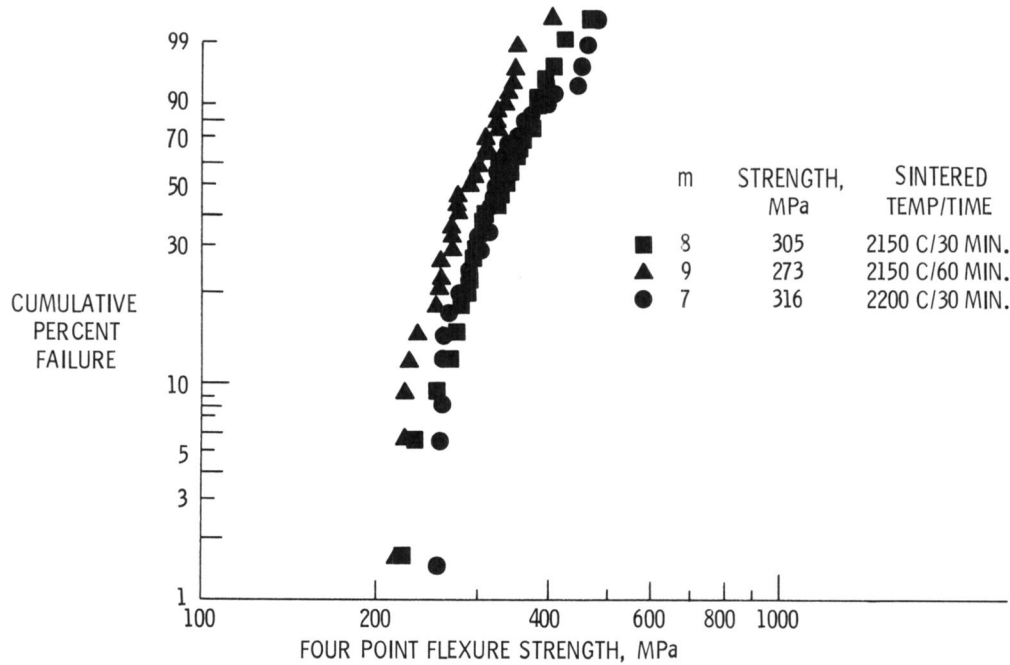
$\alpha$ - SiC TYPE	SINTERED TEMPERATURE, °C	TIME, min	DENSITY, g/cm <sup>3</sup>	MOR/TEST TEMPERATURE,	NUMBER OF SPECIMEN	MEAN MOR/ $\delta$ -D., MPa	WEIBULL/R <sup>2</sup> , m
2	2150	30	95	RT	23	353/	11/95
2	2150	60	96	RT	28	306/32	12/97
2	2200	30	97	RT	30	404/40	12/89
2	2150	30	95	1370	20	312/	7/97
2	2150	60	96	1370	24	265/32	10/94
2	2200	30	97	1370	30	316/53	7/80

CD-86-19202

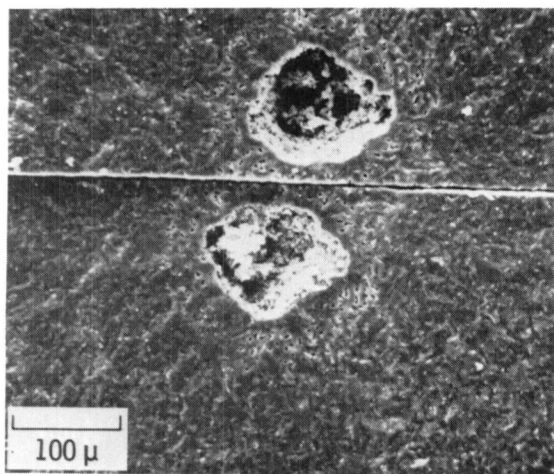
## WEIBULL PROBABILITY CHART FOR ROOM TEMPERATURE FRACTURE OF STARCK TYPE 2 $\alpha$ - SiC (B, C)



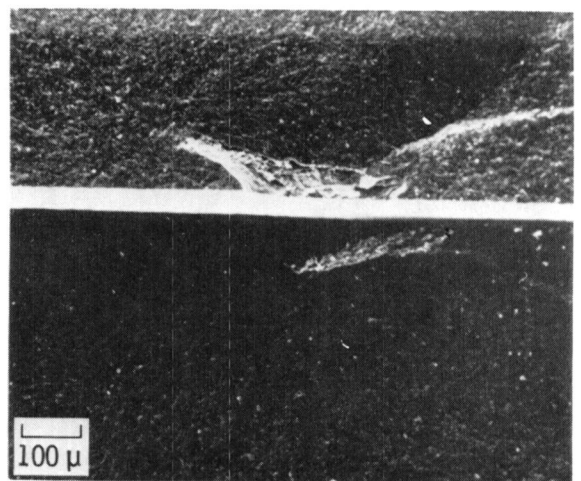
# WEIBULL PROBABILITY CHART FOR 1370° C FRACTURE OF STARCK TYPE 2 $\alpha$ -SiC (B, C)



## ROOM TEMPERATURE FRACTURE OF DRY-PRESSED/SINTERED $\alpha$ -SiC



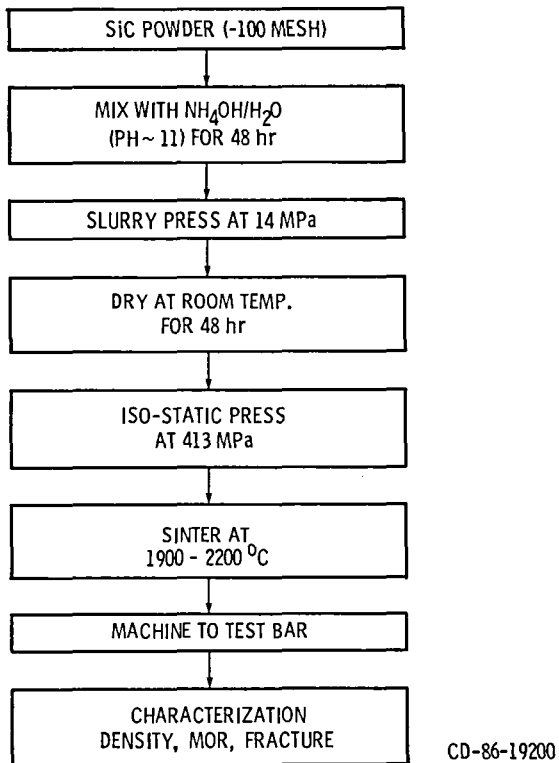
$\sigma_f$ -227 MPa



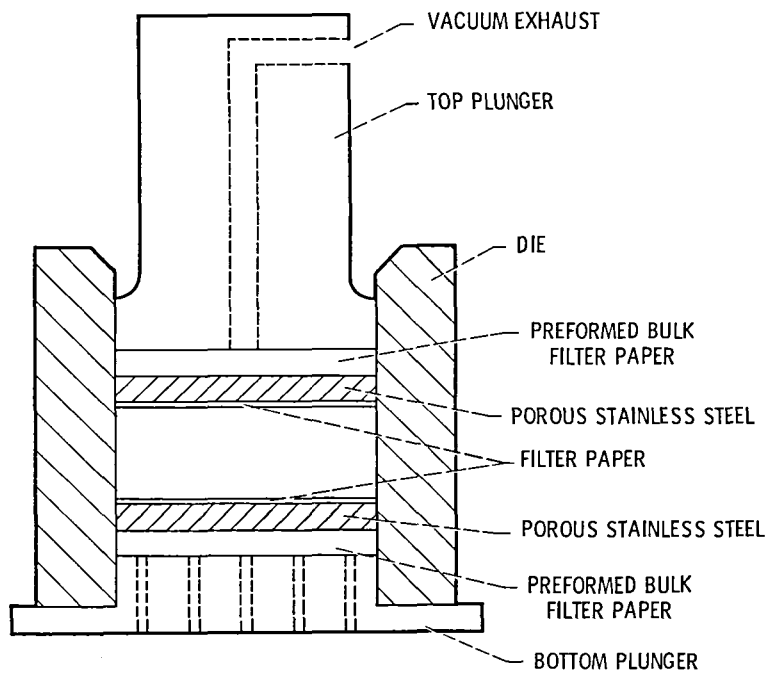
$\sigma_f$ -225 MPa

CD-86-19188

## SLURRY-PRESSING FLOW DIAGRAM



## SCHEMATIC OF SLURRY PRESSING APPARATUS



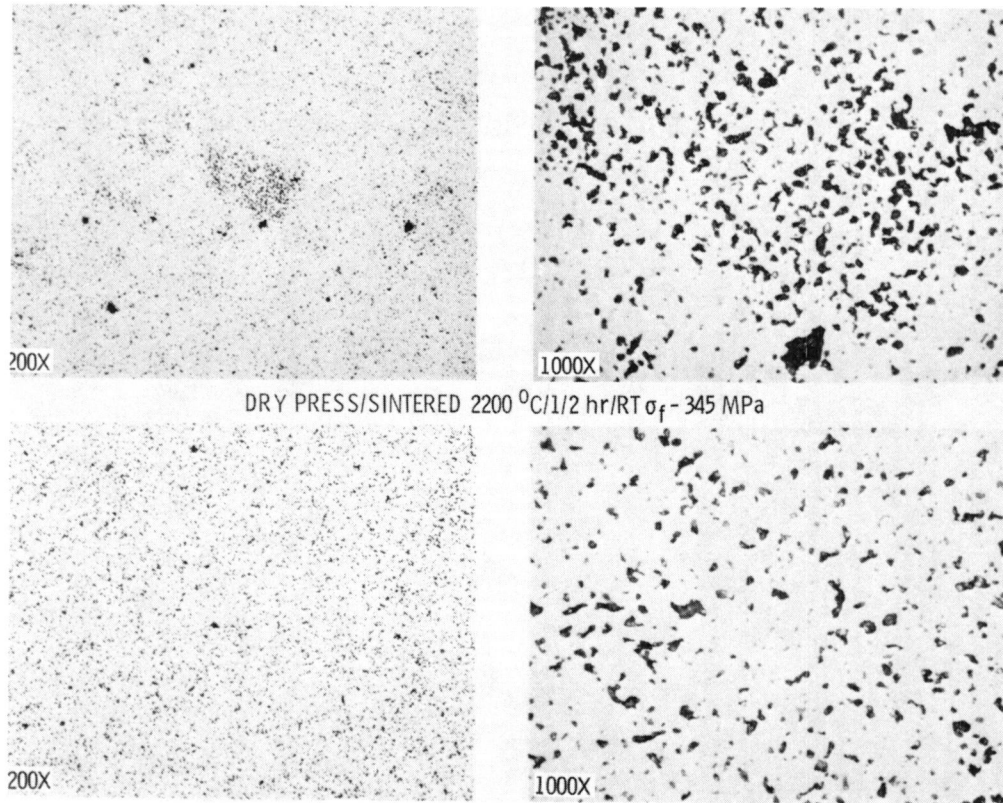
CD-86-19193

# PROPERTIES OF SINTERED VS HOT ISOSTATIC PRESSED $\alpha$ - SiC

$\alpha$ - SiC TYPE	PROCESSING METHOD	DENSIFICATION TEMPERATURE, $^{\circ}\text{C}$	TIME, min	DENSITY (% OF THEORETICAL)	MEAN MOR/6-D MPa	NO. OF SPECIMEN	WEIBULL/ $R^2$ m
2	DRY PRESS/ SINTERED	2200	30	97.4	$342 \pm 52.8$ ( $49.6 \pm 5.7$ ksi)	30	8
2	SLURRY PRESS/ SINTERED	2200	30	96.5	$416 \pm 53.3$ ( $60.3 \pm 7.7$ ksi)	22	9.3
2	SLURRY PRESS/ HIPed	1900	30	95.3	$580 \pm 77$	15	8.8
2	SLURRY PRESS/ HIPed	1800	30	80.5	N. D.	8	N. D.

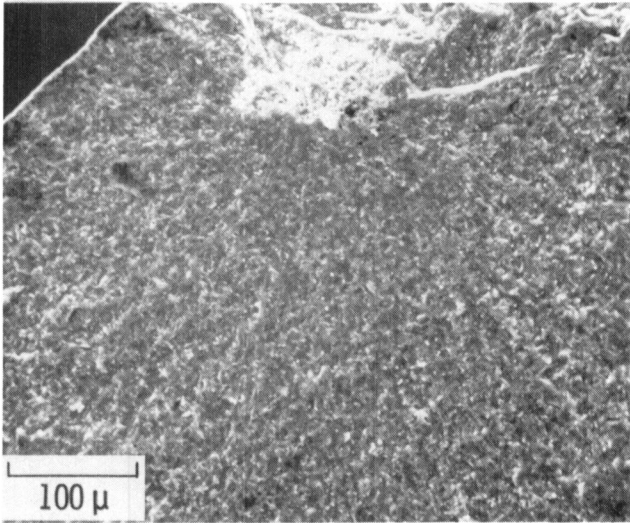
CD-86-19197

## EFFECT OF DRY PRESSING VS SLURRY PRESSING ON SINTERED MICROSTRUCTURES OF $\alpha$ -SiC

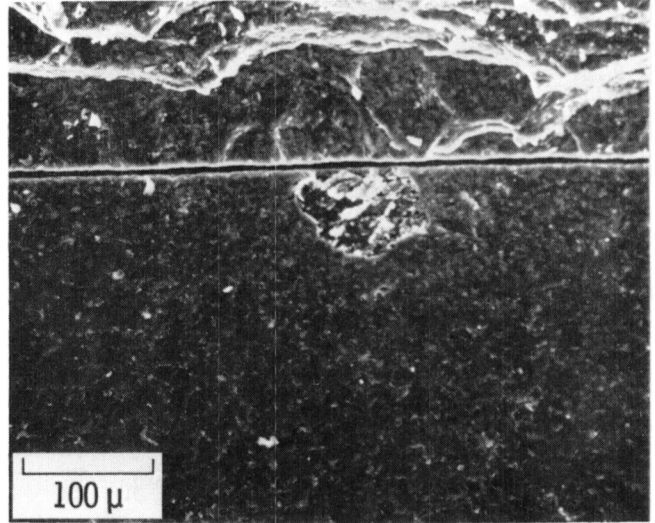


CD-86-19187

## ROOM TEMPERATURE FRACTURE OF SLURRY-PRESSED/SINTERED $\alpha$ -SiC



$\sigma_f - 340 \text{ MPa}$



$\sigma_f - 260 \text{ MPa}$

CD-86-19189

## HIPing OF STRUCTURAL CERAMICS

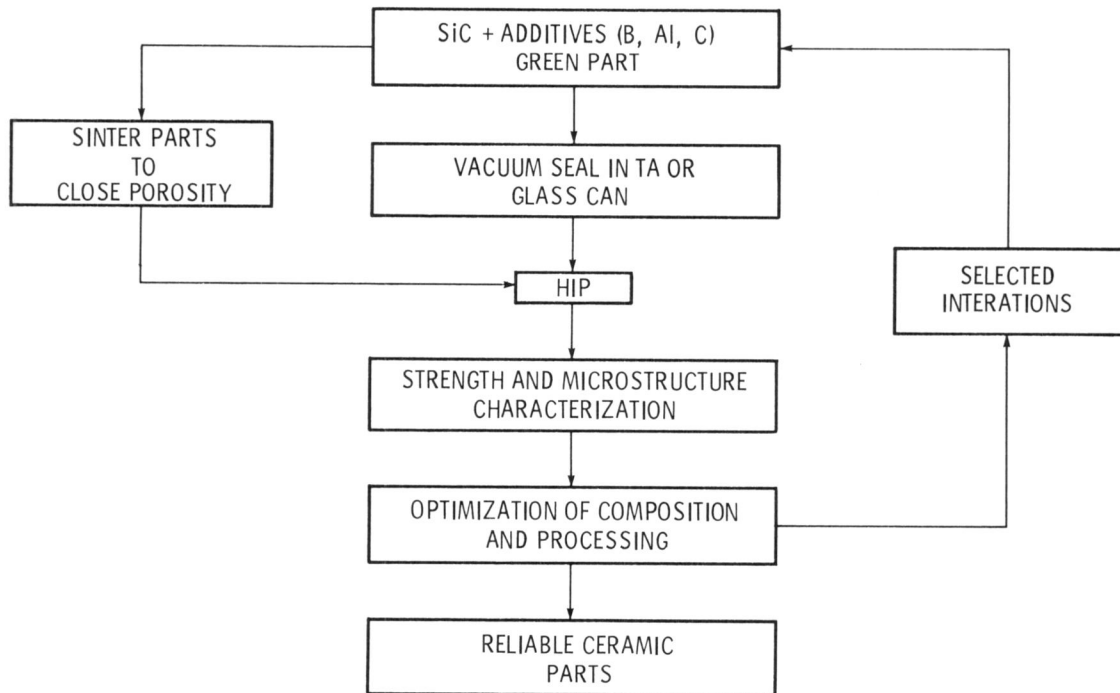
### ADVANTAGES:

HOT ISOSTATIC PRESSING (HIPing) OF STRUCTURAL CERAMICS, e.g.,  $\text{Si}_3\text{N}_4$  AND SiC.

- o ENHANCES DENSITY (APPROACHES TD)
- o IMPROVES MICROSTRUCTURE
- o SIGNIFICANTLY INCREASES STRENGTH
- o IMPROVES RELIABILITY

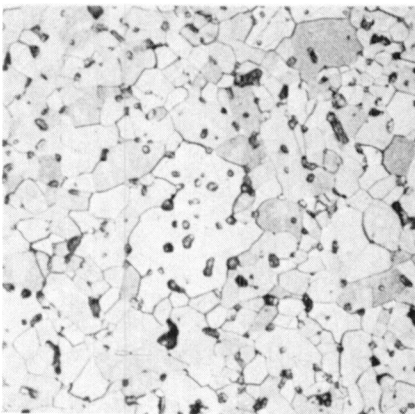
CD-86-19185

## HOT ISOSTATIC PRESSING - GENERAL FLOW CHART

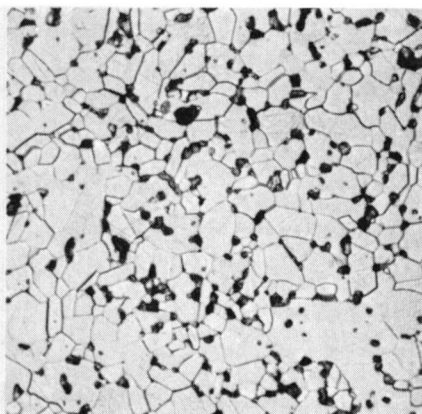


CD-86-19186

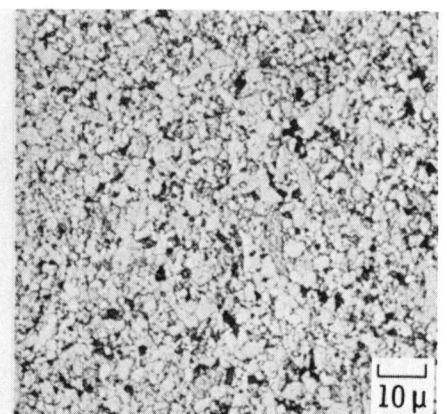
## MICROSTRUCTURE DEVELOPMENT IN SINTERED AND HOT ISOSTATIC PRESSED $\alpha$ -SiC



DRY-PRESSED/SINTERED  
2200 C / 1/2 hr

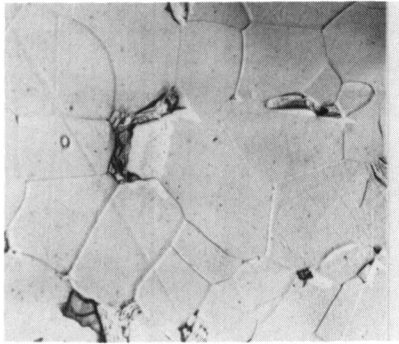


SLURRY-PRESSED/SINTERED  
2200 C / 1/2 hr

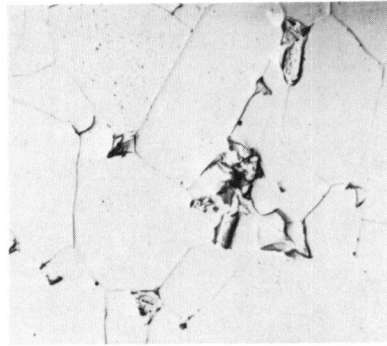


SLURRY-PRESSED/HIPed  
1900 C / 1/2 hr

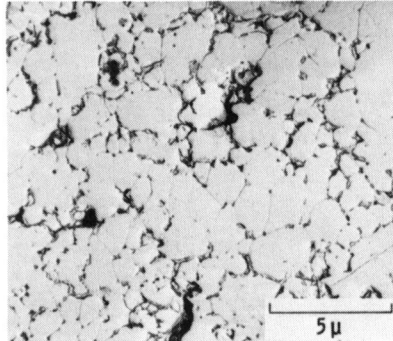
## REPLICA PHOTOMICROGRAPHS OF SINTERED AND HOT ISOSTATIC PRESSED $\alpha$ -SiC



DRY-PRESSED/SINTERED



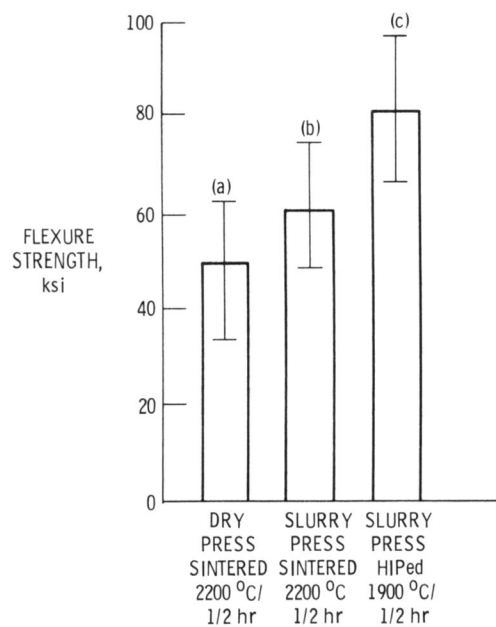
SLURRY-PRESSED/SINTERED



SLURRY-PRESSED/HIPed

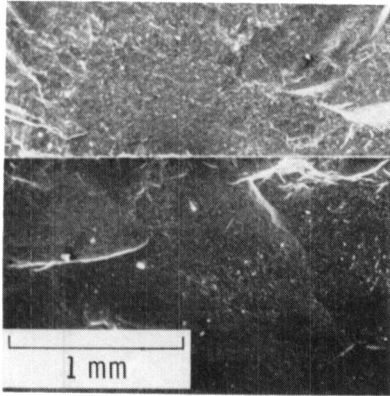
CD-86-19190

## ROOM TEMPERATURE FLEXURE STRENGTH OF SINTERED VS HIPed SILICON CARBIDE

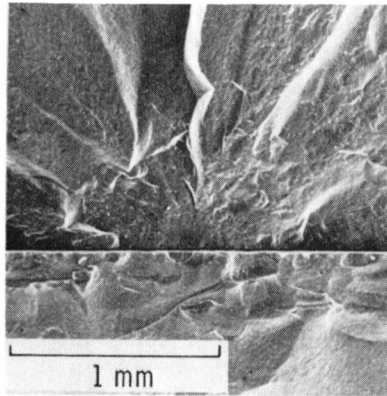


CD-86-19196

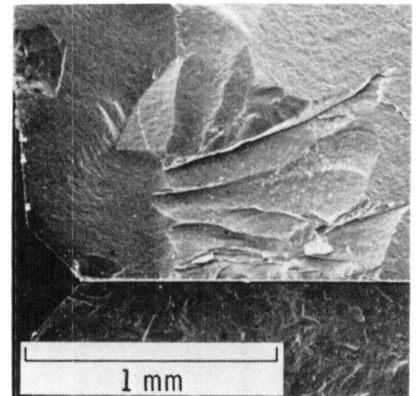
## ROOM TEMPERATURE FRACTURE OF HOT ISOSTATIC PRESSED $\alpha$ -SiC



$\sigma_f - 445$  MPa



$\sigma_f - 480$  MPa



$\sigma_f - 530$  MPa

CD-86-19191

## CONCLUSIONS

- DRY PRESSING / SINTERING OF STARCK ALPHA SILICON CARBIDE PRODUCED HIGH DENSITY BODIES WITH AN AVERAGE FLEXURE STRENGTH (4-POINT BEND) OF 350 MPa (50 ksi).
- IN CONTRAST, SLURRY PRESSING / SINTERING PRODUCED AN AVERAGE STRENGTH OF 430 MPa (62 ksi), A 30% IMPROVEMENT IN STRENGTH.
- FURTHER, SLURRY PRESSING / HOT ISOSTATIC PRESSING (HIPing) PRODUCED HIGH DENSITY BODIES AT 1850 - 1900 °C, WITH AN AVERAGE STRENGTH OF 580 MPa (84 ksi). THIS STRENGTH VALUE IS 60% HIGHER THAN THE DRY-PRESSED / SINTERED STRENGTH, AND 30% HIGHER THAN THE SLURRY-PRESSED / SINTERED STRENGTH.
- THE SLURRY-PRESSED / HIPed MATERIAL EXHIBITED AN ULTRAFINE GRAINED (0.3 - 3  $\mu$ m) MICROSTRUCTURE AS COMPARED TO 1 - 30  $\mu$ m PRODUCED BY SINTERING.
- PROCESS RELATED DEFECTS SUCH AS LARGE VOIDS, AND SHRINKAGE CRACKS WERE NOT OBSERVED IN HIPed SILICON CARBIDE.



## IMPROVED SILICON NITRIDE FOR ADVANCED HEAT ENGINES

H.C. Yeh  
AiResearch Casting Company  
Torrance, CA 90509

and

J.M. Wimmer  
Garrett Turbine Engine Company  
Phoenix, AZ

Silicon nitride is a high temperature material currently under consideration for heat engine and other applications. This presentation describes the progress made in the first 1-1/2 years of a NASA funded, 5 year program on improved  $\text{Si}_3\text{N}_4$ . The objective of this program is to improve the net shape fabrication technology of  $\text{Si}_3\text{N}_4$  by injection molding. This is to be accomplished by optimizing the process through a series of statistically designed matrix experiments. To provide input to the matrix experiments, a wide range of alternate materials and processing parameters were investigated throughout the whole program.

The improvement in the processing is to be demonstrated by a 20 percent increase in strength and a 100 percent increase in the Weibull modulus over that of the ACC baseline material. A full characterization of the baseline material/process was completed. The room temperature MOR and Weibull modulus of the as-processed test bars were established as 79.3 ksi and 7.9, respectively. In the first iteration of the MOR matrix experiments, a material with a room temperature MOR of 97 ksi and a Weibull modulus of 14 has been developed.

Material properties were found to be highly dependent on each step of the process. Several important parameters identified thus far are the starting raw materials, sinter/HIP cycle, powder bed, mixing methods, and sintering aid levels.

## OBJECTIVES

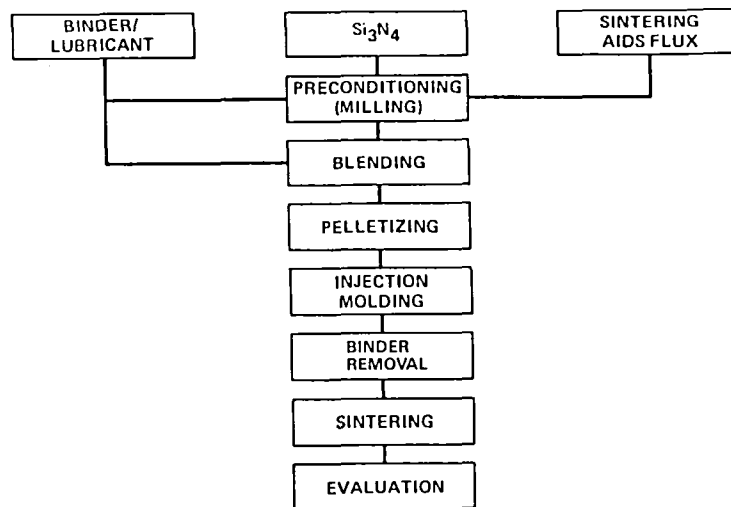
- DEVELOP FABRICATION TECHNOLOGY BASE
- INCREASE THE AS PROCESSED TEST BAR STRENGTH BY 20% (RT THRU 2550°F)
- INCREASE WEIBULL MODULUS BY 100%
- ACHIEVE INJECTION MOLDING CAPABILITY FOR LARGE COMPONENTS

## NASA WORK STATEMENT: SCHEDULE AND EFFORT

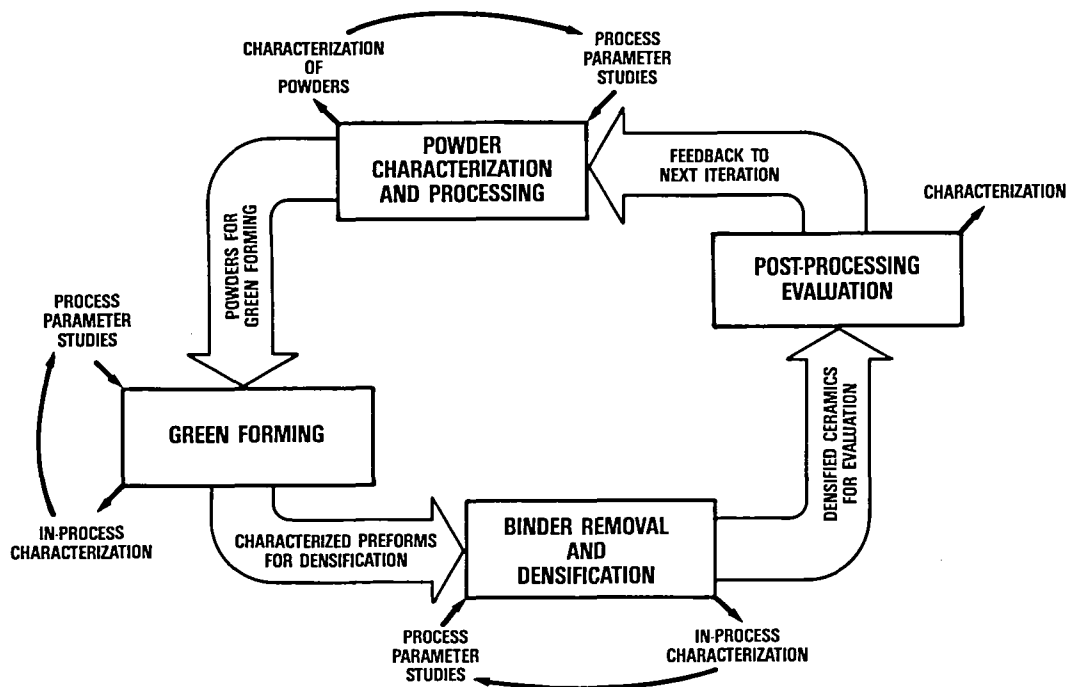
TASK NO.	DESCRIPTION	PERCENT EFFORT	YEARS FROM CONTRACT INITIATION				
			1	2	3	4	5
			← PHASE I			PHASE II →	
I.	BASLINE CHARACTERIZATION	5	■				
II.	MOR MATRIX	25		■	■		
III.	OPTIMIZED MOR	5			■		
IV.	BASLINE LARGE SHAPE	10			■	■	
V.	LARGE SHAPE MATRIX	25				■	■
VI.	OPTIMIZED LARGE SHAPE	10					■
VII.	MATERIAL/PROCESS IMPROVEMENT	15	■	■	■	■	■
VIII.	REPORTS/PROJECT MANAGEMENT	5	■	■	■	■	■

SPA 8596-74A

# INJECTION MOLDING PROCESS



## ITERATIVE APPROACH FOR IMPROVING CERAMIC MATERIAL PROPERTIES AND PROCESS CONTROLS



SPA 8777-5

## PROCESSING VARIABLES

### STARTING POWDER

- ALTERNATE  $\text{Si}_3\text{N}_4$
- ALTERNATE ADDITIVES
- LOT VARIATIONS

### COMPOSITION

- %  $\text{Al}_2\text{O}_3$ ,  $\text{Y}_2\text{O}_3$
- $\text{ZrO}_2$
- $\text{Y}_2\text{O}_3$ - $\text{SiO}_2$

### POWDER PROCESSING

- ALTERNATE MILLING
- CLASSIFICATION
- ELUTRIATION/WASHING
- MILLING AIDS
- TIME

### TOOLING

- GATE SIZE
- GATE ORIENTATION
- SEPARATION DESIGN
- TEST BARS PER SHOT

### ADDITIVES

- ALTERNATE BINDERS
- % BINDER
- PLASTICIZER
- WETTING AGENT
- LUBRICANT
- DISPERSANT
- ACID-BASE CONTROL

### MIXING

- MIXER
- TIME
- TEMPERATURE
- SHEAR RATE
- SOLVENT
- VACUUM

### INJECTION MOLDING

- MACHINE
- TEMPERATURES
- PRESSURE
- RAM SPEED
- VACUUM

### DEWAX

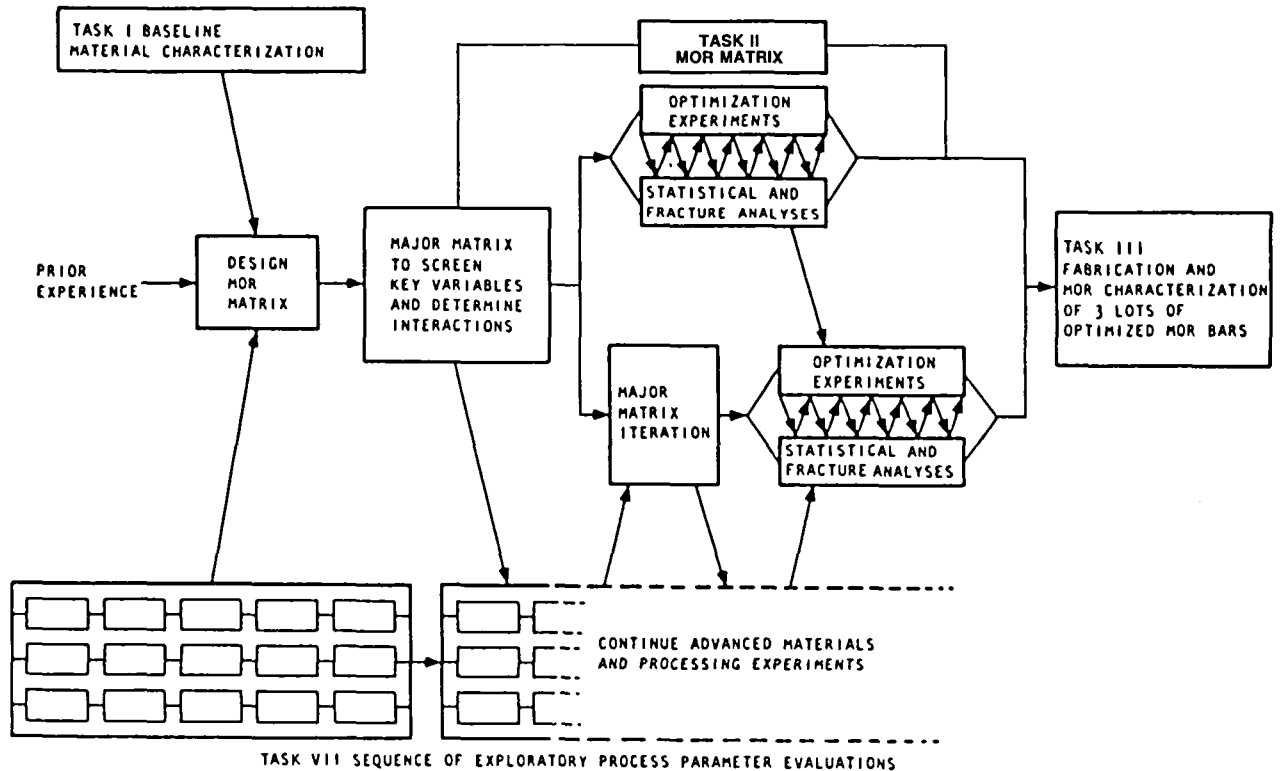
- TEMPERATURE
- PRESSURE
- CYCLE
- APPROACH
- TIME
- EQUIPMENT
- CYCLE

### SINTERING

- TIME
- TEMPERATURE
- OVERPRESSURE
- CYCLE
- EQUIPMENT
- FIXTURING

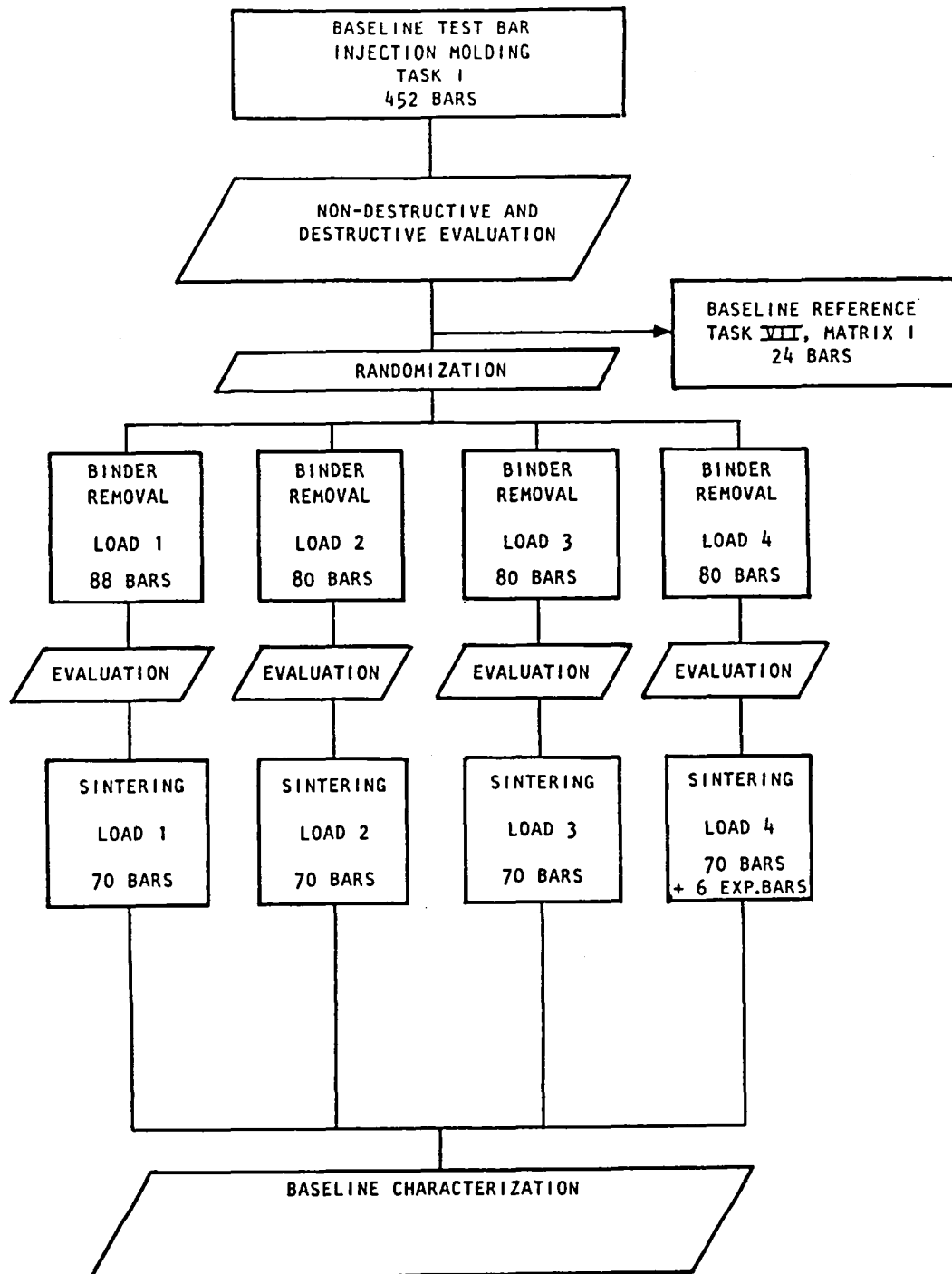
SPA 8596-191A

## PHASE I DIRECTED TOWARDS TEST BARS



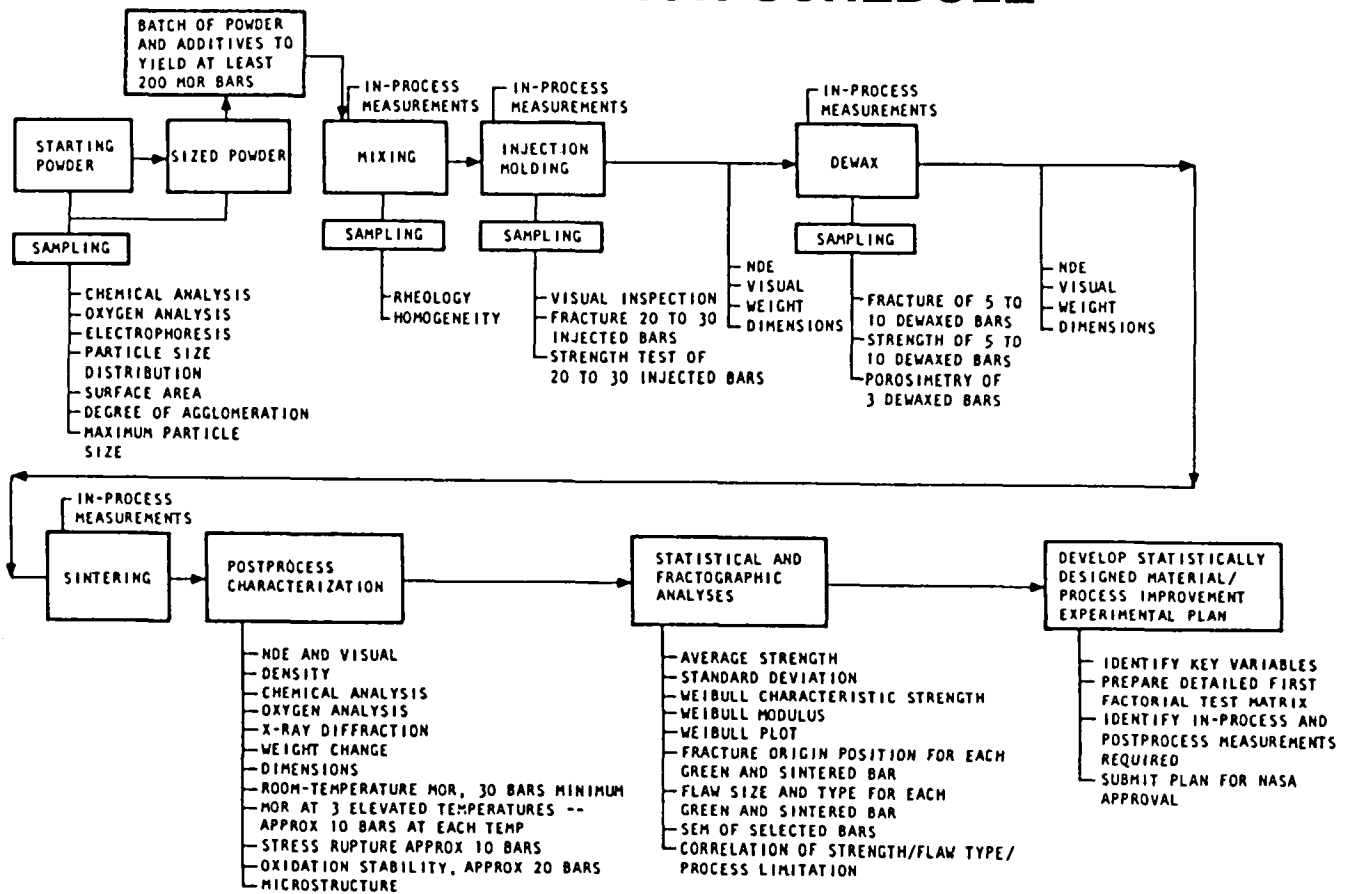
SPA 8596-79C

# NASA IMPROVED $\text{Si}_3\text{N}_4$



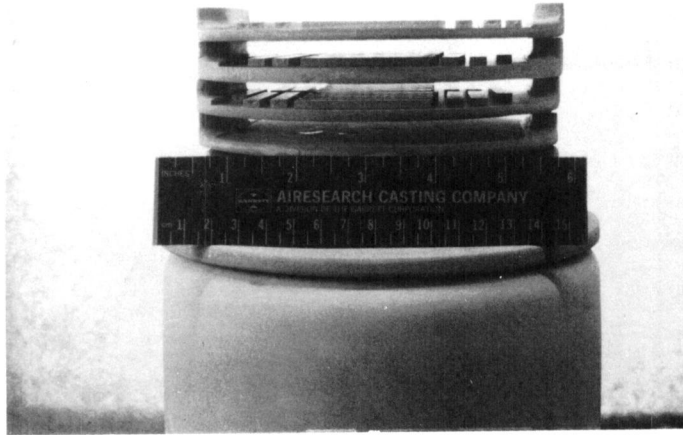
SPA 8597-48

# NASA IMPROVED $\text{Si}_3\text{N}_4$ TASK I PROCESS FLOW CHART AND CHARACTERIZATION SCHEDULE

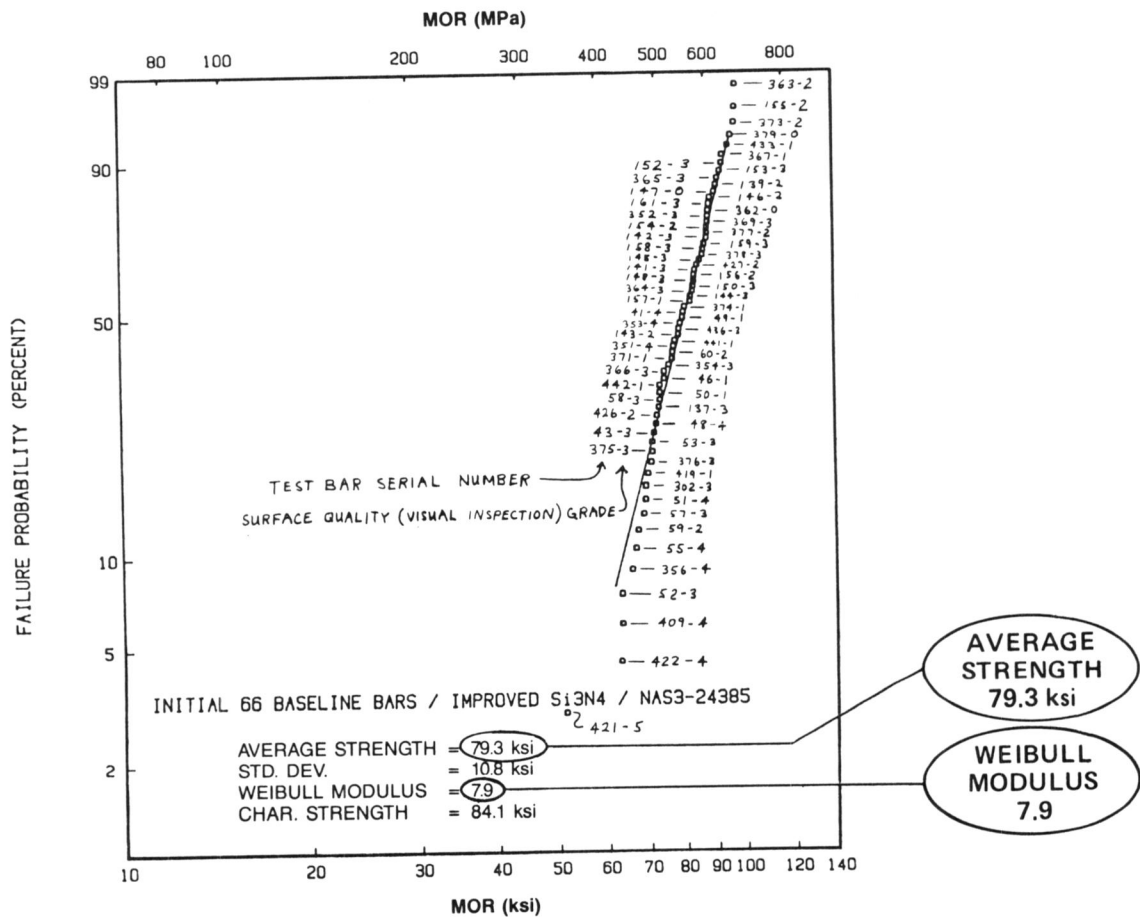


SPA 8596-80A

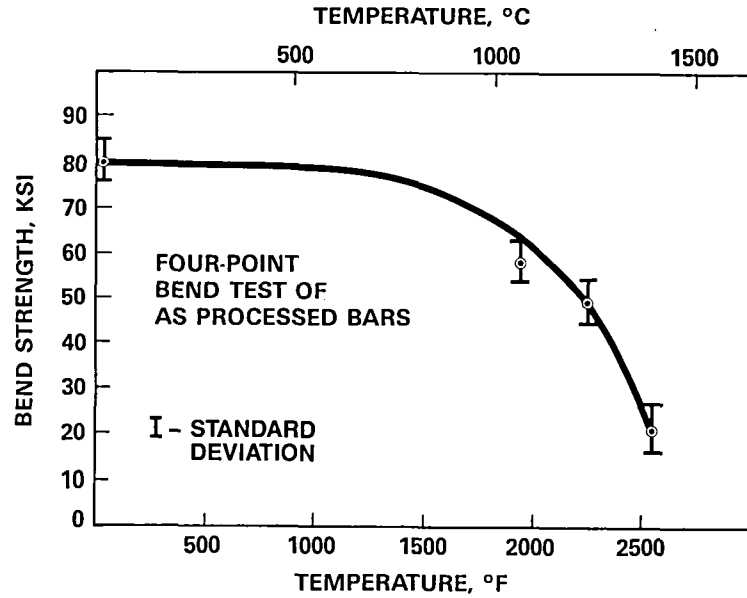
## TEST BAR SINTERING SUPPORT



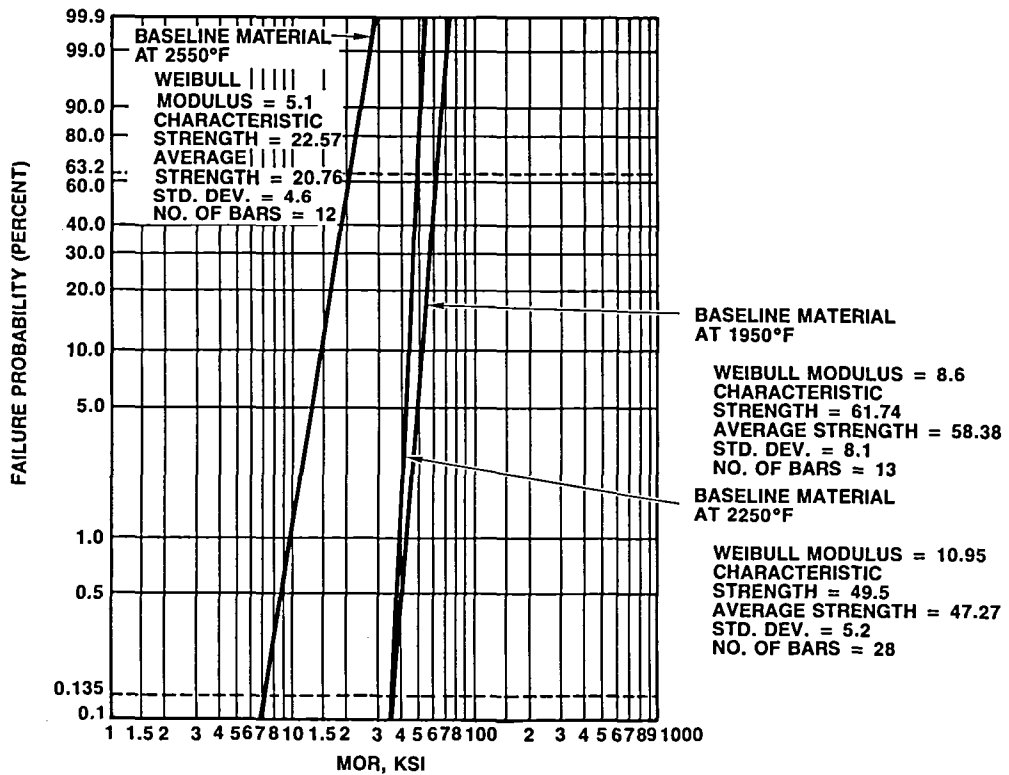
## WEIBULL ANALYSIS OF BASELINE ROOM TEMPERATURE DATA



## BASELINE STRENGTH



## WEIBULL DISTRIBUTION FOR HIGH TEMPERATURE DATA



SPA 8734-10A



# **BASELINE STRESS RUPTURE**

## **PRELIMINARY TEST CONDITIONS**

1800°F	2200°F	2500°F
10 KSI — 24 HR	10 KSI — 24 HR	10 KSI — 9 HR, 42 MIN
20 KSI — 24 HR	20 KSI — 24 HR	
30 KSI — 24 HR	30 KSI — 24 HR	
40 KSI — 1 MIN	40 KSI — 24 HR	
	50 KSI — 0	

## **FINAL TEST RESULTS**

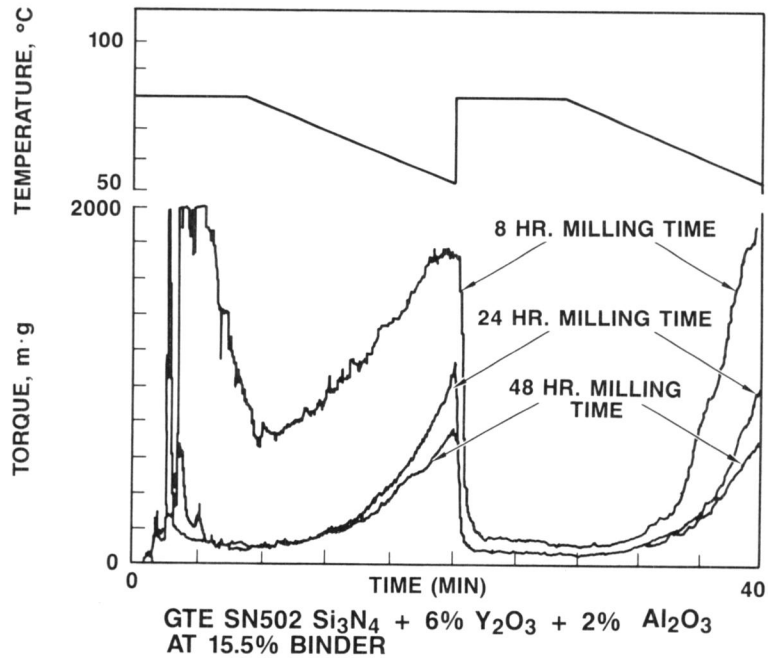
40 KSI — 7 HR, 22 MIN	40 KSI — 0	
40 KSI — 17 HR, 19 MIN	30 KSI — 1 MIN	
30 KSI — 100 HR (SURVIVED)	30 KSI — 3 HR, 38 MIN	
	30 KSI — 4 HR, 55 MIN	

SPA 8794-1

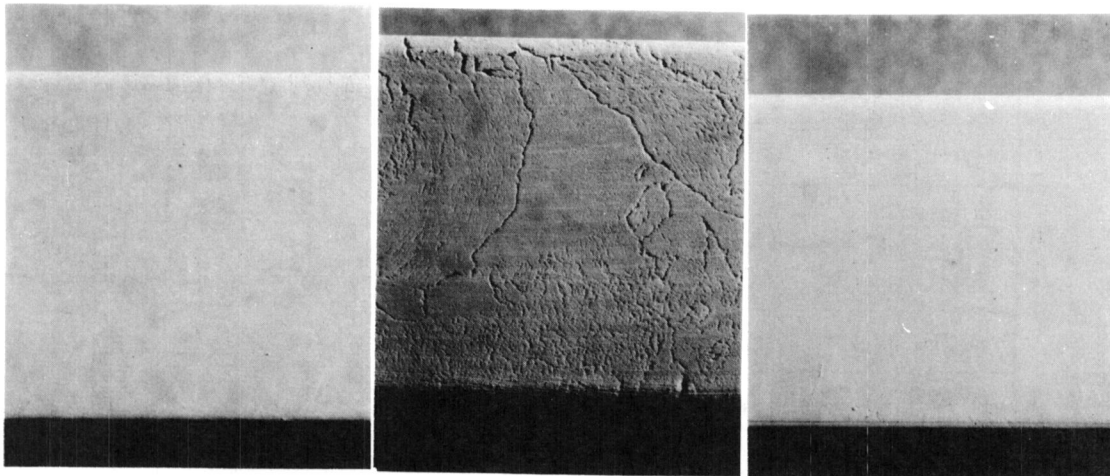
# **TASK VII EXPERIMENTAL MATRIXES**

PROCESS VARIABLE	EXPERIMENTAL MATRIX NUMBER						
	1	2	3	4	5	6	7
RAW MATERIAL	X				X	X	
BINDER		X			X	X	X
BINDER EXTRACTION			X			X	X
INJECTION MOLDING			X			X	
POWDER PREPARATION (MILLING)			X		X		
COMPOSITION				X			
SINTERING	X			X		X	

## MIXING BEHAVIOR COMPARISON ON TORQUE RHEOMETER



## AS INJECTED TEST BAR SURFACES



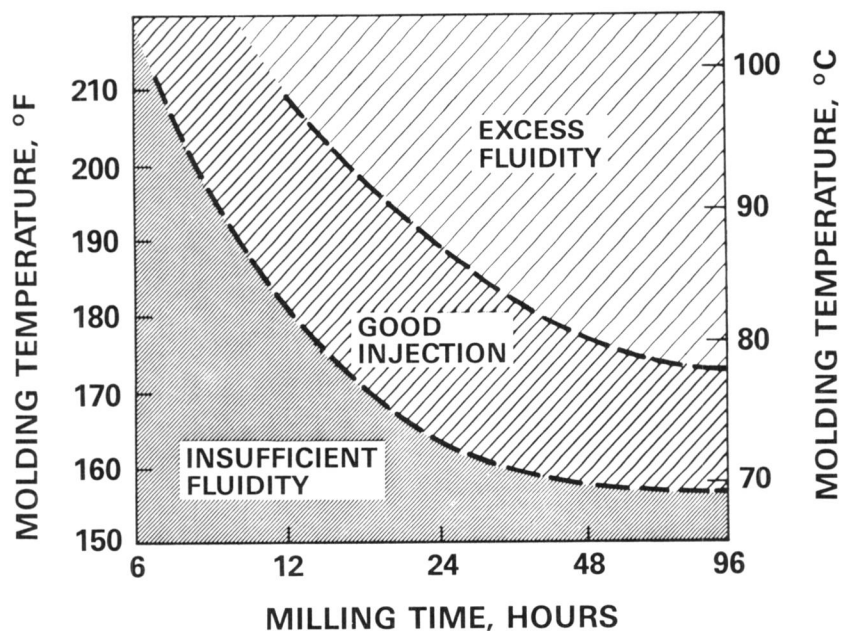
**A. 8 HR. MILLING**  
99°C (210°F) MOLDING

**B. 8 HR. MILLING**  
77°C (170°F) MOLDING

**C. 24 HR. MILLING**  
77°C (170°F) MOLDING

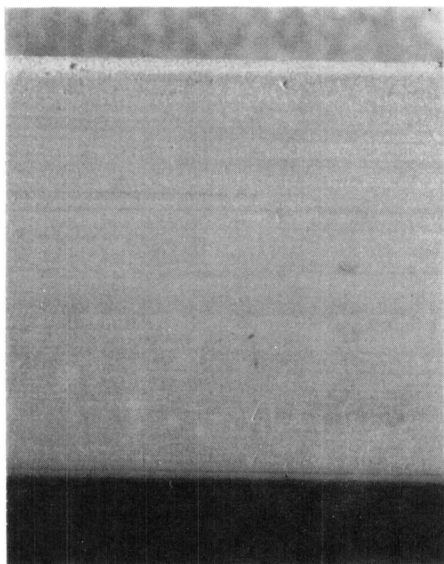
GTE SN502  $\text{Si}_3\text{N}_4$  + 6%  $\text{Y}_2\text{O}_3$  + 2%  $\text{Al}_2\text{O}_3$  AT 15.5% BINDER

## FLOW CHARACTERISTICS OF INJECTION MOLDING



## NASA IMPROVED $\text{Si}_3\text{N}_4$

SURFACE CHANGE DURING DEWAX — 96 HOUR MILLED POWDER

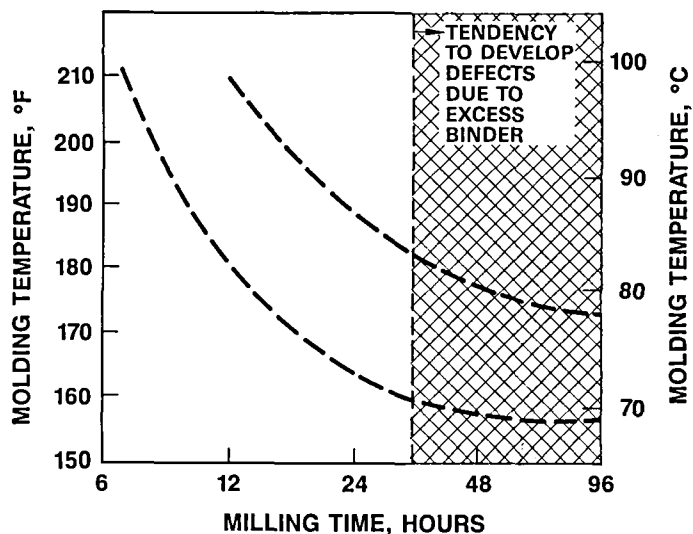


AS INJECTED



DEWAXED

## DEWAX EFFECT



## NASA IMPROVED Si<sub>3</sub>N<sub>4</sub>

### TASK II EXPERIMENTAL MATRIX 1/2 REPLICATE OF A 2<sup>5</sup> FRACTIONAL FACTORIAL DESIGN

		C+				C-			
		D+		D-		D+		D-	
		E+	E-	E+	E-	E+	E-	E+	E-
A+	B+		abcd	abce		abde			ab
	B-	acde			ac		ad	ae	
A-	B+	bcde			bd		bd	be	
	B-		cd	ce		de			1

A = CONSOLIDATION METHODS — SINTER/HIP CYCLE (A-) VS CYCLE (A+)

B = CONSOLIDATION ENVIRONMENT — WITHOUT POWDER BED (B-) VS WITH POWDER BED (B+)

C = MIXING — SIGMA MIXER (C-) VS SIGMA MIXER PLUS EXTRUDER (C+)

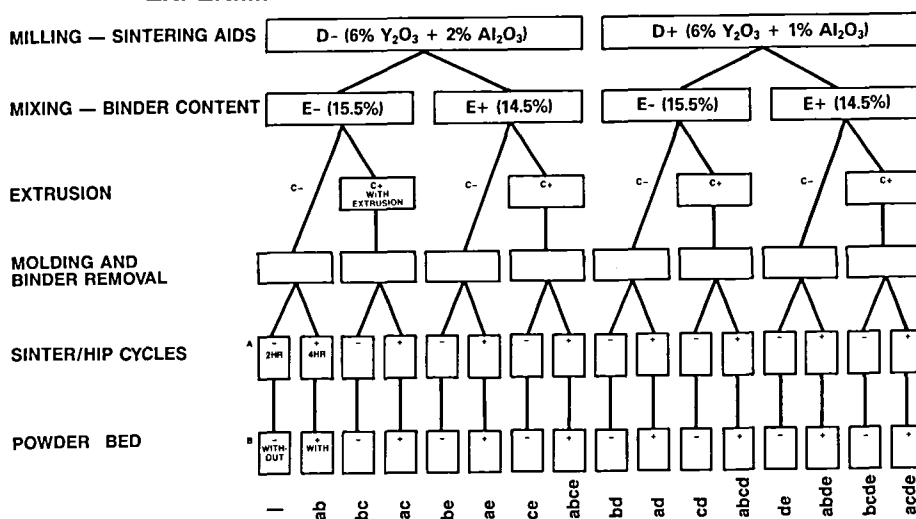
D = SINTERING AIDS — (6% Y<sub>2</sub>O<sub>3</sub> + 2% Al<sub>2</sub>O<sub>3</sub>) (D-) VS (6% Y<sub>2</sub>O<sub>3</sub> + 1% Al<sub>2</sub>O<sub>3</sub>) (D+)

E = BINDER CONTENT — 15.5% (E-) VS 14.5% (E+)

SPA 8962.97A

# NASA IMPROVED $\text{Si}_3\text{N}_4$

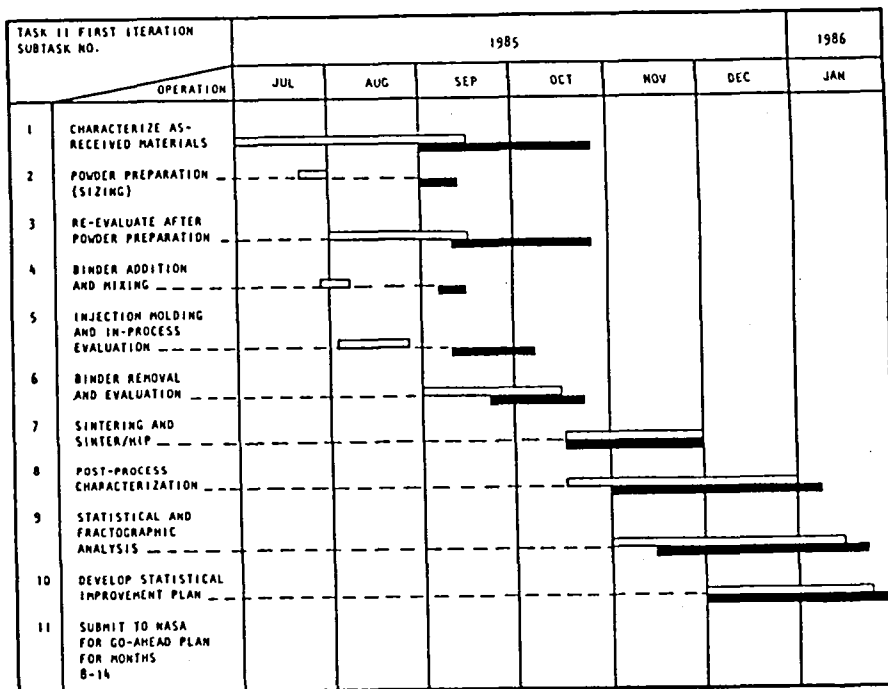
## EXPERIMENTAL MATRIX PROCESS FLOW CHART



SPA 868798A

## TASK II — MOR BAR MATRIX STUDY

MONTHS 1 THROUGH 7



## TASK II TORQUE CHARACTERIZATION

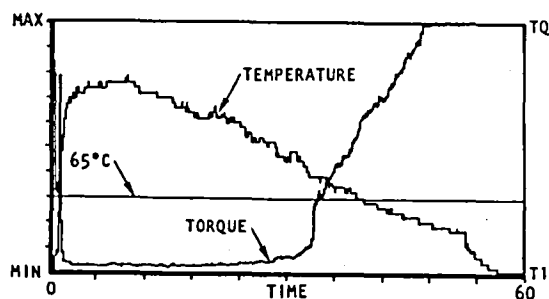
MIXING VARIATION	TORQUE AT 65°C (150°F), m·g			
	D- (6% Y <sub>2</sub> O <sub>3</sub> + 2% Al <sub>2</sub> O <sub>3</sub> )		D+ (6% Y <sub>2</sub> O <sub>3</sub> + 1% Al <sub>2</sub> O <sub>3</sub> )	
	E- (15.5% BINDER)	E+ (14.5% BINDER)	E- (15.5% BINDER)	E+ (14.5% BINDER)
MATRIX II-1 INJECTION MOLDING BATCHES				
C-	1450	1500	1386	1544
C+ (EXTRUDED)	1100	1452	762	1290
MATRIX II-2 INJECTION MOLDING BATCHES				
C-	876	1304	948	1175
C+ (EXTRUDED)	439	796	500	748

### NOTES

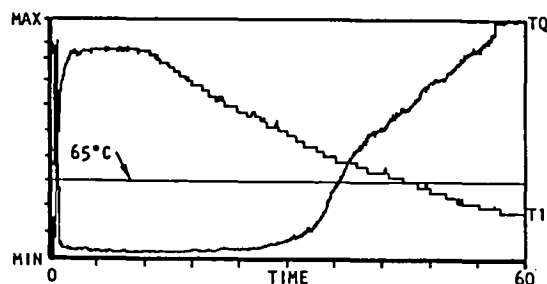
1. VALUES ARE FROM SINGLE MIXER RUNS
2. MIXER COOLING RATE WAS 1°C (1.8°F) PER MINUTE
3. m·g = meter·gram

## MATRIX II-1 TORQUE CHARACTERIZATION

### EFFECT OF BINDER CONTENT ON RHEOLOGY



15.5% BINDER



14.5% BINDER

# MATRIX II-1 AND II-2 X-RADIOGRAPHIC YIELD

## AS-INJECTED BARS

MIXING PROCEDURE	YIELD IN PERCENT			
	D- (6% Y <sub>2</sub> O <sub>3</sub> + 2% Al <sub>2</sub> O <sub>3</sub> )		D+ (6% Y <sub>2</sub> O <sub>3</sub> + 1% Al <sub>2</sub> O <sub>3</sub> )	
	E- (15.5% BINDER)	E+ (14.5% BINDER)	E- (15.5% BINDER)	E+ (14.5% BINDER)
	MATRIX II-1, STARCK H-1 Si <sub>3</sub> N <sub>4</sub> , 200 BARS INJECTED FOR EACH CONDITION			
C-	77	77	69	76
C+ (EXTRUDED)	87	92	68	92
C- C+ (EXTRUDED)	MATRIX II-2, DENKA 9FW Si <sub>3</sub> N <sub>4</sub> , 160 BARS INJECTED FOR EACH CONDITION			
	95	95	95	95
	96	96	98	96

## ROOM TEMPERATURE MOR AND WEIBULL SLOPE (MATRIX II-2)

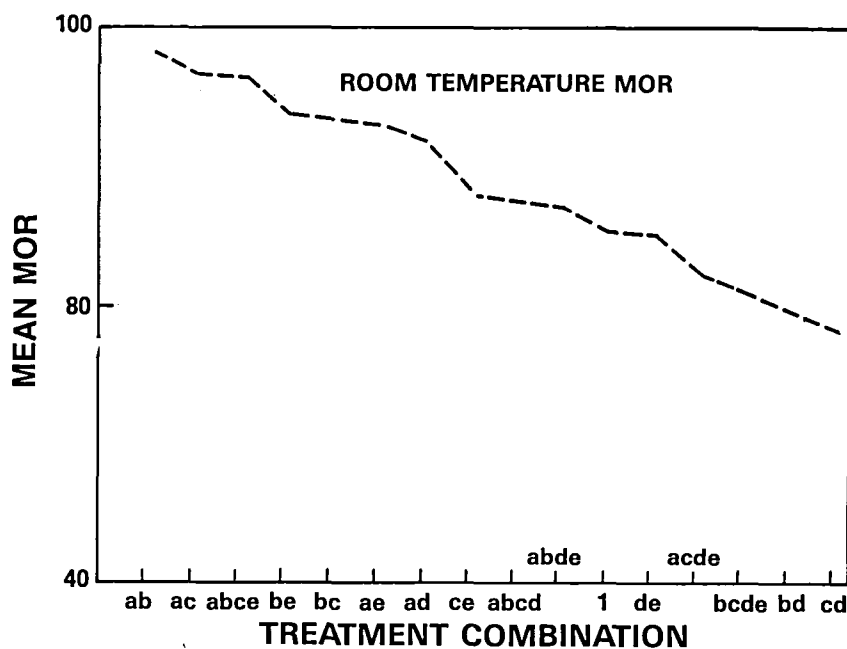
PROCESSING CONDITION	AVERAGE STRENGTH,* ksi	WEIBULL SLOPE
1	82.90	6.97
ab	97.25	13.63
bc	91.96	7.66
ac	95.58	12.73
be	92.18	10.15
ae	91.56	10.13
bd	76.20	12.84
de	82.84	7.01
ce	85.69	7.94
abce	95.28	13.44
abcd	85.02	11.24
abde	84.84	19.93
bcde	77.73	9.74
acde	78.95	5.32
ad	89.30	12.18
cd	74.40	5.64

\*30 SAMPLES TESTED FOR EACH CONDITION

---

## MATRIX II-2 MOR (DENKA 9FW)

---



---

## STATISTICAL ANALYSIS

---

### MATRIX II-2

- PROCESSING FACTORS HAVING SIGNIFICANT EFFECTS ON MOR

A, B AND D

- TWO FACTOR INTERACTIONS HAVING SIGNIFICANT EFFECTS ON MOR

B × C, B × D AND C × D

NOTE: A — SINTERED/HIP  
B — POWER BED  
C — MIXING  
D — SINTERING AID



---

## SINTER/HIP CYCLE EFFECT

---

### MATRIX II-2

SINTERING/HIP 2 HRS	SINTERING/HIP 4 HRS
83.2 ksi	89.8 ksi

DIFFERENCE = 6.6 ksi

---

## POWDER BED AND SINTERING AIDS EFFECTS

---

### MATRIX II-2

	(B+) PB*	(B-) NO PB*
(D+) 6% Y <sub>2</sub> O <sub>3</sub> + 2% Al <sub>2</sub> O <sub>3</sub>	81.0 Ksi	81.6 Ksi
(D-) 6% Y <sub>2</sub> O <sub>3</sub> + 1% Al <sub>2</sub> O <sub>3</sub>	94.3 Ksi	89.1 Ksi

\*PB: POWDER BED

---

## POWDER BED AND MIXING METHOD EFFECTS

---

### MATRIX II-2

	(B+) PB*	(B-) NO PB*
(C+) SIGMA MIXER AND EXTRUDER	87.7 Ksi	83.9 Ksi
(C-) SIGMA MIXER	87.6 Ksi	86.8 Ksi

\*PB: POWDER BED

### SUMMARY

- AVERAGE STRENGTH AND WEIBULL MODULUS OF BASELINE AS-PROCESSED, RANDOMLY SELECTED INJECTION MOLDED, SINTERED  $\text{Si}_3\text{N}_4$  SAMPLES ARE 547 MPa (79.3 ksi) AND 7.9 RESPECTIVELY
- STRENGTH AND AS-PROCESSED SURFACE QUALITY ARE CLOSELY RELATED
- TORQUE RHEOMETRY HAS THE POTENTIAL TO PREDICT INJECTION MOLDING BEHAVIOR
- GOOD QUALITY AS-INJECTED BARS CAN DEGRADE DURING DEWAX IF THEY ARE PROCESSED WITH EXCESS BINDER
- FINAL TEST BAR PROPERTIES STRONGLY DEPEND ON EACH PROCESSING STEP

(CONTINUED)

---

## SUMMARY

---

- **A MATERIAL WITH A MEAN STRENGTH OF 97 Ksi AND A WEIBULL MODULUS OF 14 HAS BEEN DEVELOPED BY A STATISTICALLY DESIGNED MATRIX EXPERIMENT**
- **STATISTICAL ANALYSIS CAN IDENTIFY KEY PROCESSING PARAMETERS AND PROCESSING VARIATIONS**



## IMPROVED PROCESSING OF $\text{Si}_3\text{N}_4$

William A. Sanders  
NASA Lewis Research Center  
Cleveland, Ohio 44135

and

George Y. Baaklini  
Cleveland State University  
Cleveland, Ohio 44115

A sintered  $\text{Si}_3\text{N}_4$ - $\text{SiO}_2$ - $\text{Y}_2\text{O}_3$  composition, NASA 6Y, was developed that reached four-point flexural average strength/standard deviation values of 857/36, 544/33, and 462/59 MPa at room temperature, 1200 and 1370 °C respectively. These strengths represented improvements of 56, 38, and 21 percent over baseline properties at the three test temperatures. At room temperature the standard deviation was reduced by more than a factor of three. These accomplishments were realized by the iterative utilization of conventional x-radiography to characterize structural (density) uniformity as affected by systematic changes in powder processing and sintering parameters. Accompanying the improvement in mechanical properties was a change in the type of flaw causing failure from a pore to a large columnar  $\beta$ - $\text{Si}_3\text{N}_4$  grain typically 40-80  $\mu\text{m}$  long, 10-30  $\mu\text{m}$  wide, and with an aspect ratio of 5:1.

# IMPROVED PROCESSING OF $\text{Si}_3\text{N}_4$

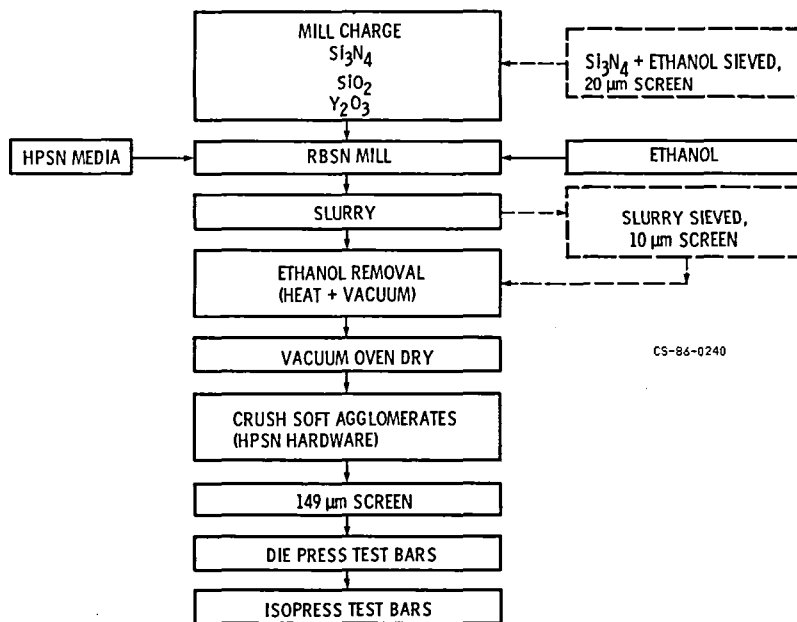
## OBJECTIVE

TO IMPROVE THE STRENGTH AND UNIFORMITY OF SINTERED SILICON NITRIDE BY A SYSTEMATIC INVESTIGATION OF POWDER PROCESSING AND SINTERING VARIABLES AS THEY AFFECT RADIO GRAPHICALLY CHARACTERIZED DENSITY GRADIENTS, AND CONSEQUENTLY THE STRENGTH LEVEL AND SCATTER OF SILICON NITRIDE

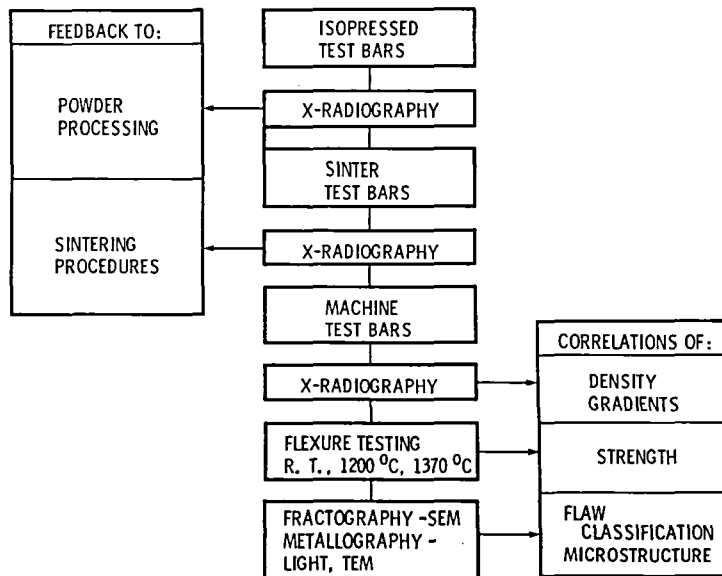
CHARACTERIZATION OF SILICON NITRIDE AND OXIDE POWDERS

MATERIAL	SOURCE	MANUFACTURERS DESIGNATION	PURITY, %	SPECIFIC SURFACE AREA, $\text{m}^2 \cdot \text{g}^{-1}$	X-RAY DIFFRACTION ANALYSIS, %			CHEMICAL ANALYSIS		
					$\alpha$	$\beta$	FREE SI	OXYGEN, wt %	CARBON, wt %	SPECTROGRAPHIC ANALYSIS, ppm
$\text{Si}_3\text{N}_4$	KBI-AME	HIGH PURITY	99.5	4.7	83.7	15.7	0.6	0.89	0.18	240Al, 60Ca, 20Co, 50Cr, 1280Fe, 20Mg, 30Mn, 40Ti, 40V, 590Y, 30Zn, 10Zr
$\text{SiO}_2$	APACHE CHEMICALS	6846	99.99	166	----	----	---	----	.16	220Al, 150Ca, 30Cr, 50Cu, 50Fe, 130Mg, 90Mn, 340Na, 40Ti
$\text{Y}_2\text{O}_3$	MOLYCORP	5600	99.9	7.5	----	----	---	---	.11	60Cu, 60Mg, 40 R. E. OXIDES

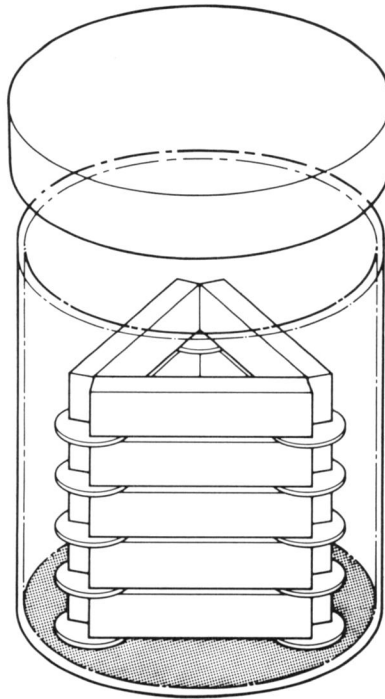
## POWDER PROCESSING OF NASA 6Y Si<sub>3</sub>N<sub>4</sub>



## EVALUATION OF NASA 6Y Si<sub>3</sub>N<sub>4</sub>

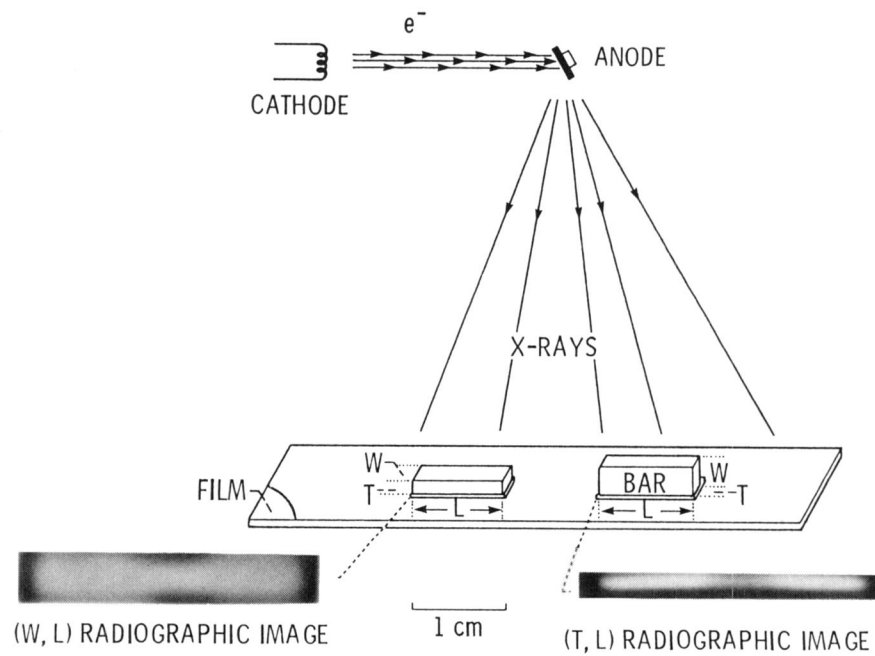


## Si<sub>3</sub>N<sub>4</sub> BAR/BN SETTER ARRANGEMENT IN W SINTER CUP



CS-86-0235

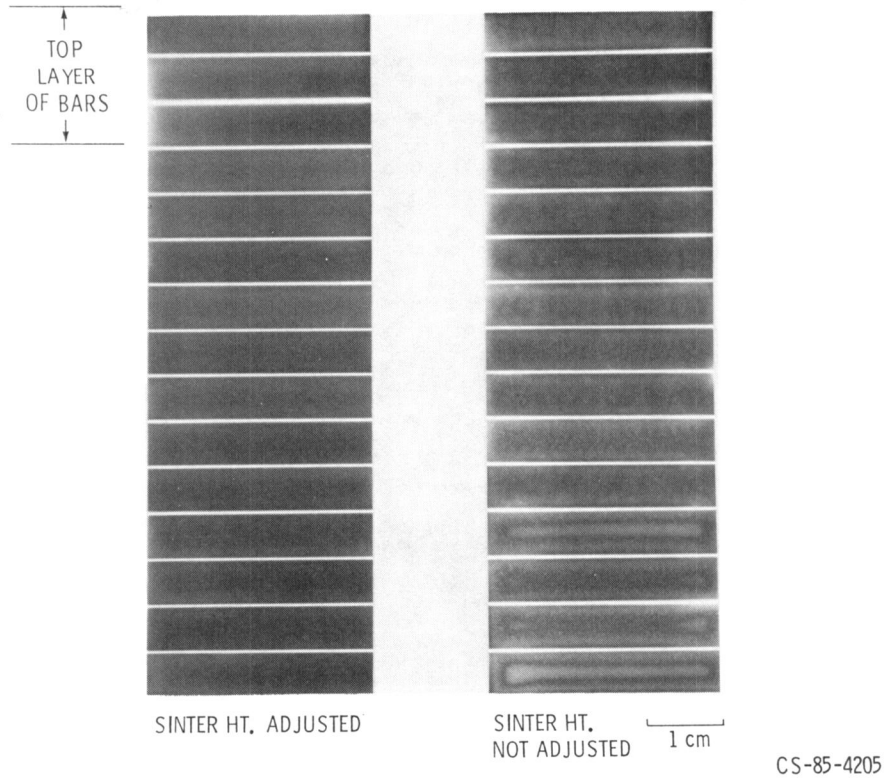
## CONVENTIONAL RADIOGRAPHY OF NASA 6Y Si<sub>3</sub>N<sub>4</sub> TEST BARS



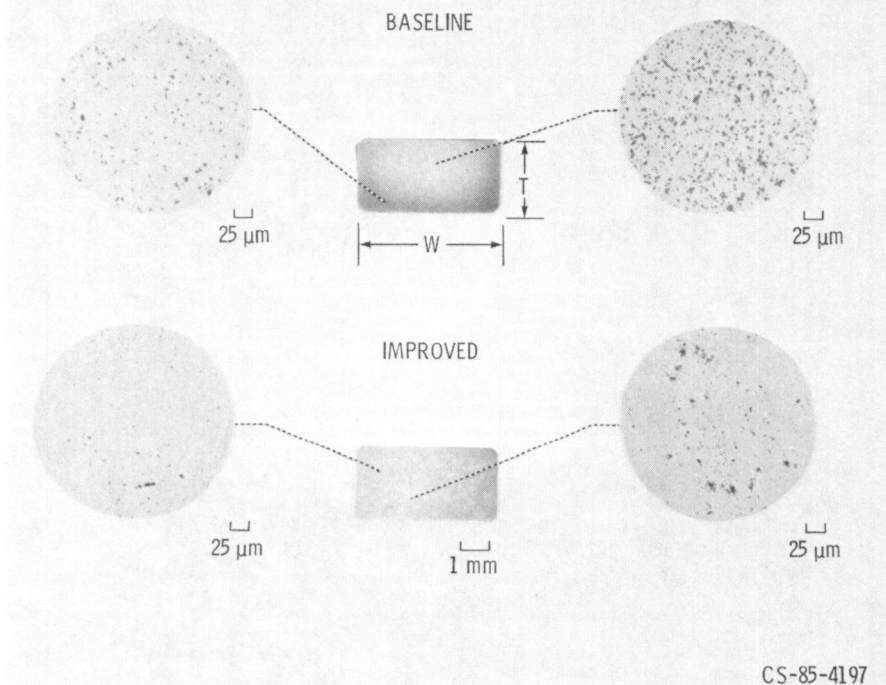
CS-85-4207



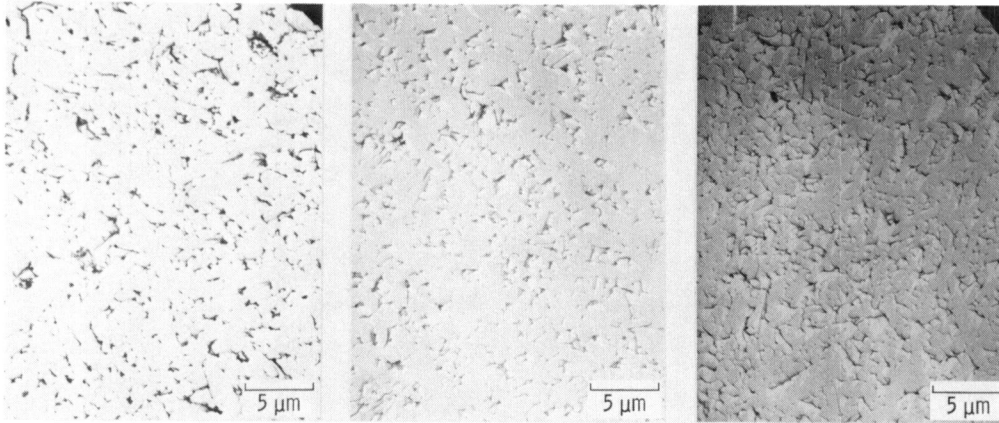
# RADIOGRAPHS OF 15-BAR SINTER-GROUPS OF NASA 6Y Si<sub>3</sub>N<sub>4</sub>



## CASE-CORE STRUCTURE COMPARISON FOR BASELINE AND IMPROVED NASA 6Y Si<sub>3</sub>N<sub>4</sub>



## TEM MICROSTRUCTURES OF NASA 6Y $\text{Si}_3\text{N}_4$ EFFECT OF GRINDING TIME



tg = 24 hr

0.3 - 4.0  $\mu\text{m}$  EQUIAX  
0.35 - 3.5  $\mu\text{m}$  COLUM. WIDTH  
1:2 TO 1:6 ASPECT RATIO  
70 VOL. % COLUM.

tg = 100 hr

0.2 - 3.5  $\mu\text{m}$  EQUIAX  
0.4 - 2.0  $\mu\text{m}$  COLUM. WIDTH  
1:2 TO 1:14 ASPECT RATIO  
40 VOL. % COLUM.

tg = 300 hr

0.2 - 3.0  $\mu\text{m}$  EQUIAX  
0.25 - 2.0  $\mu\text{m}$  COLUM. WIDTH  
1:2 TO 1:8 ASPECT RATIO  
20 VOL. % COLUM.

CS-85-4209

### SINTERING CONDITIONS AND RESULTS FOR $\text{Si}_3\text{N}_4\text{-SiO}_2\text{-Y}_2\text{O}_3$ COMPOSITION NASA 6Y SINTERED AT 2140 $^{\circ}\text{C}$

NASA 6Y BATCH NUMBER	MILLING TIME, hr	SINTERING CONDITIONS			SINTERING RESULTS <sup>a</sup>		
		TIME, hr	PN, MPa	BN SETTER CONTACT	AVERAGE WEIGHT LOSS, %	AVERAGE WIDTH SHRINKAGE, %	AVERAGE MACHINED DENSITY, $\text{g-cm}^{-3}$
BASELINE	24	1	2.5	MAX	3.85	15.6	3.12
11	100	↓	↓	MAX	5.14	17.6	3.23
13	100	↓	↓	MIN	4.93	17.6	3.24
12	300	↓	↓	MAX	5.74	18.0	3.25
14	300	↓	↓	MIN	5.42	17.5	3.24
15	24	2	5.0	↓	5.10	17.2	3.22
16	24	↓	↓	↓	4.44	16.8	3.23
17	100	↓	↓	↓	4.39	17.3	3.23
20	100	↓	↓	↓	2.81	17.2	3.22
25	300	↓	↓	↓	4.88	17.8	3.28
28 <sup>b</sup>	100	↓	↓	↓	3.77	17.3	3.21
29 <sup>b, c</sup>	100	↓	↓	↓	3.06	16.1	3.23
31 <sup>b, c</sup>	300	↓	↓	↓	3.71	17.3	3.24
21 (2050 $^{\circ}\text{C}$ )	100	↓	↓	↓	1.65	14.9	3.05

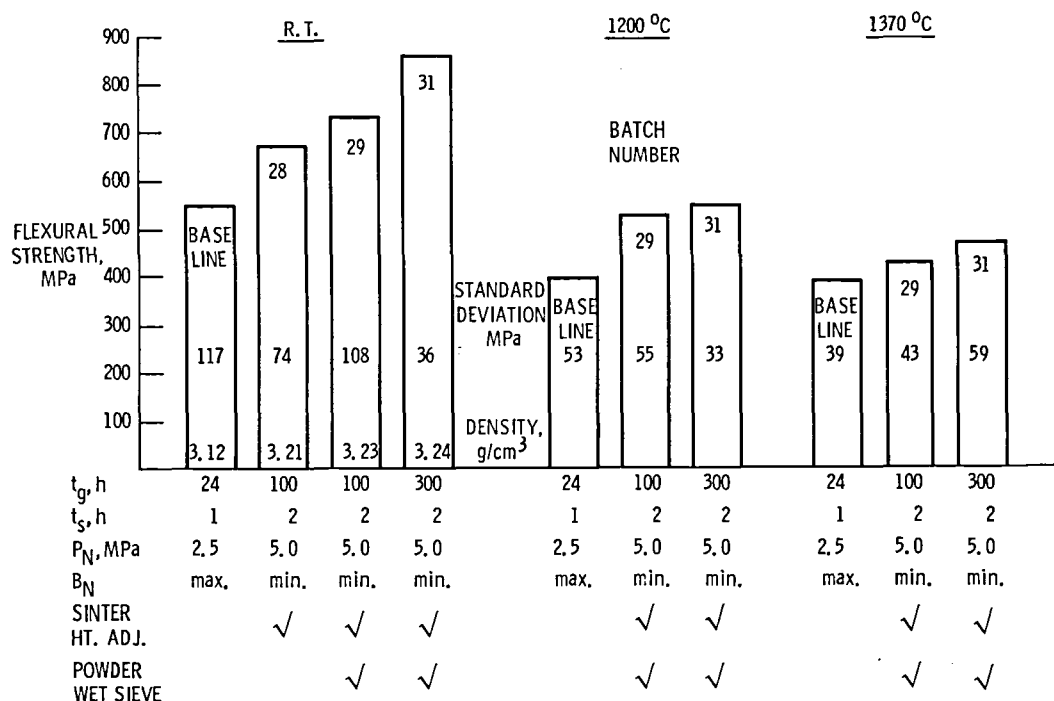
<sup>a</sup>AVERAGE FOR EACH COMPOSITION REPRESENT 30 BARS EXCEPT FOR BASELINE WHICH REPRESENTS 150 BARS AND BATCH 28 WHICH REPRESENTS 15 BARS.

<sup>b</sup>SINTER CUP RAISED 3.8 cm.

<sup>c</sup> $\text{Si}_3\text{N}_4$  POWDER WET SIEVED BEFORE AND AFTER MILLING.

CS-85-0223

# COMBINED EFFECT OF MODIFIED PROCESSING/SINTERING PROCEDURES ON THE FLEXURAL STRENGTH OF NASA 6Y Si<sub>3</sub>N<sub>4</sub>



CS-86-0232

## ASSESSMENT OF FRACTURE ORIGINS FOR NASA 6Y SINTERED Si<sub>3</sub>N<sub>4</sub>

		SUB-SURFACE PORE	SURFACE PORE	SEAM	SUB-SURFACE AGGLOMERATE	COLUMNAR GRAIN	SURFACE DEFECT	METALLIC INCLUSION
R.T. FLEXURE TEST	TOTAL FRACTURE ORIGINS IDENTIFIED	56	44	28	25	17	13	9
	PERCENT OF TOTAL	29	23	14	13	9	7	5
1200 °C FLEXURE TEST	TOTAL FRACTURE ORIGINS IDENTIFIED	23	19	9	7	14	0	18
	PERCENT OF TOTAL	26	21	10	8	15	0	20
1370 °C FLEXURE TEST	TOTAL FRACTURE ORIGINS IDENTIFIED	30	15	25	3	32	0	22
	PERCENT OF TOTAL	24	12	20	2	25	0	17

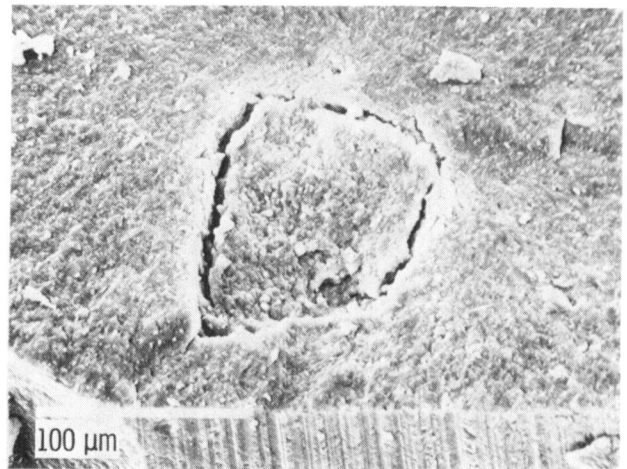
<sup>a</sup>NUMBER EXCLUDES 111, 47, AND 41 BARS FOR R.T., 1200 °C, AND 1370 °C, RESPECTIVELY, WHERE FLAW REGION OR FLAW TYPE COULD NOT BE DETERMINED.

CS-86-0234

## CRITICAL FLAWS IN R. T. FRACTURE OF NASA 6Y $\text{Si}_3\text{N}_4$



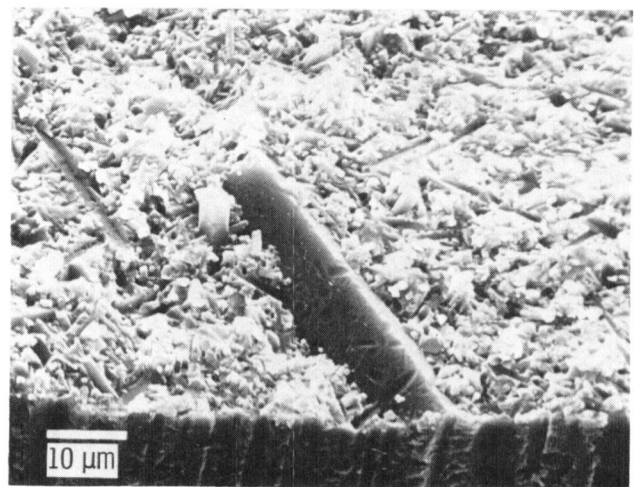
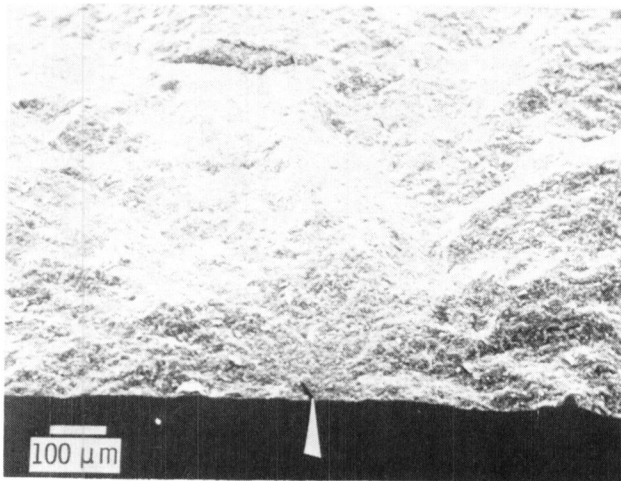
SURFACE PORE,  $\sigma_F = 620 \text{ MPa}$



AGGLOMERATE,  $\sigma_F = 470 \text{ MPa}$

CS-85-4199

## COLUMNAR $\text{Si}_3\text{N}_4$ GRAIN CRITICAL FLAW IN R. T. FRACTURE OF IMPROVED NASA 6Y $\text{Si}_3\text{N}_4$

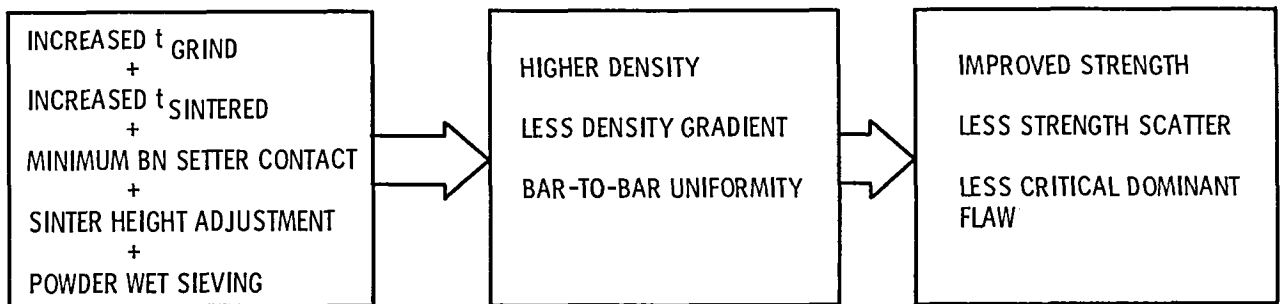


$\sigma_F = 905 \text{ MPa}$

CS-85-4201

## SUMMARY

APPLICATION OF CONVENTIONAL RADIOGRAPHY VERY BENEFICIAL IN GUIDING POWDER  
PROCESSING AND SINTERING PARAMETER CHANGES FOR IMPROVED  $\text{Si}_3\text{N}_4$





COLLOIDAL CHARACTERIZATION OF  
SILICON NITRIDE AND SILICON CARBIDE\*

Donald L. Feke  
Case Western Reserve University  
Cleveland, Ohio 44106

The colloidal behavior of aqueous ceramic slips strongly affects the forming and sintering behavior and the ultimate mechanical strength of the final ceramic product. The colloidal behavior of these materials, which is dominated by electrical interactions between the particles, is complex due to the strong interaction of the solids with the processing fluids. A surface titration methodology, modified to account for this interaction, has been developed and used to provide fundamental insights into the interfacial chemistry of these systems. Various powder pretreatment strategies were explored to differentiate between true surface chemistry and artifacts due to exposure history. The colloidal behavior of both silicon nitride and carbide is dominated by silanol groups on the powder surfaces. However, the colloid chemistry of silicon nitride is apparently influenced by an additional amine group. With the proper powder treatments, silicon nitride and carbide powder can be made to appear colloiddally equivalent. The impact of these results on processing control will be discussed.

---

\*Work done under NASA Grant NAG3-468.

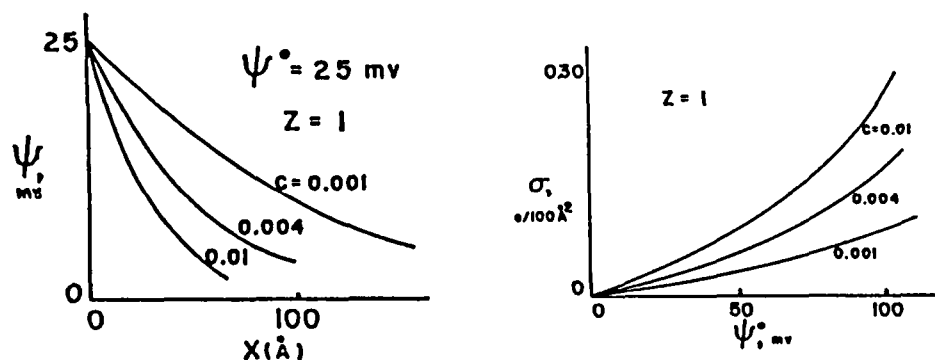
### WHY?

- \* SINTERING OF COVALENT SOLIDS  
REQUIRES SUBMICRON PARTICLES  
(PROCESSING COLLOIDAL DISPERSIONS)
  - CERAMIC POWDERS ACQUIRE  
SURFACE CHARGE AND INTERACT  
WITH IONS IN PROCESSING FLUID
  - STABILITY AND RHEOLOGY  
DOMINATED BY ELECTROSTATIC  
EFFECTS
- \* STRONG CORRELATION BETWEEN  
DISPERSION QUALITY AND FINAL  
PROPERTIES OF SINTERED CERAMIC

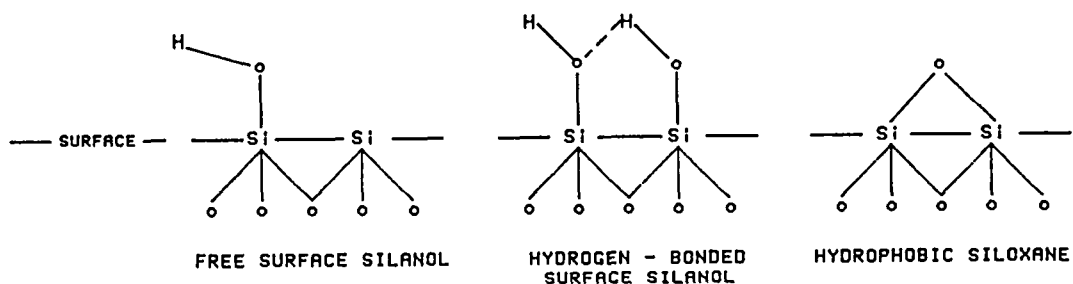
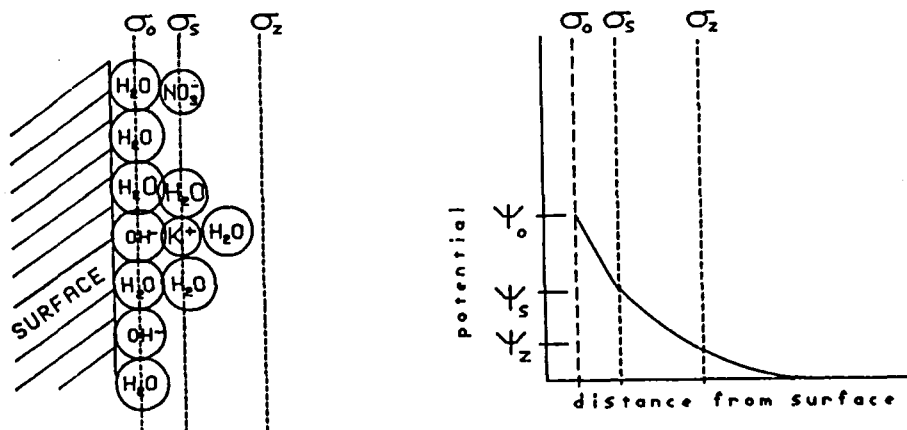
- TECHNIQUES
- SPECTROSCOPIC CHARACTERIZATION  
FTIR, ESCA, SIMS, AUGER
  - ELECTROPHORETIC CHARACTERIZATION  
ZETA POTENTIAL
  - TITRATION OF SURFACE GROUPS  
SURFACE CHARGE
  - RHEOLOGICAL CHARACTERISTICS  
VISCOMETRY
  - STABILITY CHARACTERIZATION  
SEDIMENTATION



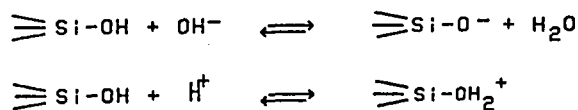
# RELATIONSHIP BETWEEN SURFACE POTENTIAL AND SURFACE CHARGE



## DEVELOPMENT OF SURFACE CHARGE AND SURFACE POTENTIAL



### ADSORPTION OF POTENTIAL DETERMINING IONS:



## ORIGIN OF SURFACE POTENTIAL

REVERSIBLE ELECTRODE --

NERNST EQUATION RELATES SURFACE POTENTIAL ( $\Psi_0$ )  
TO CONCENTRATION OF POTENTIAL DETERMINING IONS:

$$\Psi_0 = \frac{2.303RT}{ZF} \text{LOG}(C/C_{zp})$$

AMPHOTERIC OXIDE --

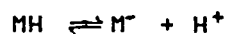
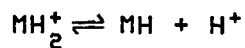
ASSUMING  $H^+$  AND  $OH^-$  ARE POTENTIAL DETERMINING  
AND EXHIBIT NERNSTIAN BEHAVIOR:

$$\Psi_0 = 59.7(pH_{pzc} - pH)$$

## ORIGIN OF SURFACE SPECIES --

### THERMODYNAMICS OF THE DOUBLE LAYER

SITE MODEL OF SOLID/LIQUID INTERFACE:



EQUATE CHEMICAL POTENTIALS:

BULK COMPONENTS--

$$\mu_j = \mu_j^0 + RT \ln a_j$$

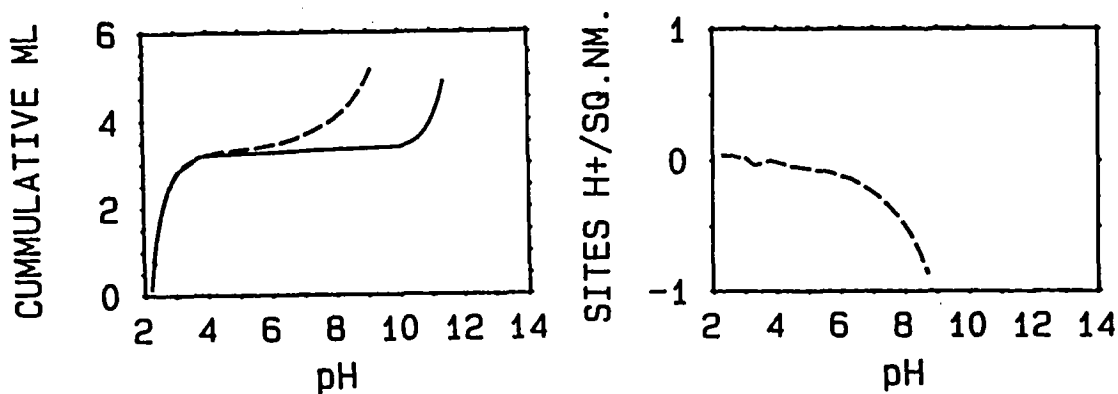
SURFACE SITES--

$$\mu_{hj} = \mu_{hj}^0 + RT \ln a_{hj} + ZF\zeta$$

## EXPERIMENTAL APPROACH

- IDENTIFY PRETREATMENT METHOD TO YIELD REPRODUCIBLE, PRISTINE SURFACE
- INVESTIGATE EFFECT OF MANUFACTURING HISTORY, SUBSTRATE ON ADSORPTION
- COMPARE SILICON NITRIDE, SILICON CARBIDE AND SILICA
- EXPLORE THE ROLE OF ELECTROLYTE
- COMPARE TITRATION RESULTS WITH RESULTS FROM OTHER METHODS

## POTENTIOMETRIC TITRATION



FOR AMPHOTERIC COLLOID:

$$\sigma_0 = F (\Gamma_{H^+} - \Gamma_{OH^-})$$

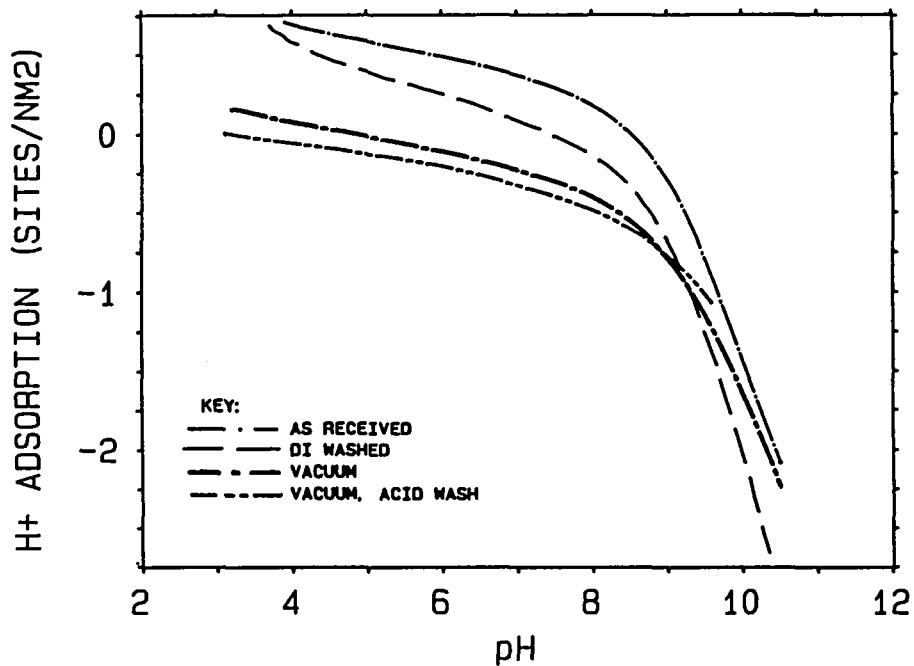
WHERE F = FARADAY'S CONSTANT

$\Gamma_{H^+}, \Gamma_{OH^-}$  = EQUIVALENTS OF H<sup>+</sup> OR OH<sup>-</sup>  
BOUND TO SURFACE

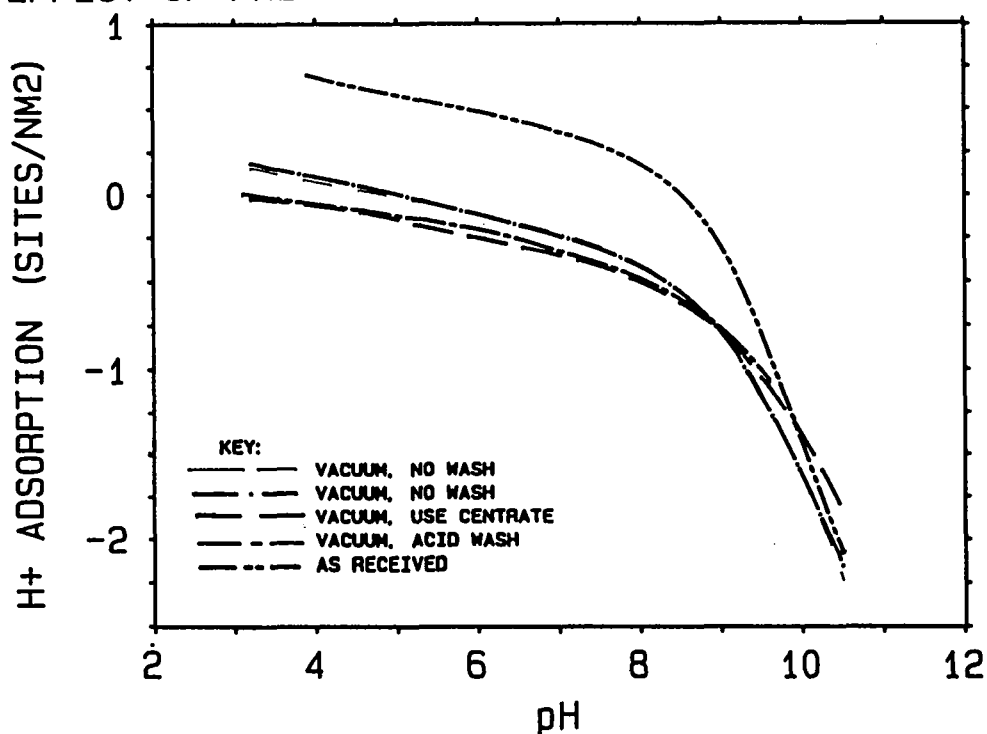
HANDLING AND PRETREATMENT:

- \* NONE (AS RECEIVED)
- \* FIRE 500°C IN ARGON
- \* FIRE 300°C IN OXYGEN
- \* WASH IN DI WATER, THEN:
  - NO DRY
  - DRY, MILD CONDITIONS
  - DRY RAPIDLY
- \* WASH IN ACIDIC ELECTROLYTE
- \* EXPOSE TO MODERATE VACUUM

EFFECT OF PRETREATMENT ON TITRATION RESULTS



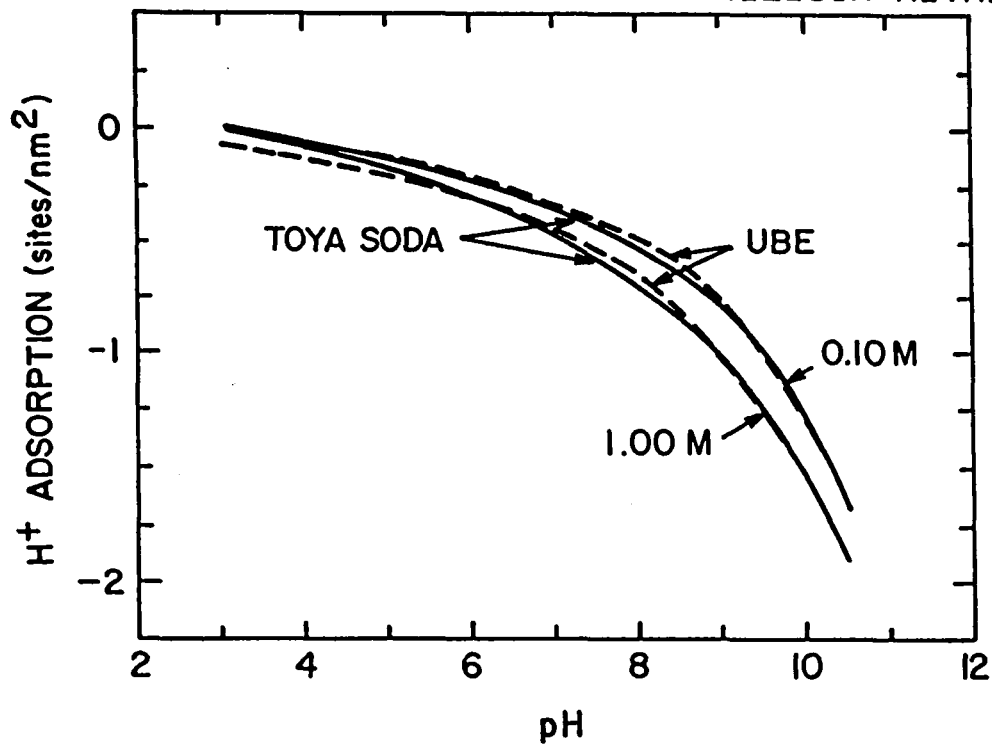
## EFFECT OF PRETREATMENT ON TITRATION RESULTS



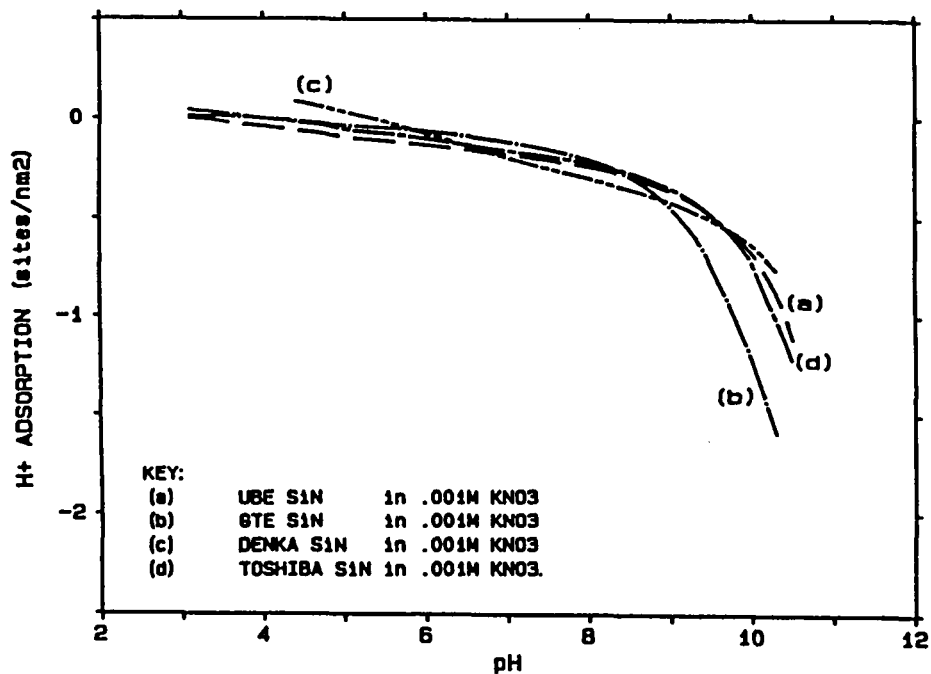
### SUMMARY OF RESULTS

- \* PHYSISORBED SPECIES REMOVED
  - BAKE IN DRY ENVIRONMENT
  - EXPOSE TO MODERATE VACUUM
- \* CHEMISORBED SPECIES DESORB RAPIDLY  
IN ACIDIC ELECTROLYTE
- \* SILICON NITRIDE REACTS WITH AQUEOUS  
SOLUTION TO RE-FORM ORIGINAL ADSORBED  
SPECIES
- \* WASHING IN ACIDIFIED SOLUTION REMOVES  
ALL ADSORBATE, BUT LEAVES SURFACE  
UNALTERED FROM "AS RECEIVED" STATE

# COMPARISON OF UBE AND TOYA SODA SILICON NITRIDE

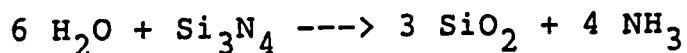


# COMPARISON OF SILICON NITRIDE FROM FOUR MANUFACTURERS

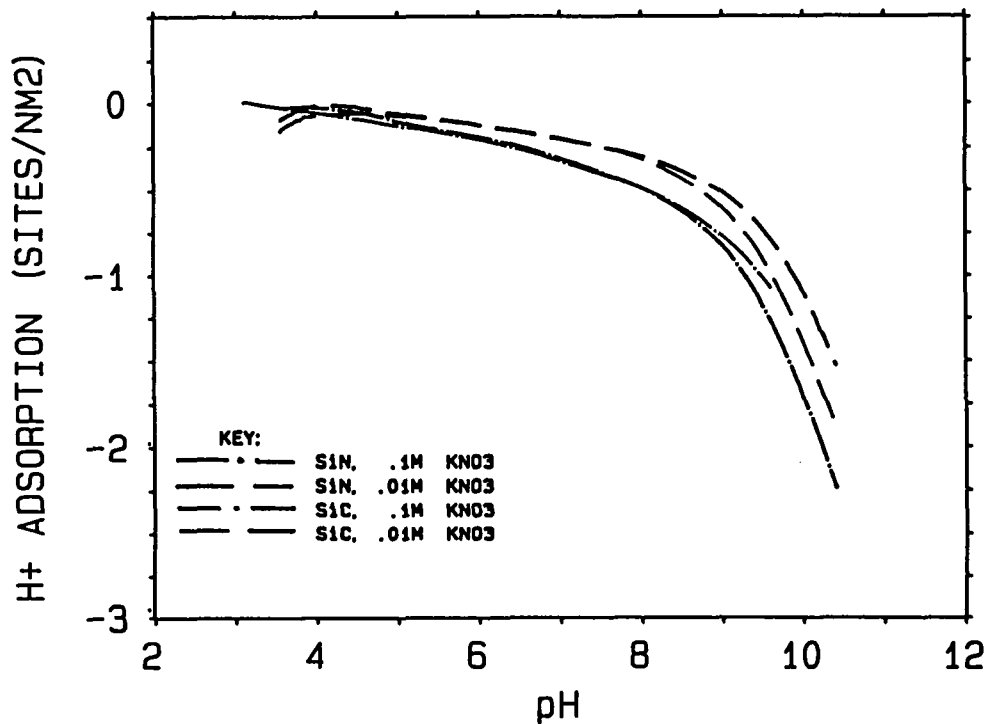


## HYPOTHESES

- \* TITRATABLE SURFACE SPECIES IS SILICA
- \* SPECIES ADSORBED ON SILICON NITRIDE IS AMMONIA
  - MOST PHYSISORBED, SOME CHEMISORBED
  - SIMILAR TO REPORTED ADSORPTION OF AMMONIA ON SILICA
- \* AMMONIA IS FORMED BY HYDROLYSIS OF SILICON NITRIDE:



## COMPARISON OF SILICON NITRIDE AND SILICON CARBIDE



SUMMARY OF SURFACE TITRATION DATA

\* SUGGEST PZC < pH 3 FOR BOTH  
SILICA AND SILICON CARBIDE

\* SUGGEST PZC > pH 6 FOR MOST  
SILICON NITRIDES

\* LITTLE DIFFERENCE AMONG VARIOUS  
MANUFACTURERS OF SILICON NITRIDE

\* LITTLE DIFFERENCE BETWEEN SILICON  
NITRIDE AND SILICON CARBIDE Si-OH  
SITE DENSITY

\* WITH CAREFUL PRETREATMENT, DATA  
IS REPRESENTATIVE OF NATIVE SURFACE  
AND IS REPRODUCIBLE



## NDE OF STRUCTURAL CERAMICS BY PHOTOACOUSTIC MICROSCOPY

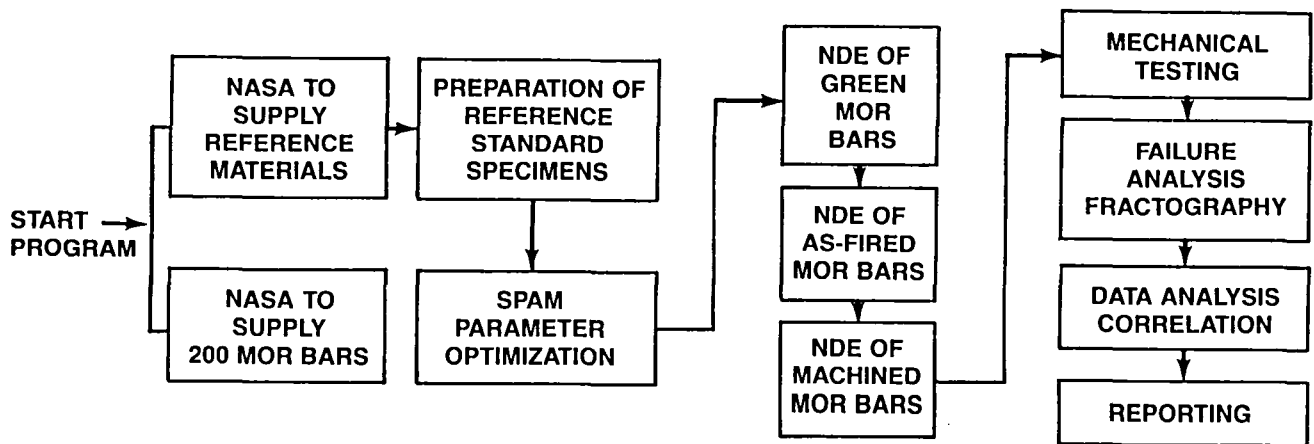
P.K. Khandelwal  
Allison Gas Turbine Division  
General Motors Corporation  
P.O. Box 420, Speed Code W-5  
Indianapolis, Indiana 46206-0420

Photoacoustic microscopy (PAM) has been utilized to detect surface and subsurface defects in structural ceramic materials. A computerized PAM data acquisition, color imaging and analysis system has been developed and used under this program. Subsurface simulated cylindrical holes can be detected to about 1 mm below the interrogating surface. Simulated tight surface cracks of 96  $\mu\text{m}$  length and 48  $\mu\text{m}$  depth can be detected in these materials under optimum conditions.

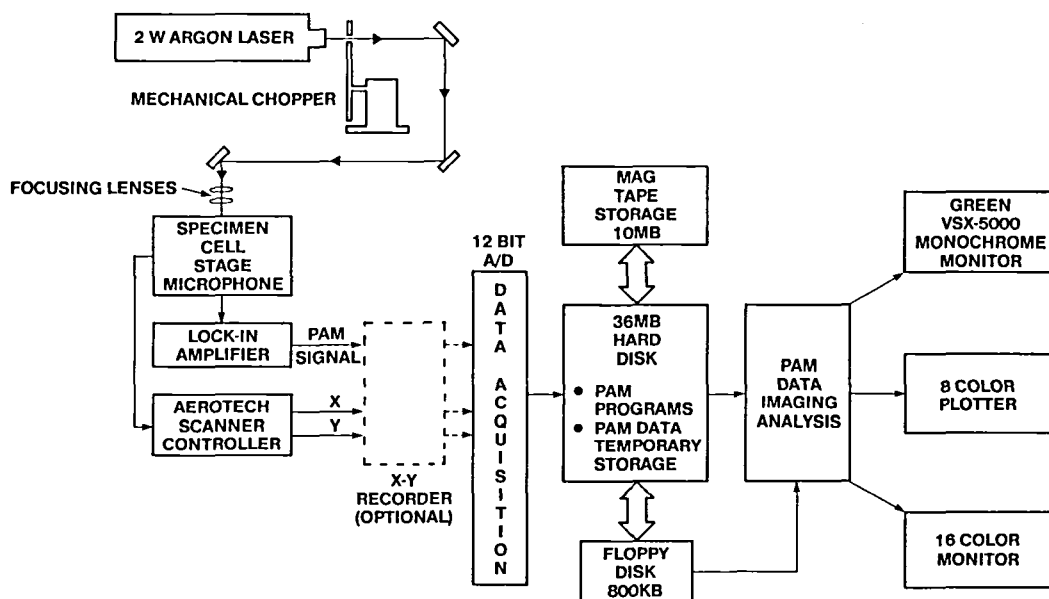
## OBJECTIVES

- o DEVELOP COMPUTERIZED CAPABILITY TO DIGITALLY ACQUIRE/RETRIEVE AND IMAGE PAM SIGNALS
- o DEVELOP CAPABILITY TO DETECT 250 $\mu$ m SIZE VOIDS/INCLUSIONS 1mm BELOW INTERROGATING SURFACE
- o DEVELOP CAPABILITY TO DETECT SURFACE CONNECTED CRACKS
- o DEMONSTRATE ABILITY OF NDE TO PREDICT FAILURE SITE ON MOR BAR CONTAINING NATURAL FLAWS

## NDE OF STRUCTURAL CERAMICS BY PHOTOACOUSTIC MICROSCOPY



# PAM FLAW DETECTION DATA ACQUISITION AND IMAGING SYSTEM



## PAM DATA ACQUISITION AND IMAGING-ANALYSIS SYSTEM

DATE  
4/10/86  
CHART NO.  
PKK

### FEATURES

- o SCANNER
  - o PROGRAMMABLE X-Y RASTER SCAN
  - o 2 $\mu$ M AXIS RESOLUTION
- o DATA ACQUISITION/IMAGING
  - o MENU DRIVEN ALGORITHMS
  - o ACQUIRES AND STORES DATA
  - o 12 BIT A/D RESOLUTION
  - o MONOCROME AND COLOR DISPLAY
  - o 8 COLOR PLOTTER
  - o EXPERIMENTAL STATISTICS
  - o MAGNIFICATION/ZOOM
  - o PAN
  - o THRESHOLDING
  - o FLAW/PAM SIGNAL SIZING
  - o HISTOGRAM OF PAM SIGNALS

CT-8040(7-86)

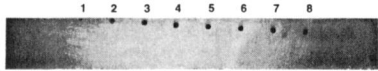
## PAM FLAW DETECTION BATCH-A AS-FIRED $\text{Si}_3\text{N}_4$



TOP VIEW

3X

HOLE #



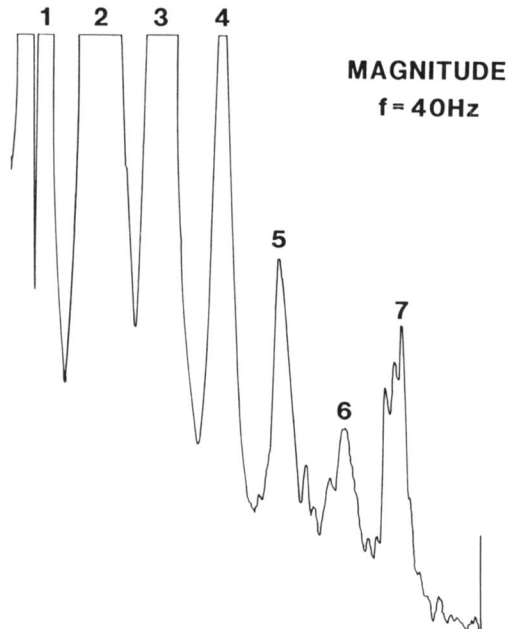
SIDE VIEW

3X

HOLE #	HOLE LOCATION FROM TOP SURFACE $\mu\text{m}$
1	OPEN TO SURFACE
2	VERY NEAR TO SURFACE BUT NOT OPEN
3	156
4	390
5	547
6	665
7	825
8	1015
NOMINAL DIAMETER $\approx 375\mu\text{m}$	
NOMINAL DISTANCE BETWEEN HOLES $\approx 2.5\text{ mm}$	
APPROXIMATE DEPTH $\approx 3.125\text{ mm}$	

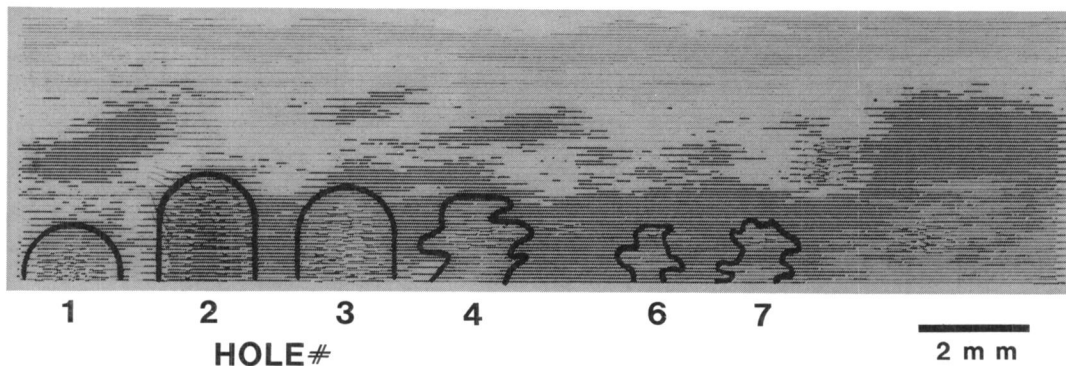
VS85-1814

## PAM SUBSURFACE FLAW DETECTION AS-FIRED SILICON NITRIDE

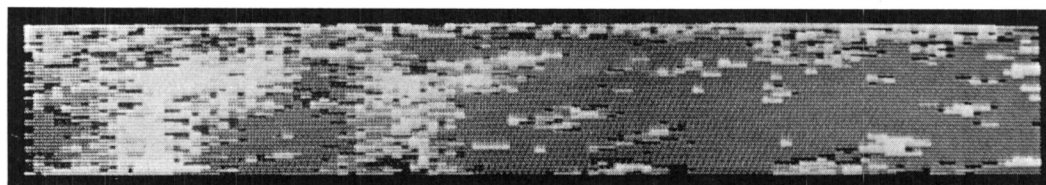
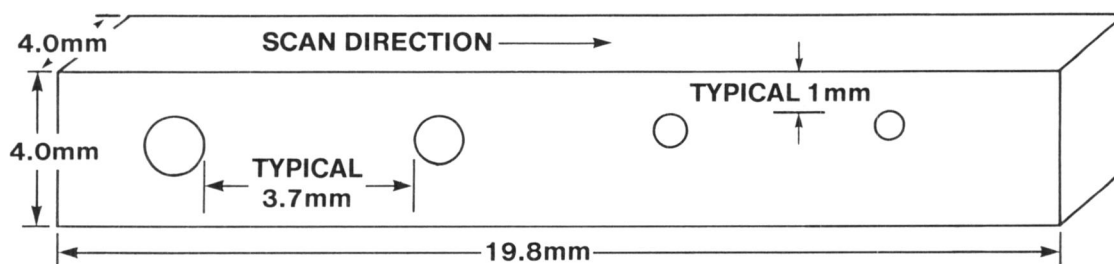


VS86-1813

# **PAM DIGITAL IMAGING- SUBSURFACE FLAWS BATCH-A AS-FIRED $\text{Si}_3\text{N}_4$**



## **PAM SUBSURFACE FLAW DETECTION AS FIRED SINTERED SILICON CARBIDE**



HOLE DIA.  $\mu\text{m}$       1000      750      500      250

PHOTOACOUSTIC MICROSCOPY  
SURFACE CRACK DETECTION

DATE  
4/10/86  
CHART NO.  
PKK

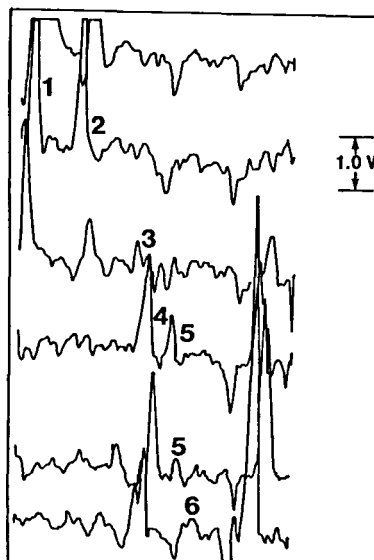
Crack #	Load (Kg)	Crack		Signal-to-Noise Ratio	
		Length (2c) $\mu\text{m}$	Depth* (a) $\mu\text{m}$	40 Hz 250 $\mu\text{m}/\text{sec}$ . 200 $\mu\text{V}$	300 Hz 250 $\mu\text{m}/\text{sec}$ 50 $\mu\text{V}$
1	12	401	200	Saturated	Saturated
2	10	323	162	9.0	13.5
3	5	234	117	2.0	4.5
4	4	205	102	3.0	5.5
5	2	140	70	N.D.	2.0
6	1	96	48	N.D.	N.D.

\*Assuming semicircular flaw,  $a = c$

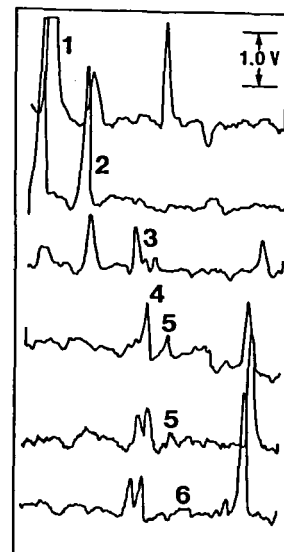
N.D. - Signal-to-noise ratio of 1  
Difficult to separate the flaw signal from the background

GT-8040(7-86)

PHOTOACOUSTIC MICROSCOPY  
SURFACE CRACK DETECTION



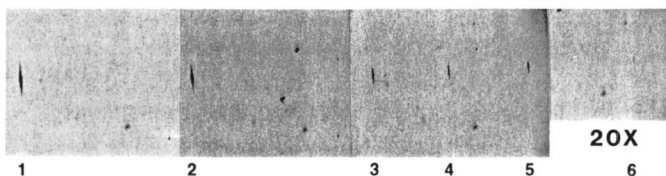
40 Hz



300 Hz

VS86-1810

# PHOTOACOUSTIC MICROSCOPY SURFACE CRACK DETECTION



OPTICAL



40Hz

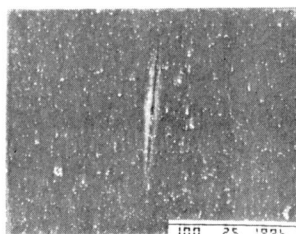


300Hz

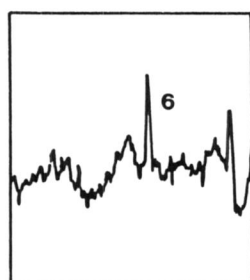
DIGITAL IMAGE

VS86-1811

# PHOTOACOUSTIC MICROSCOPY SURFACE CRACK DETECTION

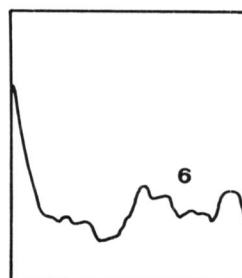


$2C = 96\mu\text{m}$   
 $a = 48\mu\text{m}$



50  $\mu\text{m/SEC}$

HPSi<sub>3</sub>N<sub>4</sub>  
 $f = 40\text{Hz}$



250  $\mu\text{m/SEC}$

VS86-1812





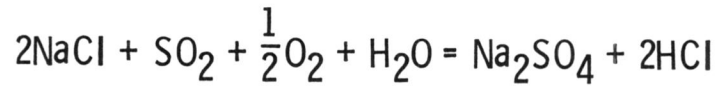
## MOLTEN SALT CORROSION OF SIC AND $\text{Si}_3\text{N}_4$

N. S. Jacobson, J. L. Smialek, and D. S. Fox  
NASA Lewis Research Center  
Cleveland, Ohio

The most severe type of corrosion encountered in heat engines is corrosion by molten sodium sulfate, which is formed by the reaction of ingested sodium chloride and sulfur impurities in the fuel. This problem has been studied extensively for superalloys, but only recently examined for ceramics. Our program at Lewis addresses this problem with laboratory studies to understand the fundamental reaction mechanisms and with burner studies to provide a more realistic simulation of the conditions encountered in a heat engine. In addition we are assessing the effect of corrosion on the strengths of these materials. Each of these aspects will be reviewed and some ideas toward possible solutions will be discussed.

## THE HOT CORROSION PROBLEM

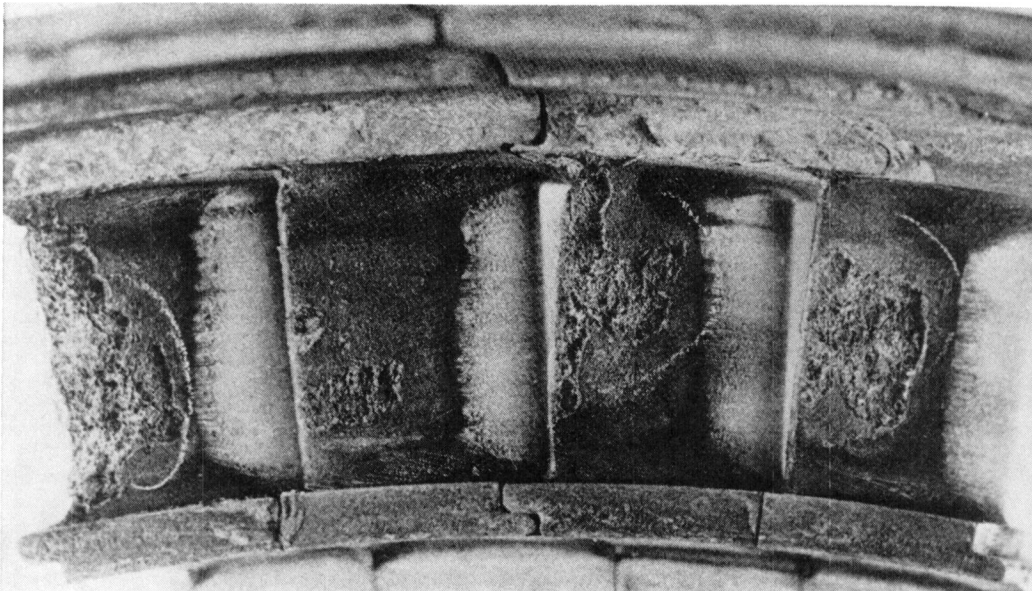
- FORMATION OF  $\text{Na}_2\text{SO}_4$



- DEPOSITION OF MOLTEN  $\text{Na}_2\text{SO}_4$  ON ENGINE PARTS  
FUNCTION OF T, P, [SALT]
- POTENTIALLY CATASTROPHIC ATTACK

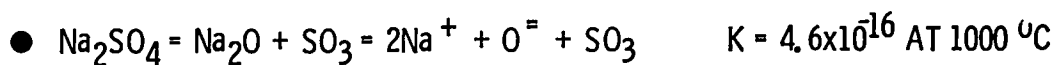
CS-86-1388

## TURBINE VANE HOT CORROSION



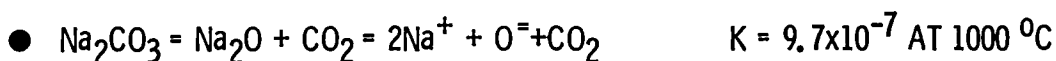
CS-73740

## BASIC AND ACIDIC MOLTEN SALTS



LOW  $P_{\text{SO}_3}$  - HIGH  $a_{\text{O}^{2-}}$  - BASIC

HIGH  $P_{\text{SO}_3}$  - LOW  $a_{\text{O}^{2-}}$  - ACIDIC



MODEL BASIC SALT

CS-86-1383

## REACTIONS WITH MOLTEN SALTS

- DISSOLUTION OF PROTECTIVE OXIDE (MO) BY MOLTEN SALT
- UNPROTECTED METAL OR CERAMIC SUSCEPTIBLE TO ATTACK

● TYPES OF DISSOLUTION

- ACIDIC       $\text{MO} = \text{M}^{++} + \text{O}^{2-}$
- BASIC       $\text{MO} + \text{O}^{2-} = \text{MO}_2^{2-}$

●  $\text{SiO}_2$  IS AN ACIDIC OXIDE

- EXPECT REACTION WITH BASIC SALT
- $\text{SiO}_2 + \text{O}^{2-} = \text{SiO}_3^{2-}$
- SILICATES LIQUID T 780 °C

CS-86-1384

## EXPERIMENTAL TECHNIQUES

### ● LABORATORY

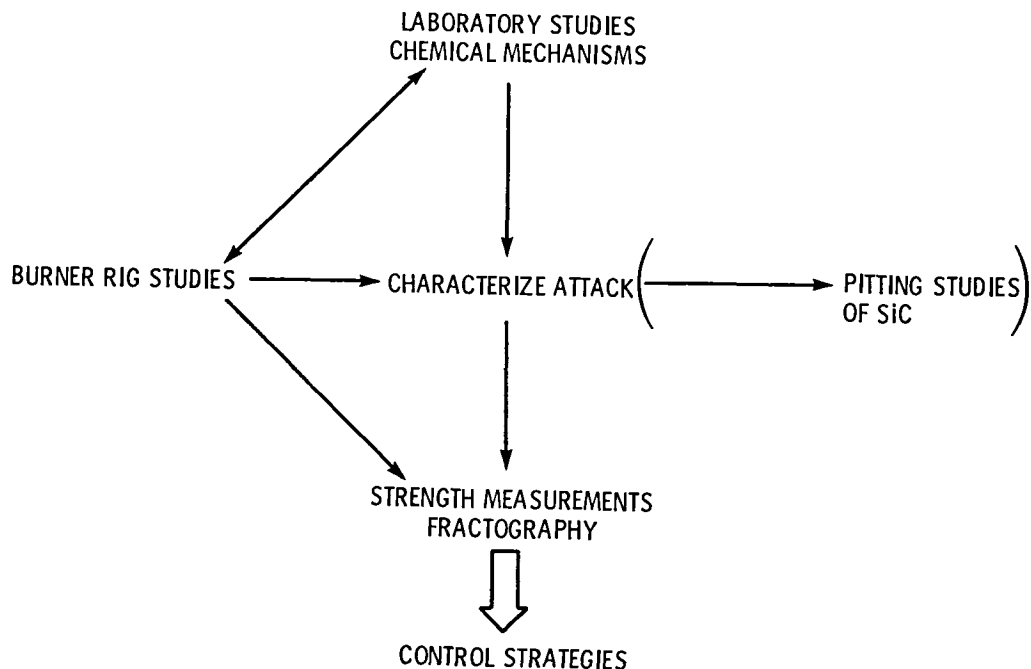
- AIRBRUSH SAMPLE WITH SALT; HEAT
- PRECISELY CONTROL PARAMETERS
- MONITOR KINETICS, MICROSTRUCTURAL CHANGES
- ONE TIME DEPOSITION OF SALT

### ● BURNER

- JET FUEL SEEDED WITH NaCl
- CONTINUOUS DEPOSITION OF SALT; CLOSER TO ENGINE CONDITIONS
- DIFFICULT TO CONTROL PARAMETERS

CS-86-1382

## LEWIS CORROSION STUDIES OF SiC AND Si<sub>3</sub>N<sub>4</sub>



CS-86-1379

## MATERIALS STUDIED

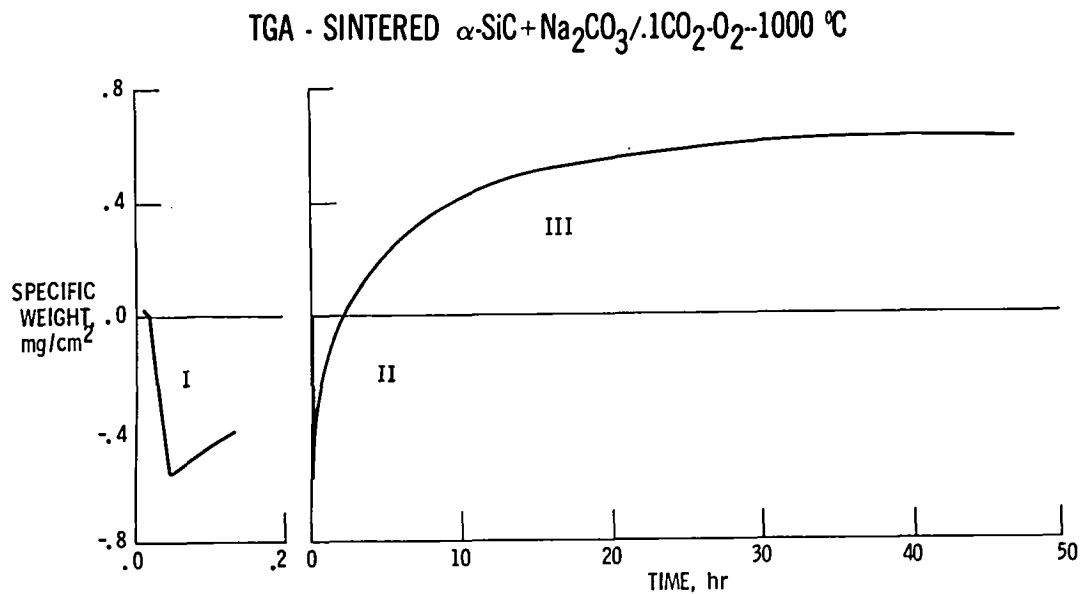
- SINTERED  $\alpha$ -SiC (B,C)

HP SiC, CVD SiC, SC SiC

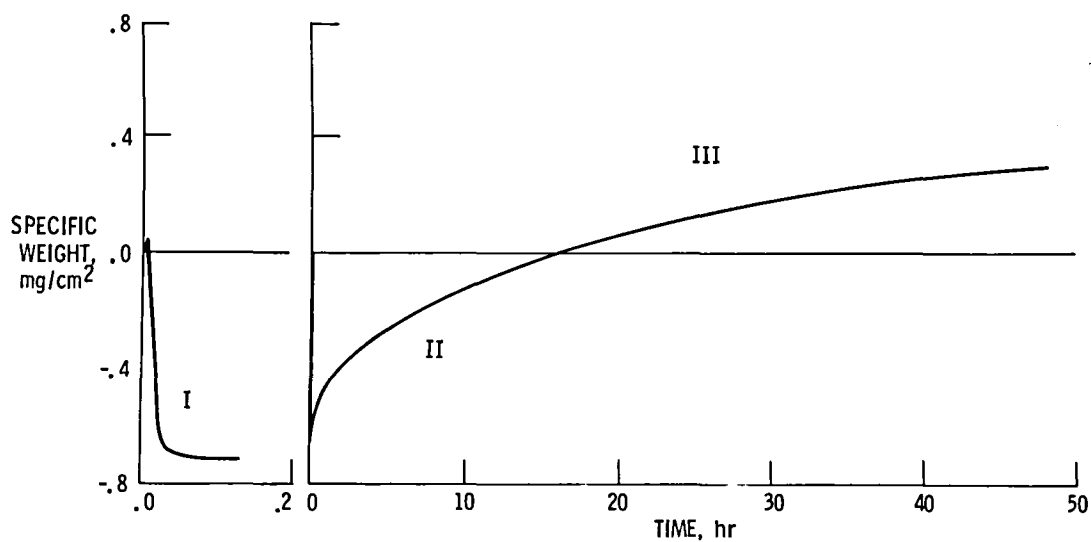
- SINTERED  $\text{Si}_3\text{N}_4$  ( $\text{Al}_2\text{O}_3$ ,  $\text{Y}_2\text{O}_3$ )

SINTERED  $\text{Si}_3\text{N}_4$  ( $\text{Y}_2\text{O}_3$ ), HIP'd RB  $\text{Si}_3\text{N}_4$

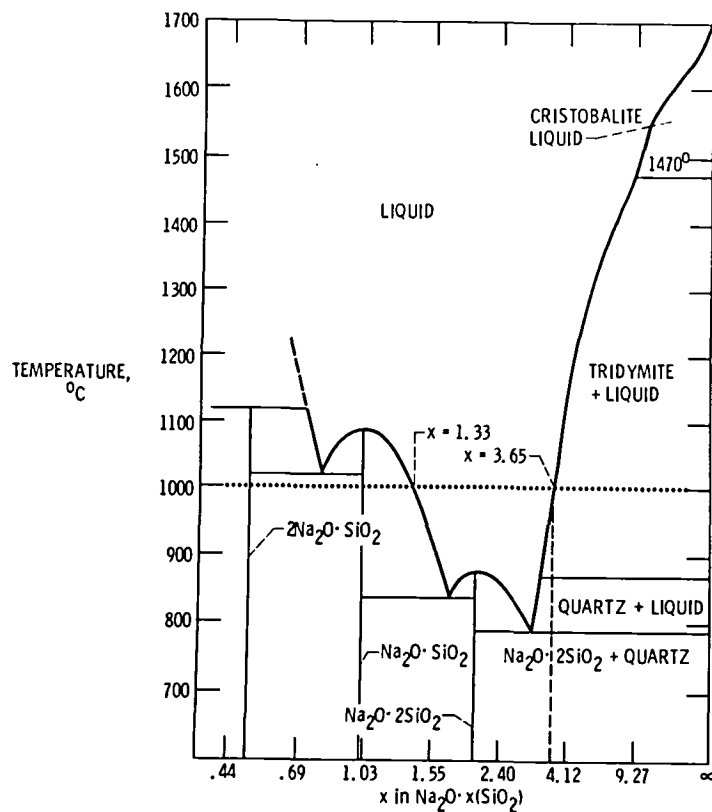
CS-86-1386



# TGA - HIP'D RBSN + $\text{Na}_2\text{CO}_3/\text{O}_2$ --1000 °C



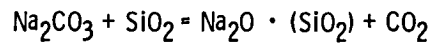
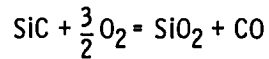
CS-84-1378



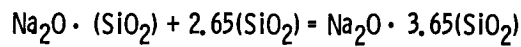
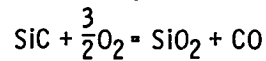
CS-85-0793

## MECHANISM OF CORROSION BY $\text{Na}_2\text{CO}_3$

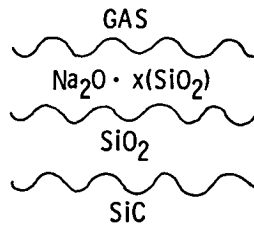
### I. DECOMPOSITION OF SALT AND SILICATE FORMATION



### II. MOVE TOWARD LIQUIDUS



### III. GROWTH OF PROTECTIVE $\text{SiO}_2$ LAYER-SLOWING OF REACTION



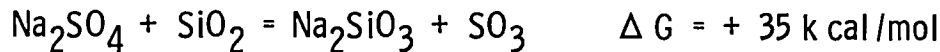
CS-86-1380

## $\text{Na}_2\text{CO}_3$ VERSUS $\text{Na}_2\text{SO}_4/\text{O}_2$

- $\text{Na}_2\text{SO}_4 = \text{Na}_2\text{O} + \text{SO}_3\uparrow$  BASIC MOLTEN SALT
- SiC - SIMILAR BEHAVIOR
- $\text{Si}_3\text{N}_4 - \text{Na}_2\text{SO}_4/\text{O}_2$  CORROSION IS SLOWER THAN  $\text{Na}_2\text{CO}_3/\text{O}_2$
- IMPORTANT SYSTEM - CLOSE TO BURNER RIG

CS-86-1381

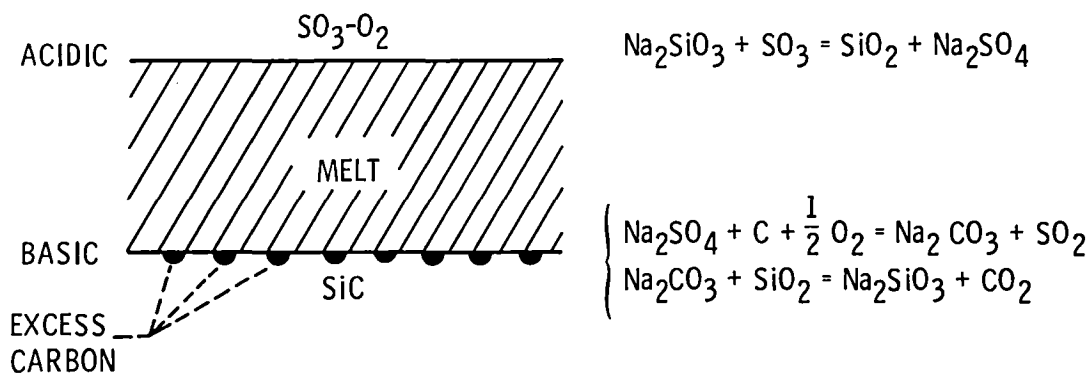
## Na<sub>2</sub>SO<sub>4</sub> / SO<sub>3</sub> CASE



- $P_{\text{SO}_3} > 10^{-6} \text{ atm}$  -- NO REACTION
- Na<sub>2</sub>SO<sub>4</sub>/10<sup>-4</sup> SO<sub>3</sub>-O<sub>2</sub> DOES NOT ATTACK
  - QUARTZ
  - HOT PRESSED (Al<sub>2</sub>O<sub>3</sub>) SiC
  - SINGLE CRYSTAL SiC
  - PREOXIDIZED (1400 °C - 23 h) SINTERED SiC
- Na<sub>2</sub>SO<sub>4</sub>/10<sup>-4</sup> SO<sub>3</sub> - O<sub>2</sub> DRAMATICALLY ATTACKS AS-GROUND SINTERED SiC

CS-85-2269

## BASIC/ACIDIC CHARACTER OF MELT



ESTABLISHES FLUXING CONDITION

CS-85-2266

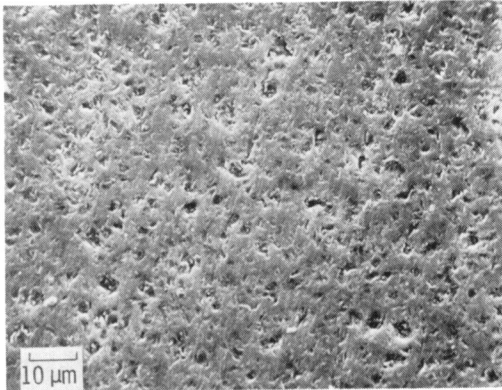


## ATTACK OF CERAMIC SUBSTRATE

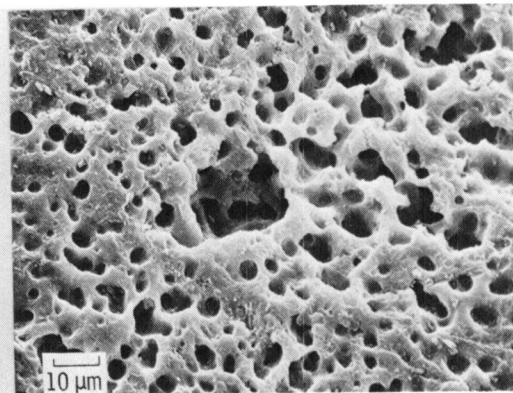
- HF REMOVES GLASSY PRODUCT LAYERS  
(CAUTION WITH  $\text{Si}_3\text{N}_4$ )
- ATTACK DOES NOT OCCUR BY EVEN RECESSION
- SiC - SEVERE PITTING ATTACK  
 $\text{Na}_2\text{CO}_3 < \text{Na}_2\text{SO}_4/\text{O}_2 < \text{Na}_2\text{SO}_4/\text{SO}_3$
- $\text{Si}_3\text{N}_4$  - SEVERE GRAIN BOUNDARY ATTACK

CS-86-1385

### CORROSION PITTING



SINTERED  $\alpha$ -SiC BEFORE CORROSION

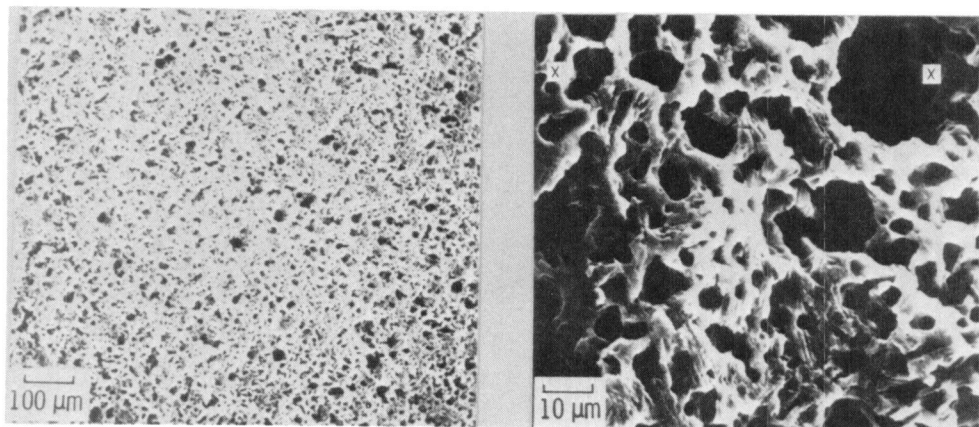


SiC AFTER CORROSION  
 $\text{Na}_2\text{CO}_3/\text{CO}_2$  - 48 hrs - 1000 °C  
PRODUCTS REMOVED WITH HF

CS-85-3407

# PITTING ATTACK MORPHOLOGY AFTER $\text{Na}_2\text{SO}_4/\text{SO}_3$ CORROSION

SCALE REMOVED BY HF DISSOLUTION

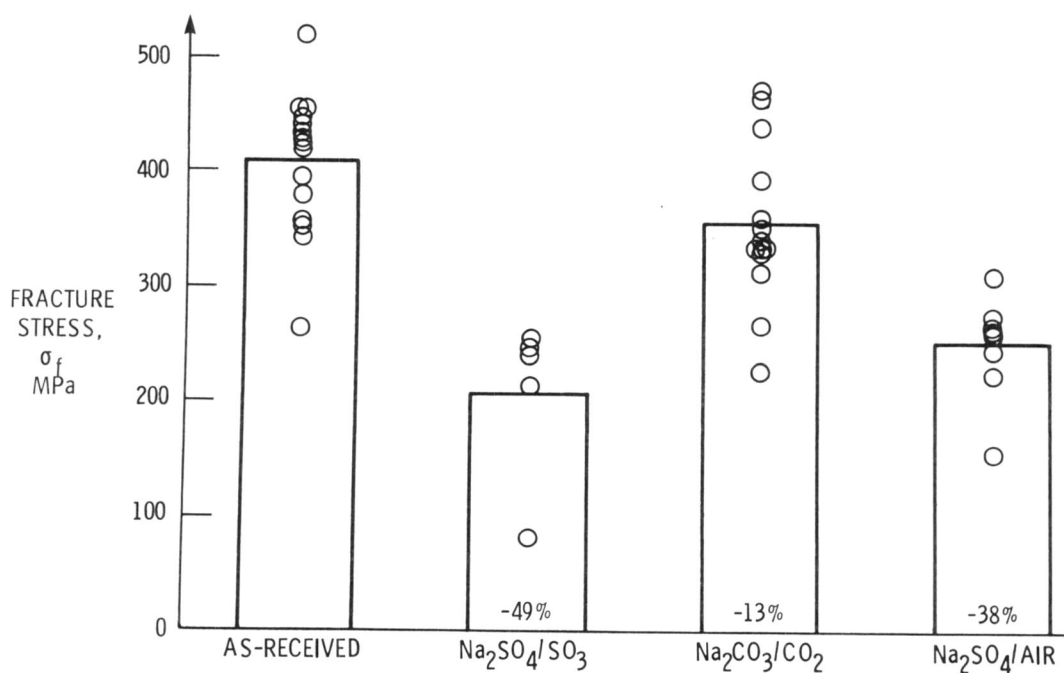


UNIFORM PITTING OBSERVED  
OVER LARGE AREAS

DETAIL OF (a) SHOWING HONEYCOMB  
PIT STRUCTURE

CS-85-2307

## STRENGTH DEGRADATION OF $\alpha$ -SiC AFTER FURNACE CORROSION TESTING



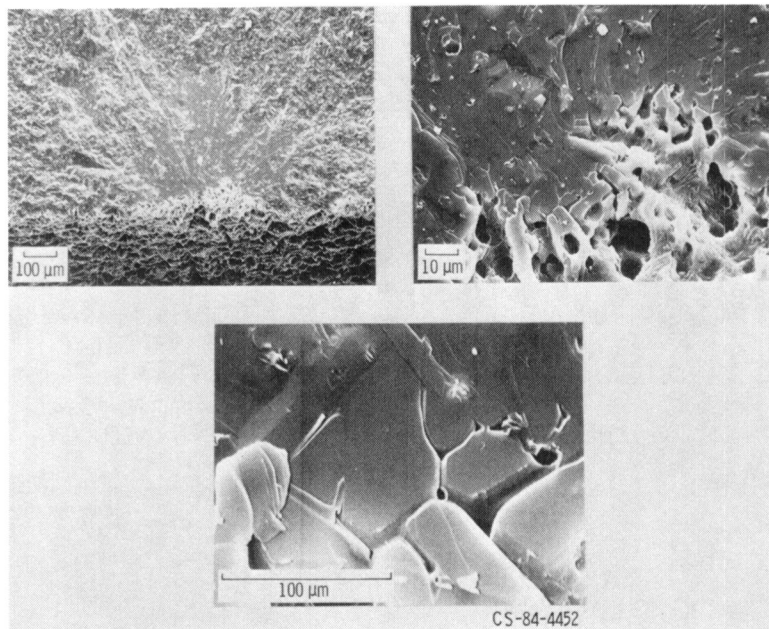
CS-85-2336

# FRACTURE ORIGIN, PITTING, AND GRAIN BOUNDARY ATTACK AFTER $\text{Na}_2\text{SO}_4/\text{SO}_3$ CORROSION

SCALE REMOVED BY HF

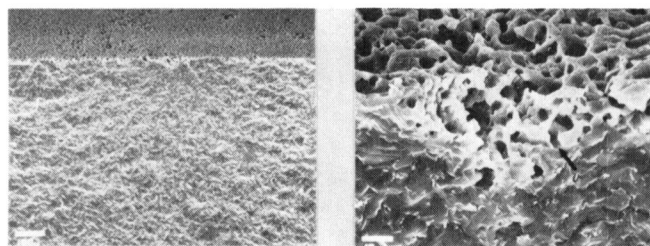
$\sigma_f = 188 \text{ MPa}$

PIT DEPTH =  $113 \mu\text{m}$



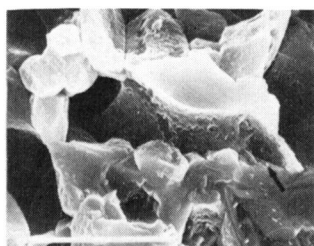
## CORROSION PIT FRACTURE ORIGIN AFTER $\text{Na}_2\text{SO}_4$ /AIR CORROSION

SCALE REMOVED BY HF DISSOLUTION;  $\sigma_f = 373 \text{ MPa}$ , PIT DEPTH =  $40 \mu\text{m}$



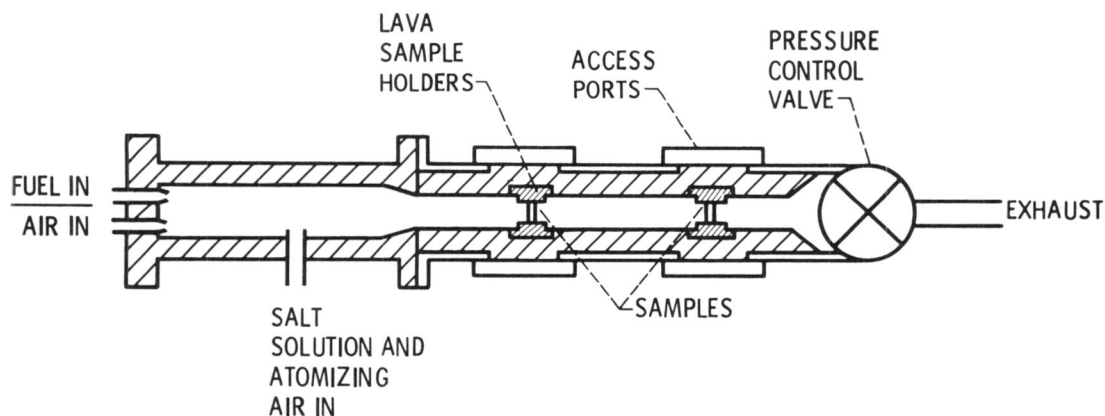
RADIAL CRACK LINES POINTING  
TO CORROSION PIT

INTERSECTION OF DEEPLY PITTED  
REGION WITH FRACTURE SURFACE



GRANULAR ATTACK MORPHOLOGY  
IN PIT

CS-85-2305



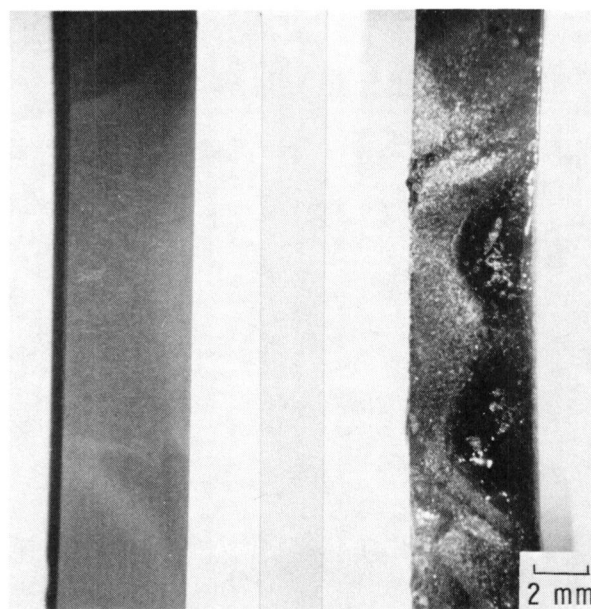
- PARALLEL TO  $\text{Na}_2\text{SO}_4/\text{O}_2$  FURNACE STUDY
- CONTINUOUS SOURCE OF  $\text{Na}_2\text{O}$
- CONTINUOUS  $\text{Na}_2\text{O} \cdot x(\text{SiO}_2)$  FORMATION

OPERATING PARAMETERS

- $T = 990 \pm 10^\circ\text{C}$
- JET A FUEL - 0.05% S
- 4 ppm Na AS NaCl
- FLOW VELOCITY - 310 ft/sec

CS-86-1376

## BURNER RIG TESTS OF $\alpha\text{-SiC}$ AT $1000^\circ\text{C}$



NO SALT  
46 hr

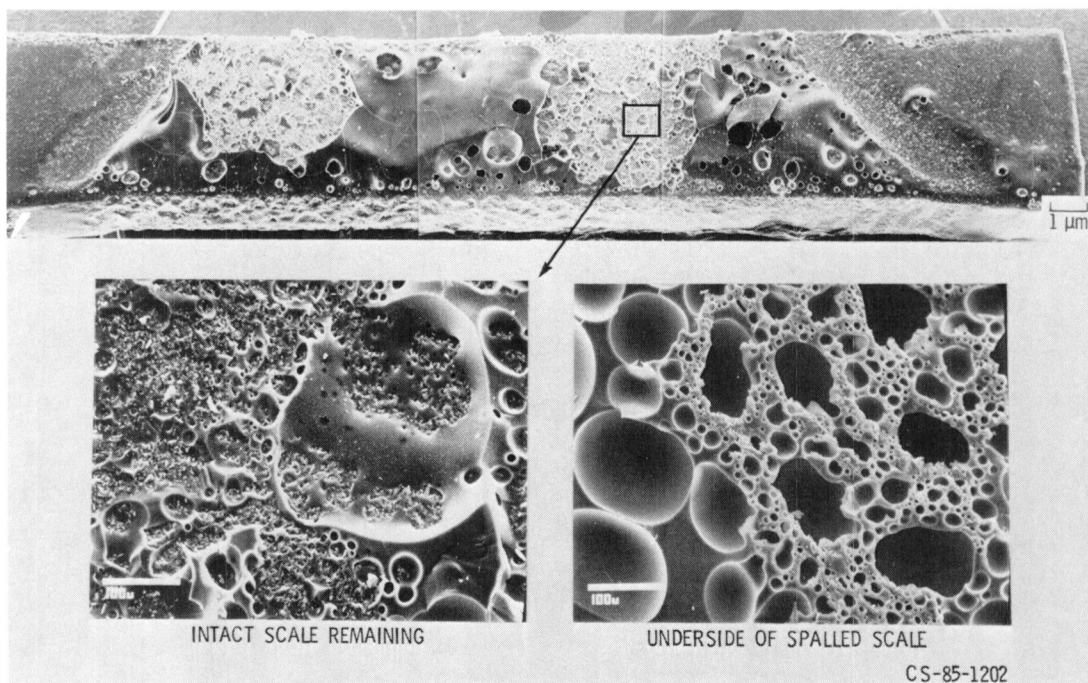
4 ppm Na  
13.5 hr

AIR FLOW →

CS-85-1205

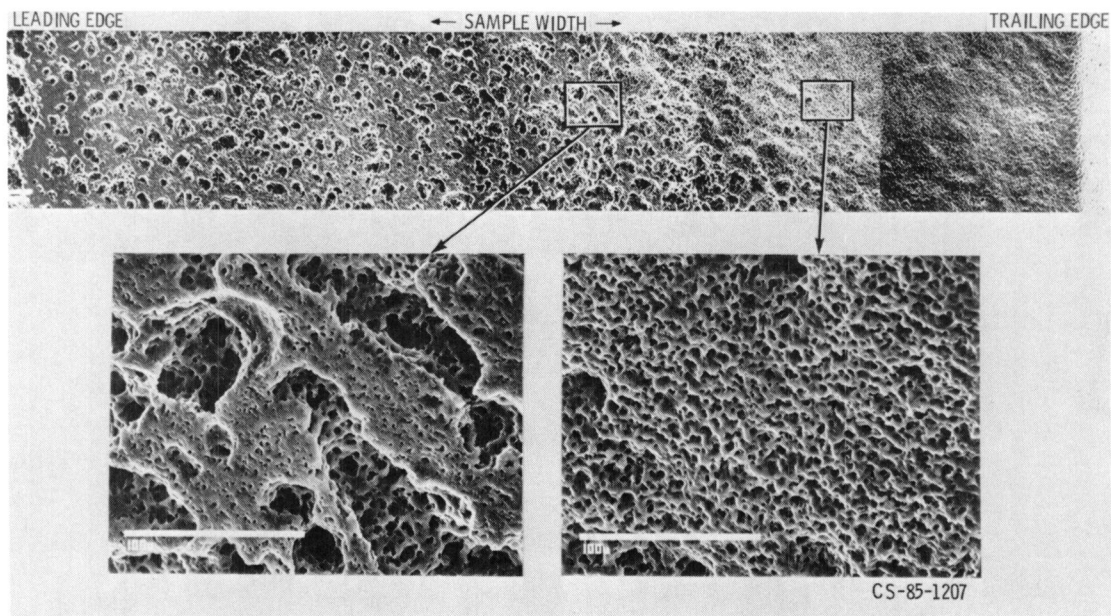
# EXTENSIVE BUBBLE FORMATION IN BURNER RIG SAMPLES

## MECHANICAL SCALE REMOVAL

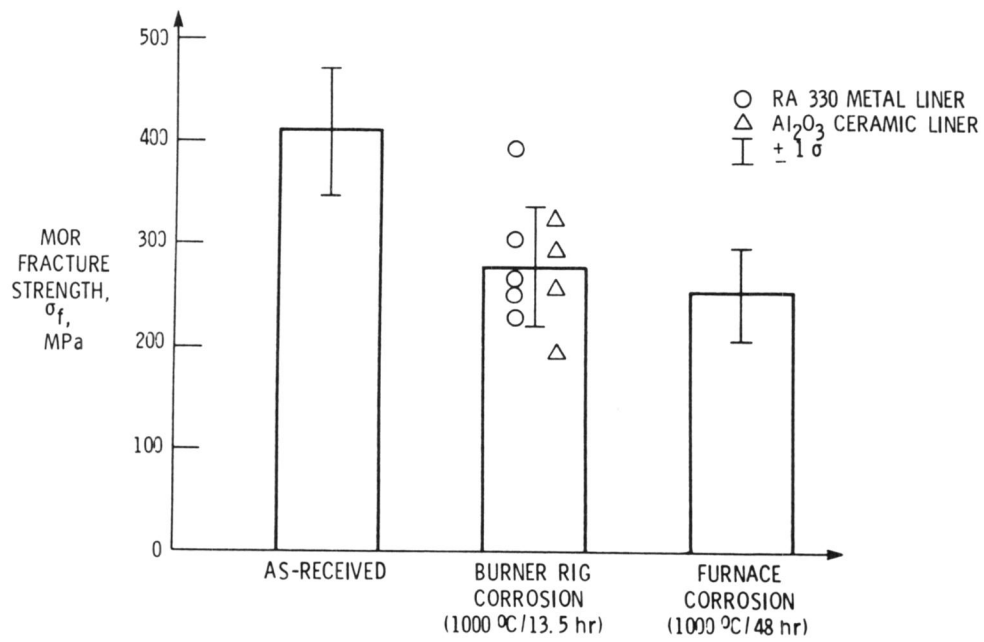


# $\alpha$ -SiC PITTING MORPHOLOGY CAUSED BY BURNER RIG CORROSION

## SCALE REMOVED BY HF DISSOLUTION

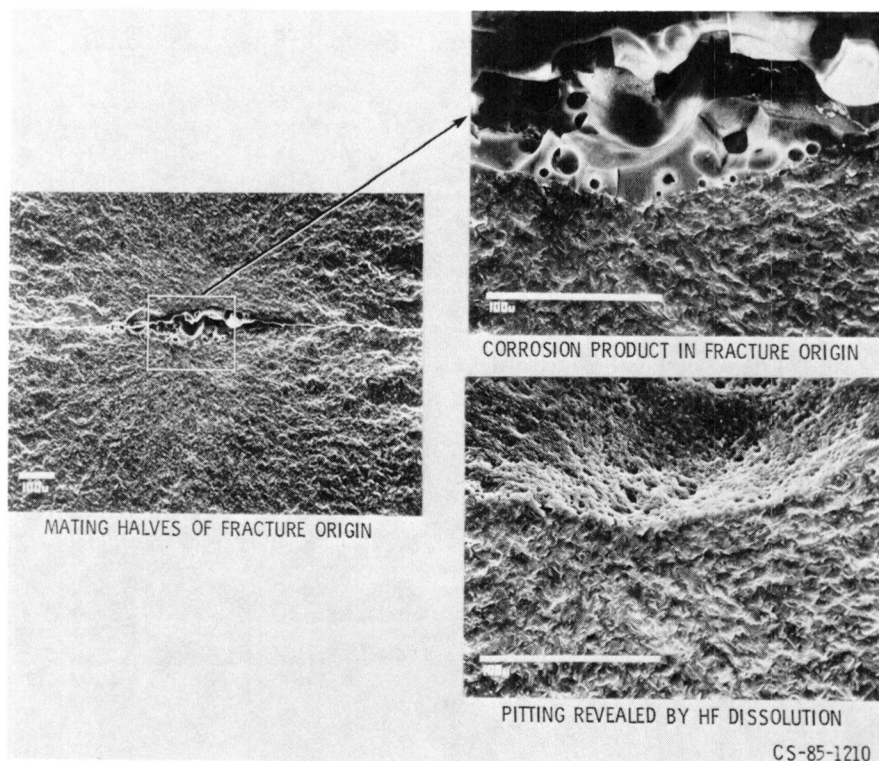


# EFFECT OF BURNER RIG HOT CORROSION ON ROOM TEMPERATURE $\alpha$ -SiC STRENGTH



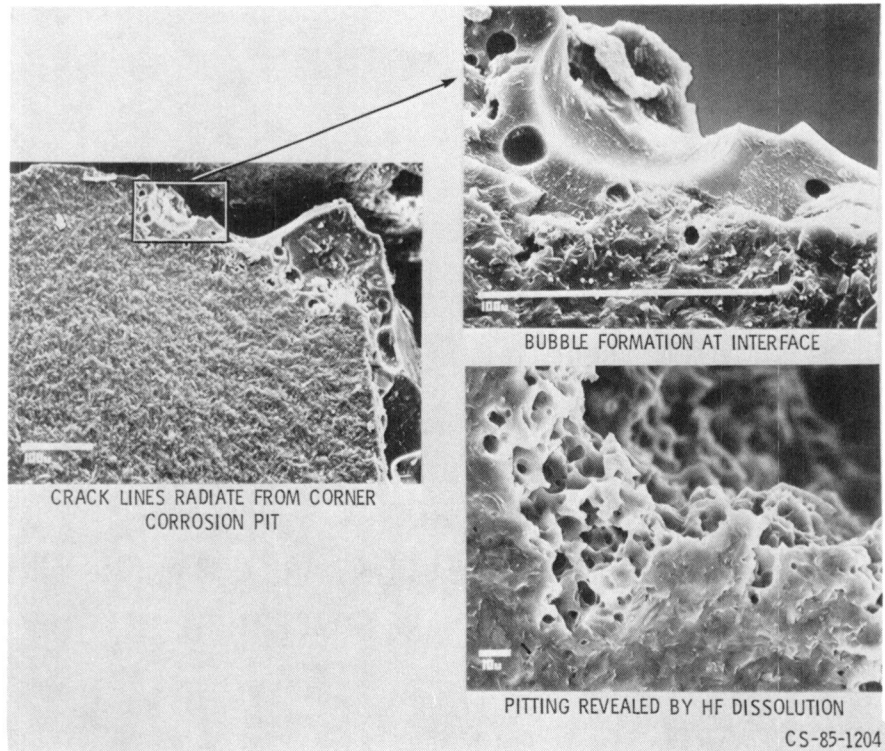
CS-85-1324

## FRACTURE ORIGIN OF BURNER RIG CORROSION SPECIMEN





## FRACTURE ORIGIN OF BURNER RIG CORROSION SPECIMEN



## SUMMARY

### LABORATORY STUDIES

- BASIC MOLTEN SALTS  
     $\text{SiO}_2$  FORMATION AND DISSOLUTION TO LIQUIDUS
- ACIDIC MOLTEN SALTS  
    NO ATTACK, UNLESS BASIC CONDITIONS AT MELT BOTTOM

### BURNER RIG

- PARALLEL TO  $\text{Na}_2\text{SO}_4/\text{O}_2$  - BASIC SALT ATTACK
- CONTINUOUS  $\text{Na}_2\text{O} \cdot x(\text{SiO}_2)$  FORMATION

### ATTACK OF CERAMICS

- $\text{SiC}$  -- SEVERE PITTING -- UP TO 50% STRENGTH REDUCTION
- $\text{Si}_3\text{N}_4$  - SEVERE GRAIN BOUNDARY ATTACK -- WORK IN PROGRESS

## SUMMARY AND CONTROL STRATEGIES

- MOLTEN SALT CORROSION
  - CAN BE CATASTROPHIC
  - ENGINEERS MUST BE AWARE CERAMICS, LIKE SUPERALLOYS, ARE SUSCEPTIBLE
- CONTROL STRATEGIES
  - WORK OUTSIDE SALT DEPOSITION REGIME
  - MAKE SALTS ACIDIC
  - COATINGS; MODIFY  $\text{SiO}_2$  LAYER

CS-86-1390



**THERMAL CYCLIC DURABILITY TESTING OF CERAMIC  
MATERIALS FOR TURBINE ENGINES**

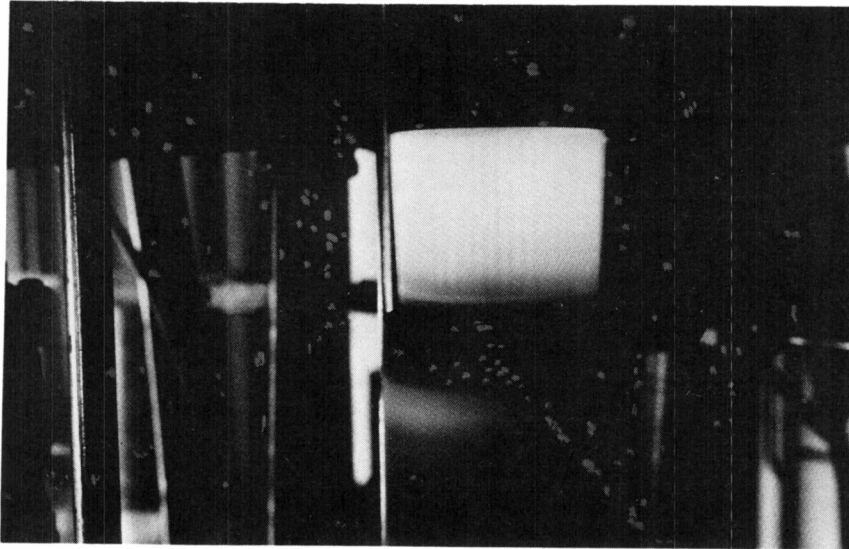
**L.J. Lindberg**

**Garrett Turbine Engine Company  
Phoenix, Arizona 85010**

The thermal cyclic durability of commercial ceramic materials for turbine engines has been under evaluation since 1978. Ceramic materials are exposed to cyclic diesel-fired burner exhaust at either 1204 or 1371C (2200 or 2500F) for up to 3500 hours. The test conditions are selected to simulate the environment experienced by the hot flow path components in an automotive gas turbine engine. The silicon nitride and silicon carbide materials tested are the same ceramic materials currently used on the AGT100 and AGT101 ceramic turbine engine programs.

This work was performed under the NASA funded program, 3500-Hour Durability Testing of Commercial Ceramic Materials, Contract DEN3-27.

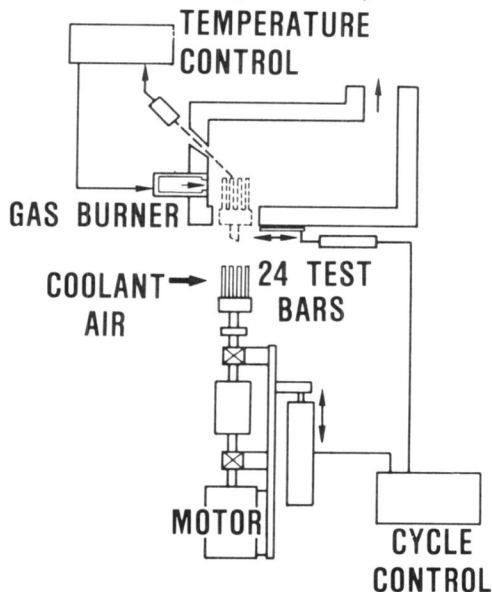
# THERMAL CYCLIC DURABILITY TESTING OF CERAMIC MATERIALS FOR TURBINE ENGINES



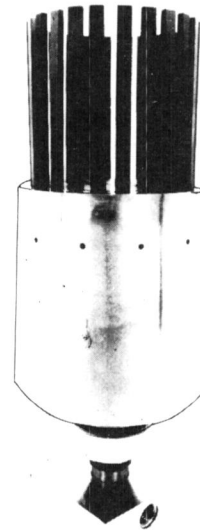
## 3500-HOUR DURABILITY TESTING OF COMMERCIAL CERAMIC MATERIALS

- OBJECTIVE
  - DETERMINE LONG-TERM DURABILITY OF CERAMIC GAS TURBINE ENGINE MATERIALS
- APPROACH
  - CYCLE CERAMIC TEST BARS FROM HIGH TEMPERATURE BURNER EXHAUST TO COLD AIR
  - MONITOR CHANGES IN STRENGTH, WEIGHT, AND DIMENSIONS WITH EXPOSURE TIME AND COMPARE TO BASELINE PROPERTIES
  - TESTING IS TERMINATED WHEN THE STRENGTH IS REDUCED TO 50 PERCENT OF THE BASELINE STRENGTH
- BENEFITS
  - IDENTIFIES CERAMIC MATERIALS CAPABLE OF LONG-TERM USE IN GAS TURBINE ENGINE
  - PROVIDES DIRECT COMPARISON OF NEW CERAMICS WITH MATERIALS PREVIOUSLY TESTED IN THIS CONTINUING PROGRAM

## NASA/GARRETT FACILITY DEVELOPED FOR 1371C (2500F) CYCLIC DURABILITY TESTING



CERAMIC TEST BAR  
DURABILITY TEST FACILITY



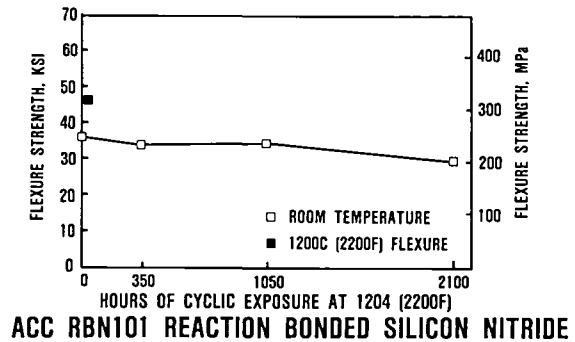
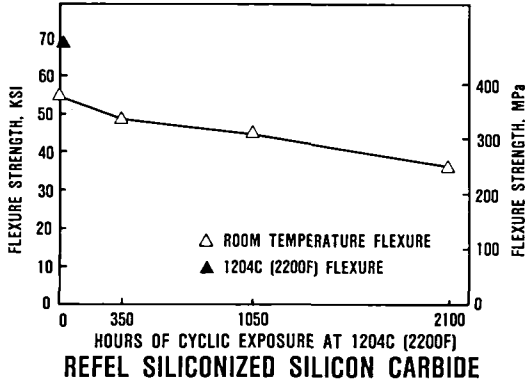
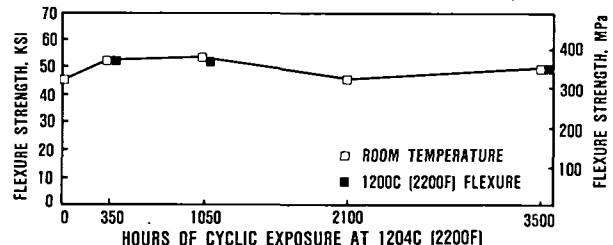
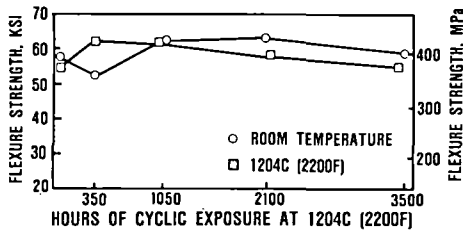
AIR COOLED CERAMIC TEST  
BAR HOLDER

G4-0255-12

## A VARIETY OF CERAMICS HAVE BEEN DURABILITY TESTED

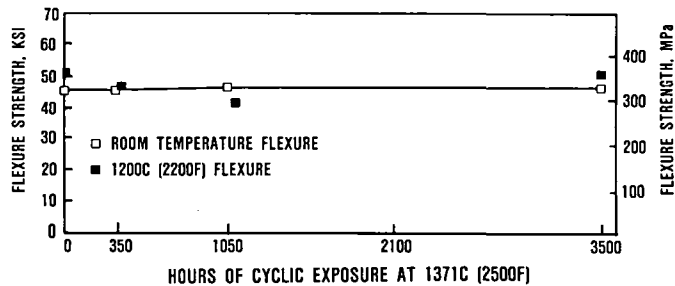
<u>MATERIAL</u>	<u>TEMP, C (F)</u>	<u>DURABILITY, HOURS</u>
SOHIO SINTERED ALPHA SILICON CARBIDE (SASC)	1204 (2200)	3500
SOHIO REACTION SINTERED SILICON CARBIDE (RSSC)	1204 (2200)	3500
ACC RBN 101 REACTION BONDED SILICON NITRIDE (RBSN)	1204 (2200)	2100
REFEL SILICONIZED SILICON CARBIDE (SiSC)	1204 (2200)	2100
NGK SN-50 SINTERED SILICON NITRIDE (SSN)	1204 (2200)	<350
GTE AY6 SSN	1204 (2200)	<350
TOSHIBA SSN	1204 (2200)	<350
ACC SSN	1204 (2200)	<350
NORTON NCX 34 HOT PRESSED SILICON NITRIDE (HPSN)	1204 (2200)	<100
SOHIO SASC	1371 (2500)	3500
ACC RBSN	1371 (2500)	2100
REFEL SiSC	1371 (2500)	<350

## SEVERAL CERAMIC MATERIALS DEMONSTRATE ACCEPTABLE PERFORMANCE AT 1204C (2200F)

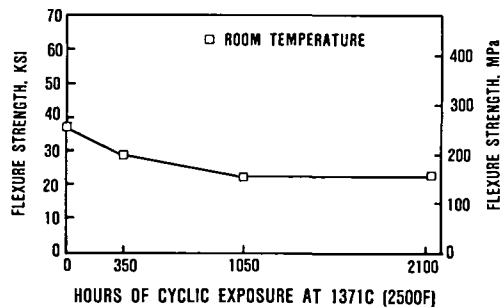


## TEST RESULTS SHOW CERAMIC DURABILITY AT 1371C (2500F)

SOHIO SINTERED  
ALPHA SILICON CARBIDE



ACC RBN101 REACTION BONDED SILICON NITRIDE



## NEW MATERIALS ARE TESTED AS THEY BECOME AVAILABLE

- KYOCERA SC201 SINTERED SILICON CARBIDE (SSC) — DURABILITY TESTING IN PROGRESS
- SOHIO SASC (INJECTION MOLDED, AS-FIRED SURFACES) — DURABILITY TESTING IN PROGRESS
- GE  $\beta$  SSC — BASELINE TESTING COMPLETE
- CORNING LAS — BASELINE TESTING COMPLETE
- NGK SN-82 SSN — BASELINE TESTING COMPLETE
- ACC CODE 2 SSN — TO BE PROCURED
- KYOCERA SN 250M OR 270M SSN — TO BE PROCURED

## BASELINE STRENGTH OF KYOCERA SINTERED SILICON CARBIDE HAS BEEN DETERMINED

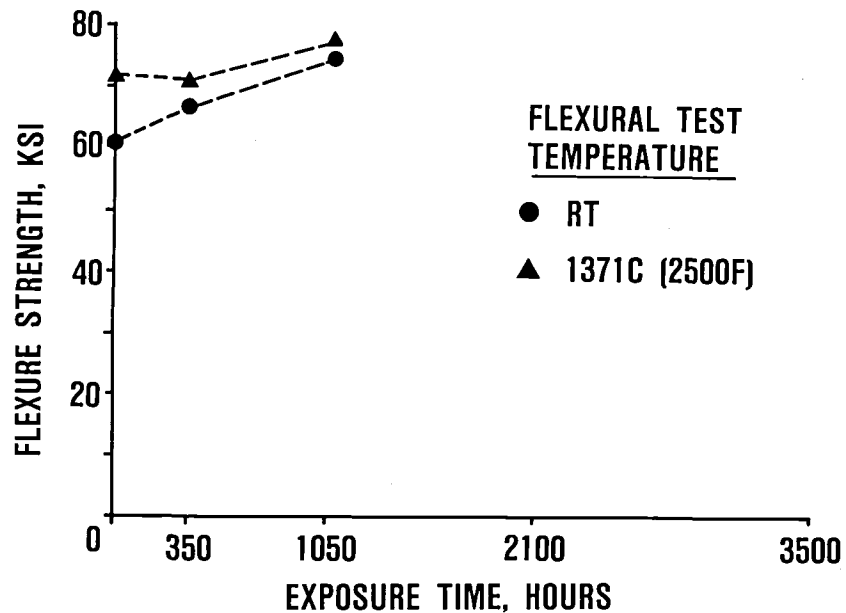
MATERIAL: KYOCERA SC201

CONDITION: AS-FIRED TEST BARS

	ROOM TEMPERATURE	1204C (2200F)	1371C (2500F)
MEAN STRENGTH, KSI (12 DATA POINTS)	61.9	66.2	71.3
STANDARD DEVIATION, KSI	11.4	8.2	8.8

CYCLIC EXPOSURE TESTING IS BEING CONDUCTED AT 1371C (2500F)

## KYOCERA SC201 HAS UNDERGONE 1050 HOURS OF CYCLIC EXPOSURE TO 1371C (2500F)



## BASELINE STRENGTH OF SOHIO INJECTION MOLDED SINTERED SiC HAS BEEN DETERMINED

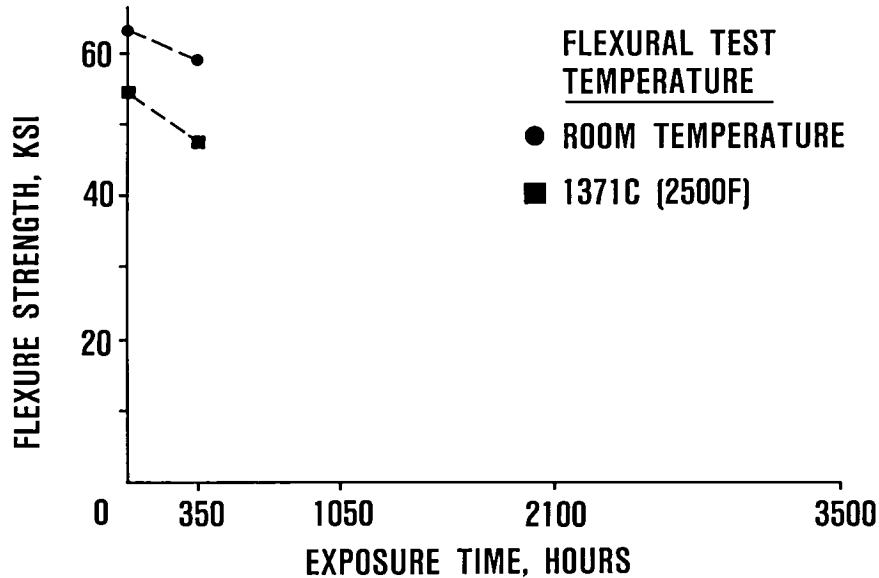
MATERIAL: SOHIO SASC

CONDITION: AS-FIRED TEST BARS

	ROOM TEMPERATURE	1204C (2200F)
MEAN STRENGTH, KSI (12 DATA POINTS)	63.5	60.7
STANDARD DEVIATION, KSI	9.2	7.6

CYCLIC EXPOSURE TESTING IS BEING CONDUCTED AT 1371C (2500F)

# **SOHIO INJECTION MOLDED SASC HAS UNDERGONE 350 HOURS OF CYCLIC EXPOSURE TO 1371C (2500F)**



## **BASELINE STRENGTH OF GE $\beta$ SILICON CARBIDE HAS BEEN DETERMINED**

**MATERIAL: GE  $\beta$  SiC**

**CONDITION: AS-FIRED TEST BARS**

	ROOM TEMPERATURE	1371C (2500F)
MEAN STRENGTH, KSI (12 DATA POINTS)	61.4	61.2
STANDARD DEVIATION, KSI	4.6	8.9

**CYCLIC EXPOSURE TESTING TO BE CONDUCTED AT 1371C (2500F)**

# BASELINE STRENGTH OF NGK SINTERED SILICON NITRIDE HAS BEEN DETERMINED

MATERIAL: NGK SN-82

CONDITION: AS-FIRED TEST BARS

	ROOM TEMPERATURE	982C (1800F)	1204C (2200F)
MEAN STRENGTH, KSI (12 DATA POINTS)	120.4	103.9	97.3
STANDARD DEVIATION, KSI	14.0	9.2	5.5

CYCLIC EXPOSURE TESTING TO BE CONDUCTED AT 1204C (2200F)

## RESULTS

- SOHIO SASC (ISOPRESSED, MACHINED SURFACES) EXPERIENCES NO NO STRENGTH DEGRADATION AFTER 3500 HOURS OF CYCLIC EXPOSURE AT 1371C (2500F)
- SOHIO RSSC EXPERIENCES NO STRENGTH DEGRADATION AFTER 3500 HOURS OF CYCLIC EXPOSURE AT 1204C (2200F)
- ACC RBSN EXPERIENCES A 20-PERCENT STRENGTH REDUCTION AT 1204C (2200F) AFTER 2100 HOURS OF EXPOSURE AND A 20-PERCENT STRENGTH REDUCTION AFTER 350 HOURS AT 1371C (2500F)
- ALL SSN MATERIALS TESTED TO DATE (NGK SN-50, ACC CODE 2, GTE AY6, TOSHIBA SSN) EITHER EXHIBITED LOW BASELINE FLEXURE STRENGTHS AND/OR SHOWED >50-PERCENT STRENGTH DEGRADATION DURING THE FIRST 350 HOURS OF CYCLIC EXPOSURE AT 1204C (2200F)



## **BASELINE FLEXURE STRENGTH AND CYCLIC DURABILITY TESTING IS SCHEDULED FOR 1986-1987**

- **CYCLIC EXPOSURE TESTING IS CURRENTLY BEING CONDUCTED ON INJECTION MOLDED SOHIO SASC WITH AS-FIRED SURFACES AND KYOCERA SSC WITH AS-FIRED SURFACES AT 1371C (2500F)**
- **CYCLIC EXPOSURE TESTING OF GE  $\beta$  SSC, CORNING LAS, NGK SN-82 SSN AND ACC CODE 2 SSN WILL BE CONDUCTED DURING 1986-1987**
- **KYOCERA SN-250M OR 270M WILL BE PROCURED FOR BASELINE AND EXPOSURE TESTING DURING 1986-1987**



# FRACTOGRAPHIC AND MICROSTRUCTURAL EVALUATION OF 3500-HOUR DURABILITY SPECIMENS

A. D. Miller  
Materials Science and Engineering  
University of Washington  
Seattle, Washington 98195

NASA Lewis Research Center has since 1978 contracted with Garrett Turbine Engine Company to conduct long-term durability testing of candidate ceramic materials for advanced gas turbine applications. Specimens of the materials are exposed to combustion atmospheres under temperature cyclic conditions for times up to 3500 hours and at peak temperatures of 1200 and 1370 C. The specimen strengths after exposure are measured at room temperature and at 1200 C. In addition, a number of physical measurements are taken, however no provision is made in the contract for microstructural examination of the specimens.

The work under this project covers examination of three materials, (1) sintered alpha silicon carbide manufactured by Carborundum Co., (2) sintered silicon nitride, manufactured by Toshiba, and (3) reaction bonded silicon nitride, grade RBN-104, manufactured by Airesearch Casting Company. The work required the development of sample preparation techniques to provide high quality thin-section specimens which can be examined by transmitted light or thinned using an ion mill for subsequent TEM examination.

Specimen preparation techniques and the results of optical and electron microscopic examination of the reaction interfaces of the selected specimens are presented and discussed.

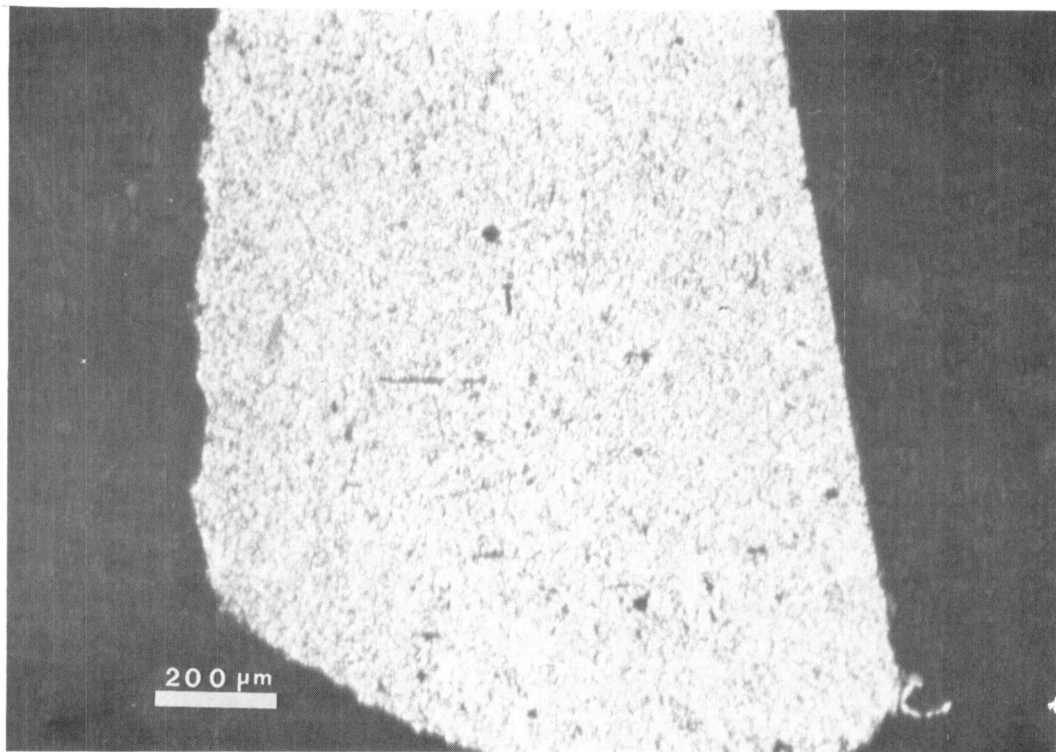


Figure 1. - Baseline SASC; crossed Nichols. 95X

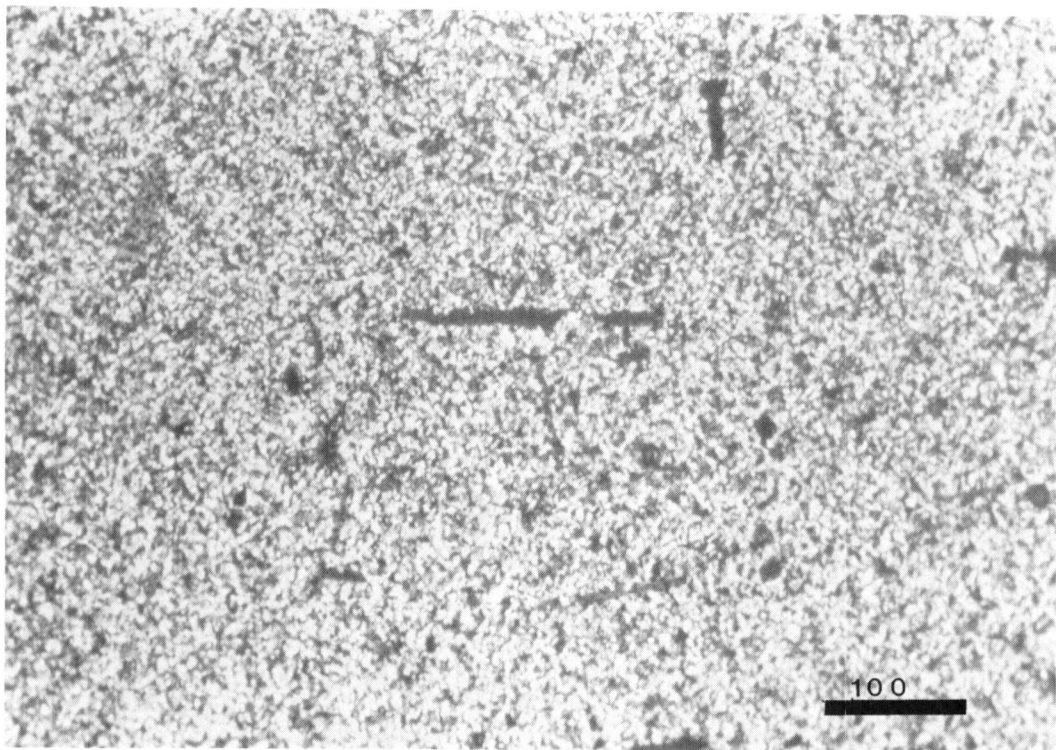


Figure 2. - Baseline SASC; crossed Nichols. 240X.

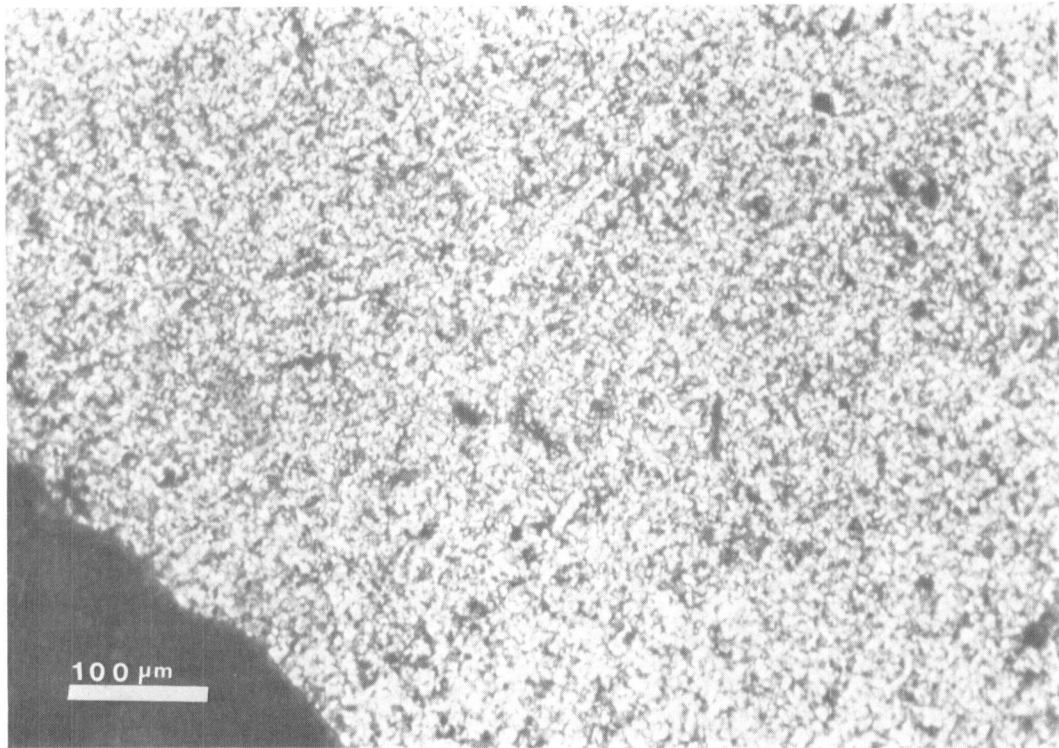


Figure 3. - Same field as fig.2; crossed Nichols, rotated 45°. 240X.

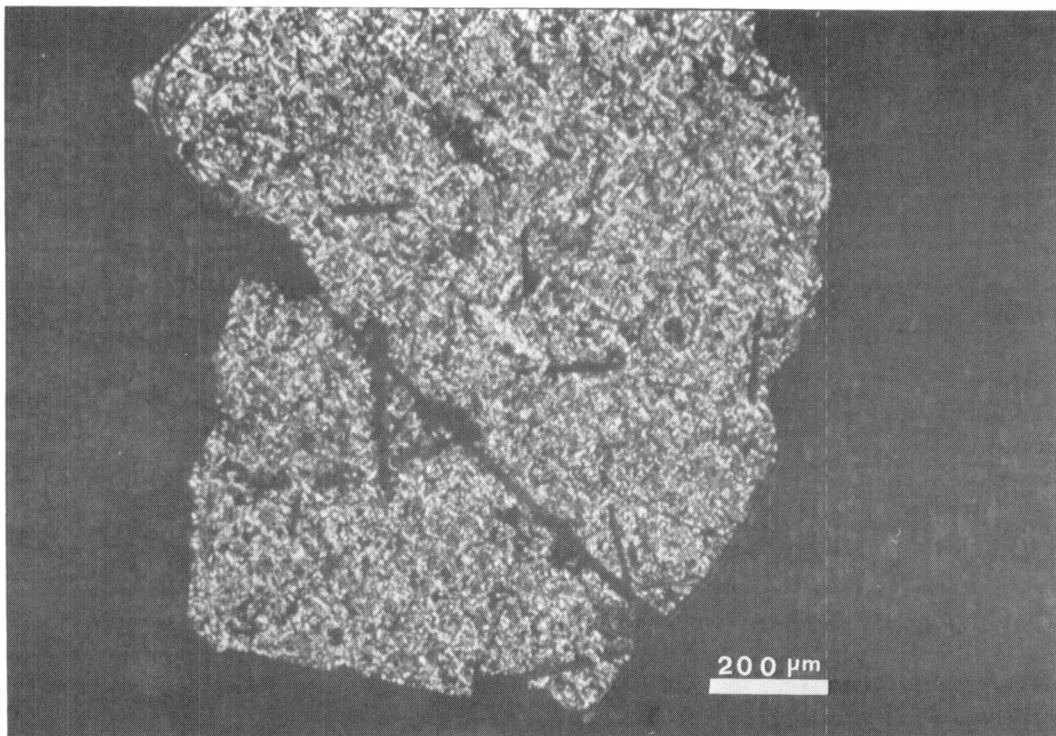


Figure 4. - SASC; 2100-hr exposure at 1370 °C; crossed Nichols. 95X.

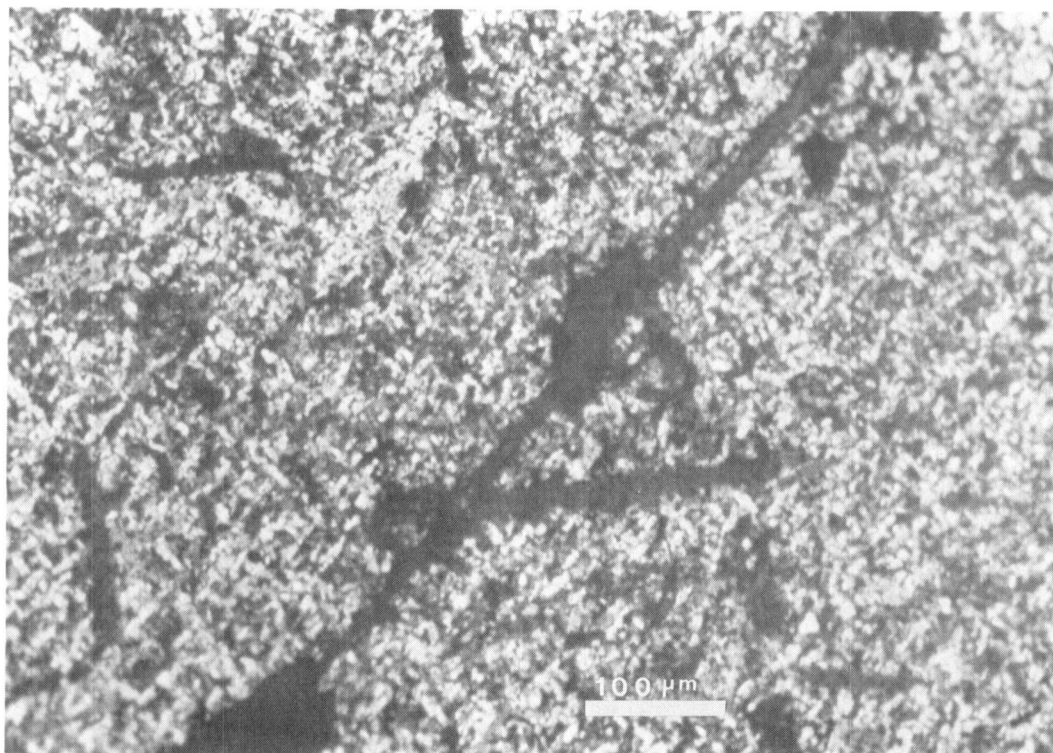


Figure 5. - Same field as fig. 4. 240X.

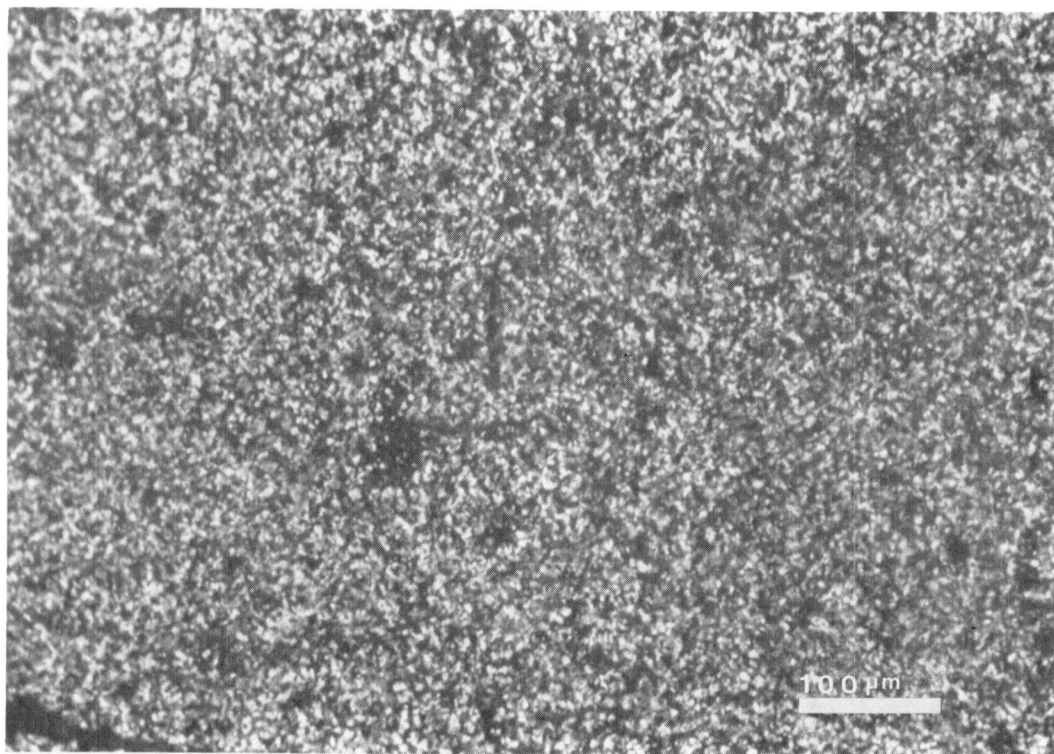


Figure 6. - SASC; 3500-hr exposure at 1370 °C; crossed Nichols. 240X.



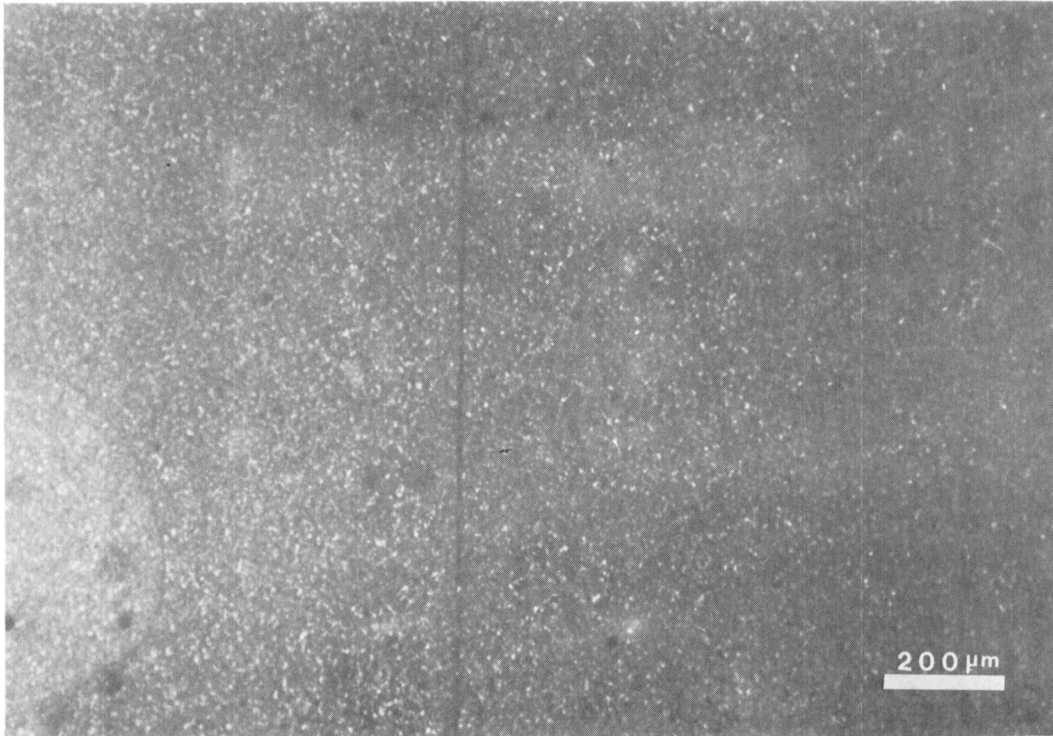


Figure 7. - Baseline Toshiba SSN; crossed Nichols. 95X.

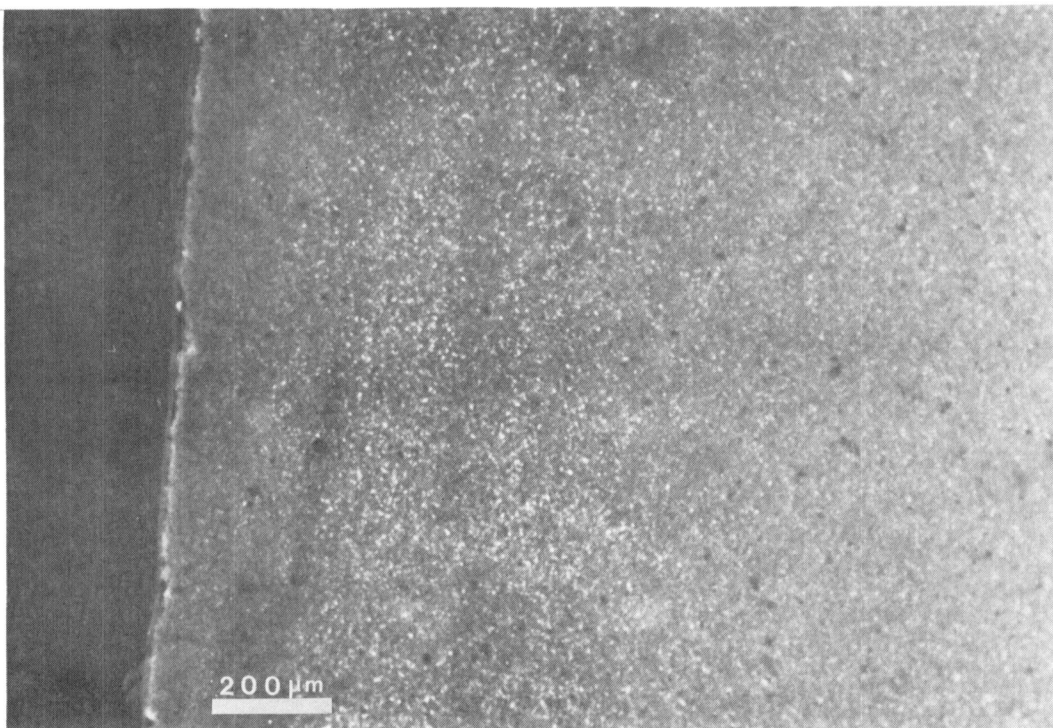


Figure 8. - Toshiba SSN; 350-hr exposure at 1205 °C; crossed Nichols. 95X.

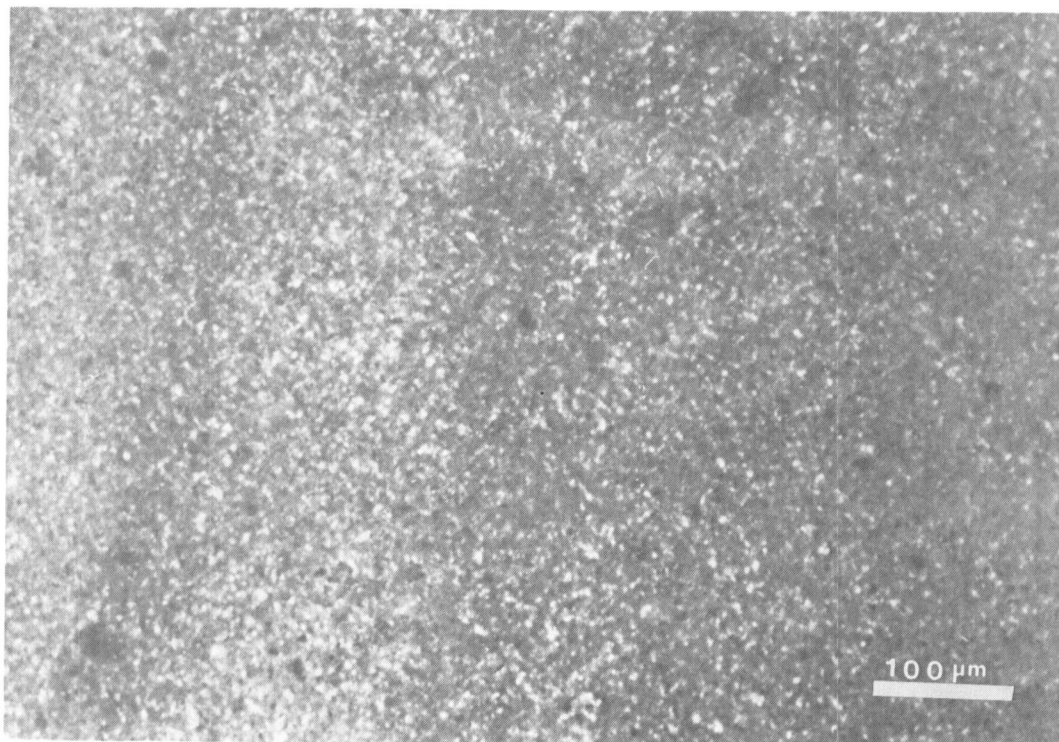


Figure 9. - Same specimen as fig. 8; field near interface; crossed Nichols. 240X

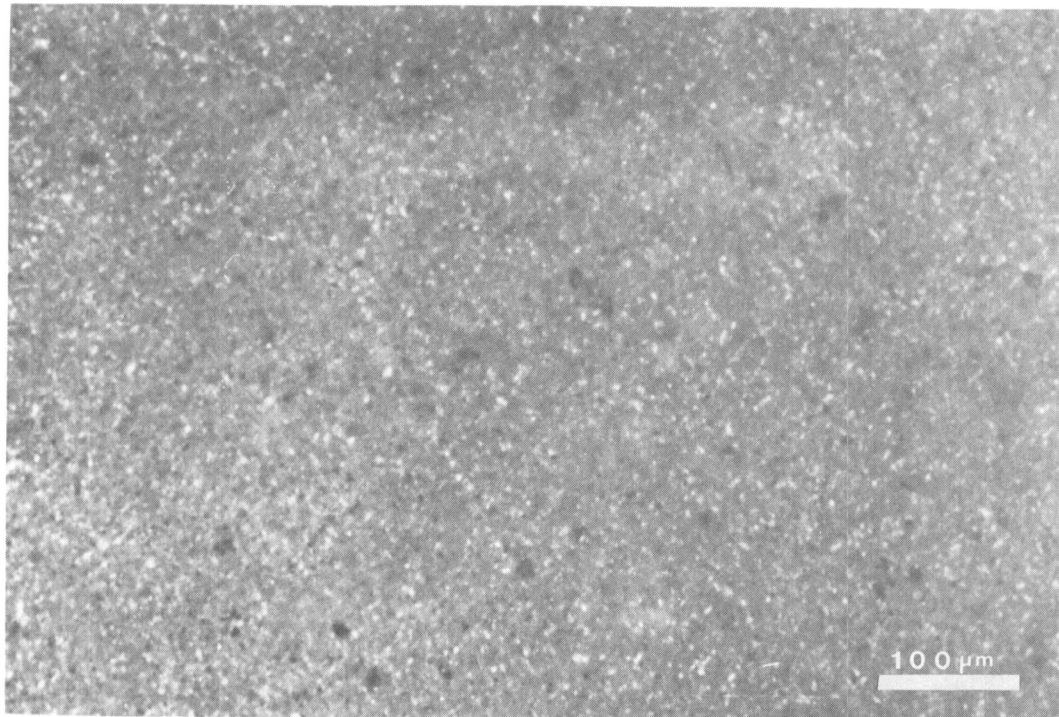


Figure 10. - Same specimen as fig 8; field far from interface; crossed Nichols. 240X.



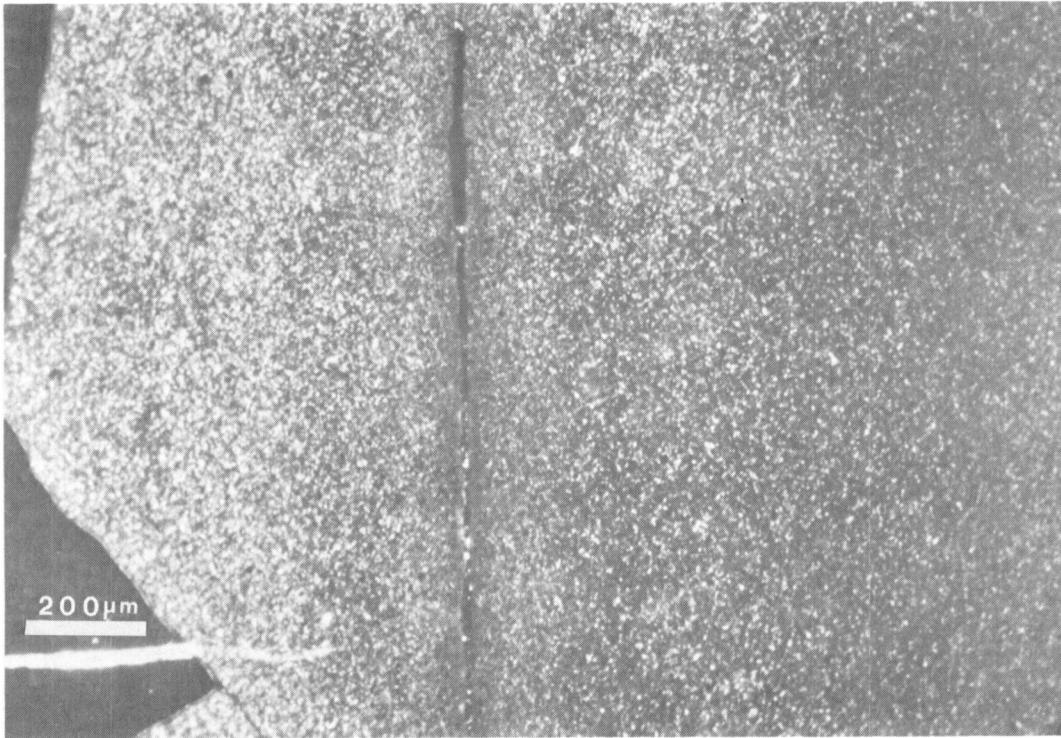


Figure 11. - Toshiba SSN; 700-hr exposure; crossed Nichols. 95X.



## CERAMIC MATRIX COMPOSITES

James A. DiCarlo  
NASA Lewis Research Center  
Cleveland, Ohio 44135

An overview is presented covering NASA Lewis research efforts aimed at materials and processing development for structurally reliable fiber-reinforced ceramic matrix composites (FRC). With the primary goal of developing technology for strong, tough Si-based FRC with use-temperatures above 1400°C, guidelines for optimum material properties and current problems in achieving these properties are discussed. Brief descriptions of particular research projects directed toward solving these problems are presented. Particular emphasis is placed on those efforts addressing the critical need of developing high performance SiC fibers with stability above 1400°C and with proper coatings for optimum composite structural performance. Based on current results for fiber and matrix development, concluding remarks are made concerning future directions for NASA Lewis FRC studies.

# CERAMIC MATRIX COMPOSITES

BY

J. DICARLO

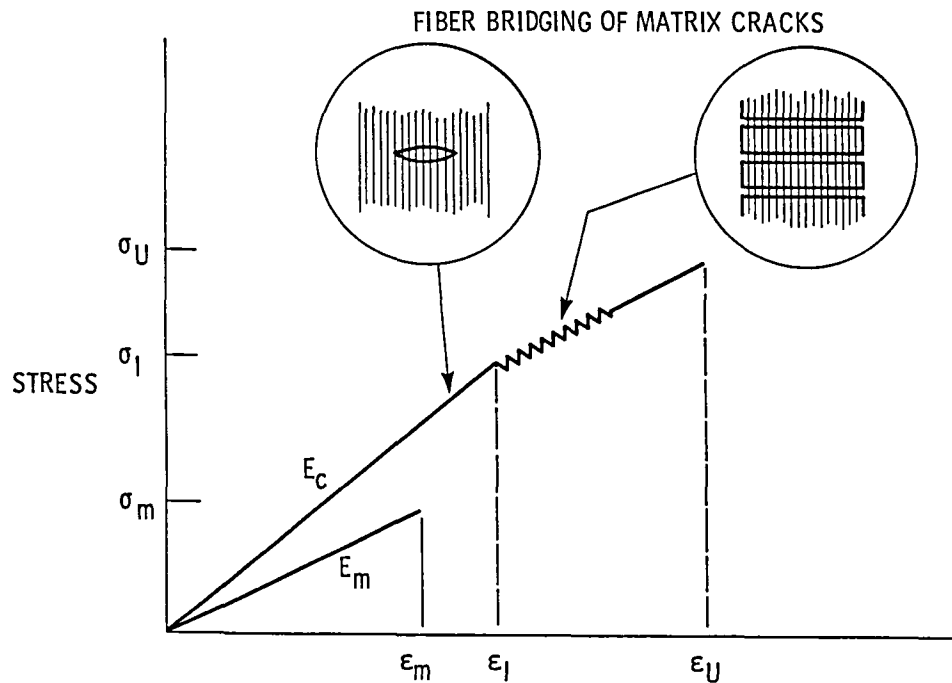
DEPUTY CHIEF, CERAMICS BRANCH

OBJECTIVE: TECHNOLOGY DEVELOPMENT FOR FABRICATION OF STRONG, TOUGH, AND RELIABLE CERAMIC COMPOSITES FOR AERO-SPACE STRUCTURAL APPLICATIONS TO 1400 °C AND ABOVE

PRIMARY

APPROACH: FIBER REINFORCED CERAMICS (FRC) - REINFORCEMENT OF Si-BASED CERAMIC MATRICES WITH CONTINUOUS HIGH PERFORMANCE CERAMIC FIBERS

## FRC DEFORMATION AND FRACTURE



CS-84-2357

## STRUCTURAL ADVANTAGES OF FIBER- REINFORCED CERAMICS

- IMPROVED STIFFNESS
  - MATRIX FRACTURE STRENGTH
  - MATRIX FRACTURE STRAIN
  - FRACTURE TOUGHNESS
  - THERMAL SHOCK
- \* METAL-LIKE STRESS-STRAIN BEHAVIOR
- \* ULTIMATE FAILURE INDEPENDENT OF MATRIX FRACTURE
- \* NONCATASTROPHIC MATERIAL FAILURE
  
- \* AVAILABLE ONLY FOR HIGH ASPECT RATIO REINFORCEMENT

## FRC - KEY TECHNICAL ISSUES

### I. FABRICATION APPROACH FOR HIGH FRC STRENGTH

- PREPARATION OF OPTIMUM MATRIX PRECURSORS
- UNIFORM PRECURSOR INFILTRATION INTO FIBER ARRAY
- MATRIX CONSOLIDATION AND DENSIFICATION WITHOUT
  - FIBER STRENGTH DEGRADATION
  - LARGE SHRINKAGE CRACKS OR POROSITY
  - NONUNIFORM FIBER DISTRIBUTION

### II. AVAILABILITY OF HIGH PERFORMANCE CERAMIC FIBERS

- HIGH STRENGTH AND STIFFNESS
- THERMAL STABILITY ABOVE 1200 °C
- SMALL DIAMETER

### III. FIBER COATINGS

- FIBER STRENGTH RETENTION UNDER FRC PROCESSING AND USE
- OPTIMUM FOR COMPOSITE TOUGHNESS AND OFF-AXIS STRENGTH

## FRC - CURRENT NASA LEWIS PROGRAMS

### I. COMPOSITE FABRICATION

PROCESSING APPROACH	PRIMARY SYSTEM	KEY ISSUES
• REACTION-BONDED $\text{Si}_3\text{N}_4$ WITH CVD SiC FIBERS	SiC/RBSN	- STRENGTH AND TOUGHNESS GREATER THAN RBSN  - THERMAL STABILITY TO 1400 °C
• CARBON MATRICES REACTION BONDED WITH SILICON	SiC/RBSC	- MATRIX MORPHOLOGY AND SILICONIZATION  - FIBER DEGRADATION
• POLYMER-DERIVED PRECURSORS TO SiC AND $\text{Si}_3\text{N}_4$ MATRICES		- HIGH CHAR YIELD  - INFILTRATION RHEOLOGY WITH CERAMIC FILLERS

## FRC - CURRENT NASA LEWIS PROGRAMS

### II. HIGH PERFORMANCE SiC FIBERS

- |   |   |
|---|---|
| • HIGH TEMPERATURE PROPERTIES<br>OF COMMERCIAL SiC FIBERS | - FIBER PROCESSING APPROACH BEST<br>SUITED FOR HIGH TEMPERATURE FRC |
| • POST PROCESSING OF NICALON<br>FIBERS AT HIGH PRESSURE   | - POTENTIAL OF HIPPING FOR IMPROVING<br>NICALON THERMAL STABILITY   |

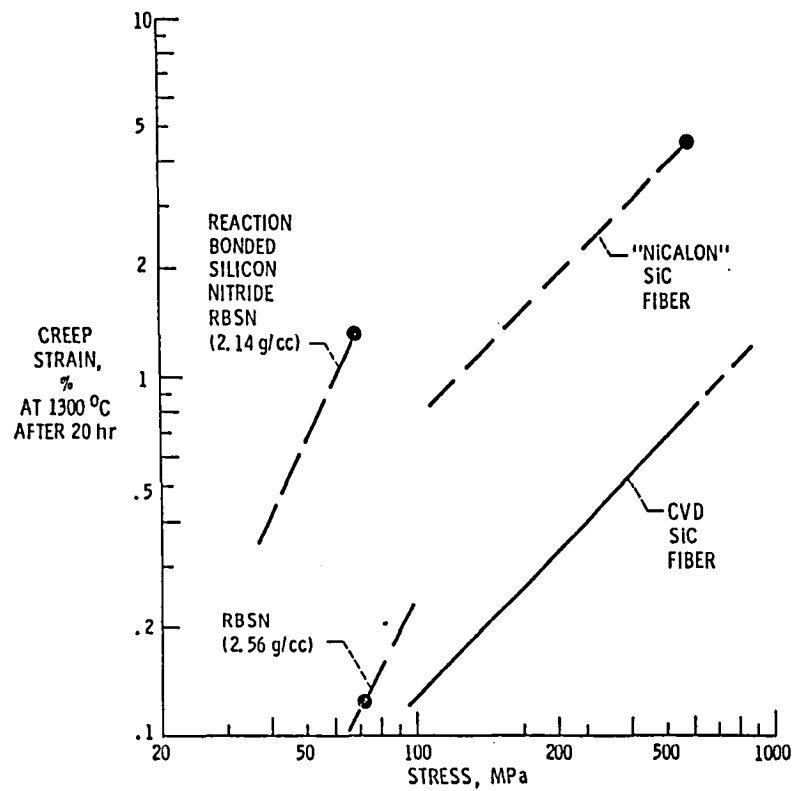
### III. FIBER COATINGS

- |   |  |
|---|--|
| • OXYGEN EFFECTS ON COMMERCIAL<br>COATINGS FOR CVD SiC FIBERS | - COATING DESIGN FOR OXIDATION<br>RESISTANCE             |
| • FIBER-MATRIX LOAD TRANSFER IN<br>SiC/RBSN COMPOSITES        | - COATING DESIGN FOR COMPOSITE<br>TOUGHNESS AND STRENGTH |

## PROPERTY COMPARISON - COMMERCIAL SiC FIBERS

TYPE:	NICALON (NIPPON CO.)	SCS (AVCO)
PRODUCTION METHOD:	POLYMER SPUN, CURED, PYROLYZED	CVD ONTO CARBON FILAMENT (1300 °C)
FORM:	MULTIFILAMENT YARN (500 PER TOW)	MONOFILAMENT
DIAMETER, $\mu\text{m}$ :	10 TO 20	142
MODULUS, GPa:	180	390
STRENGTH, GPa:		
20 °C:	2.0	>3.5
1400 °C:	<1.0	>2.5

### CVD SiC FIBERS PROVIDE CREEP RESISTANCE TO RBSN MATRICES



CS-84-0418

## ADVANTAGES OF FIBER COATINGS FOR CERAMIC MATRIX COMPOSITES

### PHYSICAL - CHEMICAL:

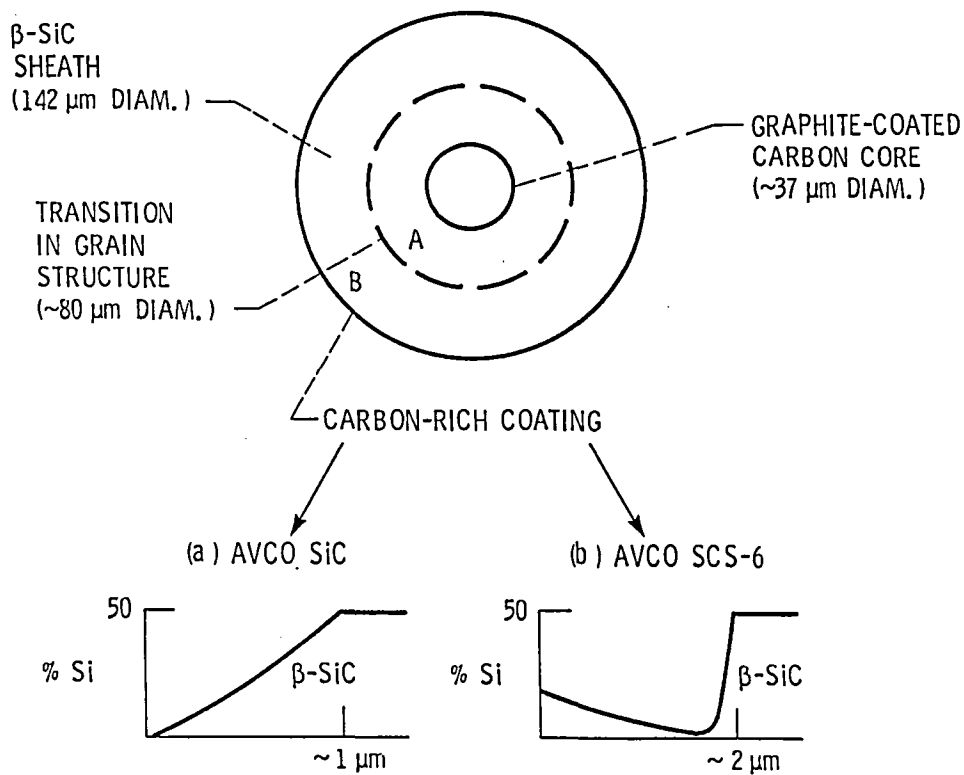
- CAN SERVE AS A DIFFUSION BARRIER INHIBITING INTERDIFFUSION AND REACTIONS WITH MATRIX AND AGGRESSIVE GASES, SUCH AS, OXYGEN
- MINIMIZE DEGRADATION OF FIBER STRENGTH AND FIBER - MATRIX INTERFACIAL BONDING

### STRUCTURAL:

- REDUCE MECHANICAL DEGRADATION DURING HANDLING AND COMPOSITE PROCESSING
- REDUCE INTERNAL DEGRADATION BY TRAPPING EVOLVING GASES
- HEAL FIBER SURFACE FLAWS AND INCREASE FIBER STRENGTH
- PROVIDE WEAK FIBER - MATRIX BONDING FOR CRACK DEFLECTION AND TOUGH COMPOSITES

CS-85-0274

### CVD SiC FIBER CROSS SECTION AND COATINGS

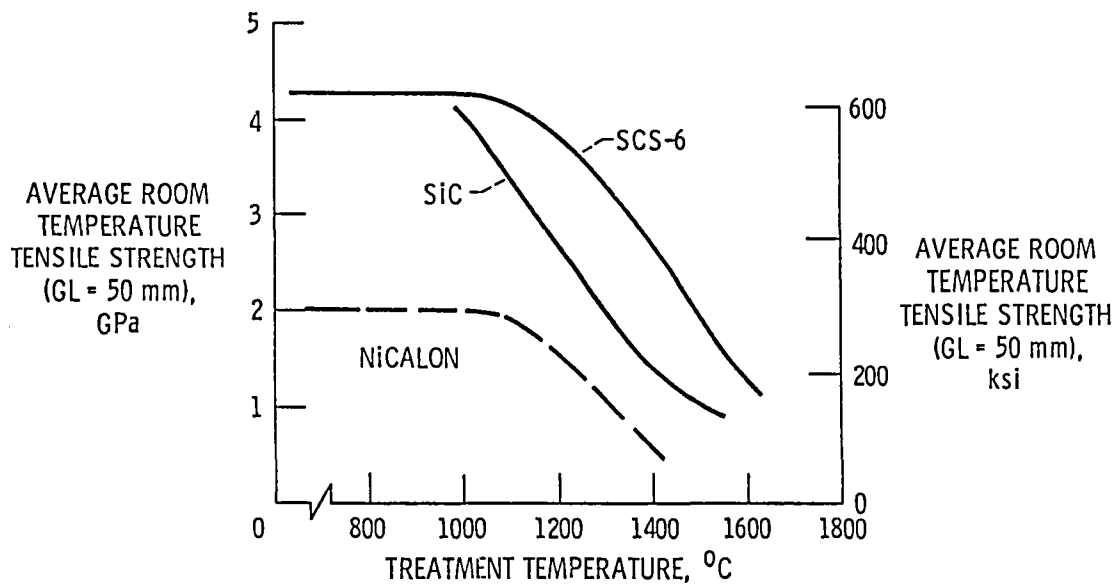


CS-84-0419



## STRENGTH RETENTION OF SiC FIBERS

ARGON OR NITROGEN, 15 min ( $10^{-4}$  ATM OXYGEN)



CS-84-2355

## CERAMIC COMPOSITES - FUTURE DIRECTIONS

### I. FRC FABRICATION

- SiC/RBSN OPTIMIZATION
- CVD-CVI PROCESSING
- COMBINED PROCESSING APPROACHES
- TOUGHENING ADDITIONS TO MATRIX
- MULTITYPE FIBERS AND FIBER WEAVES
- HYBRID MATRICES

### II. HIGH PERFORMANCE CERAMIC FIBERS

- MULTIFILAMENT TOW OF SMALL DIAMETER CVD SiC FIBERS
- SINGLE CRYSTAL SiC AND OXIDE FIBERS
- NEW INNOVATIVE PROCESSING

### III. FIBER COATINGS

- STABLE AND OPTIMIZED CVD SiC-C COATINGS
- OTHER CERAMIC COATINGS BY CVD, SOL-GEL, ETC



## Polymer Precursors for SiC Ceramic Materials

by

Morton H. Litt  
Department of Macromolecular Science  
Case Western Reserve University  
Cleveland, Ohio 44106

We have worked on precursor polymers to SiC, concentrating on polymers made from decamethyl cyclohexasilylene units. Our initial approach was to synthesize mixed diphenyl decamethyl cyclohexasilane, dephenylate and polymerize. This produced polymers which had yields of up to 50% SiC. [Theoretical yield is 75%.] Our present approach is to make polymer through the intermediate trans-1,4-diphenyl decamethyl cyclohexasilane. This should produce a crystalline polymer and high strength fibers. These will be thermally decomposed to SiC fibers. This requires new chemistry which we are studying now.

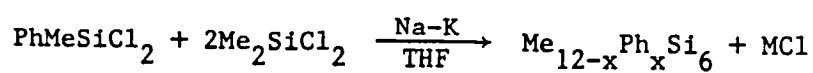
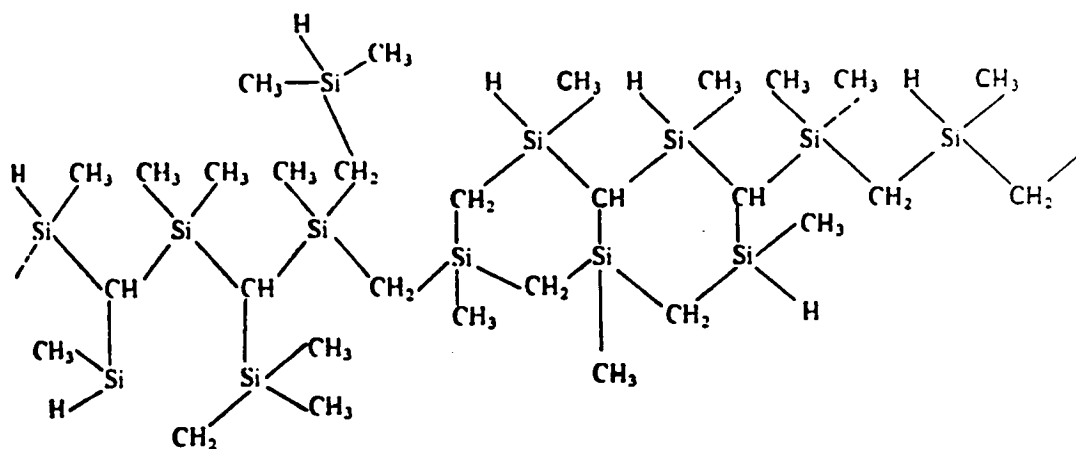
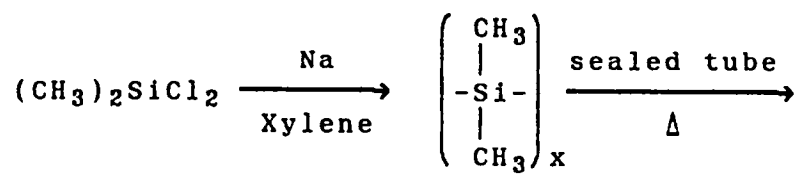


TABLE 1. PERCENT YIELD OF VARIOUS ISOLATED DERIVATIVES

$\text{Me}_{12-x}\text{Ph}_x\text{Si}_6$		<u>Yield</u>	
x	wt(%)	mol(%)	mol(%) (theoretical)
0	8	11	8.8
1	24	27	26.3
2	32	32	32.9
3	36	30	21.9
4			8.2
5			1.6
6			0.1

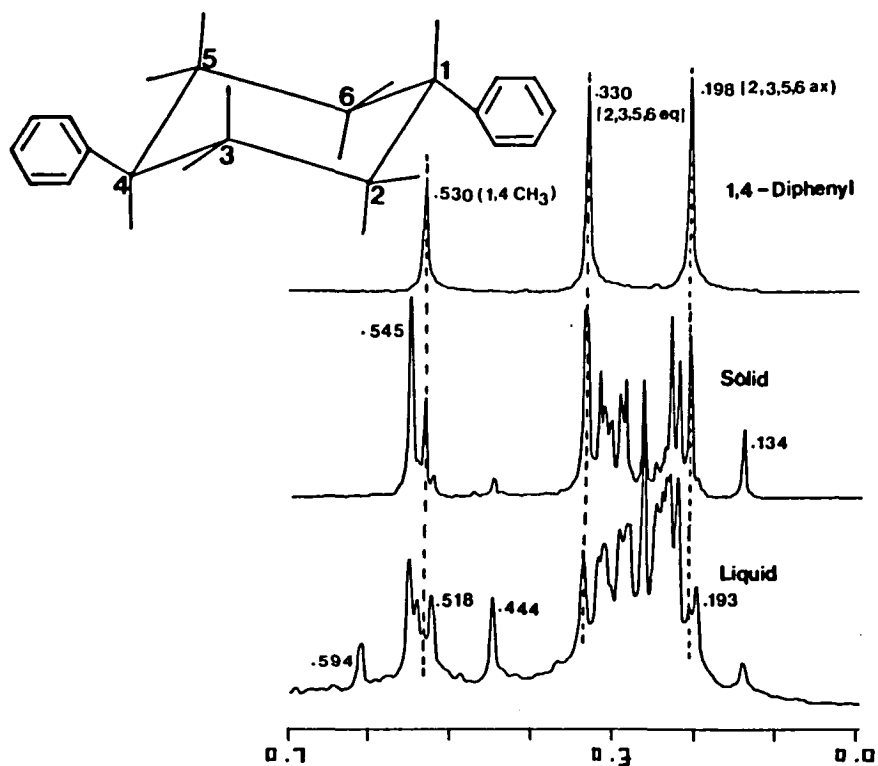


FIG 1. NMR OF DIPHENYLDECAMETHYLCYCLOHEXASILANE

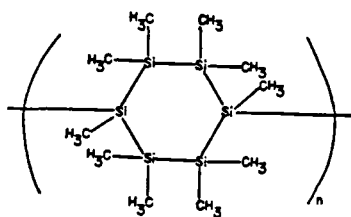
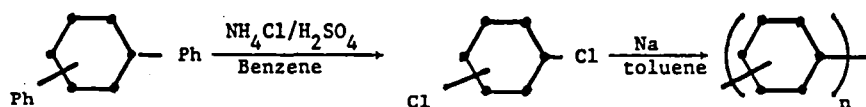
TABLE 2.  $^1\text{H}$ -,  $^{13}\text{C}$ -, AND  $^{29}\text{Si}$ - NMR CHEMICAL SHIFTS FOR PURE  
1,4-DIPHENYLDECAMETHYLCYCLOHEXASILANE

$^1\text{H}$ (No. of Methyl Groups) ( $\delta$ ppm) <sup>a</sup>	$^{13}\text{C}$ (No. of Carbon) ( $\delta$ ppm) <sup>b</sup>	$^{29}\text{Si}$ (No. of Silicon) ( $\delta$ ppm) <sup>c</sup>
0.530 (2)	-4.32 (4)	-41.08 (4)
0.330 (4)	-6.49 (2)	-41.40 (2)
0.198 (4)	-6.71 (4)	
	134.68 (o,4)	
	127.86 (p,2)	
	127.71 (m,4)	
	146.98 (i,2)	

a -  $\text{CH}_2\text{Cl}_2$  ( $\delta$  5.35) was used as an internal reference.

b -  $\text{CDCl}_3$  ( $\delta$  77.0) was used as an internal reference.

c - TMS ( $\delta$  0.0) was used as an internal reference.



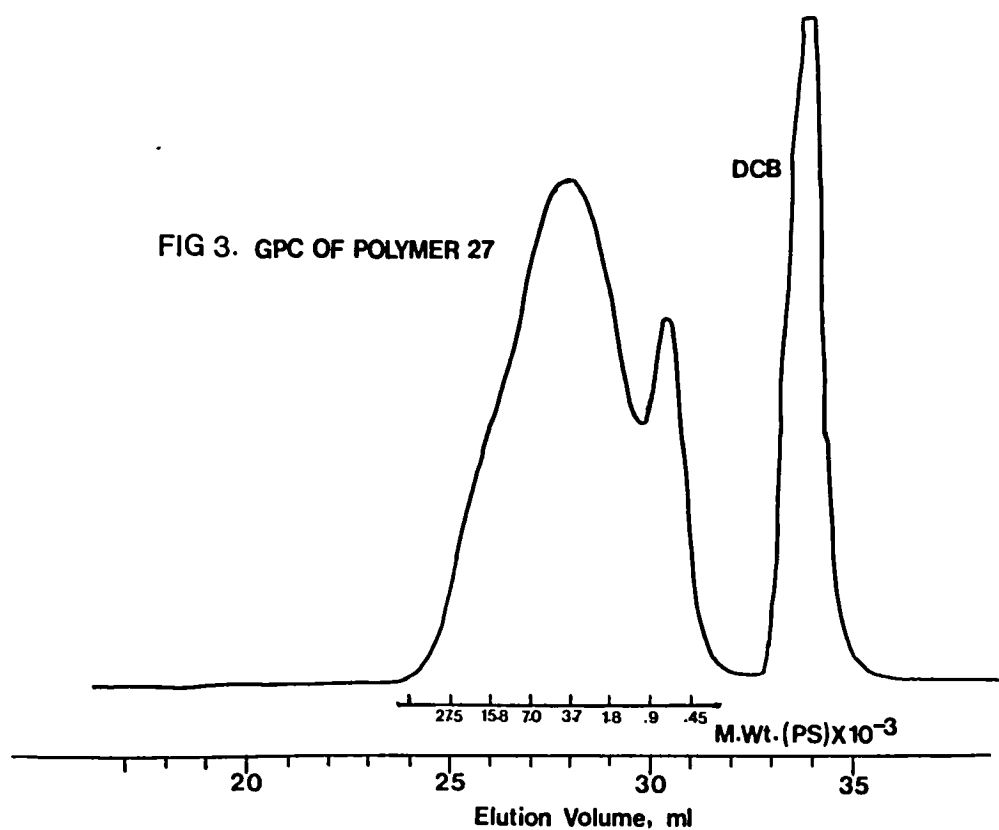
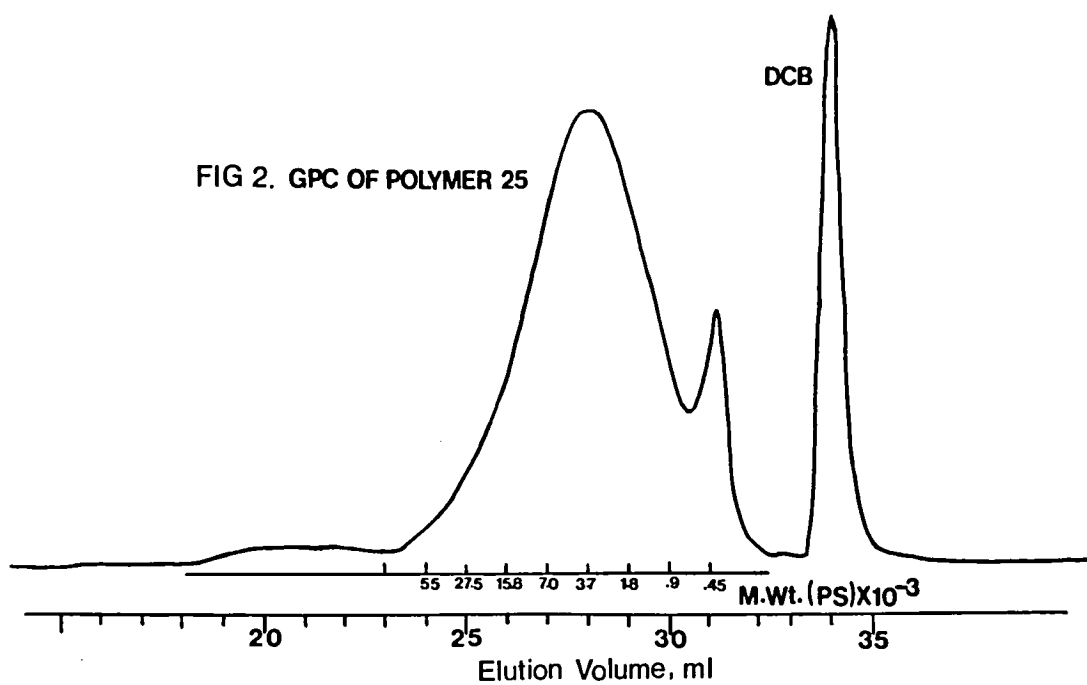


TABLE 1 ELEMENTAL ANALYSIS OF POLYMER25 AND POLYMER27

Polymer	Analytical	% C	% H	% Si	% O
Polymer25	Calcd.:	37.74	9.43	52.83	0
	Found:	33.52	8.69	48.22	9.57 (by difference)
Repeat	Found:	34.40	8.51	-----	None or Trace
Polymer27	Calcd.:	37.74	9.43	52.83	0
	Found:	38.10	9.65	48.70	3.55 (by difference)
Repeat	Found:	40.14	9.23	-----	0.16

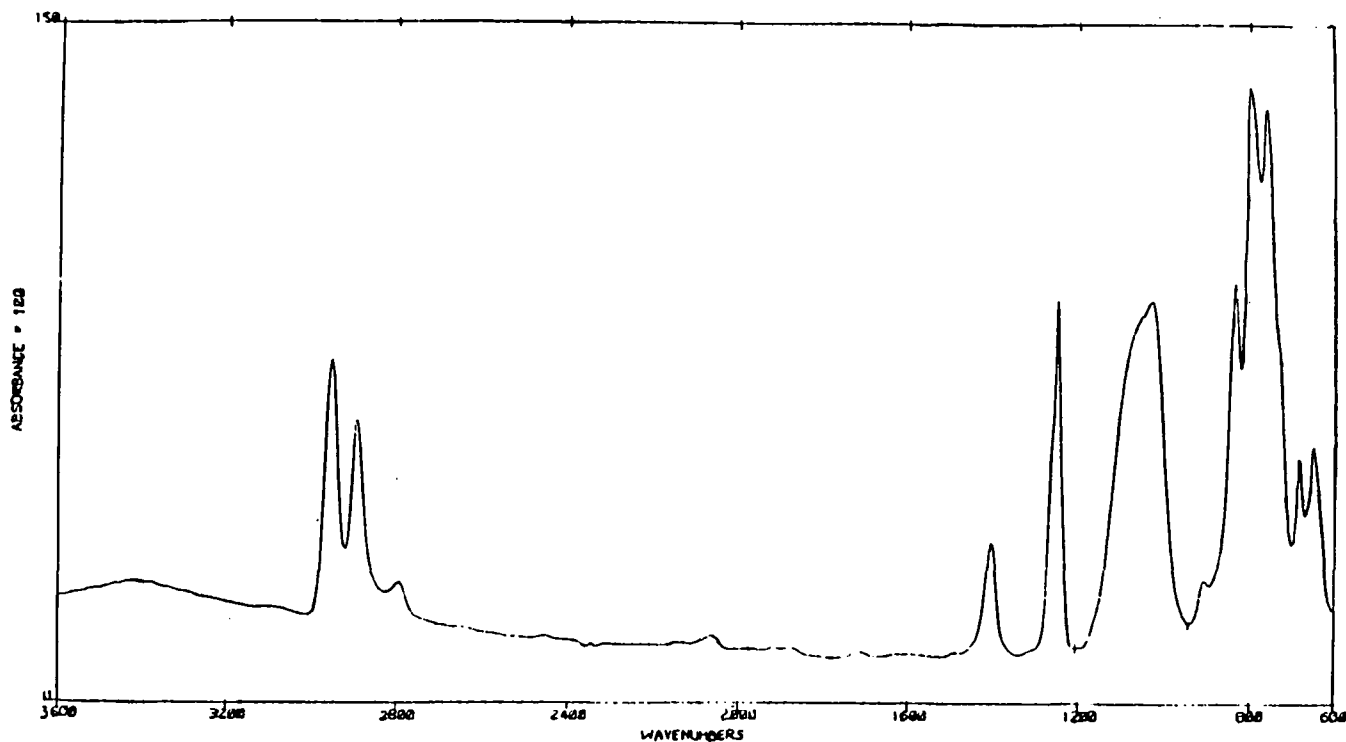


FIG 6. IR OF POLYMER25



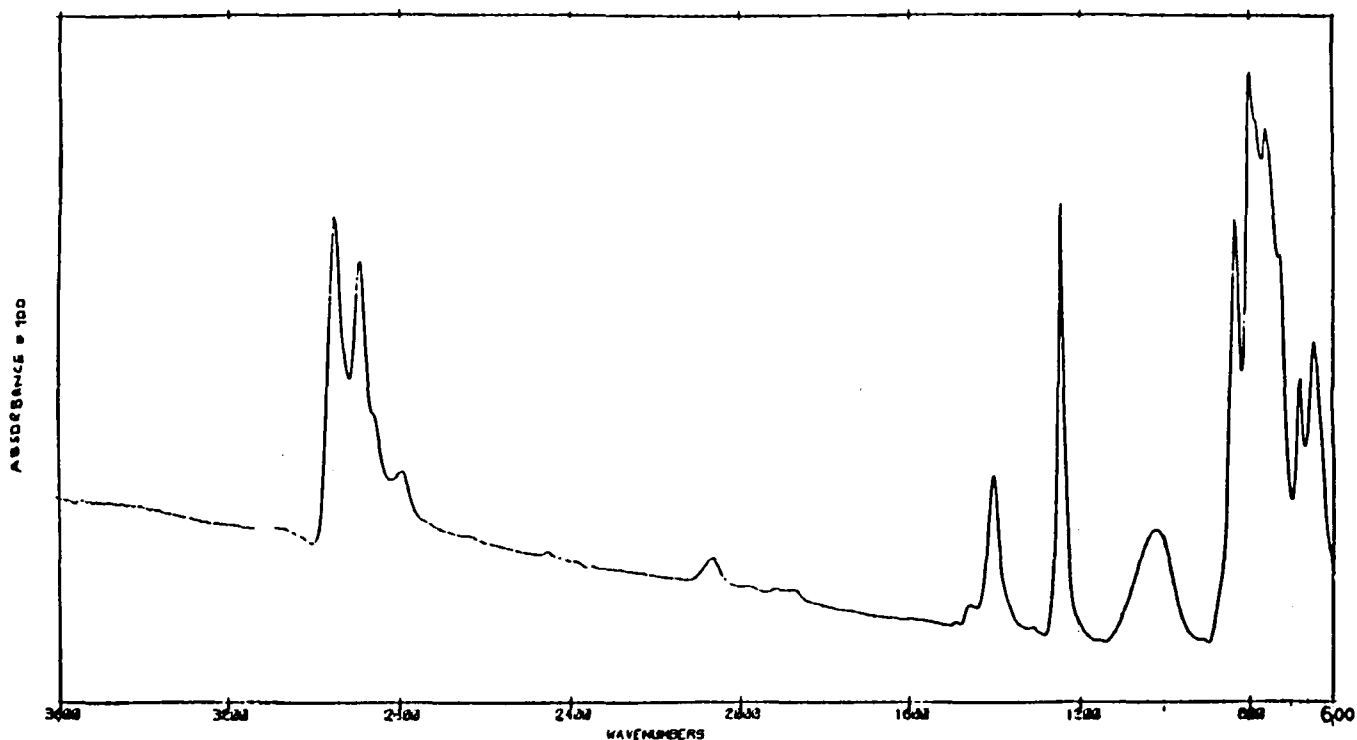


FIG 7. IR OF POLYMER27

TABLE 2 THERMOGRAVIMETRIC ANALYSIS OF POLYMER25 CURED AT VARIOUS TEMPERATURES

Temperature/Time	Char Yield %	Heating Rate
Polymer25	27.39	1.5°C/min
124° ± 4°C/4 hrs (a)	18.75	10° C/min
200° ± 1°C/5 min	20.85	10° C/min
250° ± 5°C/15 min	(a) 20.80	10° C/min
	(b) 48.27	10° C/min
200° ± 1°C/5 hrs	(c) 51.52	10° C/min
	17.74	10° C/min
	36.47	10° C/min
	25.71	15° C/min
	19.64	1.5°C/min

(a) Hexane soluble fraction (59.8% of total polymer).

(b) Gel (12.67% of the total polymer).

(c) A piece of polymer was used, rather than ground powder.

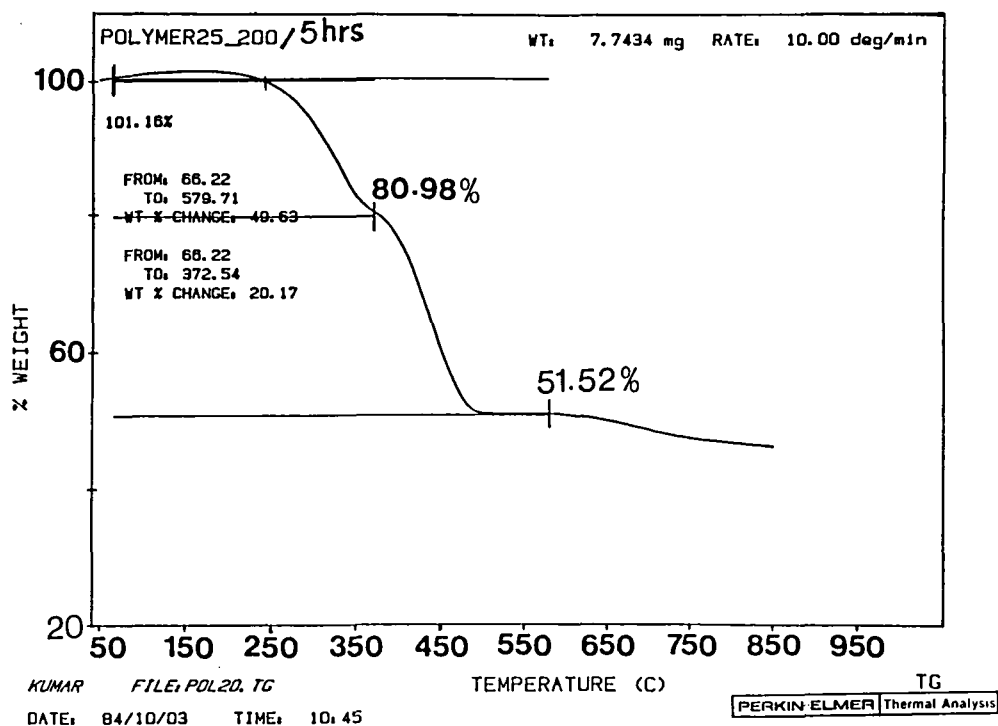
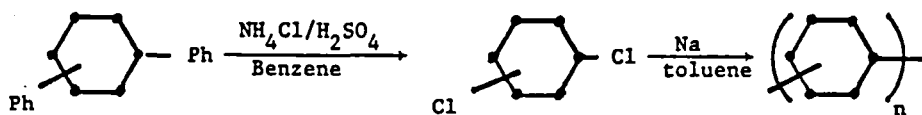


FIG 8.TGA

New Work

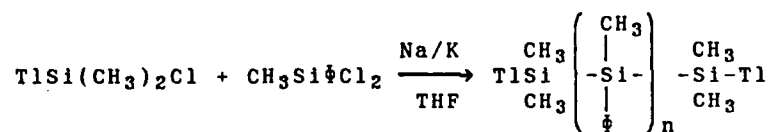
Trans-1,4-diphenyl decamethyl cyclohexasilane

mp = 169.5-170°C, yield = 0.2%



Poly(trans 1,4<sup>1</sup>-decamethyl cyclohexasilane)

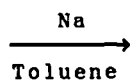
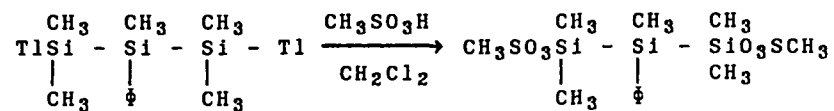
1. Crystallizable polymer.
2. Should be spinnable from solvent in nematic form.
3. Strong, stable fiber
4. Could retain strength to some degree during pyrolysis to SiC.
5. Higher yield and easier processing than present materials.



Tl = p-Tolyl      n = 0  $\longrightarrow$  ?

Theory - highest yield = 27% of n=1

Best yield so far = 20%, n=0,1,2,3,4 isolated





## POLYMER PRECURSORS FOR CERAMIC COMPOSITES

Frances I. Hurwitz  
NASA Lewis Research Center  
Cleveland, Ohio 44135

The fiber composite approach to reinforced ceramics provides the possibility of achieving ceramics with high fracture toughness relative to monolithics. Fabrication of ceramic composites, however, demands low processing temperatures to avoid fiber degradation. Formation of complex shapes further requires small diameter fibers as well as techniques for infiltrating the matrix between fibers.

Polymers offer low temperature processability, control of rheology not available with ceramic powders, and could serve as precursors to fibers of matrix. In recent years, a number of polysilanes and polysiloxanes have been investigated as potential precursors. A review of candidate polymers will be presented, including recent studies of silsesquioxanes underway at LeRC.

## NEEDS

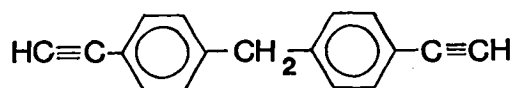
- SMALL DIAMETER CERAMIC FIBER
- HIGH TEMPERATURE, ENVIRONMENTALLY RESISTANT MATRIX

## PROBLEMS

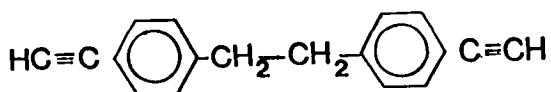
- LOW CHAR YIELD
- HIGH SHRINKAGES - VOIDS
- NEED FOR REPEATED IMPREGNATION
- DEVIATION FROM STOICHIOMETRY - CHEMICAL INSTABILITY AT HIGH TEMPERATURES



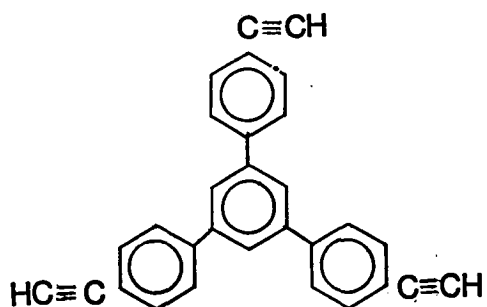
## MONOMERS



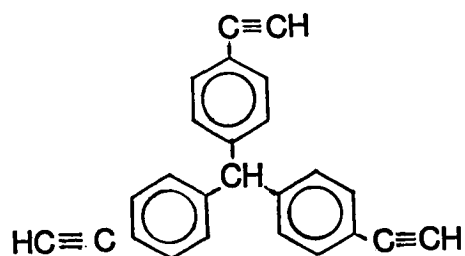
DEDPM  
diethynyldiphenylmethane



DEDPE  
diethynyldiphenylethane

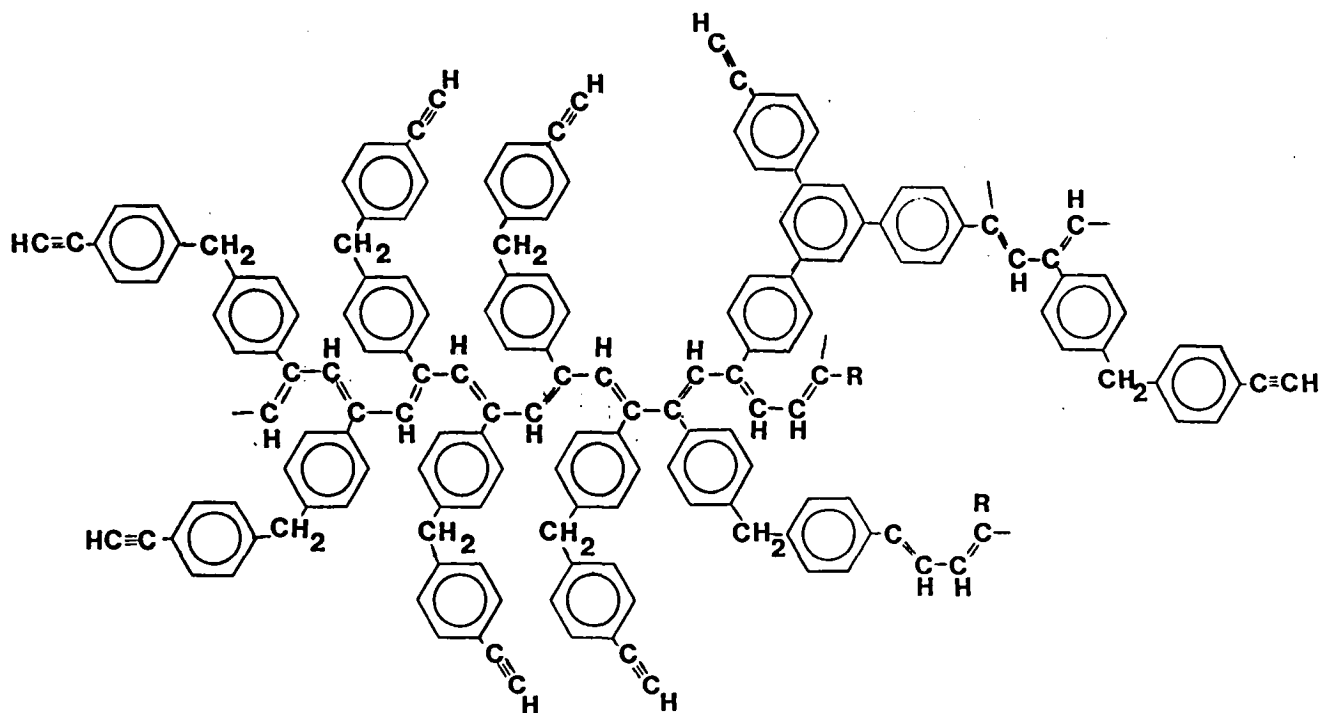


TETPB  
triethynyltriphenylbenzene



TETPM  
triethynyltriphenylmethane

## CROSSLINKED HOMOPOLYMER OR COPOLYMER



## SI CONTAINING POLYMERS

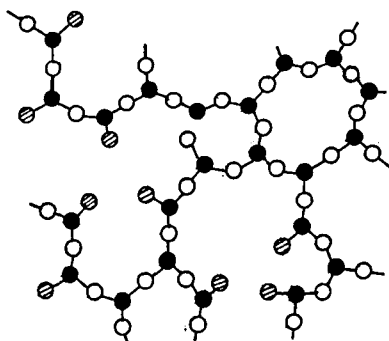
$(\text{CH}_3)_x\text{Si}_y$	METHYLPOLYSILANE
$((\text{CH}_3)_2\text{SiCH}_2\text{SiHCH}_3)_x$	POLYCARBOSILANE
$(\text{C}_6\text{H}_5\text{CH}_2\text{Si})_x((\text{CH}_3)_2\text{Si})_y$	POLYSILASTYRENE
$(\text{CH}_3\text{Si})_x(\text{CH}_2\text{CHSiCH}_3)_y$	VINYLSILANE
$(\text{CH}_3\text{HSiN})_x$	POLYMETHYLSILAZANE
$(\text{CH}_3\text{Si})_x(\text{NCH}_3)_y(\text{NHCH}_3)_z$	POLYCARBOSILAZANE
$\left( \begin{array}{c} \text{Si} - \text{Si} \\ \diagup \quad \diagdown \\ -\text{Si} \quad \text{Si}- \\ \diagdown \quad \diagup \\ \text{Si} - \text{Si} \end{array} \right)_x$	POLY (CYCLOHEXAMETHYLSILANE)

## SILSESQUIOXANES

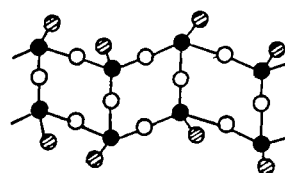


R = methyl, propyl, vinyl, phenyl

T Resin



Ladder Polymer





## SiC FIBER ANALYSIS

Martha H. Jaskowiak  
NASA Lewis Research Center  
Cleveland, Ohio 44135

Polymer derived Nicalon SiC fibers are known to be thermally unstable at temperatures beyond 1200°C. In an effort to further understand the mechanisms of fiber degradation, Nicalon fibers were heat treated at temperatures up to 2200°C and argon gas pressures varying from 0 to 1360 atm. The effects of gas pressure on the thermal stability of the fibers were determined through property comparisons between the pressure-treated fibers and vacuum-treated fibers. Investigation of the thermal stability included studies of the fiber microstructure and mechanical and physical properties before and after treatments.

# Nicalon Fiber Thermal Stability

## Problem:

- Polymer derived Nicalon SiC fibers degrade significantly in tensile strength above 1200 C in inert environments

## Probable Mechanisms:

- Creation of increased internal porosity and flaw growth caused by reactions between SiC, SiO<sub>2</sub>, C, and Si<sub>3</sub>N<sub>4</sub> in the as-produced fiber
- Grain growth of microcrystalline SiC

## Objectives

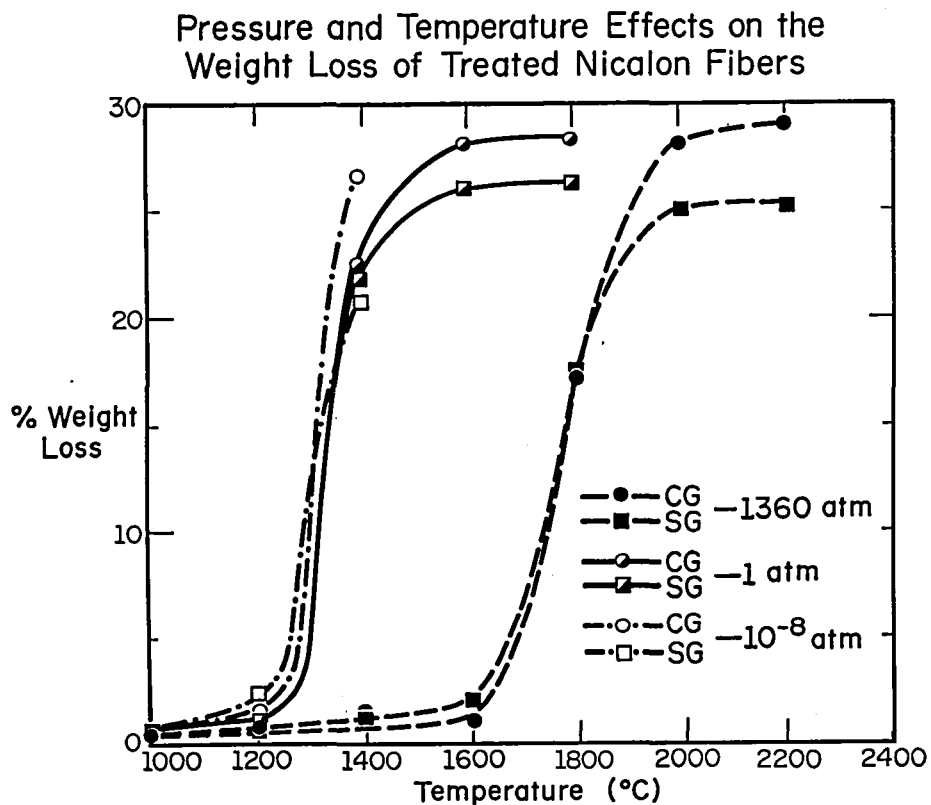
- To determine the effects of heat treatment in high pressure argon on the tensile strength and physical properties of commercially available Nicalon SiC fibers
- To determine whether Hot Isostatic Pressing can offer a viable approach to improving the thermal stability of Nicalon fibers

## Experimental Parameters

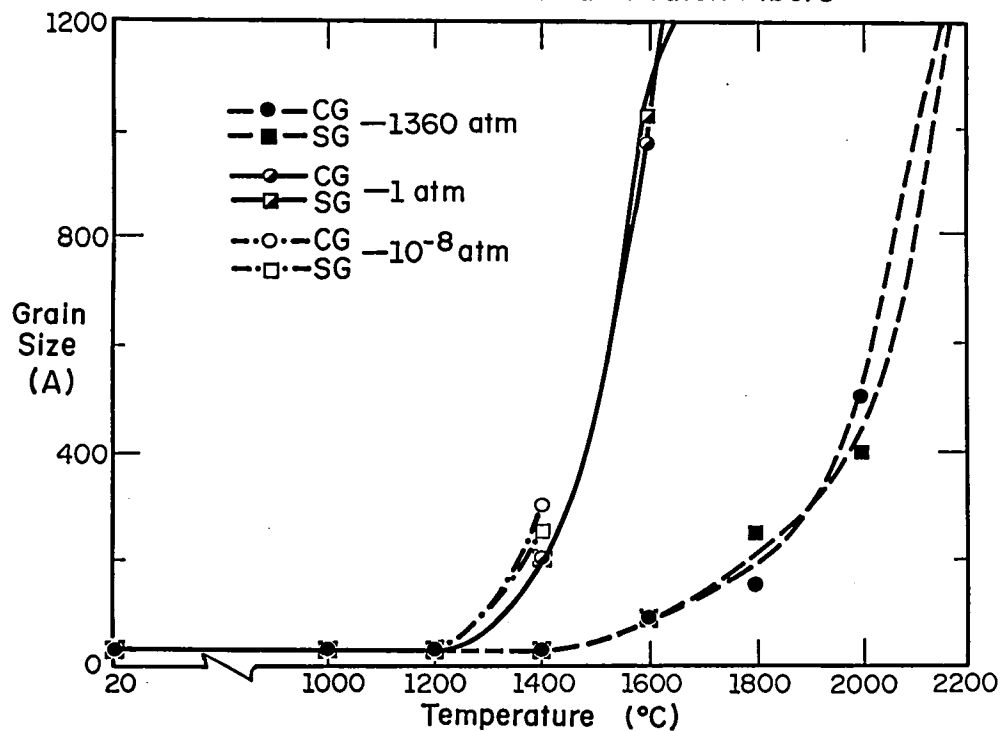
		Si	C	O	N	
Nicalon Fibers:	Ceramic Grade	~40	50	8	2	at%
	Standard Grade	~37	46	15	2	at%

Treatment Conditions: Pressure: 10<sup>-8</sup>, 1, 1360 atm Argon  
 Temperature: 1000 – 2200 C  
 Time: 1 hour

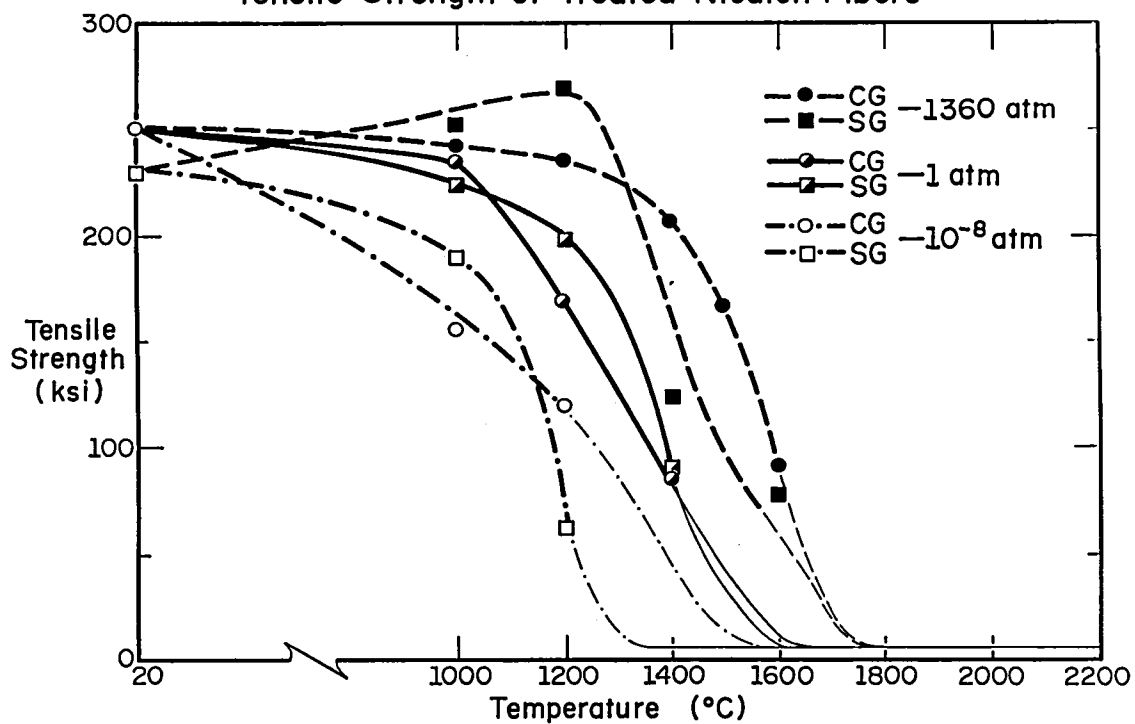
Properties: Weight Loss  
 Tensile Strength  
 Grain Size  
 Microstructure  
 Crystalline Phases



Pressure and Temperature Effects on the Grain Growth of Treated Nicalon Fibers

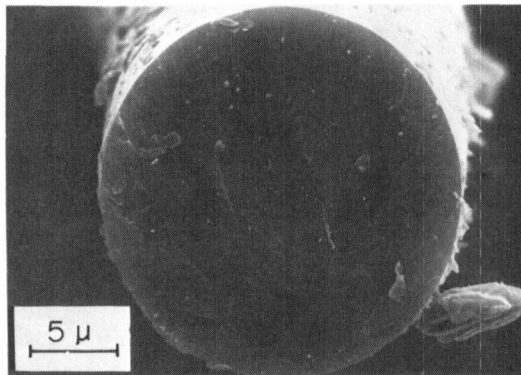


Pressure and Temperature Effects on the Tensile Strength of Treated Nicalon Fibers

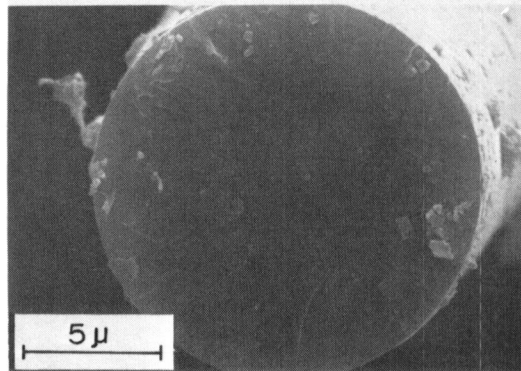


## Fracture Surfaces of As-Received Nicalon Fibers

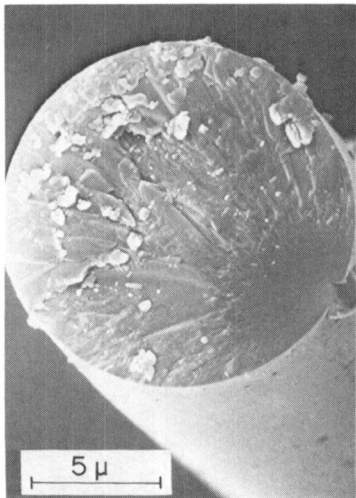
Standard  
Grade  
250 ksi



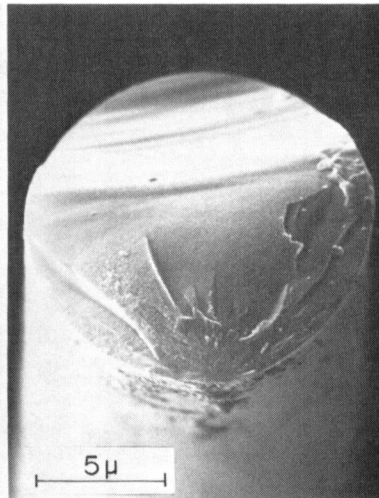
Ceramic  
Grade  
231 ksi



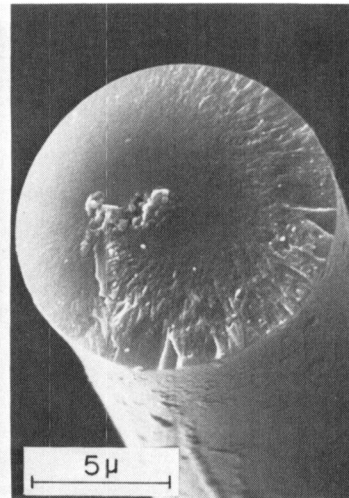
## Ceramic Grade Nicalon Heated to 1000 °C



1360 atm  
0.6 % wt loss  
240 ksi

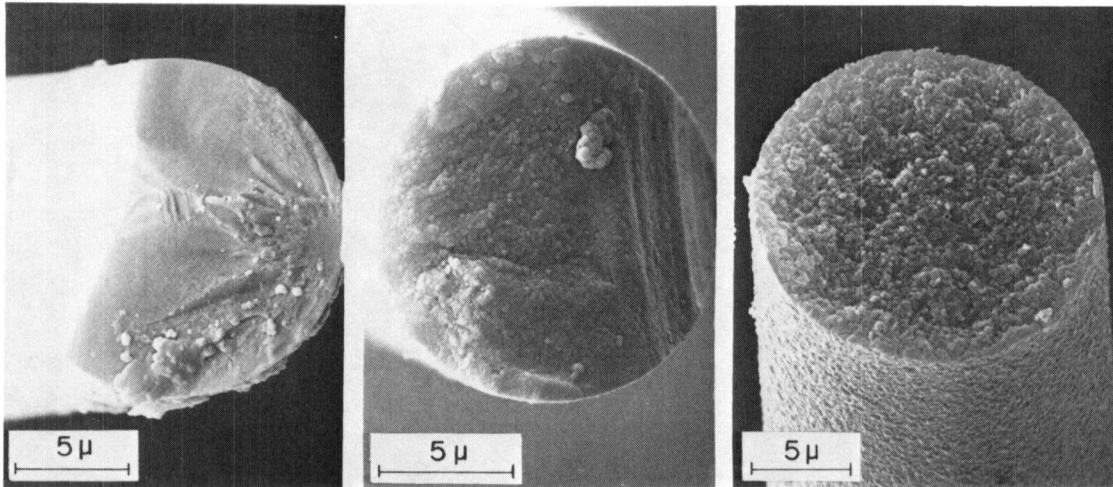


1 atm  
0.8 % wt loss  
235 ksi



10<sup>-8</sup> atm  
0.8 % wt loss  
154 ksi

### Ceramic Grade Nicalon Heated to 1400°C



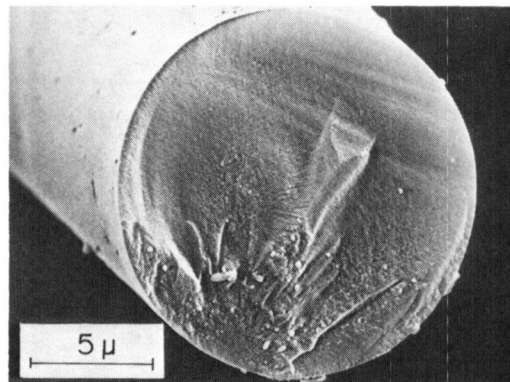
1360 atm  
1.0 % wt loss  
208 ksi

1 atm  
22 % wt loss  
85 ksi

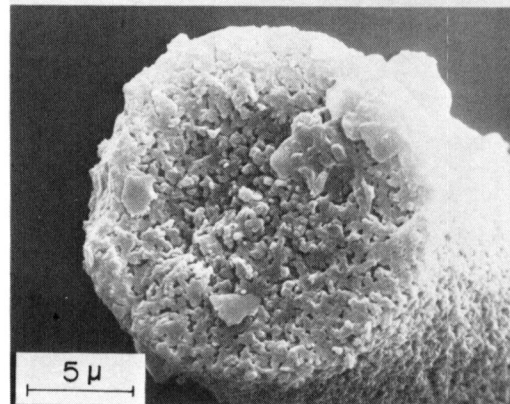
$10^{-8}$  atm  
27 % wt loss  
— ksi

### Ceramic Grade Nicalon Fibers Heated to 1600 °C

1360 atm  
0.8 % wt loss  
90 ksi

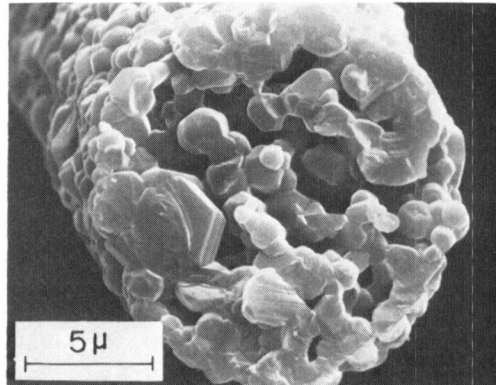


1 atm  
28 % wt loss  
— ksi

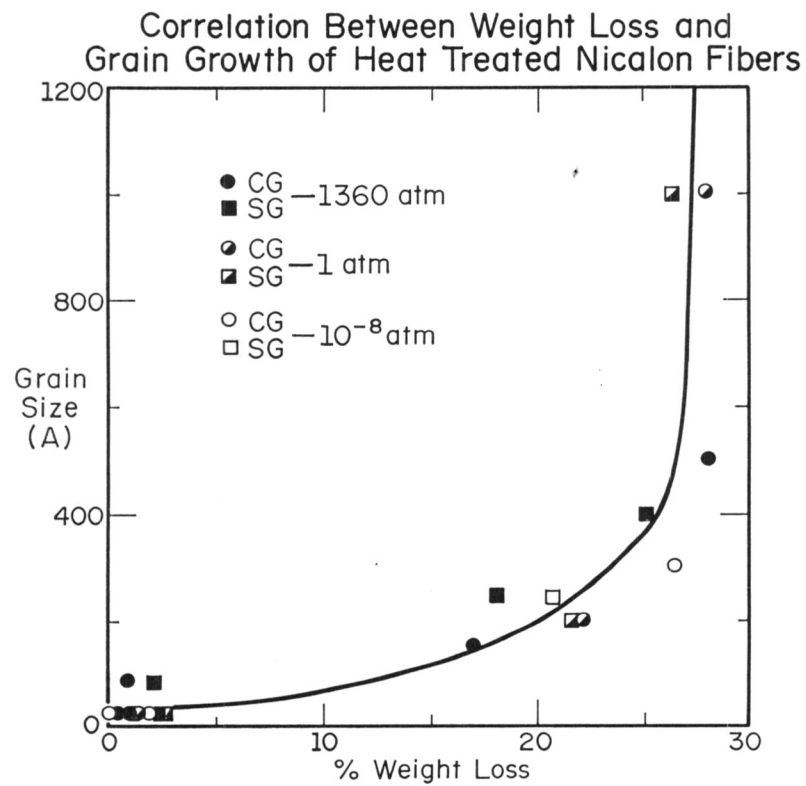
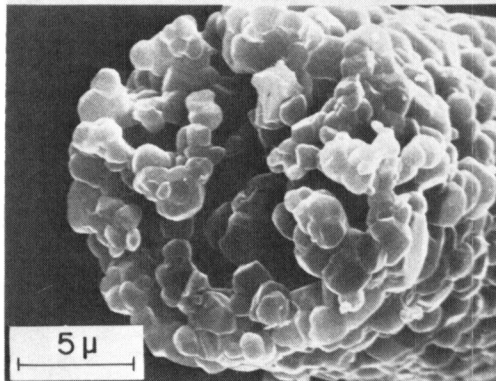


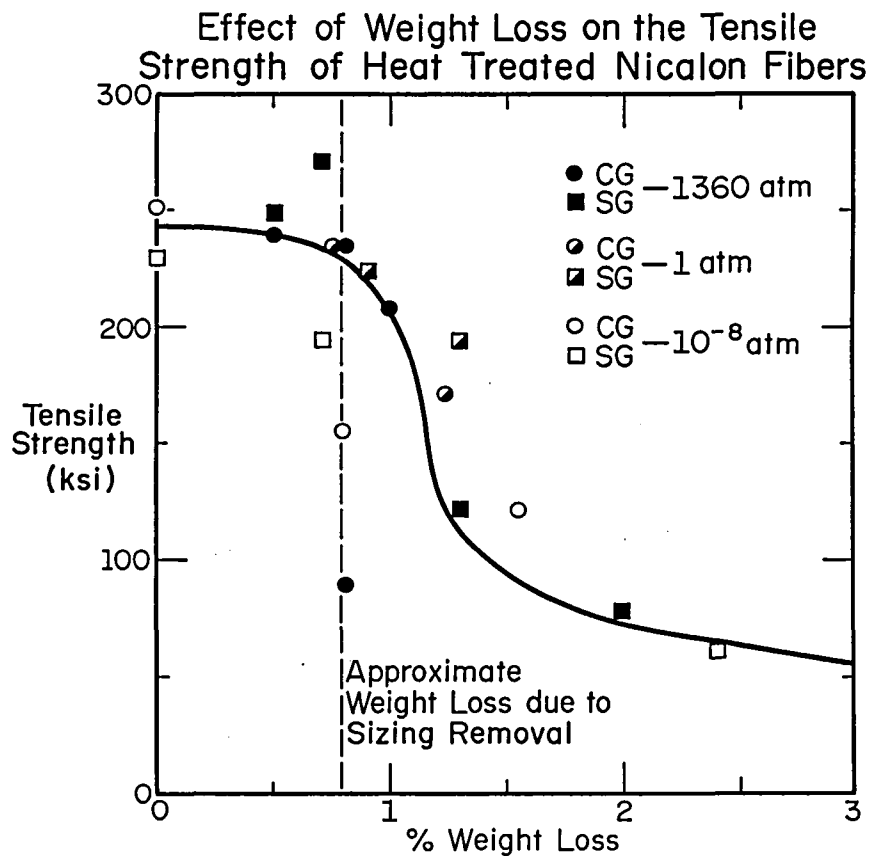
## Nicalon Fibers Heated to 2200°C

Standard  
Grade  
1360 atm  
25 % wt loss  
— ksi



Ceramic  
Grade  
1360 atm  
28 % wt loss  
— ksi





### Results of Additional Heat Treatment Tests on High Pressure Treated Nicalon Fibers

Heat Treatment Conditions	% Weight Loss	Tensile Strength (ksi)
	CG / SG	CG / SG
1200 C - 1 hr 1360 atm Ar	0.8 / 0.7	236 / 271
1200 C - 1 hr 1360 atm Ar	28 / 24	-- --
1400 C - 1 hr 1 atm Ar		
1600 C - 1 hr 1360 atm Ar	0.8 / 2.0	90 / 78
1600 C - 1 hr 1360 atm Ar	23 / 26	-- --
1400 C - 1 hr 1 atm Ar		



## Pressure Effects on Nicalon Thermal Stability

### Summary:

- High pressure treatments in Argon suppress fiber weight loss to temperatures above 1500 C
- Strength degradation and grain growth can be correlated with weight loss and thus are also inhibited by high pressure treatments
- Strength degradation occurs rapidly within the first 1% weight loss (beyond the sizing removal) whereas grain growth does not proceed as rapidly until ~20% weight is reached
- Fibers retreated at 1400 C in 1 atm Ar after high pressure treatment show no improvement in strength over as received fibers treated at 1400 C

## Pressure Effects on Nicalon Thermal Stability

### Conclusions:

- Increased external pressure creates a diffusion barrier which inhibits CO gas evolution from internal  $\text{SiO}_2$  - Carbon reactions thus suppressing fiber weight loss
- Suppression of CO gas evolution may also delay exaggerated grain growth due to the tendency of excess carbon in SiC to act as a grain growth inhibitor
- Initial and major strength degradation mechanism is most likely due to the rapid growth of pre-existing flaws near the surface
- In general, high pressure treatment of commercial Nicalon fibers offers no improvement in thermal stability unless pressure can be maintained throughout composite fabrication and fiber use
- Because of initial porosity and/or creep resistance in the as-produced Nicalon fibers Hot Isostatic Pressing does not appear to be an effective post-fabrication method for improving fiber thermal stability

## Fiber Development – Future Directions

Based on potential SiC Properties:

- High modulus ( $>400$  GPa )
- High strength ( $>4$  GPa )
- Creep resistance
- Environmental resistance
- Low density
- High thermal conductivity
- Property retention to above 1400 C

Efforts will continue to develop processing approaches for producing

- Continuous
- Small diameter
- High performance
- Multifilament tows of SiC fibers

Current results indicate CVD Processing as the optimum approach  
for the base fibers and for required fiber coatings

## SiC FIBER REINFORCED REACTION-BONDED $\text{Si}_3\text{N}_4$ COMPOSITES

Ramakrishna T. Bhatt  
NASA Lewis Research Center  
Cleveland, Ohio 44135

A technique for fabricating strong and tough SiC fiber reinforced reaction bonded  $\text{Si}_3\text{N}_4$  matrix composites (SiC/RBSN) has been developed. Using this technique, composites containing ~ 23, 30, and 40 volume fractions of aligned 140  $\mu\text{m}$  diameter, chemically vapor deposited SiC fibers have been fabricated. The room temperature physical and mechanical properties have been evaluated. The results for composite tensile strength, bend strength, and fracture strain indicate that the composite displays excellent properties when compared with the unreinforced matrix of comparable porosity. The composite stress at which the matrix first cracks and the ultimate composite fracture strength increase with increasing volume fraction of fibers, and the composite fails gracefully.

Measurements of room temperature tensile strength of SiC/RBSN composites after 100 hr exposure in flowing air at 1200°C and at 1400°C, and measurements of bend strength at temperatures up to 1300°C did not show any appreciable strength loss from the strength values of as-fabricated composites. The mechanical property data of this ceramic composite are compared with similar data for unreinforced commercially-available  $\text{Si}_3\text{N}_4$  materials and for SEP SiC/SiC composites.

## SIC FIBER REINFORCED REACTION - BONDED $\text{Si}_3\text{N}_4$

by

R. T. BHATT

NASA-LEWIS RESEARCH CENTER  
CLEVELAND, OHIO 44135

### OBJECTIVE:

- TO FABRICATE AND EVALUATE PROPERTIES OF FIBER REINFORCED  $\text{Si}_3\text{N}_4$  MATRIX COMPOSITES FOR ADVANCED HEAT ENGINE APPLICATIONS

### RATIONALE:

- $\text{Si}_3\text{N}_4$  IS A LIGHT, OXIDATION RESISTANT, THERMAL SHOCK RESISTANT, NONSTRATEGIC MATERIAL BUT LACKS DUCTILITY (TOUGHNESS) AND STRENGTH REPRODUCIBILITY

### APPROACH:

- REINFORCEMENT OF  $\text{Si}_3\text{N}_4$  BY HIGH STRENGTH, HIGH MODULUS CERAMIC FIBER SHOULD
  - IMPROVE TOUGHNESS BY CRACK DEFLECTION AT THE INTERFACE
  - INCREASE FIRST MATRIX FAILURE STRESS DUE TO INCREASE IN STIFFNESS OF MATERIAL

### PROPERTIES:

- FIRST MATRIX CRACK STRESS
- ULTIMATE STRENGTH
- INTERFACIAL SHEAR STRENGTH
- THERMAL SHOCK RESISTANCE
- THERMAL STABILITY

### TESTS:

- TENSILE STRENGTH - (ROOM TEMPERATURE)
- FLEXURE STRENGTH - (ROOM TEMPERATURE TO 1400 °C)

## MATERIALS FOR $\text{Si}_3\text{N}_4$ COMPOSITE

### FIBERS

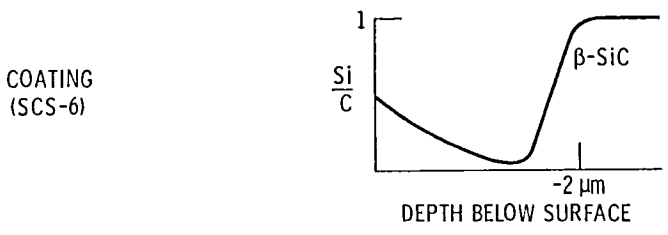
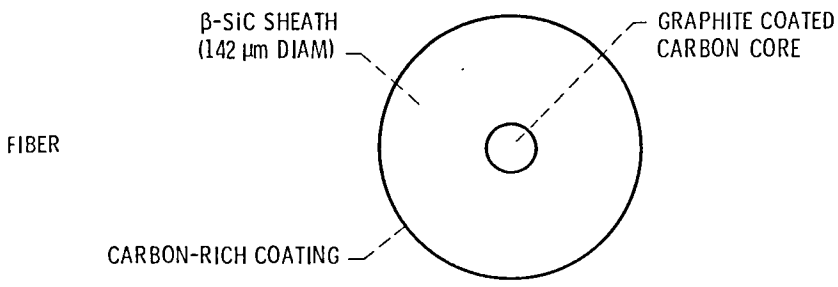
- AVCO CVD SILICON CARBIDE FIBERS
- HIGH MODULUS - 390 GPa ( $57 \times 10^6$  psi)
- HIGH STRENGTH - 3.5 GPa (500 ksi)
- HIGH PURITY
- CREEP RESISTANT
- COMPATIBLE WITH  $\text{Si}_3\text{N}_4$

### MATRIX

- REACTION-BONDED SILICON NITRIDE
- LOW MODULUS - 100-200 GPa ( $15-30 \times 10^6$  psi)
- LOW TEMPERATURE FABRICATION
- NET SHAPE PROCESSING

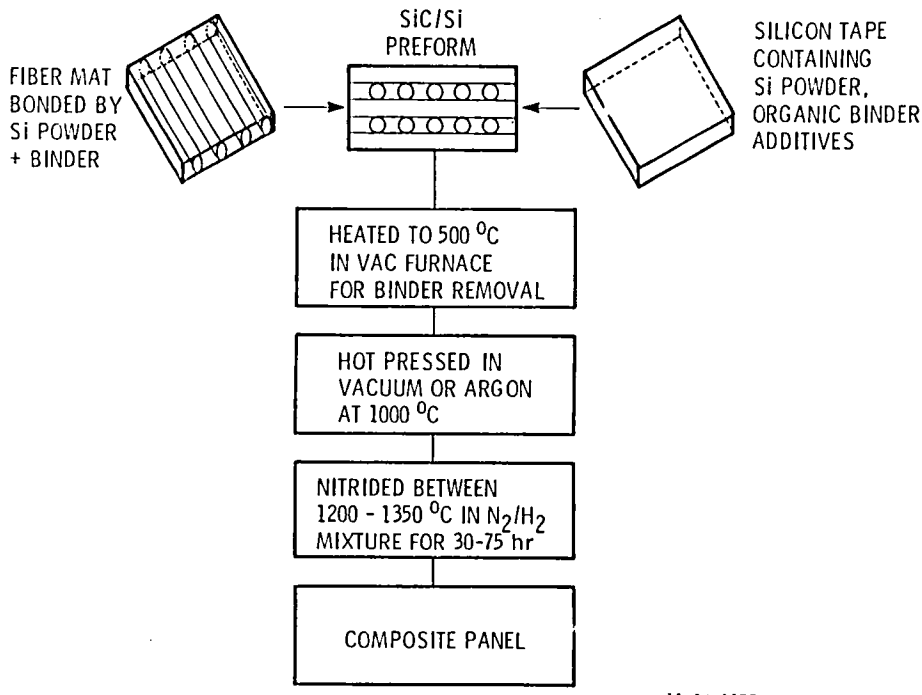
CD-85-16631

# AVCO SiC FIBER COMPOSITION



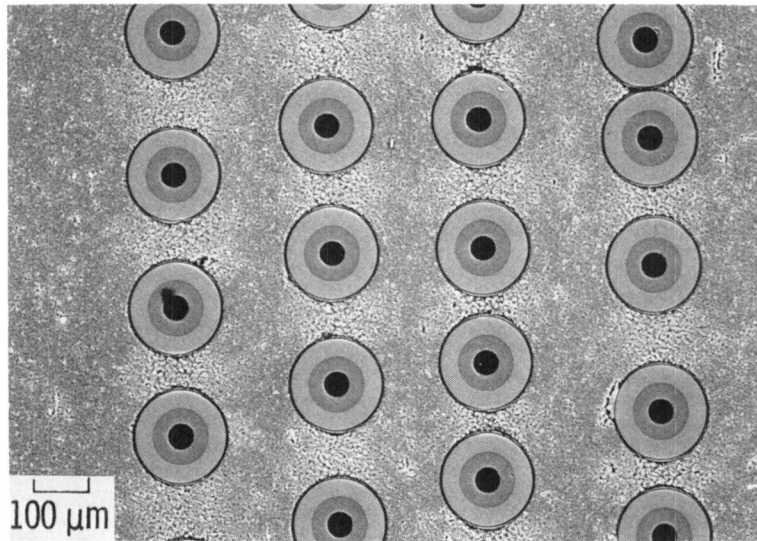
CD-85-16632  
CS-85-2221

## SiC/RBSN COMPOSITE FABRICATION



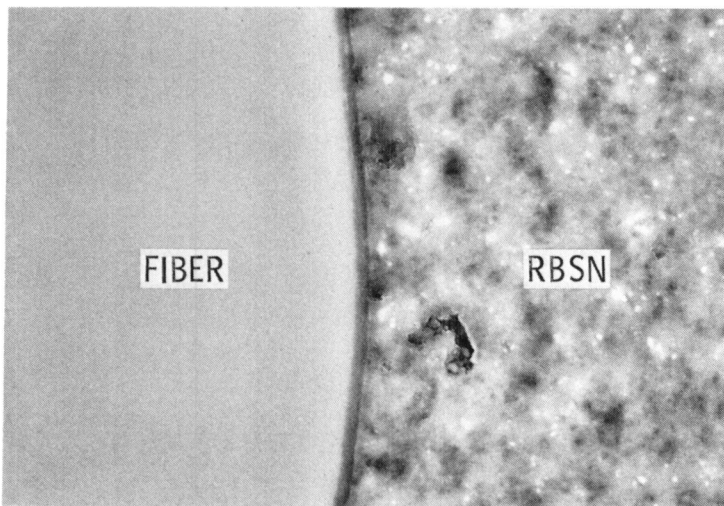
CS-85-0357

## CROSS SECTION OF 39 VOL% SiC/RBSN COMPOSITE

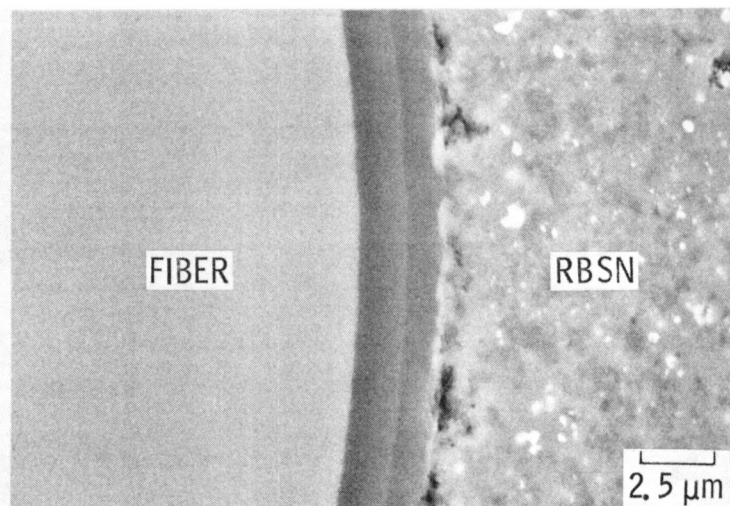


CS-86-0199

## INTERFACIAL REGION IN SiC/RBSN COMPOSITE



SCS-0 FIBER



SCS-6 (DOUBLE COATED) FIBER

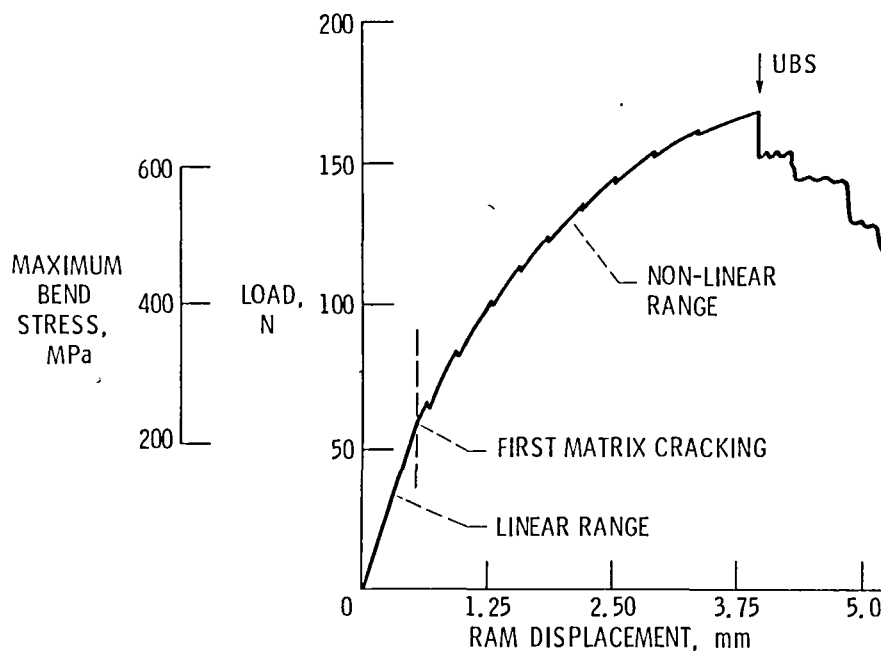
CS-86-0200

# DENSITY AND POROSITY DATA FOR SiC /RBSN COMPOSITES

VOLUME FRACTION OF FIBERS	BEFORE NITRIDATION		AFTER NITRIDATION	
	DENSITY gm /cc	MATRIX POROSITY, %	DENSITY gm /cc	MATRIX POROSITY, %
0	1.56	35	1.98	37
23 ± 3	1.70	54	2.19	39
40 ± 2	1.90	51	2.36	40

CD-85-16629

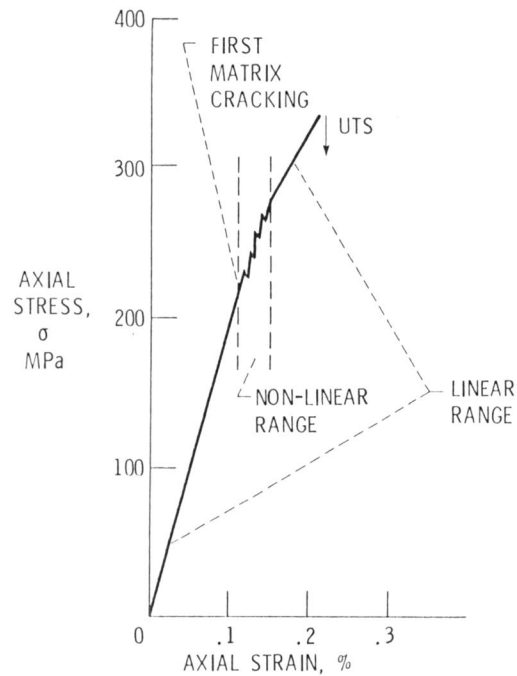
## THE LOAD-DISPLACEMENT BEHAVIOR FOR 20 vol % SiC/RBSN COMPOSITE IN 3-POINT BENDING



CD-85-16628

CS-85-2217

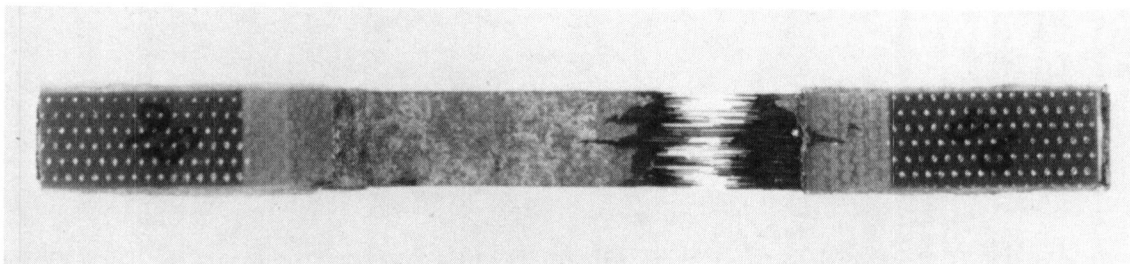
THE AXIAL STRESS-STRAIN BEHAVIOR FOR 20 vol %  
SiC/RBSN COMPOSITE



(CD 85-166X)

CS-85-2220

## FRACTURED TENSILE SPECIMEN OF SiC/RBSN COMPOSITE





## ROOM TEMPERATURE STRENGTHS OF SiC /RBSN COMPOSITE

TEST	AXIAL STRENGTH, MPa		
	0% FIBER	23 ± 3% FIBER	40 ± 2% FIBER
4 POINT BEND ( $\frac{L}{h} = 15$ ) <sup>a</sup>	107 ± 26	539 ± 48	616 ± 36
4 POINT BEND ( $\frac{L}{h} = 45$ )	-----	675 ± 42	868 ± 32
3 POINT BEND ( $\frac{L}{h} = 35$ )	-----	717 ± 80	958 ± 45
TENSILE <sup>b</sup>	-----	352 ± 73	536 ± 20

<sup>a</sup>TEST SPECIMEN HEIGHT ≈ 1.25 mm

CD-85-16641

<sup>b</sup>TEST GAUGE LENGTH 50 mm

CS-85-2218

## SiC /RBSN FRACTURE PARAMETERS

FIBER FRACTION, %	MATRIX CRACK SPACING, mm	INTERFACIAL SHEAR STRESS <sup>a</sup> , MPa	COMPOSITE STRESS AT WHICH MATRIX FIRST CRACKED, MPa	MATRIX FRACTURE STRAIN <sup>b</sup>
23 ± 3	2.0 ± 0.3	10.91	237 ± 25	0.0015
40 ± 2	0.9 ± 0.2	10.23	293 ± 15	0.0014

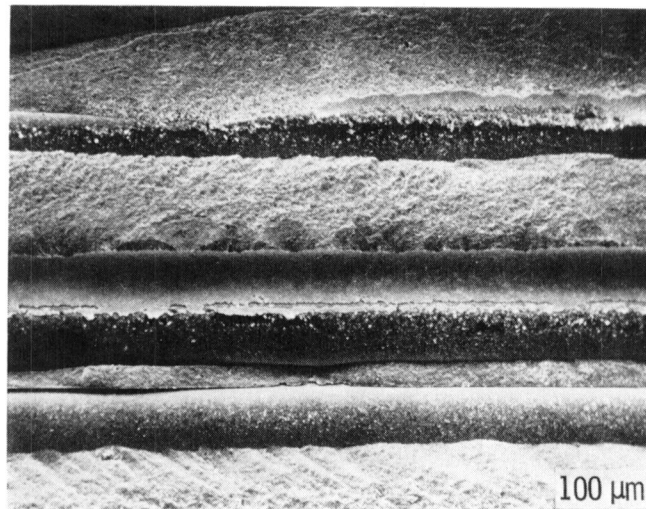
<sup>a</sup>CALCULATED FROM ACK THEORY

<sup>b</sup>CALCULATED FROM ESTIMATED COMPOSITE MODULUS

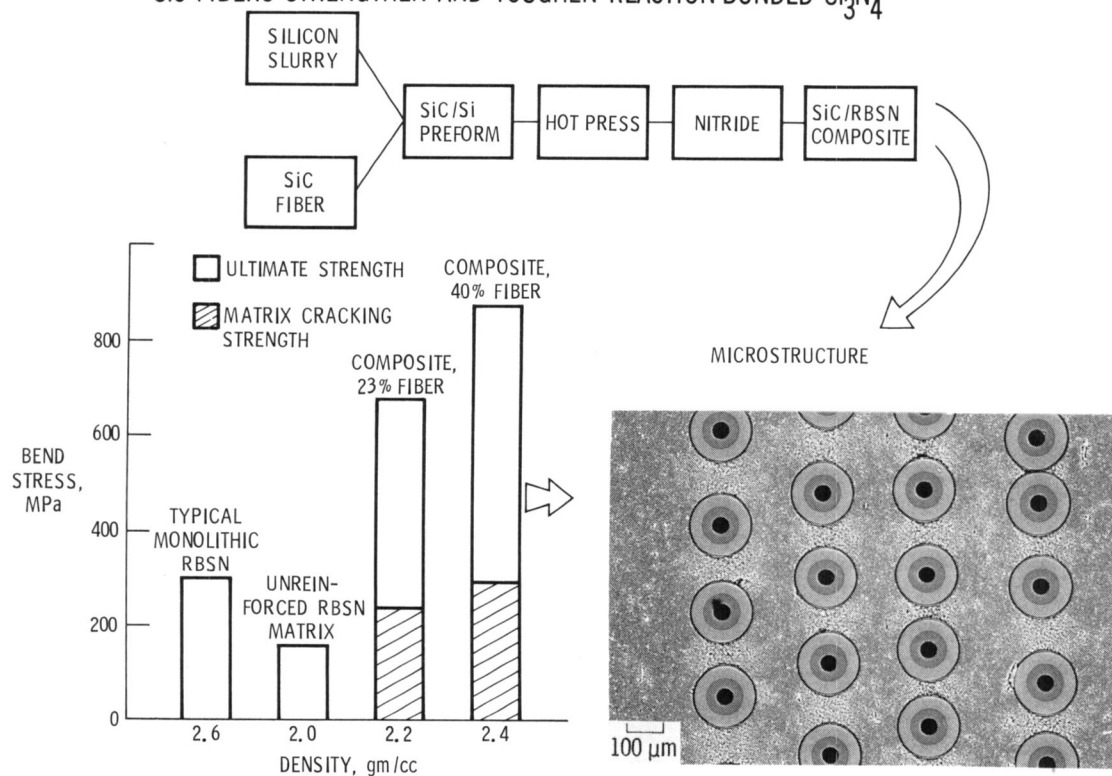
CD-85-16640

CS-85-2225

# FRACTURE SURFACE OF SiC/RBSN IN TRANSVERSE FLEXURE



## SiC FIBERS STRENGTHEN AND TOUGHEN REACTION-BONDED $\text{Si}_3\text{N}_4$



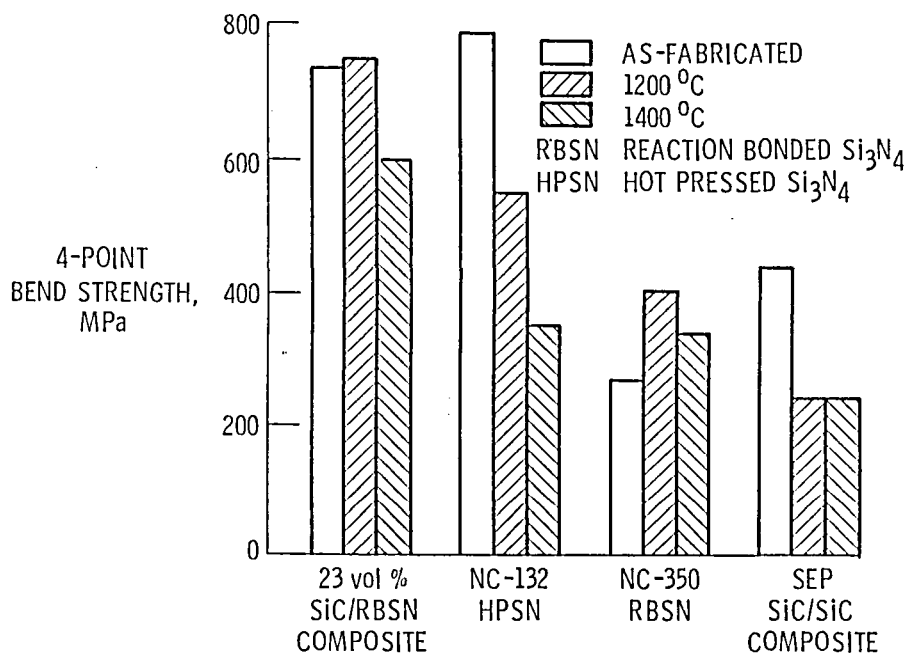
THERMAL STABILITY DATA FOR SiC/RBSN  
AND SiC/SiC COMPOSITES

TREATMENT	ROOM TEMPERATURE AXIAL ULTIMATE STRENGTH, MPa	
	30 vol % SiC/RBSN	SEP SiC/SiC
AS-FABRICATED	350 <sup>a</sup>	441 <sup>b</sup>
1200 °C, 100 hr, AIR	316 <sup>a</sup>	234 <sup>b</sup>
1400 °C, 100 hr, AIR	323 <sup>a</sup>	234 <sup>b</sup>

a-TENSILE STRENGTH.

b-4-POINT BEND STRENGTH. (NO TENSILE DATA REPORTED. TENSILE STRENGTHS WOULD BE MUCH LOWER THAN 4-POINT BEND STRENGTH.)

ELEVATED TEMPERATURE STRENGTH (4-POINT BEND) FOR  
SiC/RBSN COMPOSITE, MONOLITHIC SILICON-BASED CERAMICS, AND  
SEP SiC/SiC COMPOSITE



## SUMMARY OF RESULTS

- A STRONG AND TOUGH CERAMIC MATRIX COMPOSITE CAN BE FABRICATED BY REINFORCING RBSN BY HIGH MODULUS, HIGH STRENGTH, CONTINUOUS LENGTH CVD SiC FIBER
- REINFORCEMENT OF RBSN BY CVD SiC FIBERS ALSO MEASURABLY INCREASES COMPOSITE MODULUS AND THE COMPOSITE STRESS AT WHICH MATRIX CRACKS
- WEAK FIBER-MATRIX BONDING ALLOWS MULTIPLE CRACKING AND GRACEFUL FAILURE
- COMPOSITE IS THERMALLY STABLE AND HAS BETTER ELEVATED TEMPERATURE STRENGTH THAN MANY COMMERCIALY AVAILABLE MONOLITHIC CERAMICS
- FURTHER IMPROVEMENTS IN COMPOSITE PROPERTIES ARE POSSIBLE WITH
  - INCREASE IN MATRIX STRENGTH (DECREASE IN POROSITY)
  - SMALL DIAMETER FIBERS
  - FIBER COATING

## CURRENT AND FUTURE STUDIES

### CURRENT:

- OPTIMIZATION OF PROCESSING VARIABLES
- POST FABRICATION TREATMENTS
- LAMINATE PROPERTIES ( $0^0/90^0$ ,  $0^0/90^0/45^0$ )
- INTERFACIAL REACTION KINETICS

### FUTURE:

- MEASUREMENT OF ELEVATED TEMPERATURE TENSILE STRENGTH AND STRESS RUPTURE DATA
- THERMAL PROPERTIES
- OXIDATION

1. Report No. <b>NASA CP-2427</b>		2. Government Accession No.		3. Recipient's Catalog No.	
4. Title and Subtitle  <b>Structural Ceramics</b>				5. Report Date <b>May 1986</b>	
				6. Performing Organization Code <b>533-05-01</b>	
7. Author(s)				8. Performing Organization Report No. <b>E-3063</b>	
				10. Work Unit No.	
9. Performing Organization Name and Address  <b>National Aeronautics and Space Administration Lewis Research Center Cleveland, Ohio 44135</b>				11. Contract or Grant No.	
				13. Type of Report and Period Covered <b>Conference Publication</b>	
12. Sponsoring Agency Name and Address  <b>National Aeronautics and Space Administration Washington, D.C. 20546</b>				14. Sponsoring Agency Code	
15. Supplementary Notes					
16. Abstract  This publication is a compilation of abstracts and slides of papers presented at the NASA Lewis Structural Ceramics Workshop held at the Sheraton Hopkins Hotel, Cleveland, Ohio, on May 20 and 21, 1986. Collectively, these papers depict the scope of NASA Lewis' structural ceramics program. Each paper provides a brief overview of a technical area in which NASA Lewis Research Center has a significant research focus. The technical areas include monolithic SiC and Si <sub>3</sub> N <sub>4</sub> development, ceramic matrix composites, tribology, design methodology, nondestructive evaluation (NDE), fracture mechanics, and corrosion.					
17. Key Words (Suggested by Author(s))  <b>Ceramics Composites Polymer chemistry Nondestructive evaluation (NDE)</b>			18. Distribution Statement  <del>Foreign distribution excluded.</del> Source of Availability: NASA Industrial Applications Centers STAR Category 27		
19. Security Classif. (of this report) <b>Unclassified</b>		20. Security Classif. (of this page) <b>Unclassified</b>		21. No. of pages <b>229</b>	
				22. Price* <b>A11</b>	

LANGLEY RESEARCH CENTER



3 1176 01305 4482